CENTRE FOR ECONOMIC POLICY RESEARCH

CEPR PRESS

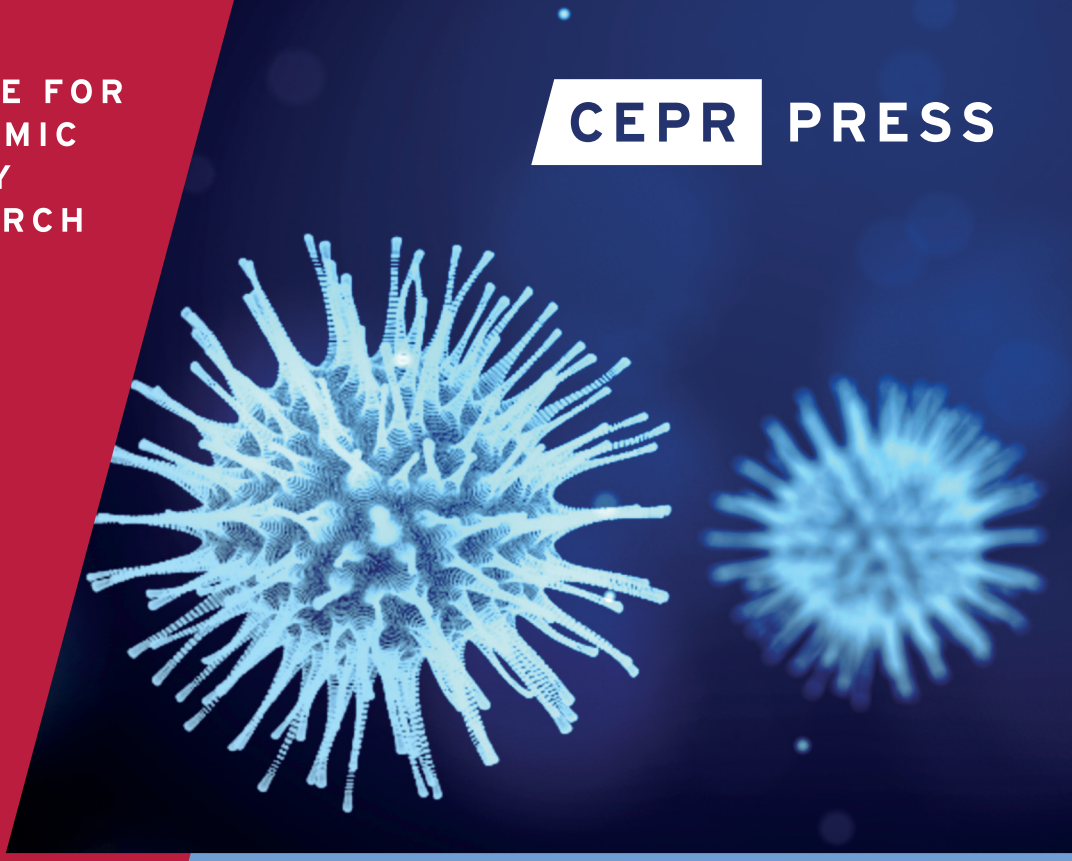

COVID ECONOMICS

VETTED AND REAL-TIME PAPERS

ISSUE 47
4 SEPTEMBER 2020

Covid Economics
Vetted and Real-Time Papers

Covid Economics, Vetted and Real-Time Papers, from CEPR, brings together formal investigations on the economic issues emanating from the Covid outbreak, based on explicit theory and/or empirical evidence, to improve the knowledge base.

Founder: Beatrice Weder di Mauro, President of CEPR
Editor: Charles Wyplosz, Graduate Institute Geneva and CEPR

Contact: Submissions should be made at https://portal.cepr.org/call-papers-covid-economics. Other queries should be sent to covidecon@cepr.org.

The Centre for Economic Policy Research (CEPR)

The Centre for Economic Policy Research (CEPR) is a network of over 1,500 research economists based mostly in European universities. The Centre's goal is twofold: to promote world-class research, and to get the policy-relevant results into the hands of key decision-makers. CEPR's guiding principle is 'Research excellence with policy relevance'. A registered charity since it was founded in 1983, CEPR is independent of all public and private interest groups. It takes no institutional stand on economic policy matters and its core funding comes from its Institutional Members and sales of publications. Because it draws on such a large network of researchers, its output reflects a broad spectrum of individual viewpoints as well as perspectives drawn from civil society. CEPR research may include views on policy, but the Trustees of the Centre do not give prior review to its publications. The opinions expressed in this report are those of the authors and not those of CEPR.

Editorial Board

Ethics

Covid Economics will feature high quality analyses of economic aspects of the health crisis. However, the pandemic also raises a number of complex ethical issues. Economists tend to think about trade-offs, in this case lives vs. costs, patient selection at a time of scarcity, and more. In the spirit of academic freedom, neither the Editors of *Covid Economics* nor CEPR take a stand on these issues and therefore do not bear any responsibility for views expressed in the articles.

Submission to professional journals

The following journals have indicated that they will accept submissions of papers featured in *Covid Economics* because they are working papers. Most expect revised versions. This list will be updated regularly.

American Economic Review
American Economic Review, Applied Economics
American Economic Review, Insights
American Economic Review, Economic Policy
American Economic Review, Macroeconomics
American Economic Review, Microeconomics
American Journal of Health Economics
Canadian Journal of Economics
*Econometrica**
Economic Journal
Economics of Disasters and Climate Change
International Economic Review
Journal of Development Economics
*Journal of Econometrics**
Journal of Economic Growth
Journal of Economic Theory
*Journal of the European Economic Association**
Journal of Finance
Journal of Financial Economics
Journal of International Economics
*Journal of Labor Economics**
Journal of Monetary Economics
Journal of Public Economics
Journal of Public Finance and Public Choice
Journal of Political Economy
Journal of Population Economics
*Quarterly Journal of Economics**
Review of Economics and Statistics
*Review of Economic Studies**
Review of Financial Studies

(*) Must be a significantly revised and extended version of the paper featured in *Covid Economics*.

Covid Economics
Vetted and Real-Time Papers

Issue 47, 4 September 2020

Contents

Covid Economics Issue 47, 4 September 2020

Test sensitivity for infection versus infectiousness of SARS-CoV-2[1]

Joshua S. Gans[2]

Date submitted: 28 August 2020; Date accepted: 30 August 2020

The most commonly used test for the presence of SARS-CoV-2 is a PCR test that is able to detect very low viral loads and inform on treatment decisions. Medical research has confirmed that many individuals might be infected with SARS-CoV-2 but not infectious. Knowing whether an individual is infectious is the critical piece of information for a decision to isolate an individual or not. This paper examines the value of different tests from an information-theoretic approach and shows that applying treatment-based approval standards for tests for infection will lower the value of those tests and likely causes decisions based on them to have too many false positives (i.e., individuals isolated who are not infectious). The conclusion is that test scoring be tailored to the decision being made.

Covid Economics 47, 4 September 2020: 1-16

1 All correspondence to joshua.gans@utoronto.ca. Disclaimer: I am an economist and not an epidemiologist. I have received no funding for this research and have no conflicts of interest. Thanks to Laura Rosella, Jakub Steiner and Alex Tabarrok for useful comments. Responsibility for all views expressed and errors made lies with the author.
2 Rotman School of Management, University of Toronto and NBER.

Covid Economics 47, 4 September 2020: 1-16

1 Introduction

An intuitive notion that guides tests for the presence of a virus in an individual is that it is preferable to have tests that have the capability to detect smaller loads of the virus in any given sample (e.g., blood, saliva or nasal mucus). As the presence of the virus is a necessary condition for someone to be infectious – that is, to have a positive probability of transmitting the virus to susceptible person – medical practitioners and government regulators often set standards for a minimum amount of a virus that a test needs to be capable of identifying before or using that test for clinical purposes. However, while being infected is a necessary condition for infectiousness, it is not sufficient. With the Covid-19 pandemic of 2020, it has been discovered that individuals who are infected – in terms of having severe acute respiratory syndrome coronavirus 2 (SARS-CoV-2) present – may not be infectious. This is because infectiousness both requires an individual to have a sufficient viral load and the virus present has to be active. This implies that, if your relevant clinical decision is to isolate an individual to prevent infections in others, as this paper will show, the intuition that you prefer a more precise test falters and less precise tests can be more valuable.[1]

The primary means of testing for SARS-CoV-2 is a reverse transcriptase-quantitative polymerase chain reaction (RT-qPCR) test. Such PCR tests use a technique (PCR) to test for viral RNA remnants in cycles where RNA segments are exponentially replicated in order to increase the likelihood of even small numbers of them being identified in a sample. The test stops once the targeted RNA is identified or, typically, after 40 cycles. If the test run completes without the RNA being found, the test result is returned as 'negative.' Otherwise, it is 'positive' and the individual is held to be infected. This process requires a laboratory, reagents and specialised machines and can cost between $50-150 per test and take between 24 and 48 hours for results to be returned.

The cost of PCR tests, along with the length of time taken for results to be communicated to medical practitioners, has led to calls for cheaper, rapid tests to be used in order to mitigate the spread of Covid-19 (the disease caused by SARS-CoV-2).[2] Larremore et al. (2020) note that a typical PCR test can detect the virus up to 10^3 copies per million (cp/ml) while point-of-care nucleic acid LAMP or rapid antigen tests can only detect up to 10^5 cp/ml. These tests are not to be as accurate as PCR tests for small viral loads but it is also noted that the threshold for infectiousness is more likely 10^6 cp/ml. Importantly, Larremore et al.

[1]Sometimes people look to rank tests according to the Blackwell (1953) criteria of informativeness. Here, the tests I will examine do not naturally correspond to that ranking and so the focus is on the value of a test per se.

[2]For example, Larremore et al. (2020) and Paltiel et al. (2020). Also, these tests require PPE for humans to administer, adding to the cost.

Covid Economics 47, 4 September 2020: 1-16

Figure 1: **Viral Load of Infected Individual Over Time**

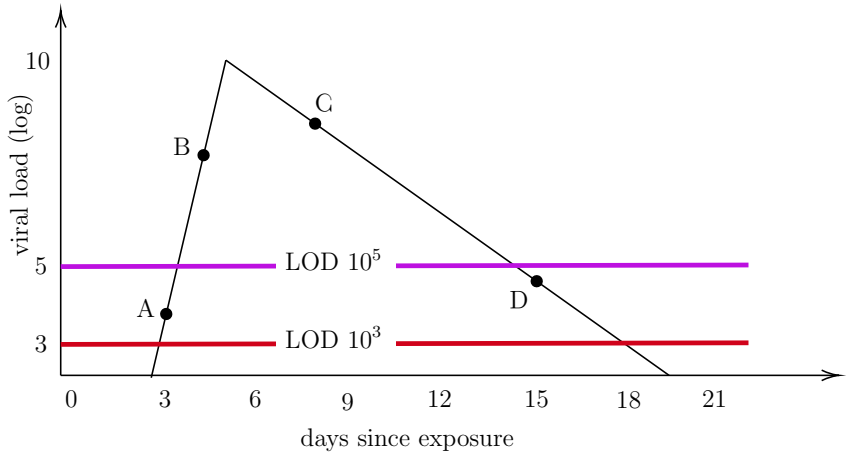

(2020) note that even if an infected patient is caught at 10^3 cp/ml, the time it takes for their load to increase above 10^5 cp/ml is short and may be negative once the time taken to process a PCR test is taken into account. Moreover, after the most infectious period in an individual, the PCR tests can still detect infections and, indeed, can detect viral remnants that may not be alive.

The typical path of the viral load for SARS-CoV-2 is shown in Figure 1.[3] Suppose that a PCR test takes 48 hours to return a result. Then if that test is taken at Day 3 (point A) then the result will be returned on Day 5 (post C) when the individual has potentially been infectious for a day. By contrast, an antigen test taken on Day 3 would return a negative result but if it were used daily and taken also on Day 4 (point B), that individual would be positive and could be isolated immediately. Thus, even though the antigen test is less accurate for identifying an infection than PCR, its cost and consequently frequency of application that allows may make it a more effective tool for mitigating the spread of Covid-19.[4] Larremore et al. (2020) conclude that "the FDA, other agencies, or state governments, encourage the development and use of alternative faster and lower cost tests for surveillance purposes, *even if they have poorer limits of detection.*" (p.7, emphasis added)

In this paper, I make a stronger claim: That even in the absence of a cost advantage or more frequent testing, a test with a higher limit of detection (e.g., an antigen test) may be more informative than a test with a lower limit of detection such as the 'gold-standard'

[3]Source: Larremore et al. (2020)

[4]Larremore et al. (2020) also point out that a test taken at Day 15 might be positive under the PCR test (e.g., point D) but, by that time, the virus itself is dead.

Covid Economics 47, 4 September 2020: 1-16

PCR test. In particular, when a test's efficacy is measured with respect to the decision being taken (isolation versus treatment), an antigen test can be more efficacious. In other words, it may not be 'poorer' but superior.

The outline for the paper is as follows. In Section 2, I provide a discussion of how tests are typically scored by regulators (using sensitivity and specificity) and also a review of the economic literature on testing. Section 3 introduces the model which involves a decision-maker choosing actions of treatment or isolation based on potential costs of a utility loss from isolation, misdiagnosed treatment or broader contagion. Section 4 then examines how to construct sensitivity measures depending on the decision-type and how this relates to the information value of a test. Section 5 considers an extension to take into account pre-symptomatic screening for infection. A final section concludes.

2 Test Scoring

The primary means of scoring tests for clinical purposes is to calculate their *sensitivity* (that is, the probability that an individual with a condition tests positive for that condition) and *specificity* (that is, the probability that an individual without that condition tests negative for that condition). These have their analogues in Type I and Type II errors with sensitivity measuring the lack of false negatives and specificity the lack of false positives. Consequently, depending on test parameters, a test designer often faces a trade-off between test sensitivity and specificity.

These measures are used to score the efficacy of tests. A PCR test for SARS-CoV-2 typically has a specificity of 99% and a sensitivity between 80-98% depending on a number of factors including how skillfully a practitioner is able to capture a sample from an individual. If the pre-test (or prior) probability that a patient is infected is 5%, a test with 90% sensitivity and 99% specificity will have a false negative rate of 1% (i.e., 1% of those who test negative are not negative) and a false positive rate of 17% (i.e., 17% of those who test positive are not positive). By contrast, an antigen test – which looks for particular chemicals associated with SARS-CoV-2 – has a specificity equivalent to PCR tests but a potentially much lower sensitivity (as low as 84-97% compared with the best practice RT-PCR);[5] implying that many, who are actually infected, will test negative for the coronavirus. However, it is important to note that (i) non-PCR tests have their sensitivity and specificity measured compared to PCR tests and (ii) PCR tests define their sensitivity and specificity with respect to infection, not infectiousness.

[5] `https://www.cdc.gov/coronavirus/2019-ncov/lab/resources/antigen-tests-guidelines.html` Döhla et al. (2020) found antigen sensitivity compared with PCR of 36%.

Covid Economics 47, 4 September 2020: 1-16

The terms sensitivity and specificity were coined by Yerushalmy (1947) who was examining the decision-theoretic foundations of using X-rays to inform on diagnosis. Sensitivity was the "probability of correct diagnosis of 'positive' cases" and specificity was the "probability of correct diagnosis of 'negative' cases." In each case, the measure was tied to the purpose of the diagnosis. With virus detection, the purpose of a test is to inform a treatment decision in which case the diagnosis is whether an individual is infected or not. By contrast, with virus mitigation, the purpose of a test is to inform an isolation or quarantine decision in which case the diagnosis is whether an individual is infectious (or contagious) or not. Because the decisions are different, so too should be the measures of sensitivity and specificity even if the underlying target is similar at a molecular level.

In the US, all clinical tests are regulated by the Federal Food and Drug Administration (FDA). When approving a test for clinical purpose this is done with regard to its usefulness in treatment. Thus, PCR tests and antigen tests are scored on the same criteria. However, as will be demonstrated, this score is misleading when the purpose of a test is for a pandemic mitigation rather than a treatment decision. For such decisions, you want to diagnose an individual as infectious or not, rather than infected or not. A test that is less sensitive for infection may be more sensitive with regard to infectiousness.

It is important to note that PCR tests can provide information that can indicate infectiousness rather than infection. As mentioned before, the number of cycles a PCR test has to go through before rendering a positive result is a measure of the viral load in an individual. This cycle count (or Ct measure) is part of any PCR test. However, the reporting of the test results is usually a binary "positive" or 'negative" outcome that discards this information. Some epidemiologists have called for a reporting of the Ct result as a matter of course (Tom and Mina (2020)).[6] In the US, labs are not legally allowed to report Ct numbers so results are binary as a matter of regulation.[7]

Thusfar, the economics literature has focused on other issues regarding testing. Notably, Galeotti et al. (2020) do provide an exposition of taking an information theoretic approach to the value of testing but do not raise issues of infectiousness (as opposed to infection). Other work that examines the informational value of testing examines how to allocate costly or scarce tasks on the basis of available data or observations that underpins pre-test probabilities (see Ely et al. (2020) and Kasy and Teytelboym (2020)). Bergstrom et al. (2020) examine the optimal frequency of testing to reduce contagion. Finally, there is a literature on the impact widespread testing might have for behavioural choices of economic agents (Eichenbaum et al.

[6]This can be particularly useful if patients have multiple tests because the change in the Ct number can indicate where they are on the lifecycle of the virus.

[7]My source for this is Michael Mini (a Harvard epidemiologist) who stated as such here `https://youtu.be/3seIAs-73G8?t=3544` I have not been able to find the specific regulation, however.

(2020); Deb et al. (2020); Acemoglu et al. (2020); Taylor (2020) and Gans (2020)). This present paper is the first that examines the particular issues that arise from testing for infectiousness in an information-theoretic way.

3 Model Setup

The decision-maker (DM) is a public health authority who chooses two actions: a treatment action, $d_i = 0$ (no treatment) and $d_i = 1$ (treatment), and an isolation action, $a_i = 1$ (don't isolate) and $a_i = 0$ (isolate) for each individual $i \in \mathcal{I} = \{1, ..., N\}$ with a payoff of:

$$\sum_{i \in \mathcal{I}} (ua_i - c((1 - d_i)I_{\theta_i \geq \underline{\theta}} + d_i I_{\theta_i < \underline{\theta}})) - C \sum_{i \in \mathcal{I}} a_i I_{\theta_i \geq \bar{\theta}}$$

where $\theta_i \in [0, 1]$ is a measure of the viral load of an individual and I is an indicator function that takes a value of 1 if the condition is met and 0 otherwise.[8] This state is not known to the DM. In contrast to Ely et al. (2020) the state, θ_i, is not binary but is a continuum with distribution function, $F(\theta)$ that is common for all individuals. There is a mass point at $F(0)$ that could be interpreted as the share of the population who are not infected with the virus.

In this setup, $u > 0$ is the utility of a non-isolated agent i, c is the individual cost of a mistreatment[9] and C is the social cost of not isolating an infected individual.[10] Thus, $\underline{\theta}$ is the threshold for the viral load, above which an individual is considered to be *infected* with the virus and can benefit from treatment. By contrast $\bar{\theta}$ is the threshold for the viral load, above which an individual is considered to be *infectious*.

3.1 Perfect information

If the DM had perfect information regarding θ_i, they would choose $d_i = 1$ if and only if $\theta_i \geq \underline{\theta}$. With respect to the isolation decision, for $\theta_i < \bar{\theta}$, DM chooses $a_i = 1$; and for $\theta_i \geq \bar{\theta}$, they choose $a_i = 0$ if $u \leq C$ and $a_i = 1$ otherwise. It will be assumed that $u \leq C$ always holds so that isolation is the optimal choice if the viral load is above the infectiousness threshold.

[8] A simplifying assumption here is that individuals are identical from the perspective of DM. This is innocuous unless there are situations where the DM has specific information about i's utility that differs from others.

[9] In reality, the cost of mistakenly treating someone and the cost of mistakenly not treating them are likely to be different. However, since the treatment decision is not the main focus of this paper, the losses are assumed to be symmetric for simplicity.

[10] This is a simplification as the marginal cost of an additional infected person who is able to interact with others depends upon the number of susceptible people remaining in the population. However, using an more complex and epidemiologically founded cost model is unlikely to change the broad conclusions of this paper.

Covid Economics 47, 4 September 2020: 1-16

3.2 No test

By contrast, suppose that the DM had no information regarding any individual's θ_i. What choice would be optimal? Beginning with the treatment decision, note that it is assumed that the costs associated with a misdiagnosis are c regardless of the 'direction' of the error. Thus, for i, $d_i = 1$ has an expected payoff of $-F(\underline{\theta})c$ while $d_i = 0$ has an expected payoff of $-(1 - F(\underline{\theta}))c$. Thus, DM will treat rather than not treat if:

$$(1 - F(\underline{\theta}))c \geq F(\underline{\theta})c \implies F(\underline{\theta}) \leq \frac{1}{2}$$

That is, blanket treatments are optimal if prevalence $(1 - F(\underline{\theta}))$ is high. For the isolation decision, the payoff from $a_i = 0$ (isolation) for all i is (by our normalisation) 0 while the expected payoff if $a_i = 1$ for all i is: $N(u - C(1 - F(\bar{\theta})))$. Thus, isolation is an optimal decision if:

$$C(1 - F(\bar{\theta})) \geq u$$

Here, high numbers of infectious individuals $(1 - F(\bar{\theta}))$ triggers a blanket isolation or lockdown decision.

4 Test Sensitivity

Suppose that there exists a test that can be deployed that will detect viral load above a certain point θ. In other words, the signal, s_i provided by a test is binary with '+' if $\theta_i \geq \theta$ and '−' otherwise. Thus, if you conduct a test on an individual i, then with probability $1 - F(\theta)$ it will return a positive result and with probability $F(\theta)$ a negative result.

4.1 Sensitivity of a test for infection

As noted in Section 2, regulators score the efficacy of clinical tests but measuring the sensitivity and specificity of those tests. However, these tests must be conducted with respect to the decision being taken and, for regulators, this is often for the purpose of informing treatment interventions (i.e., diagnosis). Thus, a test for the presence of a virus would provide information as to whether someone was infected and in need of potential treatment. This means that sensitivity and specificity would be considered with respect to $\underline{\theta}$. In medical terms this means that, prior to a test, the pre-test probability (or prior) that someone is infected is $1-F(\underline{\theta})$; likely the population level of prevalence. In the case of the test described above, specificity ($\Pr[-|\theta_i < \underline{\theta}]$) and sensitivity ($\Pr[+|\theta_i \geq \underline{\theta}]$) are:

Covid Economics 47, 4 September 2020: 1-16

Covid Economics 47, 4 September 2020: 1-16

$$\Pr[-|\theta_i < \underline{\theta}] = 1$$

$$\Pr[+|\theta_i \geq \underline{\theta}] = \frac{1 - F(\theta)}{1 - F(\underline{\theta})}$$

These are stated on the assumption that $\theta > \underline{\theta}$. This is a reasonable assumption. For instance, for Covid-19, $\underline{\theta}$ is often considered to be close 0. Under this assumption, if a patient is not infected, then they test negative for sure and so the specificity of the test is 100 percent. However, sensitivity is less than 100 percent because a negative test does not imply that the individual is negative. Note that specificity collapses to 1 as $\theta \to \underline{\theta}$ because $F(\theta) \to F(\underline{\theta})$.

What does the treatment decision look like with a test of θ? If the test is positive, the probability that you are positive is 1. If the test is negative, the probability that you are positive is:

$$\Pr[\theta_i \geq \underline{\theta}|s_i = -] = \frac{F(\theta) - F(\underline{\theta})}{F(\theta)}$$

and the probability that you are negative is:

$$\Pr[\theta_i < \underline{\theta}|s_i = -] = \frac{F(\underline{\theta})}{F(\theta)}$$

Thus, the DM will decide to not treat rather than treat on the basis of a negative test if:

$$-\Pr[\theta_i \geq \underline{\theta}|s_i = -]c - \Pr[\theta_i < \underline{\theta}|s_i = -]0 \geq -\Pr[\theta_i \geq \underline{\theta}|s_i = -]0 - \Pr[\theta_i < \underline{\theta}|s_i = -]c$$

$$\implies \Pr[\theta_i < \underline{\theta}|s_i = -] \geq \Pr[\theta_i \geq \underline{\theta}|s_i = -] \implies F(\underline{\theta}) \geq \frac{1}{2}F(\theta)$$

Note the critical role of $F(\underline{\theta})$, the pre-probability that someone is not infected, in this decision. The higher is $F(\underline{\theta})$ (i.e., the lower expected prevalence is), the more likely a negative test will trigger a decision not to treat the individual. In other words, with an imperfect diagnosis test, the DM will hold back on treatment somewhat for imperfect tests. This highlights the importance of obtaining more information regarding the likelihood of infection for an individual prior to interpreting test results (e.g., by observing for symptoms or having a recent other test).

What is the overall value of a test, θ, relative to not performing a test? Note, first, that if $F(\underline{\theta}) \leq \frac{1}{2}F(\theta)$, then treatment is a dominant action for the DM and will be chosen regardless of the signal. Thus, the test has no value. If $F(\underline{\theta}) > \frac{1}{2}F(\theta)$, then the treatment action matches the test result. DM's expected payoff prior to administering the test is:

$$(1-F(\theta))0 - F(\theta)\frac{F(\theta)-F(\underline{\theta})}{F(\theta)}c = -(F(\theta)-F(\underline{\theta}))c$$

By contrast, if no test is administered, DM's expected payoff is $\max\{-F(\underline{\theta}), -(1-F(\underline{\theta}))\}c$.

This means that the value of a test, $v(\theta)$, is:

$$v(\theta) = \begin{cases} -(F(\theta)-F(\underline{\theta}))c + (1-F(\underline{\theta}))c & F(\underline{\theta}) > \frac{1}{2} \\ -(F(\theta)-F(\underline{\theta}))c + F(\underline{\theta})c & F(\underline{\theta}) \leq \frac{1}{2} \end{cases}$$

How do these relate to sensitivity? Let $Se(\theta) \equiv \Pr[+|\theta_i \geq \underline{\theta}]$. Then $F(\theta) = 1 - S(\theta)(1-F(\underline{\theta}))$. Substituting this into the value of a test we have:

$$v(\theta) = \begin{cases} Se(\theta)(1-F(\underline{\theta}))c & F(\underline{\theta}) > \frac{1}{2} \\ (Se(\theta)(1-F(\underline{\theta})) - (1-2F(\underline{\theta})))c & F(\underline{\theta}) \leq \frac{1}{2} \end{cases}$$

Thus, a test is of most value if sensitivity, $Se(\theta)$, and prevalence, $1-F(\underline{\theta})$ are both high up to a point where $1-F(\underline{\theta}) > \frac{1}{2}$. Beyond this point, the default action without a test switches to treatment and, thus, the value of a test is reduced.

4.2 Sensitivity of a test for infectiousness

One potential way of controlling the spread of a virus is to test in order to find infectious people and isolate them. While a test for infectiousness will likely look for the similar viral markers as a test for infection, there is evidence that infectiousness is critically dependent on the viral load (Tom and Mina (2020)). Thus, the threshold for whether someone is infectious is higher than that for whether they are infected. This is captured in the assumption that $\bar{\theta} > \underline{\theta}$. Here we examine how this impacts on the measurement of sensitivity and specificity.

The first thing to note is that the pre-test probability that someone is infectious is $1-F(\bar{\theta})$ which is lower than the pre-test probability that someone is infected. For a test of infectiousness, the specificity ($\Pr[-|\theta_i < \bar{\theta}]$) and sensitivity ($\Pr[+|\theta_i \geq \bar{\theta}]$) are:

$$\Pr[-|\theta_i < \bar{\theta}] = \begin{cases} 1 & \theta \geq \bar{\theta} \\ \frac{F(\theta)}{F(\bar{\theta})} & \theta < \bar{\theta} \end{cases}$$

$$\Pr[+|\theta_i \geq \underline{\theta}] = \begin{cases} \frac{1-F(\theta)}{1-F(\bar{\theta})} & \theta \geq \bar{\theta} \\ 1 & \theta < \bar{\theta} \end{cases}$$

This demonstrates something very interesting. The monotonicity of the measures of sensitivity and specificity in θ are contingent on θ being above the threshold for an intervention.

Covid Economics 47, 4 September 2020: 1-16

Covid Economics 47, 4 September 2020: 1-16

While this was arguably a reasonable assumption for testing whether someone was infected with a virus, it is less obvious for whether someone is infectious or not. Indeed, as discussed in the introduction, many of the standard (and, indeed 'gold-standard') tests for Covid-19 were likely to detect the presence of the virus in very small concentrations. By contrast, infectiousness relies on the virus have a high concentration in an individual and, hence, those standard tests will detect the virus at levels well below $\bar{\theta}$; the threshold at which someone is said to be infectious. In this case, the test can return a positive result even where $\theta_i < \bar{\theta}$ generating a false positive with respect to infectiousness. Thus, while a test with $\theta < \bar{\theta}$ has 100 percent sensitivity, as θ falls, the specificity of the test falls implying that a DM would make more errors from false positives – i.e., isolating individuals who should not be isolated and incurring an utility loss of u each time.

Given this, how will the DM use the information from these tests to inform their isolation decision? Let's consider a test with $\theta \geq \bar{\theta}$ first. In this case, a positive test means you are infectious with probability 1. For a negative test,

$$\Pr[\theta_i \geq \bar{\theta} | s_i = -] = \frac{F(\theta) - F(\bar{\theta})}{F(\theta)}$$

$$\Pr[\theta_i < \bar{\theta} | s_i = -] = \frac{F(\bar{\theta})}{F(\theta)}$$

Thus, the DM would choose not to isolate an individual with a negative test if $\frac{F(\theta)-F(\bar{\theta})}{F(\theta)} \leq \frac{u}{C}$. If this condition did not hold, the test would have no value at that time. Given this, if the test has value, DM's expected payoff from administering the test is:

$$(1 - F(\theta))0 + F(\theta)(u - \frac{F(\theta) - F(\bar{\theta})}{F(\theta)}C) = F(\theta)(u - C) + F(\bar{\theta})C$$

If no test is administered, DM's payoff is $\max\{u - (1 - F(\bar{\theta}))C, 0\}$. Thus, the value of a test for infectiousness, $V(\theta)$ is:

$$V(\theta) = \begin{cases} F(\theta)(u - C) + F(\bar{\theta})C - u + (1 - F(\bar{\theta}))C & 1 - F(\bar{\theta}) < \frac{u}{C} \\ F(\theta)(u - C) + F(\bar{\theta})C & 1 - F(\bar{\theta}) \geq \frac{u}{C} \end{cases}$$

We can consider how these relate to sensitivity by letting $\bar{Se}(\theta) \equiv \Pr[+|\theta_i \geq \bar{\theta}]$. Then $F(\theta) = 1 - \bar{Se}(\theta)(1 - F(\bar{\theta}))$. Substituting this into the value of a test we have:

$$V(\theta) = \begin{cases} -\bar{Se}(\theta)(1 - F(\bar{\theta}))(u - C) & 1 - F(\bar{\theta}) < \frac{u}{C} \\ -\bar{Se}(\theta)(1 - F(\bar{\theta}))(u - C) + u - (1 - F(\bar{\theta}))C & 1 - F(\bar{\theta}) \geq \frac{u}{C} \end{cases}$$

This is increasing in $\bar{Se}(\theta)$ by our earlier assumption that $u \leq C$.

Now, consider the case where $\theta < \bar{\theta}$. In this case, a negative test means i is not infectious with probability 1 as sensitivity is equal to 100 percent. For a positive test,

$$\Pr[\theta_i \geq \bar{\theta} | s_i = +] = \frac{1 - F(\bar{\theta})}{1 - F(\theta)}$$

$$\Pr[\theta_i < \bar{\theta} | s_i = +] = \frac{F(\bar{\theta}) - F(\theta)}{1 - F(\theta)}$$

Thus, the DM would choose to isolate an individual with a positive test if $\frac{1-F(\bar{\theta})}{1-F(\theta)} \geq \frac{u}{C}$. If this condition did not hold, the test would have no value. Given this, if the test has value, DM's expected payoff from administering the test is:

$$(1 - F(\theta)) + F(\theta)u = F(\theta)u$$

If no test is administered, DM's payoff is $\max\{u - (1 - F(\bar{\theta}))C, 0\}$.

$$V(\theta) = \begin{cases} F(\theta)u - u + (1 - F(\bar{\theta}))C & 1 - F(\bar{\theta}) < \frac{u}{C} \\ F(\theta)u & 1 - F(\bar{\theta}) \geq \frac{u}{C} \end{cases}$$

We can consider how these relate to specificity by letting $\bar{Sp}(\theta) \equiv \Pr[-|\theta_i < \bar{\theta}]$. Then $F(\theta) = \bar{Sp}(\theta)F(\bar{\theta})$. Substituting this into the value of a test we have:

$$V(\theta) = \begin{cases} \bar{Sp}(\theta)F(\bar{\theta})u - u + (1 - F(\bar{\theta}))C & 1 - F(\bar{\theta}) < \frac{u}{C} \\ \bar{Sp}(\theta)F(\bar{\theta})u & 1 - F(\bar{\theta}) \geq \frac{u}{C} \end{cases}$$

This is increasing in $\bar{Sp}(\theta)$.

4.3 The optimal test for infectiousness

It has been demonstrated above that the value of a test for infection, $v(\theta)$ is decreasing in θ until $\theta = \underline{\theta}$. By contrast, let's examine the impact of θ on a test for infectiousness.

Proposition 1 *$V(\theta)$ is increasing in θ for $\theta < \bar{\theta}$ and decreasing in θ for $\theta > \bar{\theta}$ with a maximum at $\theta = \bar{\theta}$.*

Proof. When $\theta < \bar{\theta}$, $V(\theta) = -(1-F(\theta))u+(1-F(\bar{\theta}))C$ if $1-F(\bar{\theta}) < \frac{u}{C}$ and $F(\theta)u$ otherwise. In each case, $V'(\theta) = f(\theta)u > 0$. When $\theta > \bar{\theta}$, $-(1 - F(\theta))(u - C)$ if $1 - F(\bar{\theta}) < \frac{u}{C}$ and $F(\theta)(u - C) + F(\bar{\theta})C$ otherwise. In each case, $V'(\theta) = f(\theta)(u - C) < 0$. ■

Covid Economics 47, 4 September 2020: 1-16

Covid Economics 47, 4 September 2020: 1-16

Figure 2: **Value of Tests for Infectiousness**

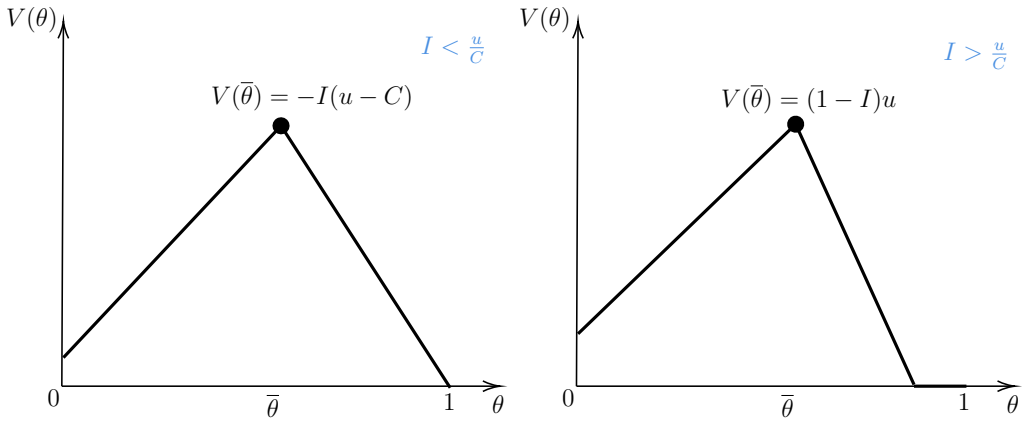

Figure 2 plots $V(\theta)$ is a function of θ for the cases where, the current share of infectious agents, $I \equiv 1 - F(\bar{\theta}) < (>)\frac{u}{C}$. Because $F(0) > 0$, each starts at a positive value at $\theta = 0$, rises until $\theta = \bar{\theta}$ and falls thereafter.

This is the main result of the paper. When tests are scored on the basis of sensitivity with regard to infection (for the purposes of a treatment decision), these favour tests with a lower θ. However, when these tests are below $\bar{\theta}$, the threshold for infectiousness, requiring a lower θ *reduces* the value of those tests. This result arises even though we have not taken into account the cost of tests, where a test cost is likely to be higher the lower is θ, nor their frequency. In other words, scoring tests for infectiousness on the basis of sensitivity of tests for infection, leads to *less* informative tests for infectiousness and hence, would end up isolating too many individuals. This would be economically wasteful.

5 Pre-infectiousness

The above analysis assumes that when $\theta_i < \bar{\theta}$, the optimal decision is to not isolate i. For a virus like SARS-CoV2, the viral load only rises above $\bar{\theta}$, if at all, after three or so days from the point the individual becomes infected. Unless tests are being conducted very frequently – of the order of every 1-2 days around the time a person becomes infected – it would also be optimal to isolate someone with a low viral load who has just been infected. Thus, examining whether $\theta_i \geq \bar{\theta}$ or not is insufficient to obtain the optimal decision.

While frequent testing can overcome this difficulty, here I want to note how to adjust the sensitivity of a test for infectiousness to take this into account. Figure 3 shows a typical path

Covid Economics 47, 4 September 2020: 1-16

for the viral load and compares a (perfect) PCR test for infection (i.e., $\theta = \underline{\theta}$) with a (perfect) Antigen test for infectiousness (i.e., $\theta = \bar{\theta}$). In this figure, the optimal decision is to isolate the patient from period t_0 to t_3. If $1-F(0)$ is the probability that an individual carries some amount of the virus, then the probability that they test negative for an antigen test with a threshold of $\bar{\theta}$ is $\frac{F(\bar{\theta})}{1-F(0)}$ which is a false result with probability $\frac{t_2-t_0}{T-t_0-(t_3-t_2)}$. By contrast, a negative PCR test, which happens with probability $\frac{F(\underline{\theta})}{1-F(0)}$ is false for infectiousness with probability $\frac{t_1-t_0}{T-t_0-(t_3-t_2)}$.

Given this, the specificity and sensitivity of the PCR test for infectiousness is:

$$\Pr[-|\theta_i < \bar{\theta}, \{0 < \theta_i, t \in [t_2, T]\}] = \frac{F(\underline{\theta})}{F(0) + \frac{T-t_3}{T-t_0-(t_3-t_2)}(F(\bar{\theta}) - F(0))}$$

$$\Pr[+|\theta_i \geq \bar{\theta}, \{\theta_i > 0, t \in [t_0, t_2]\}] = \frac{1 - F(\bar{\theta}) + \frac{t_2-t_1}{t_4-t_1-(t_3-t_2)}(F(\bar{\theta}) - F(\underline{\theta}))}{1 - F(\bar{\theta}) + \frac{t_2-t_0}{T-t_0-(t_3-t_2)}(F(\bar{\theta}) - F(0))}$$

The difference between these measures and those provided earlier arises due to the recognition of potential infectiousness between t_0 and t_2. When this gap disappears, these measures converge to the earlier ones for the case where $\theta = \underline{\theta} < \bar{\theta}$.

For the antigen test, the specificity and sensitivity for infectiousness become:

$$\Pr[-|\theta_i < \bar{\theta}, \{0 < \theta_i, t \in [t_2, T]\}] = \frac{F(\bar{\theta})}{F(0) + \frac{T-t_3}{T-t_0-(t_3-t_2)}(F(\bar{\theta}) - F(0))}$$

Figure 3: **Sensitivity with Pre-Infectiousness**

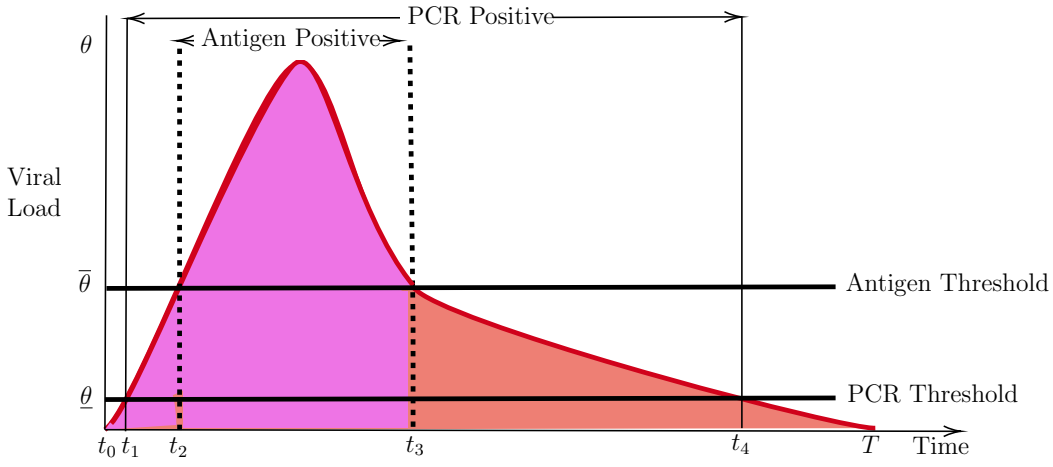

$$\Pr[+|\theta_i \geq \bar{\theta}, \{\theta_i > 0, t \in [t_0, t_2]\}] = \frac{1 - F(\bar{\theta})}{1 - F(\bar{\theta}) + \frac{t_2 - t_0}{T - t_0 - (t_3 - t_2)}(F(\bar{\theta}) - F(0))}$$

Comparing this with the measures for the PCR test, the antigen test still has higher specificity but the ranking on sensitivity becomes less clear cut. The PCR test risks false positives, as they did before, of people who have already been infectious but are still infected but picks up, in a way that the antigen test does not, the pre-infectious but infected individuals (that is, $\frac{t_2 - t_1}{t_4 - t_1 - (t_3 - t_2)}(F(\bar{\theta}) - F(\underline{\theta}))$). In particular, the antigen test, even with $\theta = \bar{\theta}$, is less than 100 percent sensitive because of the presence of pre-infectious individuals.

This adjustment does not alter the broad conclusion of Proposition 1 that a test for infectiousness should not require a threshold θ to be as low as possible. It does suggest that the optimal test may involve $\theta \in (\underline{\theta}, \bar{\theta})$. These analyses presume that an infected individual receives at most one test while they are infected. Of course, if the tests were conducted more frequently (something possible with cheaper antigen tests that have immediate results), then the information they provided together could be used to form a clearer picture of where in the viral life-cycle an infected individual was.

6 Conclusion

This paper has examined the consequences of choosing a test scoring method that does not match the decision being taken. If sensitivity standards for test of SARS-CoV-2 infection are used to score tests for infectiousness, the value of tests in informing an isolation decision is reduced. Insisting on treatment sensitivity requirements leads to more false positives in the isolation decision; that is, individuals are isolated even though they are not infectious. This similarly leads to other costs not modelled here. The decision to release someone from isolation is usually predicated on a negative test which, if made on the basis of infection, would cause people to be isolated for too long. Indeed, they are even safer given that they have previously been infectious. In contact tracing, a positive PCR test is used to inform a costly exercise in tracking down contacts and isolating them. It is likely that most of those efforts are wasted unless those decisions are informed by a test more suited for infectiousness or, alternatively, using the viral load (or Ct) information in the PCR test. Currently, that information is not collected or reported.

Covid Economics 47, 4 September 2020: 1-16

References

Acemoglu, D., Makhdoumi, A., Malekian, A., and Ozdaglar, A. (2020). Testing, voluntary social distancing and the spread of an infection. Technical report, National Bureau of Economic Research.

Bergstrom, T., Bergstrom, C. T., and Li, H. (2020). Frequency and accuracy in proactive testing for covid-19. mimeo, UC Santa Barbara.

Blackwell, D. (1953). Equivalent comparisons of experiments. *The annals of mathematical statistics*, pages 265–272.

Deb, R., Pai, M., Vohra, A., and Vohra, R. (2020). Testing alone is insufficient. *Available at SSRN 3593974*.

Döhla, M., Boesecke, C., Schulte, B., Diegmann, C., Sib, E., Richter, E., Eschbach-Bludau, M., Aldabbagh, S., Marx, B., Eis-Hübinger, A.-M., et al. (2020). Rapid point-of-care testing for sars-cov-2 in a community screening setting shows low sensitivity. *Public health*.

Eichenbaum, M., Rebelo, S., and Trabandt, M. (2020). The macroeconomics of testing during epidemics. mimeo, Rochester.

Ely, J., Galeotti, A., and Steiner, J. (2020). Optimal test allocation. Technical report, Mimeo.

Galeotti, A., Steiner, J., and Surico, P. (2020). Merit of test: Perspective of information economics.

Gans, J. S. (2020). The economic consequences of r= 1: Towards a workable behavioural epidemiological model of pandemics. Technical report, National Bureau of Economic Research.

Kasy, M. and Teytelboym, A. (2020). Adaptive targeted infectious disease testing. *Oxford Review of Economic Policy*.

Larremore, D. B., Wilder, B., Lester, E., Shehata, S., Burke, J. M., Hay, J. A., Tambe, M., Mina, M. J., and Parker, R. (2020). Test sensitivity is secondary to frequency and turnaround time for covid-19 surveillance. *MedRxiv*.

Paltiel, A. D., Zheng, A., and Walensky, R. P. (2020). Assessment of sars-cov-2 screening strategies to permit the safe reopening of college campuses in the united states. *JAMA network open*, 3(7):e2016818–e2016818.

Taylor, C. (2020). Information and risky behavior: Model and policy implications for covid-19. mimeo, Stanford.

Tom, M. R. and Mina, M. J. (2020). To interpret the sars-cov-2 test, consider the cycle threshold value. *Clinical Infectious Diseases*.

Yerushalmy, J. (1947). Statistical problems in assessing methods of medical diagnosis, with special reference to x-ray techniques. *Public Health Reports (1896-1970)*, pages 1432–1449.

Covid Economics 47, 4 September 2020: 1-16

Covid Economics Issue 47, 4 September 2020

Asset pricing during pandemic lockdown[1]

Yuta Saito[2] and Jun Sakamoto[3]

Date submitted: 29 August 2020; Date accepted: 31 August 2020

This paper examines the implications of lockdown policies for asset prices using a susceptible-infected-recovered model with microeconomic foundations of individual economic behaviours. In our model, lockdown policies reduce (i) labour income by decreasing working hours and (ii) precautionary savings by decreasing susceptible agents' probability of getting infected in the future. We qualitatively show that strengthening lockdown measures negatively impacts asset prices at the time of implementation. Our empirical analysis using data from advanced countries supports this finding. Depending on parameter values, our numerical analysis displays a V-shaped recovery of asset prices and an L-shaped recession of consumption. The rapid recovery of asset prices occurs only if the lockdown policies are insufficiently stringent to reduce the number of new periodic cases. This finding implies the possibility that lenient lockdowns have contributed to rapid stock market recovery at the beginning of the COVID-19 pandemic.

Covid Economics 47, 4 September 2020: 17-34

1 Saito acknowledges financial support from Grant-in-Aid for Scientific Research (Start-up) from the Ministry of Education, Culture, Sports, Science and Technology of Japan No. 19K23239 . Sakamoto acknowledges financial support from Grant-in-Aid for Scientific Research (Start-up) from the Ministry of Education, Culture, Sports, Science and Technology of Japan No. 19K23212 . Any remaining errors are our own.

2 Assistant Professor, Faculty of Economics, Kobe International University.
3 Assistant Professor, Faculty of Economics, Kobe International University.

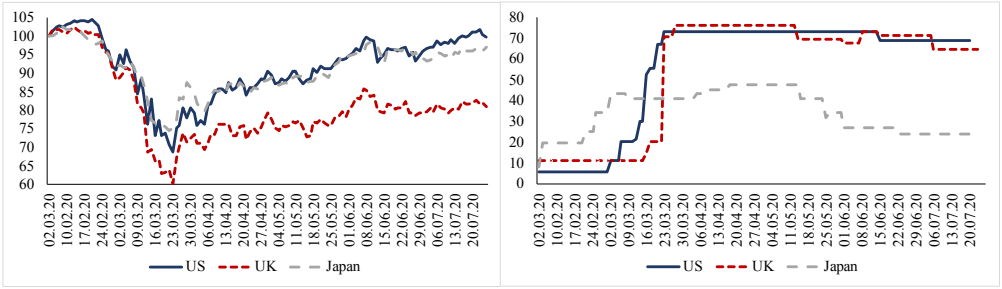

(a) Stock Price (b) Lockdown Stringency

Figure 1: Stock Price and Lockdown Stringency

Note: The data on stock prices are obtained from the MSCI World Index. Figure (b) plots the government stringency index, provided by the Oxford COVID-19 Government Response Tracker (OxCGRT), which ranges from 0 to 100, recording wide range of government's responses to the pandemic.

Covid Economics 47, 4 September 2020: 17-34

1 Introduction

The COVID-19 pandemic has been plunging the global economy into a severe recession.[1] By contrast, stock markets have been recovering amidst strict lockdown restrictions. (see Figure 1). To decipher the causes of the divergence between the two markets, this paper develops a framework to provide primary economic implications of lockdown policies for asset prices.

We consider a consumption-based economy à la Lucas (1978) combined with Kermack and McKendrick' (1927) s susceptible-infected-recovered (SIR) model. The population is divided into susceptible, infected and recovered agents. Susceptible agents receive a time endowment, which is inelastically supplied to the labour market. The length of their working hours affects their probability of getting infected in the next period. Recovered agents are immune to the virus and inelastically supply their time endowments. To eliminate transmission of the virus, the government (or social planner) can reduce a fraction of time endowments. We refer to this government restriction as lockdown.

Our qualitative analysis shows that the impacts of lockdown restrictions on asset prices are twofold. First, lockdowns decrease labour income (and hence consumption) at the period of its implementation. If a lockdown is immediately implemented at the current period, then it decreases current consumption, asset accumulation and asset prices. In contrast, a future lockdown allows agents to expect a reduction in their future labour income. Thus a future lockdown increases asset accumulation and asset prices at the period of implementation. Second, lockdowns decrease susceptible agents' future risks of infection and their precau-

[1]According to the World Bank forecasts, for instance, economic activities of advanced and developing economies in 2020 are expected to decrease by 7% and 2.5%, respectively.

Covid Economics 47, 4 September 2020: 17-34

tionary saving motives toward the risk of losing future labour income. This effect decreases asset demand and prices at the period of implementation.

Our numerical experiments examine the impact of different lockdown schedules on asset price dynamics. We show that a stringent lockdown schedule negatively impacts stock prices. The finding is consistent with our empirical analysis of data from advanced countries during the COVID-19 pandemic. We also show that an L-shaped consumption trajectory associated with a V-shaped asset price trajectory across periods. The V-shaped recovery of asset markets happens only if the number of new cases increases due to the insufficiently strict lockdowns. In cases where lockdowns are sufficiently strict and can reduce new periodic cases, by contrast, introducing lockdowns only flattens the declining asset price slope. The finding implies the possibility that lenient lockdowns have contributed to the stock market recovery at the beginning of the COVID-19 pandemic.

We also study the effects of an exogenous increase in cash handouts to agents on asset prices. Unlike lockdowns, cash handouts do not influence the spread of infection and only increase agents' disposable income at the period of lockdown. Thus cash handouts enhance current asset prices if they are implemented at the current period. By contrast, future cash transfers negatively affect present asset prices by dis-incentivising asset accumulation.

Several studies have theoretically investigated asset pricing during pandemics. Rietz (1988), Barro (2006), and Barro (2009) study the effects of existing risk of rare disasters on asset markets. Toda (2020) numerically studies the effect of the COVID-19 pandemic on a production-based asset pricing model and shows negative relationship between stock prices and the number of infected agents.[2] Caballero and Simsek (2020) analyses the impact of central banks' asset purchases on asset markets during a pandemic. Detemple (2020) studies a production-based asset pricing model and shows that stock prices and interest rates behave cyclically during a pandemic. Compared with the studies above, current study focuses on lockdown policies and provides qualitative results that deliver intuitive implications to assess asset markets during a pandemic.

This paper is also related with the growing literature on empirical studies of financial markets during the COVID-19 pandemic. The list of the literature includes Al-Awadhi et al. (2020), Akhtaruzzaman et al. (2020), Ashraf (2020), Baker et al. (2020), Giglio et al. (2020), Pagano et al. (2020), Sharif et al. (2020) and Zhang et al. (2020). Notably, Baker et al. (2020) argue that stock market volatility during the COVID-19 pandemic is largely the consequence of governments' responses–such as lockdowns, business shutdown, and direct cash transfers.

Finally, this paper contributes to the emerging debate on the macroeconomic impacts of a pandemic. Using macroeconomic-SIR models, numerous studies have investigated the

[2] Toda (2020) also estimates the model and investigates the optimal mitigation policy.

Covid Economics 47, 4 September 2020: 17-34

economic consequences of pandemic shocks and their implications for welfare and policy-making. An incomplete list of those studies includes Acemoglu et al. (2020), Albanesi et al. (2020), Alon et al. (2020), Alvarez et al. (2020), Atkeson (2020), Bodenstein et al. (2020), Eichenbaum et al. (2020), Ferguson et al. (2020), Fernández-Villaverde and Jones (2020), Glover et al. (2020), Jones et al. (2020), Kaplan et al. (2020), Krueger et al. (2020) and Toxvaerd (2020).

The rest of the paper is organised as follows. Section 2 shows how our model illustrates lockdown and economic activities during a pandemic. Section 3 qualitatively and qualitatively studies how pandemic policies affect the asset prices, provides supporting evidence on our theoretical predictions, and discuss intuitions. Lately, Section 4 concludes the paper by discussing the limitations of our analysis.

2 Model

This section illustrates our modelling of a pandemic and describes the individual economic behaviours and conditions satisfied in equilibrium.

2.1 Pandemic and Lockdown

We consider a version of the SIR epidemic model where economic behaviour and public policies affect the spread of a disease. Times are discrete: $t = 0, 1, 2, \ldots$. In each period t, total population N_t is divided into three groups, namely, susceptible S_t, infected I_t, and recovered agents R_t. Hence it holds that:

$$N_t = S_t + I_t + R_t \tag{1}$$

where $N_t = 1$ is assumed for all t. Susceptible agents are those who have never been infected and have not had immunity to the virus. Infected agents are those who have been infected before and not recovered at the present period. They will recover in the next period with probability $\gamma > 0$ and will continuously be ill in the next period with probability $1 - \gamma$. When the infected agents meet the susceptible agents, they transmit the virus at a rate of $\delta > 0$. Recovered agents are those who had been previously infected but have recovered from the disease. We suppose they are immune to the virus. We specify the law of motion of S_t, I_t and R_t are given by the following respectively:

$$S_{t+1} = (1 - \delta L_t^S I_t) S_t, \tag{2}$$

Covid Economics 47, 4 September 2020: 17-34

$$I_{t+1} = (1 + \delta S_t L_t^S - \gamma) I_t, \tag{3}$$

$$R_{t+1} = R_t + \gamma I_t. \tag{4}$$

L_t^S captures susceptible agents' degree of participation in labour activities compared with the days before the outbreak. If $L_t^S = 1$, then people work similarly to before the outbreak, whereas if $L_t^S = 0$, then they do not work at all. Note that Eqs. 2–4 coincide with the standard SIR model if $L_t^S = 1$ for all t.

Throughout the paper, we suppose that $S_1, I_1 > 0$ and L_t^S is an exogenous working time endowment that depends on the stringency of the lockdown policy at the period. Let $\epsilon_t \in [0, 1]$ represent the stringency of lockdown at t, and time endowments are given by:

$$L_t^i = \begin{cases} 1 - \epsilon_t & if\ i \in \{S, R\}, \\ 0 & otherwise. \end{cases} \tag{5}$$

Here lockdowns are supposed to reduce the transmissions of infections by decreasing agents' working hours. Note that (because they are ill) recovered agents do not receive any time endowment irrespective of stringency of the lockdown. The next property shows a necessary condition of lockdowns to decrease the number of cases in the next period.

Proposition 1.

The number of infected agents at $t+1$ decreases if the lockdown at t satisfies:

$$\epsilon_t > \underline{\epsilon_t}(S_t|\delta, \gamma), \tag{6}$$

where $\underline{\epsilon_t}(S_t|\delta, \gamma) \coloneqq 1 - \frac{\gamma}{\delta S_t}$. A higher value of $\underline{\epsilon_t}(S_t|\delta, \gamma)$ implies that a stricter lockdown is required to reduce the number of infected agents, and vice versa. The value of $\underline{\epsilon_t}(S_t|\delta, \gamma)$ is higher in an economy with (i) a small γ, implying high-quality medical care, (ii) a large δ, implying high public hygiene, and (iii) a large S_t, implying a large population susceptible individuals who may get infected in the future. Note that for all S_t, δ and γ, we have $\underline{\epsilon_t}(S_t|\delta, \gamma) < 1$. This condition implies that the number of new cases can be decreased without imposing complete business shutdown (i.e., $\epsilon_t = 1$).

2.2 Economy

The economy is based on Lucas (1978). Each period t there are k_t of identical infinitely-lived trees, which are the only assets existing in the economy. Each tree generates dividend d_t

Covid Economics 47, 4 September 2020: 17-34

that cannot be stored. We suppose that each tree's dividend stream is i.i.d., and given by:

$$d_t = \begin{cases} d^H & w.p.\ \pi \\ d^L & w.p.\ 1-\pi \end{cases} \tag{7}$$

where $\pi \in [0,1]$ and $d^H > d^L$. Agents in state $\theta_t \in \{S, I, R\}$ at t face the following budget constraint:

$$c_t(\theta_t) + p_t k_{t+1}(\theta_t) = w_t L_t(\theta_t) + (p_t + d_t)k_t(\theta_{t-1}) + b_t. \tag{8}$$

where w_t is the wage rate, c_t is the amount of consumption, b_t is the monetary endowment and p_t is the market price of a tree.

Susceptible and infected agents are uncertain about their future states. In contrast, recovered agents are certain about their future state (they know they are immune to the virus). Let $q_{t+1}^{\theta_{t+1}|\theta_t}$ denote the probability of an agent in state θ_t at t will become in state θ_{t+1} at $t+1$. Then Eqs. 2–4 imply $q_{t+1}^{S|S} = 1-\delta L_t I_t$, $q_{t+1}^{I|S} = \delta L_t I_t$, $q_{t+1}^{R|S} = 0$, $q_{t+1}^{S|I} = 0$, $q_{t+1}^{I|I} = 1-\gamma$, $q_{t+1}^{R|I} = \gamma$, $q_{t+1}^{S|R} = 0$ and $q_{t+1}^{I|R} = 0$.

Agents at t evaluate the intertemporal utility as follows:

$$\mathbb{E}_t \left[\sum_{\omega=0}^{\infty} \beta^{\omega} \left[u(c_{t+\omega}(\theta_{t+\omega})) \right] \right] \tag{9}$$

where $\beta \in (0,1)$ is their discount factor and $\mathbb{E}_t$ is the expectation operator at t. The instant utility u is assumed to be strictly increasing, concave and twice continuously differentiable.

Each agent i maximises the intertemporal utility 9 subject to the budget constraint 8. By arranging the first-order conditions, we obtain the following Euler equation:

$$u'(c_t(\theta_t)) = \beta \mathbb{E}_t \left[u'(c_{t+1}(\theta_{t+1})) \left(\frac{p_{t+1} + d_{t+1}}{p_t} \right) \right]. \tag{10}$$

In equilibrium, aggregate dividend is all consumed and asset market clears. Thus we have $S_t c_t^S + I_t c_t^I + R_t c_t^R = d_t K_t$, and $S_t k_t^S + I_t k_t^I + R_t k_t^R = K_t$.

3 Analysis

This section discusses the results and the implications of our analyses.

Assumption 1. $S_t \approx N_t$

This assumption can be interpreted as the pandemic is in an early stage when only a marginal fraction of population is infected. We consider this assumption as reasonable to analyse the early impacts of the COVID-19 pandemic lockdowns when the cumulative confirmed cases are relatively small—for instance, as of June 10, 2020, the number of cumulative confirmed cases divided by the total population is 0.0006% in China, 0.2219% in Germany, 0.3842% in Italy, 0.0138% in Japan, 0.0230% in South Korea, 0.5091% in Spain, 0.5803% in the US and 0.4076 in the UK.[3]

Proposition 2.

Suppose Assumption 1. Then

$$p_t \approx \tilde{p}_t = \frac{1}{u'(c_t^S)} \mathbb{E}_t [m] \tag{11}$$

where

$$m \coloneqq \beta \left(\sum_{\theta_{t+1} \in \{S,I\}} q_{t+1}^{\theta_{t+1}|S} u'(c_{t+1}(\theta_{t+1})) \right) d_{t+1} + \beta^2 \left(\sum_{\theta_{t+1} \in \{S,I\}} q_{t+1}^{\theta_{t+1}|S} \sum_{\theta_{t+2} \in \{S,I,R\}} q_{t+2}^{\theta_{t+2}|\theta_{t+1}} u'(c_{t+2}(\theta_{t+2})) \right) d_{t+2} + \cdots$$

The asset price at t is determined by the present discounted value of the stream of future endowments. The probabilities and consumption are influenced by the policies implemented by the government. The next section studies the effect of lockdown on the asset price at t.

3.1 Qualitative Analysis and Supporting Evidence

3.1.1 Qualitative Analysis

Corollary 1. (Impact of Lockdown on Asset Prices)

Suppose ϵ_t satisfies the condition 6 for all t. Then

$$\frac{d\tilde{p}_t}{d\epsilon_t} = \underbrace{\overbrace{\frac{d\tilde{p}_t}{dc_t^S}}^{+} \overbrace{\frac{dc_t^S}{d\epsilon_t}}^{-} \overbrace{\mathbb{E}_t [m]}^{+}}_{-} + \underbrace{\overbrace{\frac{1}{u'(c_t^S)}}^{+} \overbrace{\mathbb{E}_t \left[\frac{dm}{d\epsilon_t} \right]}^{-}}_{-} < 0 \tag{12}$$

[3]The data are obtained from Our World in Data, whose original source is published by the European CDC.

$$\frac{d\tilde{p}_t}{d\epsilon_{t+\omega}} = \underbrace{\overbrace{\frac{d\tilde{p}_t}{dc^S_{t+\omega}}}^{-}\overbrace{\frac{dc^S_{t+\omega}}{d\epsilon_{t+\omega}}}^{-}\overbrace{\mathbb{E}_t\left[m\right]}^{+}}_{+} + \underbrace{\overbrace{\frac{1}{u'(c^S_t)}}^{+}\overbrace{\mathbb{E}_t\left[\frac{dm}{d\epsilon_{t+\omega}}\right]}^{-}}_{-} \gtreqless 0,\ \forall \omega \in \mathbb{N}_+ \tag{13}$$

Proof.

$u'(c_t) > 0$ implies $\frac{d\tilde{p}_t}{dc_t} > 0$ and $\frac{d\tilde{p}_{t+s}}{dc_{t+s}} < 0$ for all $s \in \mathbb{N}_+$. Since $\frac{dc^S_t}{d\epsilon_t} = -w < 0$, we have $\frac{d\tilde{p}_t}{dc^S_t}\frac{dc^S_t}{d\epsilon_t} < 0$ and $\frac{d\tilde{p}_t}{dc^S_{t+s}}\frac{dc^S_{t+s}}{d\epsilon_{t+s}} > 0$ for all $s \in \mathbb{N}_+$. Note that

$$\frac{dm}{d\epsilon_t} = \beta\left(\sum_{\theta_{t+1}\in\{S,I\}} \frac{dq^{\theta_{t+1}|S}_{t+1}}{d\epsilon_t} u'(c^j_{t+1})\right) d_{t+1} + \beta^2\left(q^{S|S}_{t+1}\sum_{\theta_{t+2}\in\{S,I\}} \frac{dq^{\theta_{t+2}|S}_{t+2}}{d\epsilon_t} u'(c^j_{t+2})\right) d_{t+2} + \cdots.$$

By the definitions of $q^{S|S}_{t+1}$, $q^{I|S}_{t+1}$ and $L_t = 1 - \epsilon_t$, we have $\frac{dq^{S|S}_{t+1}}{d\epsilon_t} = \delta I_{t+1} > 0$ and $\frac{dq^{I|S}_{t+1}}{d\epsilon_t} = -\delta I_{t+\omega} < 0$. For all $\omega > 1$, if condition (6) is satisfied, then we have $\frac{dI_{t+\omega-1}}{d\epsilon_t} < 0$. Hence by the definitions of $q^{S|S}_{t+\omega}$ and $q^{I|S}_{t+\omega}$, we have

$$\frac{dq^{S|S}_{t+\omega}}{d\epsilon_t} = -\delta\left(\frac{dI_{t+\omega-1}}{d\epsilon_t} L^S_{t+\omega-1}\right) > 0,$$

$$\frac{dq^{I|S}_{t+\omega}}{d\epsilon_t} = \delta\left(\frac{dI_{t+\omega-1}}{d\epsilon_t} L^S_{t+\omega-1}\right) < 0,$$

for all $\omega > 1$. Since $u'(c_t) > 0$, $u''(c_t) < 0$, and $c^S_{t+\omega} > c^I_{t+\omega}$ imply $u'(c^S_{t+\omega}) - u'(c^I_{t+\omega}) < 0$, we have

$$\sum_{\theta_{t+\omega}\in S,I} u'(c^S_{t+\omega})\frac{dq^{\theta_{t+\omega}|S}_{t+\omega}}{d\epsilon_t} = \frac{dq^{S|S}_{t+\omega}}{d\epsilon_t}\left(u'(c^S_{t+\omega}) - u'(c^I_{t+\omega})\right) < 0$$

for all t and $\omega \geq 0$. Hence $\frac{d\Delta}{d\epsilon_t} < 0$ and the results immediately follow.□

The results show how different lockdown schedule causes different impacts on asset prices. Strengthening current-period lockdown decreases asset price at the time, whereas while the impacts of strengthening future-periods lockdowns are unclear. An increase in lockdown stringency affects the asset price at t, regardless of the timing of implementation, by decreasing (i) consumption and (ii) future probabilities of getting the virus.

The first terms in the right-hand-sides of Eqs. 12–13 represent the economic impacts of strengthening lockdown measures on consumption. A stricter lockdown decreases working hours, asset demand and its price at the period of implementation. If the government com-

Covid Economics 47, 4 September 2020: 17-34

Covid Economics 47, 4 September 2020: 17-34

mits to a stricter lockdown in the future, then individuals expect a reduction in future labour endowment. To prepare for that, individuals demand additional assets. This behaviour hikes present asset prices.

The second terms in the right-hand-sides of Eqs. 12–13 illustrate the effects of strengthening lockdown measures on the spread of infection. A stricter lockdown decreases susceptible agents' future risks of infection and precautionary saving motives towards the risk of losing working hours. As a result, asset demand and its present prices decrease.

These analyses raise the following questions. First an introduction of lockdown induces individuals to expect that it will continue for several periods. This situation means that the effects of Eqs.12–13 arise at the same time and present asset prices depend on the entire lockdown schedule. In Section 3-2, we numerically deal with this issue by supposing that individuals believe a lockdown schedule $\{\epsilon_t, \epsilon_{t+1}, \epsilon_{t+2}, ...\}$ at an initial period t.

Second if the condition 6 is not satisfied, then strengthening lockdown measures does not necessarily reduce the number of infected agents. For instance, consider a scenario where the government does not impose any economic activity restrictions and *herd immunity* is reached at $t = 100$ (i.e. $\epsilon_t = 0$ for all t and $q_{100}^{I|S} = 0$) .Then, strengthening restrictions at period $t = 10$ may reduce new cases at $t = 11$ but may delay the date of achieving herd immunity (i.e., it holds that $q_{100}^{I|S} > 0$ and $\frac{dq_{100}^{I|S}}{d\epsilon_{10}} > 0$, and the sign of 12 is not always negative). Our numerical experiments in Section 3-2 examines scenarios with $\epsilon_t < \underline{\epsilon}$ and how asset prices react to lenient lockdowns.

We now consider the effect of cash handouts to agents on the asset prices. For simplicity, we suppose b_t is an exogenous endowment and do not consider its effect on the government budget constraint.

Corollary 2. (Effect of Cash Handouts on Asset Prices)

$$\frac{d\tilde{p}_t}{db_t} = \underbrace{\overbrace{\frac{d\tilde{p}_t}{dc_t^S}}^{+}\overbrace{\frac{dc_t^S}{db_t}}^{+}\overbrace{\mathbb{E}_t\left[m\right]}^{+}}_{+} > 0 \tag{14}$$

$$\frac{d\tilde{p}_t}{db_{t+\omega}} = \underbrace{\overbrace{\frac{d\tilde{p}_t}{dc_{t+\omega}^S}}^{-}\overbrace{\frac{dc_{t+\omega}^S}{db_{t+\omega}}}^{+}\overbrace{\mathbb{E}_t\left[m\right]}^{+}}_{-} < 0,\ \forall \omega \in \mathbb{N}_+. \tag{15}$$

Table 1: Summary of Data

(a) Summary Statistics

	N	Mean	Std.dev	Min	Max
ΔStringency Index	295	2.944	11.262	-47.220	50.000
ΔEconomic Support Index	57	28.289	25.170	-25.000	100.000
Return	2643	0.000	0.027	-0.186	0.130

(b) Correlation Matrix

	ΔStringency Index	ΔEconomic Support Index	Return
ΔStringency Index	1.000	0.518	-0.295
ΔEconomic Support Index	0.518	1.000	-0.028
Return	-0.295	-0.028	1.000

Note: The indexes of stock returns are obtained from the MSCI World Index. ''Stringency index'' and ''economic support index'' are obtained from OxCGRT.

Proof.

Note that $\frac{dc_t}{db_t} = 1$ *for all* $t \in \mathbb{N}_+$. $\frac{d\tilde{p}_t}{dc_t} > 0$ *implies the first result.* $\frac{d\tilde{p}_t}{dc_{t+s}} < 0 \; \forall s \in \mathbb{N}_+$ *implies the second result.* □

In contrast to lockdowns, cash handouts increase the disposable income and do not affect the spread of infection. An increase in monetary transfer only enhances asset demand and prices at the period. Expected future cash handouts decrease current asset prices by disincentivising asset accumulation.

3.1.2 Supporting Evidence

Using indexes from OxCGRT, this section tests our theoretical prediction that strengthening lockdown measures and decreasing monetary transfers negatively affect asset prices at the time of implementation. Table 1 summarise the data.

Table 2 shows the correlation between each developed country's stock return index and the changes in government responses. ''Government response index'' measures overall government response, including lockdown, testing policy, and economic support. ''Stringency index'' only records the strictness of ''lockdown style'' policies. Δ represents change in the variable from the day before.

Most countries have negative correlations between stock returns and an increase in the stringency of restrictions from the day before. The finding implies that the negative impacts of increasing the stringency of lockdowns (Eq. 12), surpassed the positive impacts on implementing economic supports, such as direct cash handouts (Eq. 14). Stock returns and the change in the number of new cases are also positively correlated. This is consistent with our

Covid Economics 47, 4 September 2020: 17-34

Covid Economics 47, 4 September 2020: 17-34

Table 2: Correlation Between Stock Price and Variable Changes

Countries	ΔGovernment Response Index	ΔStringency Index	Δ New Cases Per Million
Australia	0.133	0.014	0.013
Austria	-0.442	-0.491	0.092
Belgium	-0.361	-0.384	0.075
Canada	-0.572	-0.718	0.186
Denmark	-0.025	0.002	-0.039
Finland	-0.411	-0.465	0.178
France	-0.338	0.047	0.020
Germany	-0.105	-0.124	0.147
Ireland	-0.328	-0.372	0.096
Israel	-0.382	-0.372	0.077
Italy	-0.215	-0.268	0.029
Japan	-0.154	-0.075	0.071
Netherlands	-0.468	-0.617	0.111
New Zealand	-0.143	-0.121	0.141
Norway	-0.182	-0.326	0.060
Portugal	-0.405	-0.327	0.157
Singapore	-0.026	-0.027	0.084
Spain	-0.391	-0.459	0.085
Sweden	-0.109	-0.239	0.065
Switzerland	0.098	0.084	0.113
United Kingdom	-0.021	-0.533	0.122
United States	-0.620	-0.593	0.135

Note: Data on the number of new cases (new cases per million) are obtained from Our World in Data, whose original source is published by the European CDC.

Table 3: Result of Regression

	Model 1	Model 2	Model 3
ΔStringency Index	-0.0006^{***}		-0.0013^{**}
	(0.0002)		(0.0004)
ΔEconomic Support Index		0.0001	0.0002^{**}
		(0.0001)	(0.0001)
R^2	0.8462	0.8662	0.9658
Adj. R^2	0.7681	0.7118	0.8633
Num. Obs.	295	57	21
RMSE	0.0193	0.0251	0.0206

Note: Robust standard errors in parentheses ** and *** represent significance at 5% and 1%, respectively.

Covid Economics 47, 4 September 2020: 17-34

theoretical prediction that an increase in the number of new cases increases the asset prices by incentivising susceptible agents' precautionary saving motives.

We now estimate the effects of strengthening lockdowns and economic supports on market returns using the following model:

$$r_t^i = \lambda_1 \Delta Stringency\ Index_t^i + \lambda_2 \Delta Economic\ Support\ Index_t^i + \eta_t + u_t^i \tag{16}$$

where r_t^i represents the market returns of country i at time t, $\Delta Stringency\ Index_t^i$ represents the difference of the OxCGRT "stringency index" at country i from time $t-1$ to t, and $Economic\ Support\ Index_t^i$ represents the difference of the OxCGRT "economic support index" at country i from time $t-1$ to t.[4]

The results are reported in Table 3. The coefficient on $\Delta Stringency\ Index_t^i$ is negative and strongly significant in Model 1 and Model 3. The result means that increasing the lockdown stringency decreases stock returns at the time. The result is consistent with our theoretical prediction 12. The coefficient on $\Delta Transfer_t^i$ is positive and strongly significant in Model 3, meaning that strengthening economic support hikes stock returns at the time. The result is consistent with our theoretical prediction 14.

3.2 Numerical Experiments

We now demonstrate quantitative studies where a lockdown schedule $\{\epsilon_t, \epsilon_{t+1}, \epsilon_{t+2}, ...\}$ is committed at the beginning of period t. Throughout our numerical analysis, we suppose instant utility from consumption is constant relative risk aversion (CRRA):

$$u(c_t) = \frac{c_t^{1-\sigma}}{1-\sigma}. \tag{17}$$

Table 2 presents the parameter values for our computations. We assume that the annual discount rate is 4%, which means that the daily discount factor is: $\delta = exp(-0.04/365) \approx 0.999$. The infection rate is supposed at $\beta = 0.20$, meaning that the daily increase in active cases would be 20 percent without any lockdown. The parameter γ, the probability that an infected agent recovers in a day, is set to $\gamma = 1/18$, which means that the expected duration of illness is 18 days as Atkeson (2020).

Figures 2 demonstrates the outcomes of our benchmark cases, where lockdown is constant in every period, that is, $\epsilon_t = \epsilon \in \{0.719, 0.721, 0.723\}$ for all t. In the case of $\epsilon = 0.719$ (dotted lines), the committed lockdown schedule sufficiently decreases the population of infected agents across periods (i.e., condition 6 is satisfied for all t). In the case of $\epsilon = 0.721$ (slashed

[4]The market returns are calculated using the data from the MSCI Country Indexes.

Covid Economics 47, 4 September 2020: 17-34

Table 4: Parameter Values

Economic Parameters	SIR Parameters
$\delta = 0.999,\ \rho = 2,\ \pi = 0.7,\ d^H = 0.01,\ d^L = 0.001$	$\beta = 0.20,\ \gamma = 1/18,\ I_0 = 0.0002,\ S_0 = 1 - I_0$

lines), the number of new cases initially increases but decreases later. This trajectory is caused by gradual reductions in S_t and $\underline{\epsilon_t}(S_t|\delta, \gamma)$, which let $\epsilon = 0.721$ to satisfy condition 6. In the case of $\epsilon = 0.723$ (solid lines), lockdowns are lenient and the number of new cases increases across periods (condition 6 is not satisfied for all t).

Asset prices are higher in the cases of lenient lockdowns where susceptible agents face a high probability of infections and have high precautionary saving motives. Thus asset demand and prices are high in those cases. Moreover, asset prices increase across periods in those cases whereas they decrease in the scenarios of severe lockdowns. This behaviour is also caused by the dynamics of the number of infected agents. As new cases increase, susceptible agents have precautionary saving motives, and vice versa.

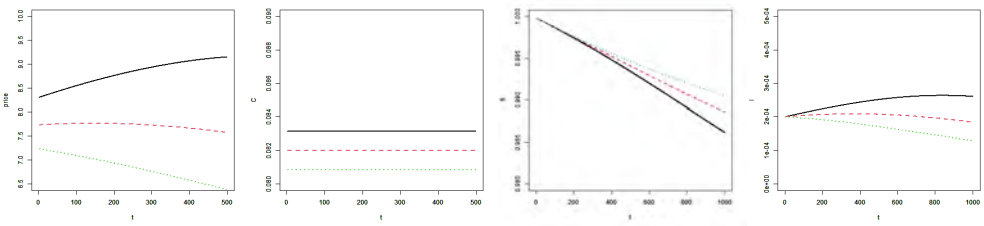

(a) Asset Price (b) Consumption (c) Population of S_t (d) Population of I_t

Figure 2: Constant Lockdowns (The solid-lines suppose $\epsilon = 0.719$, the slashed-lines suppose $\epsilon = 0.721$, and the dotted-lines suppose $\epsilon = 0.723$.)

Figure 3 supposes that lockdown stringency changes across periods. We let $\varepsilon_t = 0$ from $t = 0$ to 50 and $\epsilon_t = \epsilon \in \{0.719, 0.721, 0.723\}$ from $t = 51$. Before implementing lockdowns, prices drastically fall in each case. After implementing lockdowns, asset prices rebound in the lenient case, in which 6 is not satisfied, due to the same mechanism as the lenient constant lockdown scenario in Figure 3. As a result, the asset prices illustrate a V-shaped trajectory, whereas consumption continues to in a low value.

CEPR PRESS

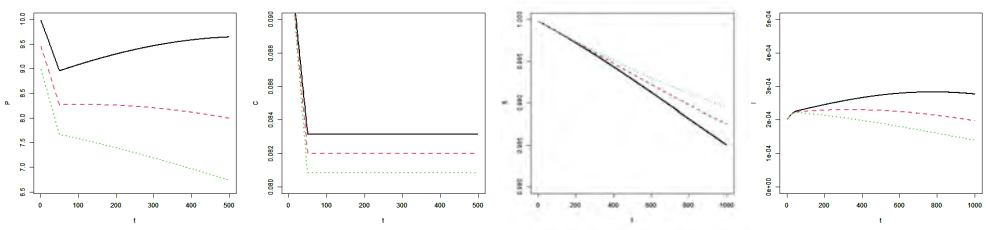

(a) Asset Price (b) Consumption (c) Population of S_t (d) Population of I_t

Figure 3: Time-variant Lockdown (For $t \in [0, 50]$, $\epsilon_t = 0$ for all scenarios. For $t > 50$, the solid lines suppose $\epsilon = 0.719$; the slashed lines suppose $\epsilon = 0.721$; and the dotted lines suppose $\epsilon = 0.723$.)

4 Conclusion

We conclude by discussing the limitations of our study and promising future extensions. First, assumption 1 is inadequate to analyse scenarios where a large fraction of population has been infected. In those cases, an increase in recovered agents' population may reduce asset prices since their asset demand is not high, unlike that of susceptible agents, due to the lack of their precautionary saving motives.

Second, we have not considered the effects of increasing cash handouts on the government budget constraints. In reality, an increase in fiscal expenditure may enable the agents to anticipate future tax hikes. Its effects on economic activities depend on the fiscal resources (e.g., committing an increase in labour income tax rate in the future may incentivise present asset accumulation, whereas committing an increase in future capital income tax rate may dis-incentivise it).

Finally, we have supposed rational expectations, which may be an inadequate assumption in an unprecedented situation. If the public is supposed to be optimistic towards the effects of lockdown on infection control, then asset demand may shrink by reducing the precautionary saving motives. On the contrary, if the individuals are pessimistic, then asset demand may increase.[5]

[5]In a similar context, using investor survey data Giglio et al. (2020) found that investors who were initially pessimistic and optimistic differed in their subsequent portfolio rebalancing.

Covid Economics 47, 4 September 2020: 17-34

Covid Economics 47, 4 September 2020: 17-34

References

Daron Acemoglu, Victor Chernozhukov, Iván Werning, and Michael D Whinston. A multi-risk sir model with optimally targeted lockdown. Technical report, National Bureau of Economic Research, 2020.

Md Akhtaruzzaman, Sabri Boubaker, and Ahmet Sensoy. Financial contagion during covid–19 crisis. *Finance Research Letters*, 101604, 2020.

Abdullah M Al-Awadhi, Khaled Al-Saifi, Ahmad Al-Awadhi, and Salah Alhamadi. Death and contagious infectious diseases: Impact of the covid-19 virus on stock market returns. *Journal of Behavioral and Experimental Finance*, 100326, 2020.

Stefania Albanesi, Rania Gihleb, Jialin Huo, and Jiyeon Kim. Household insurance and the macroeconomic impact of the novel coronavirus. Unpublished Manuscript, University of Pittsburgh, 2020.

Titan M Alon, Matthias Doepke, Jane Olmstead-Rumsey, and Michele Tertilt. The impact of covid-19 on gender equality. *Covid Economics: Vetted and Real Time Papers*, 4, 2020.

Fernando E Alvarez, David Argente, and Francesco Lippi. A simple planning problem for covid-19 lockdown. *Covid Economics: Vetted and Real Time Papers*, 14, 2020.

Badar Nadeem Ashraf. Stock markets' reaction to covid-19: cases or fatalities? *Research in International Business and Finance*, 101249, 2020.

Andrew Atkeson. What will be the economic impact of covid-19 in the us? rough estimates of disease scenarios. Technical report, National Bureau of Economic Research, 2020.

Scott R Baker, Nicholas Bloom, Steven J Davis, and Stephen J Terry. Covid-induced economic uncertainty. Technical report, National Bureau of Economic Research, 2020.

Robert J Barro. Rare disasters and asset markets in the twentieth century. *The Quarterly Journal of Economics*, 121(3):823–866, 2006.

Robert J Barro. Rare disasters, asset prices, and welfare costs. *American Economic Review*, 99(1):243–64, 2009.

Martin Bodenstein, Giancarlo Corsetti, and Luca Guerrieri. Social distancing and supply disruptions in a pandemic. *Covid Economics: Vetted and Real Time Papers*, 19, 2020.

Ricardo J Caballero and Alp Simsek. A model of asset price spirals and aggregate demand amplification of a" covid-19" shock. Technical report, National Bureau of Economic Research, 2020.

Jerome Detemple. Asset prices and pandemics. Available at SSRN 3587432, 2020.

Martin S Eichenbaum, Sergio Rebelo, and Mathias Trabandt. The macroeconomics of epidemics. Technical report, National Bureau of Economic Research, 2020.

Neil Ferguson, Daniel Laydon, Gemma Nedjati Gilani, Natsuko Imai, Kylie Ainslie, Marc Baguelin, Sangeeta Bhatia, Adhiratha Boonyasiri, ZULMA Cucunuba Perez, Gina Cuomo-Dannenburg, et al. Report 9: Impact of non-pharmaceutical interventions (npis) to reduce covid19 mortality and healthcare demand. Technical report, Imperial College, 2020.

Jesús Fernández-Villaverde and Charles I Jones. Estimating and simulating a sird model of covid-19 for many countries, states, and cities. Technical report, National Bureau of Economic Research, 2020.

Stefano Giglio, Matteo Maggiori, Johannes Stroebel, and Stephen Utkus. Inside the mind of a stock market crash. Technical report, National Bureau of Economic Research, 2020.

Andrew Glover, Jonathan Heathcote, Dirk Krueger, and José-Víctor Ríos-Rull. Health versus wealth: On the distributional effects of controlling a pandemic. *Covid Economics: Vetted and Real Time Papers*, (14), 2020.

Callum J Jones, Thomas Philippon, and Venky Venkateswaran. Optimal mitigation policies in a pandemic: Social distancing and working from home. Technical report, National Bureau of Economic Research, 2020.

Greg Kaplan, Benjamin Moll, and Gianluca Violante. Pandemics according to hank. Unpublished Manuscript, 2020.

William Ogilvy Kermack and Anderson G McKendrick. A contribution to the mathematical theory of epidemics. *Proceedings of the royal society of london. Series A, Containing papers of a mathematical and physical character*, 115(772):700–721, 1927.

Dirk Krueger, Harald Uhlig, and Taojun Xie. Macroeconomic dynamics and reallocation in an epidemic. *Covid Economics: Vetted and Real Time Papers*, 5, 2020.

Robert E Lucas. Asset prices in an exchange economy. *Econometrica*, 46(6):1429–1445, 1978.

Covid Economics 47, 4 September 2020: 17-34

Marco Pagano, Christian Wagner, and Josef Zechner. Disaster resilience and asset prices. *Covid Economics: Vetted and Real Time Papers*, 21, 2020.

Thomas A Rietz. The equity risk premium a solution. *Journal of Monetary Economics*, 22 (1):117–131, 1988.

Arshian Sharif, Chaker Aloui, and Larisa Yarovaya. Covid-19 pandemic, oil prices, stock market, geopolitical risk and policy uncertainty nexus in the us economy: Fresh evidence from the wavelet-based approach. *International Review of Financial Analysis*, 101496, 2020.

Alexis Akira Toda. Susceptible-infected-recovered (sir) dynamics of covid-19 and economic impact1. *Covid Economics: Vetted and Real Time Papers*, 43, 2020.

Flavio Toxvaerd. Equilibrium social distancing. *Covid Economics: Vetted and Real Time Papers*, 110, 2020.

Dayong Zhang, Min Hu, and Qiang Ji. Financial markets under the global pandemic of covid-19. *Finance Research Letters*, 101528, 2020.

Covid Economics 47, 4 September 2020: 17-34

Appendix: Sensitivity of Epidemiology Parameters

Since the information on COVID-19 is yet incomplete, there could be misspecification on the parameters. In Figure 4, we investigate the effect of changing the parameters on the virus's characteristics on our results. Figure 4 shows both a greater δ and a smaller γ lead to higher asset prices. In a nutshell, both effects increase the number of infected agents per period: increasing δ directly increases the probability of getting the virus; decreasing γ increases the average periods of an infected agent staying at the state. Also, the impacts of decreasing γ (increasing δ) on asset prices are greater in the cases of a higher δ (lower γ). In the severer lockdown case ($\epsilon_t = 0.723$), however, the effects of changing the SIR parameters on asset prices are relatively small compared to the results of $\epsilon_t = 0.721$. In this case, agents do not interact with each other in the first place, so changing the virus's characteristics does not greatly influence the spread of infections.

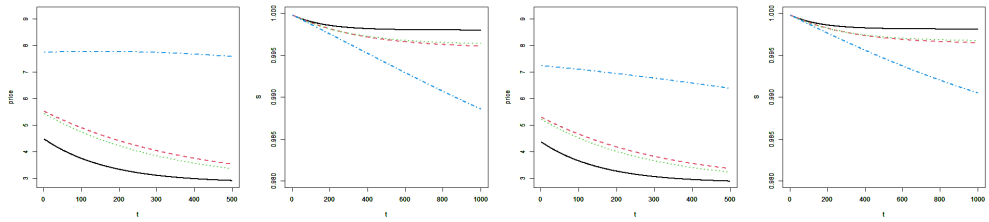

(a) Asset Price ($\epsilon_t = 0.721$ for all t)
(b) Population of S_t ($\epsilon = 0.721$ for all t)
(c) Asset Price ($\epsilon_t = 0.723$ for all t)
(d) Population of S_t ($\epsilon_t = 0.723$ for all t)

Figure 4: Impacts of δ and γ

Note: The solid lines suppose $\{\delta = 0.19, \gamma = 1/17\}$; the dashed lines suppose $\{\delta = 0.19, \gamma = 1/18\}$; the dotted line suppose $\{\delta = 0.20, \gamma = 1/17\}$ and the dotted dashed lines suppose $\{\delta = 0.20, \gamma = 1/18\}$.

Covid Economics 47, 4 September 2020: 17-34

Pandemic shocks and household spending[1]

David Finck[2] and Peter Tillmann[3]

Date submitted: 26 August 2020; Date accepted: 31 August 2020

We study the response of daily household spending to the unexpected component of the COVID-19 pandemic, which we label as pandemic shock. Based on daily forecasts of the number of fatalities, we construct the surprise component as the difference between the actual and the expected number of deaths. We allow for state-dependent effects of the shock depending on the position on the curve of infections. Spending falls after the shock and is particularly sensitive to the shock when the number of new infections is strongly increasing. If the number of infections grows moderately, the drop in spending is smaller. We also estimate the effect of the shock across income quartiles. In each state, low-income households exhibit a significantly larger drop in consumption than high-income households. Thus, consumption inequality increase after a pandemic shock. Our results hold for the US economy and the key US states. The findings remain unchanged if we choose alternative state-variables to separate regimes.

Covid Economics 47, 4 September 2020: 35-69

1 We thank Carola Binder, Daniel Grabowski, Salah Hassanin, Peter Winker and the team from Opportunity Insights for helpful discussions.
2 PhD student, Justus Liebig University Gießen.
3 Professor of Economics, Justus Liebig University Gießen.

Covid Economics 47, 4 September 2020: 35-69

I Introduction

The global spread of the COVID-19 pandemic since January 2020 led to a sharp contraction of economic activity in almost all economies affected by the virus. Between January and April, real personal consumption expenditures declined by more than 15%. With personal consumption expenditures accounting for 68% of US GDP in 2019, this decline in spending casts shadow on overall economic activity in 2020. Consumption recovered in May and June, partly driven by government transfers which led to an increase in real disposable income.

In this paper, we provide an analysis of the causal effect of the pandemic on household spending. Spending, such as consumption in general, should mostly be driven by unexpected shocks. According to the theory of permanent income, predictable fluctuations in future income should prompt households to tap the capital market and smooth consumption, such that consumption exhibits very little fluctuations.[1] Initially, the spread of the pandemic might be considered unpredictable. After that, and in particular with the beginning of the second wave of infections in June, however, a large part of the development should have been predictable.

We look at the unexpected element of the pandemic and analyze how it affects spending decisions. We draw on forecasts of the number of fatalities due to COVID-19 in the US provided by Gu (2020) and contrast the one day-ahead forecast with the actual number of deaths. A positive forecast error is consistent with an under-prediction of the number of fatalities or a surprise in the severity of the pandemic, respectively. We refer to this series of unexpected deaths as a pandemic shock and use it as the key explanatory variable for household spending.

Our measure of household spending is provided by Chetty et al. (2020) and consists of debit and credit card transactions in the US. The key advantage of the data is timeliness. We can track spending on a daily frequency for the entire US economy as well as for US states. In a series of local projections, see Jordà (2005), we estimate the response of spending to a pandemic shock.

There are at least three channels through which a pandemic shock can affect spending. First, an adverse pandemic shock could prompt households to restrain consumption voluntarily. This is because the virus spreads through

[1] See Jappelli and Pistaferri (2010) for a survey of the field.

social interaction such as shopping in retail stores, dining or entertainment. Anxious households could reduce these activities even before official lockdown measures are in place.[2] Second, households might be barred from consumption due to a lockdown of selected activities or even shelter-in-place orders. An adverse pandemic shock makes these measures more likely. Third, households could perceive an unexpected change in future income and adjust their spending accordingly. Even if a household is not itself affected by the virus, the future of entire industries is at risk. Workers in the service sector, for example, cannot resort to working from home and experience a large drop in future income.[3]

While we cannot disentangle these transmission channels, we take account of an important property that all three channels have in common: the effect of a pandemic shock should be stronger if the virus spreads more rapidly. The more widespread the virus is, the larger the reluctance to shop offline, the more likely stricter lockdown measures and the more severe the drop in future income will be. Thus, the effect of the pandemic shock should depend on the position of the economy on the infection curve.

Therefore, we generalize our model and allow the pandemic shock to have regime-dependent effects. In our baseline setting, we chose the growth of the daily number of new infections as our state variable. This figure is omnipresent, especially in the media, and provides information on where the economy stands on the infection curve. The transition between states is driven by either a non-parametric model introduced by Born et al. (2020) or a parametric approach proposed by Auerbach and Gorodnichenko (2012).

We show that a pandemic shock originating when the number of new infections is growing fast has a strongly negative effect on spending. We find a significant drop of about 1% in spending after a pandemic shock of one standard deviation. The drop in consumption is consistent with recent macroeconomic models of the effect of income expectations and uncertainty on consumption, see Dietrich et al. (2020), or the feedback between the spread of the pandemic and macroeconomic aggregates, e.g. Eichenbaum et al. (2020). The pandemic shock explains more than 20% of fluctuations

[2]Goolsbee and Syverson (2020) show that consumer behavior during the pandemic is more driven by fear of infection than formal restrictions.

[3]In a survey conducted early in the pandemic, Binder (2020) finds that households expect an increase in unemployment due to the pandemic.

Covid Economics 47, 4 September 2020: 35-69

in spending.

If the shock occurs in a situation in which the virus spreads less rapidly, spending drops by 0.5% only with the peak response occurring after one week. Throughout the paper, we find that the nexus between spending and the pandemic shock is strongly depending on the underlying regime. In almost all cases, we can reject the null hypothesis of equal spending responses across regimes. We estimate the model not only for the whole US economy, but also for the 10 largest US states. Across all states, the regime-dependent sensitivity of spending to pandemic shocks is very similar. The results remain unchanged if we use alternative state variables such as the level of new infections rather than the growth rate of infections.

We also study the spending response across income quartiles. We use spending data for residents of ZIP codes with low, middle and high median household income. This allows us to estimate the response of household spending across income groups to a pandemic shock. The first two of the three transmission channels discussed before, voluntary and forced consumption restraint, should apply equally to high-and low-income households.

The third, however, should imply that low-income households reduce their spending by more compared to high-income households. This is because the drop in lifetime income should be particularly pronounced for low-productivity workers, e.g. workers in the service sector.[4] We do indeed find that in the regime with a strong growth of the number of infections, high-income households reduce their spending by 0.5%, while low-income households cut expenditures by 1%. This is remarkable because the initial fall in spending was larger for high-income households as documented by Chetty et al. (2020). Our results suggest that the economic burden of the pandemic in terms of consumption falls more on low-income households.[5] The difference in spending responses is highly statistically significant in both

[4]Even if the drop in income were equal across income groups, we expect the marginal propensity to consume (MPC) to be higher for low-income quartiles. In fact, Karger and Rajan (2020) track spending of recipients of governmental transfer payments during the COVID-19 pandemic. They find an MPC of 0.68 for hand-to-mouth consumers and 0.23 for savers.

[5]See Mongey et al. (2020) for an analysis of the effect of social distancing across workers. They find significant differences in the burden from social distancing.

Covid Economics 47, 4 September 2020: 35-69

Covid Economics 47, 4 September 2020: 35-69

regimes. Thus, the pandemic contributes to a growing of consumption inequality.

This paper contributes to the recent work on household behavior based on innovative datasets. In an early paper, Baker et al. (2020) use transaction-level data for the US in order to document the changes in consumption patterns after the outbreak of the coronavirus. Cox et al. (2020) extend this line of research and shed light on the response of consumption and saving across the income distribution. Using transaction-level data from the largest Danish bank, Andersen et al. (2020) show that the decline in spending increases in the exposure of households to the economic consequences of the pandemic. Surico et al. (2020) use data from a fintech company based in the UK to track the behavior of spending. These authors also document the build-up of financial stress as well as consumption and income inequality across households. Carvalho et al. (2020) use six billion transactions of customers of Spain's second-largest bank to track consumption over the crisis. Coibion et al. (2020) estimate the effect of lockdowns on spending and household expectations based on survey data. They make use of the asynchronous timing of lockdown measures in order to identify a causal effect. The occurrence of the first corona infection is used to instrument local lockdown restrictions. They find that lockdown restrictions explain most of the fall in consumer spending since March 2020.[6]

Most of these papers, with the exception of Coibion et al. (2020), provide descriptive evidence based on massive new datasets or estimate the response of spending to observable events. Instead, we aim at estimating the sensitivity of spending to unexpected changes in the severity of the pandemic.

The paper is organized as follows. Section 2 presents the data and discusses the derivation of our pandemic shock. Section 3 lays out our estimation strategy. Our results are discussed in Section 4. Section 5 presents results for alternative state variables. Section 6 concludes.

[6] Alexander and Karger (2020) analyze consumer spending and cellphone records in the US and show the causal effect of stay-at-home orders on spending.

II Data

To investigate the response of consumption to the unexpected spread of the pandemic, we rely on two data sets. The first contains information on daily household spending since the outbreak of the coronavirus and the second reports daily historical forecasts on the number of fatalities due to COVID-19.

A. *Household spending*

Throughout the paper, the dependent variable is a measure of household spending. We have daily observations ranging from April 3 up to July 26. We use the series provided by Chetty et al. (2020), which are open source and available at https://tracktherecovery.org.[7]

We also have spending broken down into ZIP codes with high, middle and low median income. Below, we will refer these subgroups of households as high- and low-income households, although we do not have information on household income, only on median income of the ZIP code of residency.

Because the original data on spending exhibits substantial periodic fluctuations across days, the publicly available series are 7-day moving averages in order to smooth daily fluctuations. Furthermore, data on consumer spending exhibits strong weekly fluctuations which are autocorrelated across years. To account for this, Chetty et al. (2020) divide all spending series by its corresponding value from 2019. Lastly, the seasonally adjusted data are indexed to its pre-pandemic level, namely the mean of the 7-day moving average from January 8-28.[8] Hence, our series are given in percent, such that a value of two percent in t corresponds to an increase of spending by two percent relative to its average value in January.

[7] Chetty et al. (2020) collect the data on spending from Affinity Solutions Inc. This company aggregates information on credit and debit card spending. The data is available for nation-wide aggregates as well as for each US state.

[8] It should be mentioned that the spending data for the entire sample is available on a daily basis. Since July 5th, however, it is based on the average of the last 7 days. More precisely, the daily data available from July 6th onward is interpolated as line segments connecting the weekly data points. For more details on the construction of the data, see Chetty et al. (2020).

Covid Economics 47, 4 September 2020: 35-69

Covid Economics 47, 4 September 2020: 35-69

Figure 1: Total Spending and Spending by Income Quartile

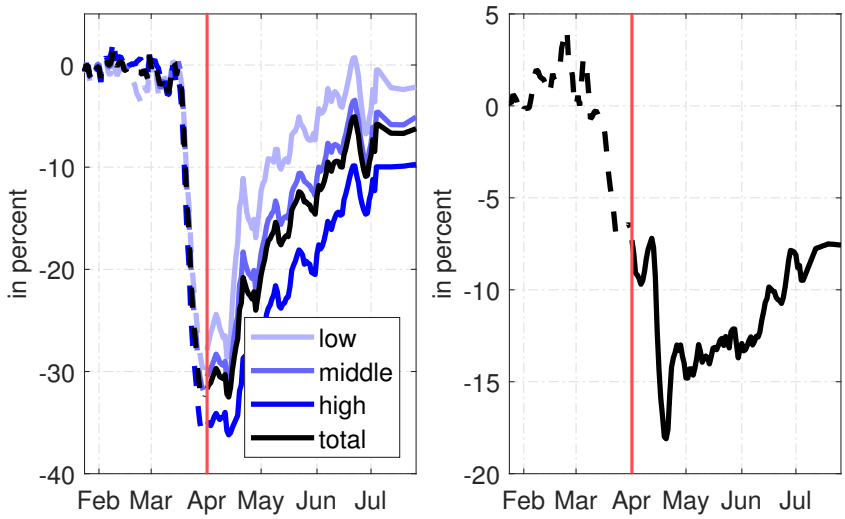

Notes: The left panel shows the difference of actual spending relative to its level in January 2020 by customers living in ZIP codes with different income classes, namely high (top quartile) median income, middle (middle two quartiles) median income as well as low (bottom quartile) median income. The right panel shows the difference in spending of customers living in ZIP codes with high median income and customers living in ZIP codes with low median income. In both samples, the start of our estimation sample (April 3rd) is highlighted by the red vertical lines.

The left panel of Figure (1) shows that for all income households, spending fell sharply in mid-March, when national emergency was declared. In early April, spending fell by 36.4% for high-income households, 32% for low-income households and 29.8% for middle-income households. The right panel shows relative spending, i.e. the difference between spending of high- and low-income households. The reversion of spending to the pre-pandemic level differs remarkably, with the level of low-income households being almost back to the pre-pandemic level. Spending from high-income households fell more and recovered less - a finding that we need to keep in mind because below we show that the sensitivity of high-income households to pandemic shocks is actually smaller than that of low-income households.

B. *The surprise number of fatalities*

Consumption should respond to the unexpected severity of the pandemic. Hence, in order to investigate the consumption response, we need a series of the surprise component of the pandemic. We formulate the surprise in terms

of the unexpected number of fatalities due to COVID-19, i.e. the difference between expected and realized deaths.

We retrieve daily real-time projections on deaths and the unrevised reported number of deaths due to COVID-19 in the US from Gu (2020). This data is open source and can be downloaded from www.covid19-projections.com. The author takes a (machine learning) data-driven approach rooted in epidemiology to forecast infections and deaths from the coronavirus epidemic in the US (and around the world).[9] These forecasts have been covered by almost all major US media outlets.

Importantly, we do not only have the latest forecast, but also the historical forecasts. The forecasts are updated on a daily basis. We use this data to derive a pandemic shock, i.e. the unexpected number of deaths due to COVID-19. To do so, denote $\mathbf{d}_{t|t-1}$ the forecast made in $t-1$ for deaths occurring in t. Thus, we focus on one day-ahead forecasts. Our pandemic shock is calculated as the difference between the actual outcome for t and the forecast number of deaths, that is

$$\mathbf{e}_t = \mathbf{d}_t - \mathbf{d}_{t|t-1}. \tag{1}$$

That is, our pandemic shock is the difference of today's number of reported deaths and yesterday's forecast for today.[10] Notice that the number of reported deaths exhibits transient drops on weekends, typically followed by increases during the week. We therefore purify our shock by regressing it on a set of dummies for each day of the weak. Formally, we regress

$$\mathbf{e}_t = \gamma \mathbf{D}_t + \phi \mathbf{e}_{t-1} + \varepsilon_t. \tag{2}$$

Note that the estimated residuals for ε_t can be interpreted as the pandemic shock, which cannot be explained neither by the set of daily dummies cap-

[9]Details on the forecasting model, including assumptions on the model parameters are available at https://covid19-projections.com/model-details.

[10]We cannot rule out that some households have different beliefs about how the virus will progress and might even mistrust the official data about new cases and deaths, e.g. Fetzer et al. (2020).

Covid Economics 47, 4 September 2020: 35-69

tured in $\mathbf{D}_t$ nor by yesterday's forecast error.[11]

Table 1: Descriptive Statistics for Shocks

			RAW SHOCK				
MIN	MAX	MEAN	MEDIAN	5^{th}	95^{th}	Q-STAT.	p−VAL.
-1007	2416	52.86	63	-587.1	745.40	184.65	0.000
			PURIFIED SHOCK				
MIN	MAX	MEAN	MEDIAN	5^{th}	95^{th}	Q-STAT.	p−VAL.
-632.10	1865.36	0.00	-29.68	-468.59	465.68	10.61	0.717

Notes: Numbers are in deaths per day. Shocks are calculated based on unrevised real-time data. The last two columns report Q-statistics and p−values for a Ljung-Box test with the null hypothesis of zero autocorrelation up to 14 lags.

Table (1) reports some descriptive statistics for both the raw shock $\mathbf{e}_t$ and the purified shock ε_t. It is noteworthy that a large fraction of outliers can be explained by our daily dummies. This is because for the purified shock, the 5th and 95th percentiles are much close to zero than for the raw shock. Also for the minimum and maximum values of our shock, a notable fraction seems to be grounded on the seasonal patterns that is apparent in the reported number of deaths. The purified shock is almost iid and has no serial correlation for up to fourteen lags. Finally, in order to interpret our shock in terms of standard deviations, we subtract the mean and divide the series by the sample standard deviation.

Figure (2) shows the underlying data we use to derive the shock as well as our shock series. Starting with the right panel, the bars show the actual daily reported number of deaths over time. The black solid line corresponds to the one-step ahead forecasts. One can immediately recognize the seasonal pattern mentioned before. The reported number of deaths increased up to 2000 per day until the end of April and started to steadily decrease afterwards, with daily deaths (on average) below 500 by the end of June. However, since early July, the number of daily deaths started to increase again. Interestingly, the forecasts follow the overall direction of the actual number of reported deaths with positive forecast errors being equally likely

[11] We checked whether other control variables have explanatory power, including the daily number of cases and a lag polynomial for up to seven lags. However, it turns out that the dynamics jointly explained by these variables is negligible. We therefore exclude them from our regression.

Covid Economics 47, 4 September 2020: 35-69

Figure 2: Raw vs Purified Shock

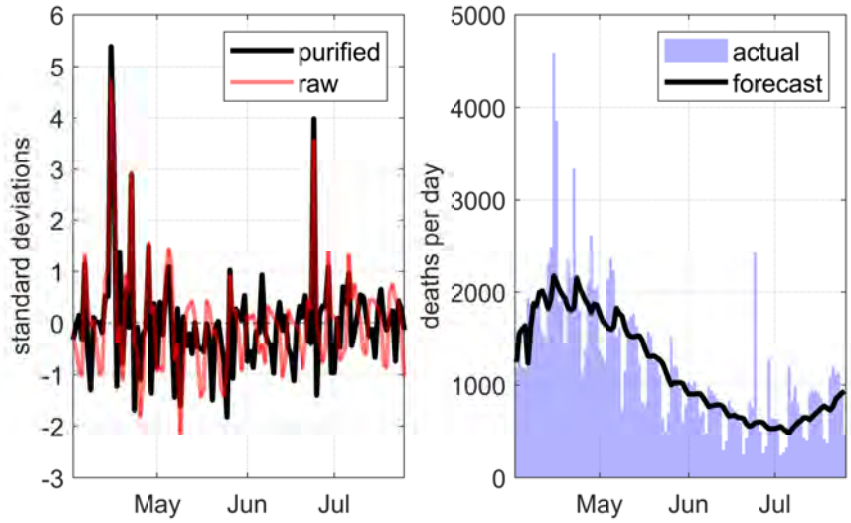

Notes: The left panel shows the raw shock calculated as $\mathbf{e}_t = \mathbf{d}_t - \mathbf{d}_{t|t-1}$ as well as the shock after our purification procedure, i.e. ε_t. The right panel shows the reported number of deaths per day (in real-time) of people infected with the coronavirus (purple bars) as well as the real-time one-step-ahead forecasts.

to negative forecast errors/ones. The left panel shows the raw and the purified shock series constructed as described above. While the raw series clearly exhibits seasonal patterns, the purified shock series now looks very much like an iid process. Moreover, especially from May onwards, we can now see that a significant fraction of the swings disappears when taking seasonality into account.

III Methodology

We investigate the effects of pandemic shocks via local projections as proposed by Jordà (2005). Local projections provide a flexible framework and are easy to implement. Moreover, they offer a straightforward way to condition the short-run effects of pandemic shocks on the state of the pandemic.

A. *Setup*

The linear model of departure reads

$$y_{t+h} = \alpha_h + \beta_h \varepsilon_t + \delta_h t + \gamma_h \mathbf{x}_t + \varphi_h \mathbf{D}_t + u_{t+h}, \tag{3}$$

Covid Economics 47, 4 September 2020: 35-69

where y_{t+h} is the response of the dependent variable at time $t+h$ to a shock ε_t occurring in t. In our model, the dependent variable is household spending and ε_t is the pandemic shock introduced before. The coefficient α_h corresponds to a fixed effect at horizon h and δ_h measures the effect of a deterministic linear trend. The vector γ_h contains the effects of the lagged endogenous variable and other control variables (including our shock) at horizon h captured in the vector $\mathbf{x}_t$ and φ_h contains the effects of daily dummy variables. Finally, u_{t+h} is assumed to have a zero mean and a (strictly) positive variance.

Our vector $\mathbf{D}_t$ in (4) includes the stringency index provided by researchers from the University of Oxford as well as two dummy variables to account for (1) the stimulus payment under the CARES Act that started in April 15, the Paycheck Protection Program signed into law by President Trump on April 24, and (2) the three FOMC meetings since April.[12] In our baseline setting, $\mathbf{x}_t$ includes one lag of the endogenous variable, one lag of the Economic Policy Uncertainty Index (EPU) as well as one lag of our structural shock. This lag structure is the recommendation of the Bayesian Schwarz Criterion.[13]

The model presented before is linear. We now generalize the model to allow for state-dependent effects, that is we condition the impact of the shock on different regimes. Our preferred version throughout this paper conditions the response on the growth rate of new infections. Therefore, we estimate a smooth transition model of the form

$$y_{t+h} = F(z_t)\left(\alpha_h^I + \beta_h^I \varepsilon_t + \gamma_h^I \mathbf{x}_t\right) + (1 - F(z_t))\left(\alpha_h^{II} + \beta_h^{II} \varepsilon_t + \gamma_h^{II} \mathbf{x}_t\right) + \delta_h t + \varphi_h \mathbf{D}_t + u_{t+h}, \tag{4}$$

where the fixed effects, the effects of controls and the lagged endogenous variable captured in $\mathbf{x}_t$ as well as the effect of our shock are now allowed to differ across regimes I and II at each horizon h, respectively. That is, the

[12] The stringency index is meant to measure the strictness of policies restricting people's behavior and lies between 1 and 100. The data is available on a daily frequency at https://www.bsg.ox.ac.uk/research/research-projects/coronavirus-government-response-tracker. The index is aggregated from 17 indicators of government responses, economic policies and health system policies.

[13] The results are insensitive to using the Akaike Information Criterion instead.

Covid Economics 47, 4 September 2020: 35-69

indicator function $F(z_t)$, which lies between 0 and 1, determines the weight of each regime, whereby $F(z_t)$ depends on outcomes of the state variable z_t, which in our case is the growth rate of new infections.

In effect, the response of our endogenous variables to a shock is a weighted average of regimes I and II conditional on z_t and reads

$$\left.\frac{\partial y_{t+h}}{\partial \varepsilon_t}\right|_{z_t} = F(z_t)\beta_h^I + (1 - F(z_t))\,\beta_h^{II}. \tag{5}$$

In the next subsection, we will describe the specification of $F(z_t)$ in detail. However, it is important to note that our framework allows us to easily compare the sensitivity to shocks across both regimes without making explicit assumptions (as in the case of VAR models) on the economy staying in either regime I or II. That is, we can draw inference on the difference between β_h^I and β_h^{II} based on $t-$type tests.

B. *State-Dependent Dynamics*

Our approach follows Born et al. (2020) and relies on specifying the transition function $F(z_t)$ based on the empirical cumulative density function (CDF)

$$F(z_t) = \frac{1}{T}\sum_{t=1}^{T} \mathbb{1}_{z_j<z_t}, \tag{6}$$

where T is the sample size and $\mathbb{1}_{z_j<z_t} = 1$ if $z_j < z_t$ and zero otherwise. That is, $\mathbb{1}_{z_j<z_t}$ denotes the indicator function of the event $z_j < z_t$. We refer to this approach as non-parametric, as we do not need to specify parameters driving the transition.

We choose the weekly growth rate of new infections as our state variable. Since the outbreak of the pandemic, numbers on new infections are reported every day in almost all media outlets. Public policies geared towards "flattening of the curve" made this statistic particularly popular. The left panel of Figure (3) shows the weekly growth rate of new infections with the coronavirus over time. The right panel shows the transition functions $F(z_t)$ based

Covid Economics 47, 4 September 2020: 35-69

Covid Economics 47, 4 September 2020: 35-69

on the empirical cumulative density function over time.[14]

Starting with the left panel, after a well-pronounced decline with the growth rate falling from 60% to almost zero throughout mid of April, the growth rate of new infections fluctuates around zero until the beginning of June. Since then, however, we observe a strong increase in the growth rate with a rise in cases of above 40% in mid June, which declines again at the end of our sample.

Figure 3: Deriving the state variable

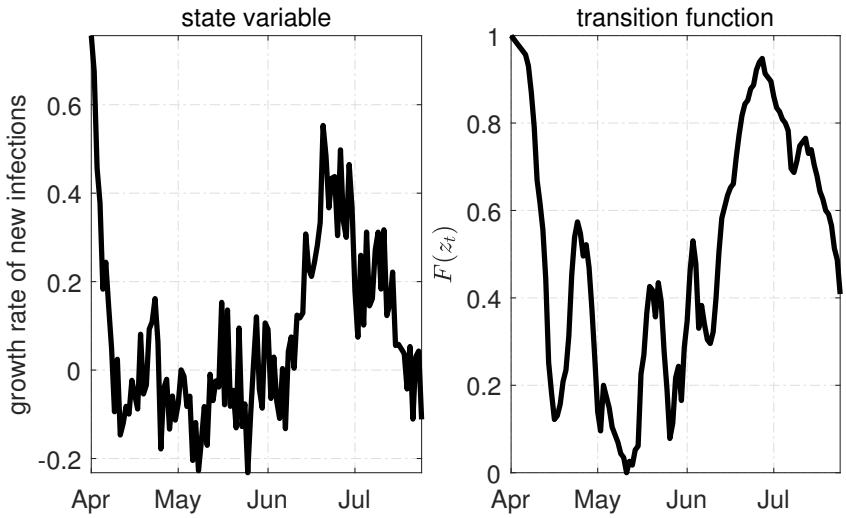

Notes: The left panel shows the weekly growth rate of daily cases of new infections with the coronavirus that causes COVID-19. The right panel shows the transition functions $F(z_t)$ based on parametric approach drawing on the empirical cumulative density function.

The right panel of Figure (3) shows the resulting transition function calculated as described above. While we see a sharp fall of $F(z_t)$ at the beginning of our sample, saying that the economy swiftly moves from regime I to regime II, the sudden rise in daily cases translates into a fast reversion from regime II to regime I from mid June onwards. As a result, we observe that a high weight is attached to regime I throughout June and July.

[14] In order to further get rid of noise in the data, we take a 7-day moving average before calculating the transition function. It must be stressed, however, that we get exactly the same results if we abandon the moving average and use the un-smoothed growth rate.

C. *Inference*

We regress the dependent variable at different horizons on the same set of control variables. This will likely result in autocorrelated residuals. In order to calculate standard errors that account for the possibility of serially correlated residuals both within and across equations, we follow the strategy of Ramey and Zubairy (2018) and Tenreyro and Thwaites (2016) and estimate seemingly unrelated equations as proposed by Driscoll and Kraay (1998). That is, we estimate the parameters of interest of each equation separately and, in a second step, average the moment conditions across horizons $h = 0, ..., H$ when deriving Newey-West standard errors. As a result, Driscoll and Kraay (1998) standard errors account for autocorrelation across both, time t and horizons h.

Finally, we follow standard practice (see Jordà, 2005) and set the maximum autocorrelation lag for the Newey-West procedure to $L = h + 1$.[15]

IV Results

In this section, we first set out our baseline results. In the baseline setting, the idea is to uncover possible asymmetries across regimes in the responses of consumer spending to a standardized pandemic shock. That is, the baseline regression focuses on the effects of pandemic shocks conditional on the state of the infection curve. The sample size covers data from April 3 to July 26, consisting of 115 observations. After adjusting for leads and lags, the effective sample size starts in April 4 and ends in July 12 and, thus, consists of 100 observations. The section also reports results for different income levels as well as for the ten largest US states.

[15]Note that for each horizon h, our null hypothesis is $H_0 : (\beta_h^I - \beta_h^{II}) = 0$. Since we test the same null hypothesis for each $h = 0, ..., H$, one could argue that our $t-$statistics will result in a multiple testing problem as we test $H+1$ null hypotheses at a significance level α and, in effect, would - on average - reject αn true hypotheses. However, as pointed out by Tenreyro and Thwaites (2016), the multiple testing problem is negligible when the $t-$statistics for adjacent horizons are correlated, which is what we will see when we discuss our results.

Covid Economics 47, 4 September 2020: 35-69

Covid Economics 47, 4 September 2020: 35-69

A. *Baseline Results*

Figure (4) shows the state-dependent impulse responses of total spending following a pandemic shock. Remember that throughout the paper, all spending variables are given in percent change relative to the average level of January. That is, a value of one corresponds to an increase in spending of one percent relative to January. In the left column, the red-solid line depicts the impulse response coefficients in regime I following a pandemic shock. Regime I corresponds to a situation with a high growth rate of new infections. The shaded area corresponds to the 90 percent confidence bands based on Driscoll-Kraay standard errors. For the purpose of comparison, we also report the corresponding coefficients from the linear model (red-dashed line). Accordingly, the second column reports the corresponding values for regime II, i.e. the regime with a modest growth rate of new infections. The third column shows the t-statistics testing the null hypothesis $H_0 : \beta_h^I - \beta_h^{II} = 0$ for adjacent horizons $h = 0, ..., H$, where the shaded area covers the $t-$critical values for a 90 percent confidence interval, i.e. ± 1.645.

In this context, it is important to stress that a perfectly symmetric transmission of pandemic shocks would imply that $\beta_h^I = \beta_h^{II}\ \forall h = 0, ..., H$. In other words, a pandemic shock as identified in the previous section would have the same effects across both regimes. Contrary to this, we would refer to asymmetric effects when the difference between β_h^I and β_h^{II} is significantly different from zero.

Starting with the results from the left panel, i.e. the impulse response coefficients in regime I, we see a significant drop in total spending. That is, following a pandemic shock, total spending falls by about 0.5 percent on impact relative to its average value in January. Spending decreases even further on subsequent days and peaks at a decrease of 0.8% three to four days after the shock. Afterwards, total spending starts to steadily revert to its mean which is reached after eight days. In other words, having recognized the pandemic shock as bad news, households respond with a significant decline in aggregate spending when the reported daily number of new infections is relatively high.

However, we see a different pattern in regime II, i.e. when the growth rate of new infections is relatively small. Following a pandemic shock of the same size, spending remains unchanged for the first week. After that, we

Figure 4: Response of Total Spending

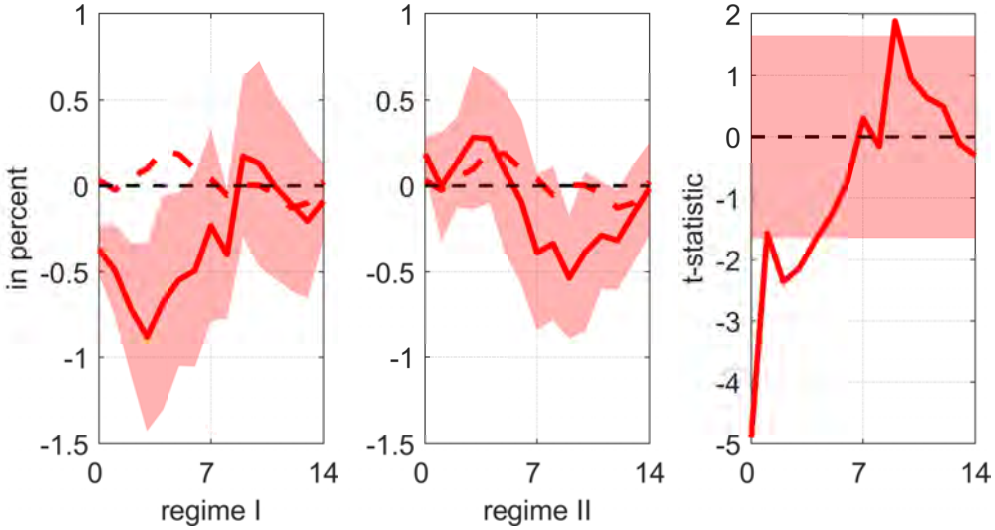

Notes: The first column shows the impulse response coefficients (red-solid) β_h^I for $h = 0, ..., H$ in regime I following a pandemic shock (one standard deviation); the second column shows the corresponding impulse response coefficients β_h^{II} in regime II. In both cases, the red-shaded area corresponds to the 90 percent confidence interval relying on Driscoll-Kraay standard errors. The red-dotted lines in the first two columns correspond to the impulse response coefficients from the linear model without allowing for state-dependent effects. The third column shows the $t-$statistics testing the null that $H_0 : \beta_h^I - \beta_h^{II} = 0$ for each horizon using the Driscoll-Kraay method. The red-shaded area covers the $t-$critical values for a 90% confidence interval, i.e. ±1.645.

find a drop by about 0.5%. The $t-$statistics in the right panel shows that the difference between the response in regime I and regime II is significantly different from zero for the first five days. This being said, we reject the null hypothesis of symmetric effects and find strong evidence for a regime-dependent response of spending to a pandemic shock.

As discussed in the introduction, the effect of the pandemic on household spending, whether it works through voluntary or force consumption restraint or an unexpected fall in lifetime income, should increase in the spread of the pandemic. If few people are affected by the virus, the need to reduce spending, either voluntarily or through governmental restrictions, remains limited. Likewise, the drop in lifetime income remains small since a shock does not call entire industries or job profiles into question. If, in contrast, the number of infections is large, the shock should have stronger effects. Our results are consistent with this notion because the effect of the shock is sig-

Covid Economics 47, 4 September 2020: 35-69

nificantly larger in regime I compared to regime II. As we will see now, the shock impact across income quartiles is also consistent with this. Low-income households work more in contact-intensive jobs. With low-income household bearing the burden of social distancing, the future of these jobs is uncertain in a situation with many infections, while high-income households have jobs in which social distancing is possible. The impact of the shock in regime I should therefore be larger for low-income compared to high-income households.

Next, we take a closer look on the response of spending and investigate how the impulse responses differ across income quartiles. This is possible because we have data on spending by customers living in ZIP codes with different income levels, namely high (top quartile) median income, middle (middle two quartiles) median income as well as low (bottom quartile) median income. This encourages us to estimate the response of spending to our pandemic shock across different income classes.

Figure (5) reports the results for spending of all three different income categories. Starting with panel A, it stands out that, prompted by a pandemic shock, high-income households significantly reduce spending when the growth rate of new infections is relatively high (regime I). After four days, spending drops by about 0.8% and starts to revert to its mean which is reached after one week. The reaction to the same shock has no significant effect in regime II, i.e. when the spread of the virus is slower.

We have a similar picture in panels B and C. While the qualitative picture is similar to the one of high-income households, it stands out that the response of households in regime I seems to be negatively correlated with lifetime income. That is, we see a larger drop in spending for middle-income households and an even larger drop for low-income households. In regime I, spending of low-income households drops by 1% percent, i.e. low-income households are more sensitive to the shock than high-income households.

For all income groups, the response to a pandemic shock depends strongly on where the economy is at the infections curve. Our results indicate that over the first week after the shock the response is much stronger in regime I and is significantly different from the response in regime II. For each income quartile, we cannot reject the null that $\beta_h^I = \beta_h^{II}$ over the first few days considered. Hence, the response of household spending is asymmetric across regimes.

Covid Economics 47, 4 September 2020: 35-69

Covid Economics 47, 4 September 2020: 35-69

Figure 5: Response of Spending by Income Quartile

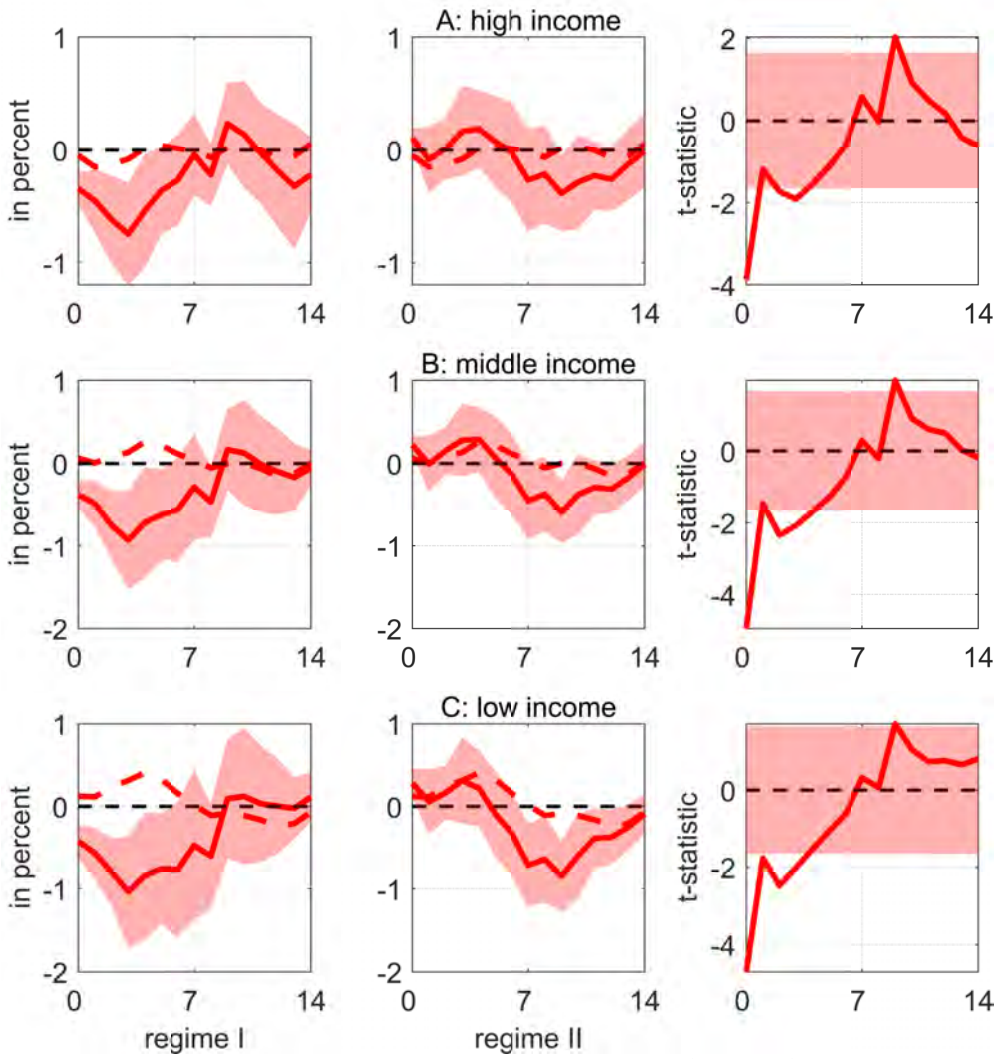

Notes: The first column shows the impulse response coefficients (red-solid) β_h^I for $h = 0, ..., H$ in regime I following a pandemic shock (one standard deviation); the second column shows the corresponding impulse response coefficients β_h^{II} in regime II. In both cases, the red-shaded area corresponds to the 90 percent confidence interval relying on Driscoll-Kraay standard errors. The red-dotted lines in the first two columns correspond to the impulse response coefficients from the linear model without allowing for state-dependent effects. The third column shows the $t-$statistics testing the null that $H_0 : \beta_h^I - \beta_h^{II} = 0$ for each horizon using the Driscoll-Kraay method. The red-shaded area covers the $t-$critical values for a 90% confidence interval, i.e. ±1.645.

Covid Economics 47, 4 September 2020: 35-69

These findings can be rationalized based on the notion that the fall in lifetime income as a result of a pandemic shock is larger for low-income households. Workers in the service and hospitality sector, for example, face uncertainty about whether and when they can return to their old jobs. In addition, our results resemble what is found in the literature dealing with the nexus between household characteristics and the marginal propensity to consume (MPC). Aggregate MPC is typically found to depend on how aggregate shocks are distributed across households (see, for instance, Carroll et al., 2017; Carroll, 2009; Gelman, 2020; Calvet and Comon, 2003). In this context, higher marginal propensities to consume, as typically found in the literature, can explain why our pandemic shock has a larger impact on lower-income households. In the context of the COVID-19 pandemic, Karger and Rajan (2020) show an MPC of 0.68 for hand-to-mouth consumers and 0.23 for households with access to assets. [16]

Figure 6: Response of Relative Spending (High Income - Low Income)

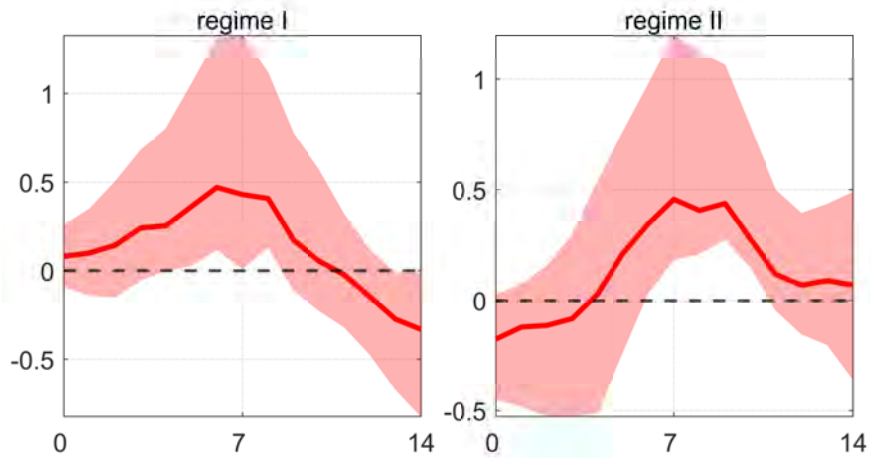

Notes: Difference of estimated coefficients $\beta_h^{high,I} - \beta_h^{low,I}$ in regime I and $\beta_h^{high,II} - \beta_h^{low,II}$ in regime II. The shaded areas cover the 5^{th} and 95^{th} percentiles from the distribution of the block bootstrap procedure as described in the text.

The previous graph revealed a significant state-dependence of the spending responses. However, we could not infer whether the response of high-income households is significantly different from low-income households. To shed light on the responses across quartiles, we proceed as follows: we

[16]Explanations include households' wealth or employment status and the accompanying heterogeneity with respect to liquidity constraints.

generate 2,000 samples of contiguous blocks (with replacement) of four consecutive observations each. Within each replication, for each $h = 0, ..., H$ we then estimate the impulse response coefficients and calculate the sign of $\beta_h^{high,j} - \beta_h^{low,j}$ in regime j =I, II.[17] We then use the distribution of our bootstrap and report the 5^{th} and 95^{th} percentiles.

We show the results in Figure (6). Starting with the left panel, i.e. regime I, we find a significantly positive difference, which peaks at about 0.5% after six days. To interpret this finding, recall that the actual response for both income quartiles was negative. Hence, the positive value means that, following a pandemic shock, low-income households reduce spending significantly more than high-income households. The results are consistent with the view that the pandemic prevents low-income households from returning to their jobs, while high-income households can reconcile their jobs with the necessary degree of social distancing. As a result, the drop in permanent income is larger for low-income households. Also in regime II, i.e. when the number of new infections is growing less strongly, we find that the drop in spending is significantly stronger for low-income households. Hence, a pandemic shock prompts an increase in consumption inequality.

B. *The Quantitative Significance of Pandemic Shocks*

So far our results imply that spending is significantly responsive to our identified pandemic shock. However, we do not yet know the overall quantitative significance of our shock. If the shock we have identified is indeed an important driver of consumer spending, this should also be reflected in the variance of the forecast errors. In this section, we therefore apply the strategy of Gorodnichenko and Lee (2019) for forecast error variance decompositions (FEVDs) within the local projection framework and assess the contribution of our pandemic shock to the variation of forecast errors at different horizons. In a first step, we estimate the same model as before, but

[17] One difficulty in our application is that our set of control variables includes two dummies which have mostly 0-entries. It is therefore likely that inverting the matrix of right-hand side variables is not possible due to multicollinearity. To overcome this issue, we add another step and make sure that each bootstrap sample contains at least once those observations (not blocks) where the dummy variables are equal to one. From a practical point of view, this should not be a problem, since the dummy variables only improve the in-sample fit.

Covid Economics 47, 4 September 2020: 35-69

this time we leave out the contemporaneous effect of the shock

$$y_{t+h} = F(z_t)\left(\alpha_h^I + \gamma_h^I \mathbf{x}_t\right) + (1 - F(z_t))\left(\alpha_h^{II} + \gamma_h^{II}\mathbf{x}_t\right) + \delta t + \varphi_h \mathbf{D}_t + u_{t+h}. \quad (7)$$

In a second step, we take the estimated forecast errors $\widehat{u}_{t+h}$ and regress them on the shock ε_t occurring between t and $t+h$, while accounting for our regimes I and II from our baseline setting

$$\widehat{u}_{t+h} = F(z_t)\left(\omega_0^I \varepsilon_t + \cdots + \omega_h^I \varepsilon_{t+h}\right) + (1 - F(z_t))\left(\omega_0^{II}\varepsilon_t + \cdots + \omega_h^{II}\varepsilon_{t+h}\right) + \eta_{t+h}, \quad (8)$$

where ω_j^i for $j = 0, ..., h$ and $i = \text{I, II}$ measures the state-dependent effect of the pandemic shock on the estimated forecast error. Note that the coefficient of determination of this regression gives us the share of the forecast error variance which is explained by our pandemic shock. As shown by Gorodnichenko and Lee (2019), the R^2-method of the above regression is a natural estimator of the population share of variance explained by the future innovations ε_t in the total variations of our endogenous variable.

Inference is based on the distribution of the R^2s from a block bootstrap procedure including a bias-correction step as recommended by Gorodnichenko and Lee (2019).[18]

Remember that we do not have a VAR-based benchmark for our local projection-based FEVD, which is due to the novelty of the data. However, theoretically, and based on our results so far, we expect pandemic shocks to be a major driver of fluctuations in household spending. This is what we see in Figure (7), which shows the estimated share of the forecast error variance that can be explained by our pandemic shock by income quartiles. The red dots correspond to the explained share of the forecast error variance. The green bars cover 90% of the distribution the R^2s obtained by our bootstrap procedure. For all groups, our pandemic shock seems to be an important

[18] To do so, we generate $B = 2000$ samples consisting of contiguous blocks of four consecutive observations each. Our bias is calculated as the difference between the mean over all bootstrap-based $R^{2,(b)}$ and the R^2 from our baseline procedure, i.e. $\text{bias}_h = B^{-1}\sum_{b=1}^{B} R^{2,(b)} - R^2$. Hence, our bias-corrected variance decomposition reads $R^{2,bc} = R^2 - \text{bias}_h$. As in the previous section, to improve the robustness of our estimates, we adjust our bootstrap algorithm and manually add the dummy observations equal to one in our bootstrap samples.

Covid Economics 47, 4 September 2020: 35-69

Figure 7: FEVD by Income Quartiles

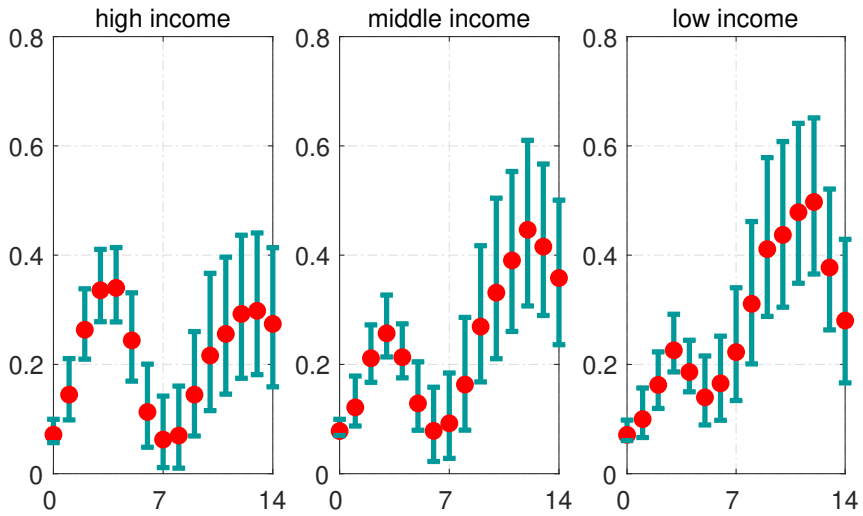

Notes: Explained share of forecast error variance after the bias-correction procedure (red dots) and the 5^{th} and 95^{th} percentiles of the distribution of the block bootstrap procedure

driver of spending. Over the first week, our shock explains up to above 20% of the forecast error variance. While we observe a drop in the explained share for all income quartiles after the first week (especially for high-income households), the quantitative significance increases sharply and reaches its maximum after around 12 days. We see again, with an explained share of above 40% after nearly two weeks, that spending for low-income households is most responsive to our pandemic shock. Interestingly, the 5^{th} percentiles are above zero across all income quartiles and for all horizons considered. Our results therefore point to an important role of the pandemic shock in the variation of consumer spending. While after 12 days about 29% of the forecast variance can be explained for high-income households, this share is almost twice as large for low-income households. In other words, our results imply that for low-income households all other shocks together play a lesser role in the fluctuations of spending than our pandemic shock alone.

Thus, we conclude that our pandemic shock is a significant driver for all income groups, but especially for low-income households.

Covid Economics 47, 4 September 2020: 35-69

V Results on the State Level

Our data on spending is also available on the level of US states. We therefore repeat our exercise from the previous subsection and now investigate the responsiveness of spending for the ten states with the largest population.

Figure 8: Response on the State Level

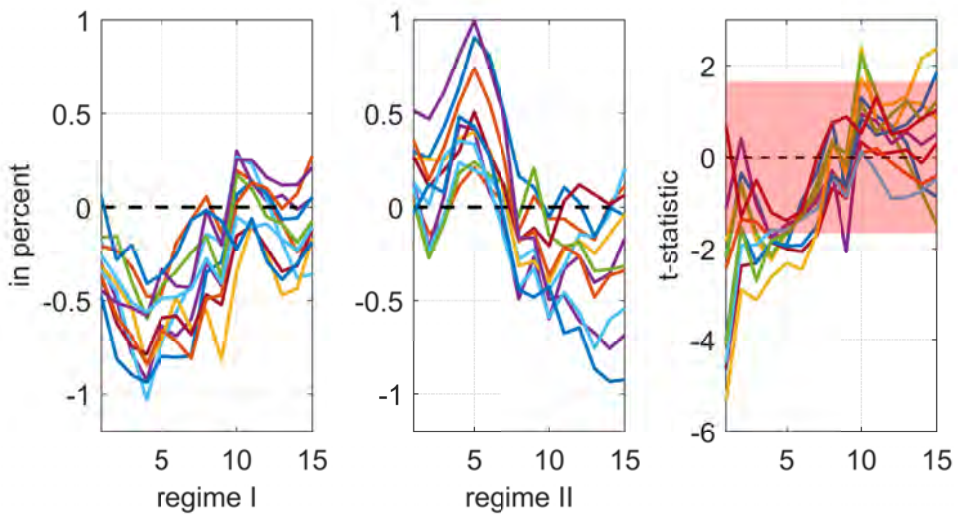

Notes: The first column shows the impulse response coefficients β_h^I for $h = 0, ..., H$ in regime I following a pandemic shock (one standard deviation), the second column shows the corresponding impulse response coefficients β_h^{II} in regime II. The third column shows the $t-$statistics testing the null that $H_0 : \beta_h^I - \beta_h^{II} = 0$ for each horizon using the Driscoll-Kraay method. The red-shaded area covers the $t-$critical values for a 90% confidence interval, i.e. ±1.645.

We estimate the baseline model with spending in each of the ten largest US states as the dependent variable. The driving variable remains the nation-wide pandemic shock and the state-variable is still the nation-wide growth of new infections.

Figure (8) shows the mean impulse responses of total spending following a pandemic shock for ten states. It stands out that the qualitative pattern in regime I appears to be very homogeneous across all states. In regime I, we observe a sharp drop in spending in all states. Spending peaks after four or five days before it returns to its mean after two weeks. Also in regime II,

Covid Economics 47, 4 September 2020: 35-69

the overall direction of the responses looks quite similar across all states. The third column shows that, for the first five days, in many cases we reject the null of equal responses across regimes.

While there are no error bands shown in Figure (8), Figure (9) shows the corresponding impulse response coefficients across states with ±1.645 standard deviations for selected periods, namely four, eight and twelve periods after the pandemic shock. For reasons of comparison, the transparent horizontal lines report the coefficients on the national level.

In almost all states, spending after four days is significantly reduced in regime I. In regime II, in contrast, we see an insignificant response for most states. Let us focus on two states, Michigan and New York, in which spending behaves differently than in most other states. Eight days after the occurrence of the shock in regime I, the drop in spending is sharpest in Michigan, while the response in New York is also well below the nationwide average response. Household spending in Michigan and New York deviates from the nationwide recovery after 12 days since spending in regime I is below spending in regime II.

VI Alternative State-Variables

In our baseline setting, we choose the growth rate of daily infections as our state variable. While figures about new infections are omnipresent in the media, the drawback of this state variable is that it does not necessarily provide information on where the economy stands on the infection curve. In fact, households may condition their spending behavior on the overall level of the infections curve, rather than the slope of the curve.

As a first alternative, we therefore repeat our estimation and use a binary indicator as our state variable. The indicator variable is 0 if the temporary peak of new infections is not yet reached and 1 if the total number of new infections decreases (alternative I). To do so, we set our indicator function to 1 until April 9th, to 0 from April 10th to June 8th, and to 1 again afterwards. These are roughly the cut-off dates that reflect a reversal of the current infection pattern.[19]

[19]Holding anything else constant, we replace $F(z_t)$ with an indicator variable $I(z_t)$, where $I(z_t)$ is equal to zero from April 10 to June 8 and equal to one otherwise.

Covid Economics 47, 4 September 2020: 35-69

Covid Economics 47, 4 September 2020: 35-69

Figure 9: Response of Total Spending on the State Level

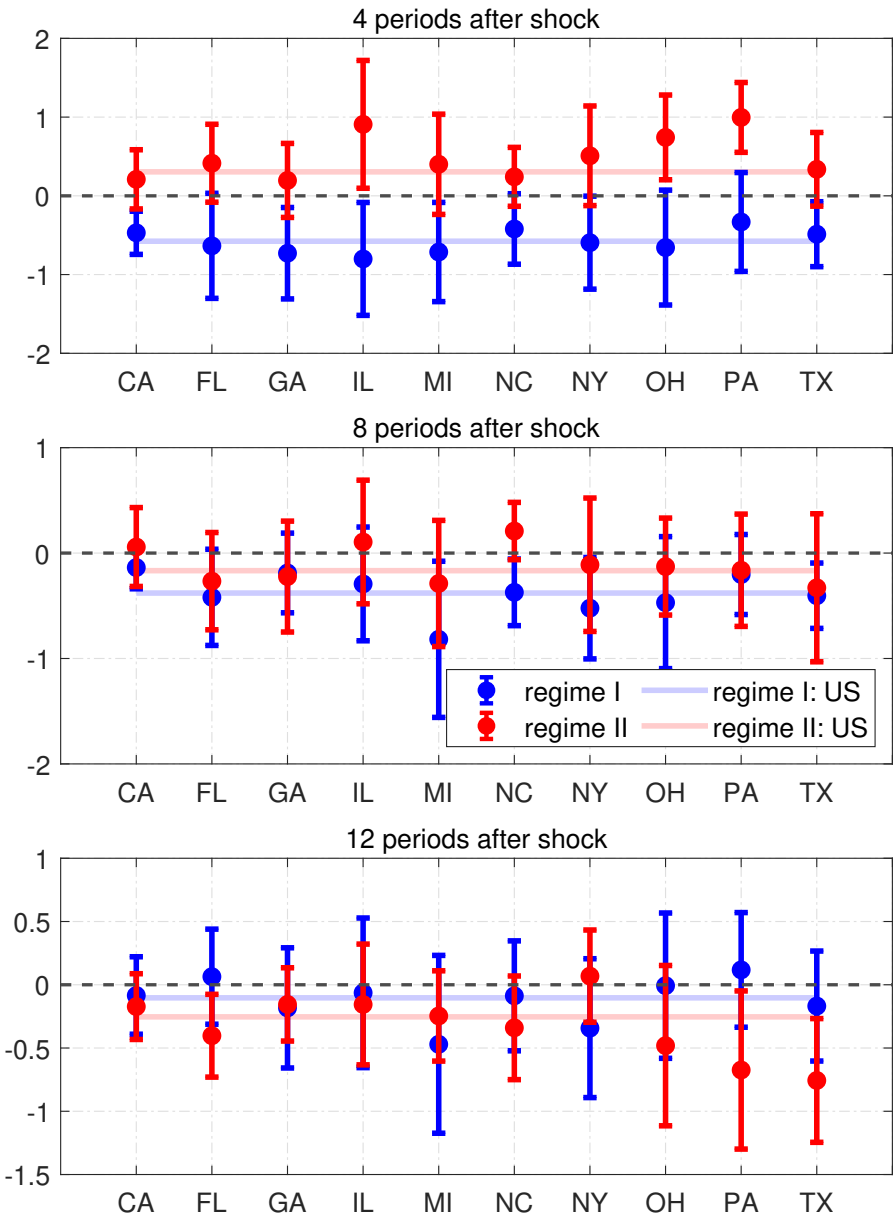

Notes: The dots correspond to the point estimates for regime I (red) and regime II (blue) after 4 periods (upper panel), 8 periods (middle panel) and 12 periods (bottom panel). The edges indicate 1.645 standard deviations in order to cover a 90% confidence interval, based on Driscoll-Kraay standard errors. The horizontal lines reflect the nation-wide effects in each regime.

As a second alternative, we specify $F(z_t)$ as a logistic function of the form

$$F(z_t) = \frac{\exp\left(\kappa \frac{z_t - \mu}{\sigma_z}\right)}{1 + \exp\left(\kappa \frac{z_t - \mu}{\sigma_z}\right)}, \tag{9}$$

where μ is used to control the proportion of the sample the economy spends in either state, and σ_z is the sample standard deviation of the state variable z_t. The parameter κ controls how abruptly the economy switches from one state to the other following movements of the state variable. In other words, higher values of κ mean that small movements of the state variable suffice to induce a switch from one regime to the other. However, although the parametric approach has the disadvantage that we have to make explicit assumptions about the parameters determining the behavior of switching from one state to the other, this approach is well understood and relies on the idea of Granger and Terasvirta (1993) and is, among others, used in Auerbach and Gorodnichenko (2012), Ramey and Zubairy (2018) and Tenreyro and Thwaites (2016). We set $\kappa = 3$ which implies an intermediate intensity of in- tensity of regime-switching and set $\mu = \text{med}(z_t)$. Figure (10) shows both alternative regimes. The left panel shows the actual number of daily new infections and the distinction of regimes I and II as indicated by the black vertical lines on the cut-off dates. The right panel shows the transition function based on the parametric approach (blue-dashed). The alternative transition function looks very much like our baseline transition function, although we observe a higher weight of regime I at the end of our sample.

Figures (11) to (14) in the appendix show the corresponding impulse response functions for total spending and spending across income quartiles for both alternative regime classifications. It stands out that our results from the first alternative state look exactly like the results in the previous section. That is, total spending significantly decreases in regime I, i.e. when the growth rate of new infections is relatively high. The peak is reached after 3-4 days with a drop of 0.7 percent. Moreover, the responses in regime II resemble those from our baseline results. Finally, we also observe a significant difference in the responses across regimes which is consistent with asymmetric effects. The responses across different income quartiles are similar to those in the benchmark model.

The results from our alternative state variable (alternative II) exhibit a sim-

Covid Economics 47, 4 September 2020: 35-69

Figure 10: Alternative States

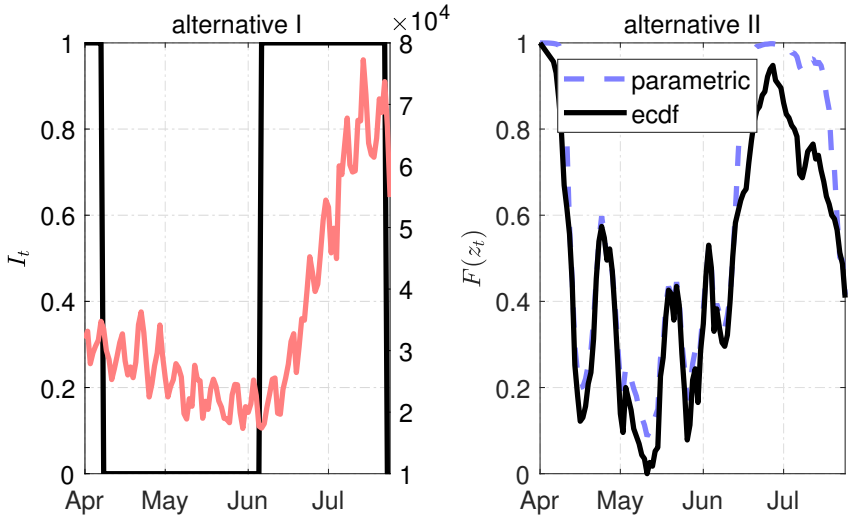

Notes: The left panel shows daily new infections (red-solid) and the corresponding alternative regimes as described in the main text. The right panel shows the alternative transition function obtained by the parametric approach as described in the text.

ilar picture. Both the shape of the impulse responses and the magnitudes of the effects are remain unchanged. This being said, our results indicate that spending reacts more strongly when the number of new infections is high. Again, we find that the difference across regimes I and II is stronger for low-income households.

VII Conclusion

We provided evidence on the causal effect of unexpected news about the COVID-19 pandemic on spending of US households. Our first finding is that a pandemic shock, the forecast error about the number of fatalities, has a negative effect on spending: a surprise increase in the number of deaths leads to a sharp reduction in expenditures. We also showed that this effect is depending on the position of the US economy with respect to the infection curve. With the number of new infections increasing, the effect of a shock is much stronger. If the growth rate of the number of infections is small, in contrast, the pandemic shock has almost no effect. A second finding pertains to the effect across income quartiles. If the number of infections is increasing

Covid Economics 47, 4 September 2020: 35-69

strongly, the shock prompts a much larger adjustment of spending from low-income households compared to high-income households. Hence, the pandemic shock increases consumption inequality.

Our results have two implications for economic policies designed to stabilize aggregate economic activity. First, policy measures should target low-income households more than high-income households. Spending of low-income households is particularly sensitive to a pandemic shock, such that support packages will be more effective when targeting relatively poor households. Second, economic support through direct and indirect transfers should be conditioned on the state of the pandemic in order to stabilize consumption effectively. Transfers will be more effective when the number of infections is large, because in this state households would reduce spending the most.

References

Alexander, D. and E. Karger (2020) "Do Stay-at-Home Orders Cause People to Stay at Home? Effects of Stay-at-Home Orders on Consumer Behavior," Working Paper 2020-12, Federal Reserve Bank of Chicago.

Andersen, A. L., E. T. Hansen, N. Johannesen, and A. Sheridan (2020) "Consumer Responses to the COVID-19 Crisis: Evidence From Bank Account Transaction Data," *Covid Economics*, No. 7, 88-114, April 2020.

Auerbach, A. and Y. Gorodnichenko (2012) "Fiscal Multipliers in Recession and Expansion," in *Fiscal Policy After the Financial Crisis*, 63–98: University of Chicago Press.

Baker, S. R, R. A. Farrokhnia, S. Meyer, M. Pagel, and C. Yannelis (2020) "How does Household Spending Respond to an Epidemic? Consumption During the 2020 COVID-19 Pandemic," *Covid Economics*, No. 18, 73-108, May 2020.

Binder, C. (2020) "Coronavirus Fears and Macroeconomic Expectations," *The Review of Economics and Statistics*, forthcoming.

Born, B., G. Müller, and J. Pfeifer (2020) "Does Austerity Pay Off?," *Review of Economics and Statistics*, 102 (2), 323–338.

Covid Economics 47, 4 September 2020: 35-69

Calvet, L. and E. Comon (2003) "Behavioral Heterogeneity and the Income Effect," *Review of Economics and Statistics*, 85 (3), 653–669.

Carroll, C. (2009) "Precautionary Saving and the Marginal Propensity to Consume out of Permanent Income," *Journal of Monetary Economics*, 56 (6), 780–790.

Carroll, C., J. Slacalek, K. Tokuoka, and M. White (2017) "The Distribution of Wealth and the Marginal Propensity to Consume," *Quantitative Economics*, 8 (3), 977–1020.

Carvalho, J. R., V. M. an Garcia, S. Hansen, A. Ortiz, T. Rodrigo, J. V. Rorriguez Mora, and P. Ruiz (2020) "Tracking the COVID-19 Crisis with High-Resolution Transaction Data," unpublished, University of Cambridge.

Chetty, R., J. Friedman, N. Hendren, M. Stepner, and the Opportunity Insights Team (2020) "How Did COVID-19 and Stabilization Policies Affect Spending and Employment? A New Real-Time Economic Tracker Based on Private Sector Data," NBER Working Paper 27431, National Bureau of Economic Research.

Coibion, O., Y. Gorodnichenko, and M. Weber (2020) "The Cost of the COVID-19 Crisis: Lockdowns, Macroeconomic Expectations and Consumer Spending," *Covid Economics*, No. 20, 1-51, May 2020.

Cox, N., P. Ganong, P. Noel, J. Vavra, A. Wong, D. Farrell, and F. Greig (2020) "Initial Impacts of the Pandemic on Consumer Behavior: Evidence fom Linked Income, Spending, and Savings Data," unpublished, University of Chicago.

Dietrich, A. M., K. Kuester, G. J. Müller, and R. S. Schoenle (2020) "News and Uncertainty about COVID-19: Survey Evidence and Short-Run Economic Impact," Working Paper 20-12, Federal Reserve Bank of Cleveland.

Driscoll, J. and A. Kraay (1998) "Consistent Covariance Matrix Estimation with Spatially Dependent Panel Data," *Review of Economics and Statistics*, 80 (4), 549–560.

Covid Economics 47, 4 September 2020: 35-69

Eichenbaum, M. S., S. Rebelo, and M. Trabandt (2020) "The Macroeconomics of Pandemics," unpublished, Northwestern University.

Fetzer, T., L. Hensel, J. Hermle, and C. Roth (2020) "Coronavirus Perceptions and Economic Anxiety," *The Review of Economics and Statistics*, forthcoming.

Gelman, M. (2020) "What Drives Heterogeneity in the Marginal Propensity to Consume? Temporary Shocks vs Persistent Characteristics," *Journal of Monetary Economics, forthcoming*.

Goolsbee, A. and C. Syverson (2020) "Fear, Lockdown, and Diversion: Comparing Drivers of Pandemic Economic Decline," NBER Working Paper 27432, National Bureau of Economic Research.

Gorodnichenko, Yuriy and Byoungchan Lee (2019) "Forecast Error Variance Decompositions with Local Projections," *Journal of Business & Economic Statistics*, 1–24.

Granger, C. and T. Terasvirta (1993) "Modelling Non-Linear Economic Relationships," *Oxford: Oxford University Press*.

Gu, Youyang (2020) "COVID-19 Projections Using Machine Learning," *Retrieved July*, 13, 2020, https://covid19-projections.com.

Jappelli, T. and L. Pistaferri (2010) "The Consumption Response to Income Changes," *Annual Review of Economics*, 2 (1), 479–506.

Jordà, Ò. (2005) "Estimation and Inference of Impulse Responses by Local Projections," *American Economic Review*, 95 (1), 161–182.

Karger, E. and A. Rajan (2020) "Heterogeneity in the Marginal Propensity to Consume: Evidence from Covid-19 Stimulus Payments," Working Paper 2020-15, Federal Reserve Bank of Chicago.

Mongey, S., A. Weinberg, and L. Pilossoph (2020) "Which Workers Bear the Burden of Social Distancing Policies?," *Covid Economics*, No. 12, 69-86, May 2020.

Covid Economics 47, 4 September 2020: 35-69

Ramey, V. and S. Zubairy (2018) "Government Spending Multipliers in Good Times and in Bad: Evidence from US Historical Data," *Journal of Political Economy*, 126 (2), 850–901.

Surico, P., D. Känzig, and S. Hacioglu (2020) "Consumption in the Time of COVID-19: Evidence From UK Transaction Data," CEPR Working Paper 14733, Centre for Economic Policy Research.

Tenreyro, S. and G. Thwaites (2016) "Pushing on a String: US Monetary Policy is Less Powerful in Recessions," *American Economic Journal: Macroeconomics*, 8 (4), 43–74.

Covid Economics 47, 4 September 2020: 35-69

Appendix

Figure 11: Response of Total Spending: alternative I

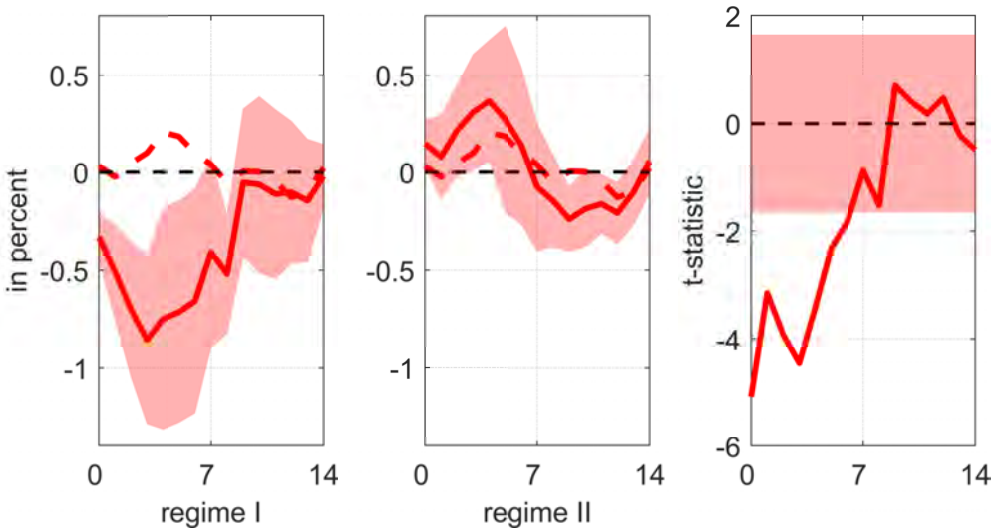

Notes: The first column shows the impulse response coefficients (red-solid) β_h^I for $h = 0, ..., H$ in regime I following a pandemic shock (one standard deviation); the second column shows the corresponding impulse response coefficients β_h^{II} in regime II. In both cases, the red-shaded area corresponds to the 90 percent confidence interval relying on Driscoll-Kraay standard errors. The red-dotted lines in the first two columns correspond to the impulse response coefficients from the linear model without allowing for state-dependent effects. The third column shows the $t-$statistics testing the null that $H_0 : \beta_h^I - \beta_h^{II} = 0$ for each horizon using the Driscoll-Kraay method. The red-shaded area covers the $t-$critical values for a 90% confidence interval, i.e. ±1.645.

Covid Economics 47, 4 September 2020: 35-69

Covid Economics 47, 4 September 2020: 35-69

Figure 12: Response of Spending Across Income Quartiles: alternative I

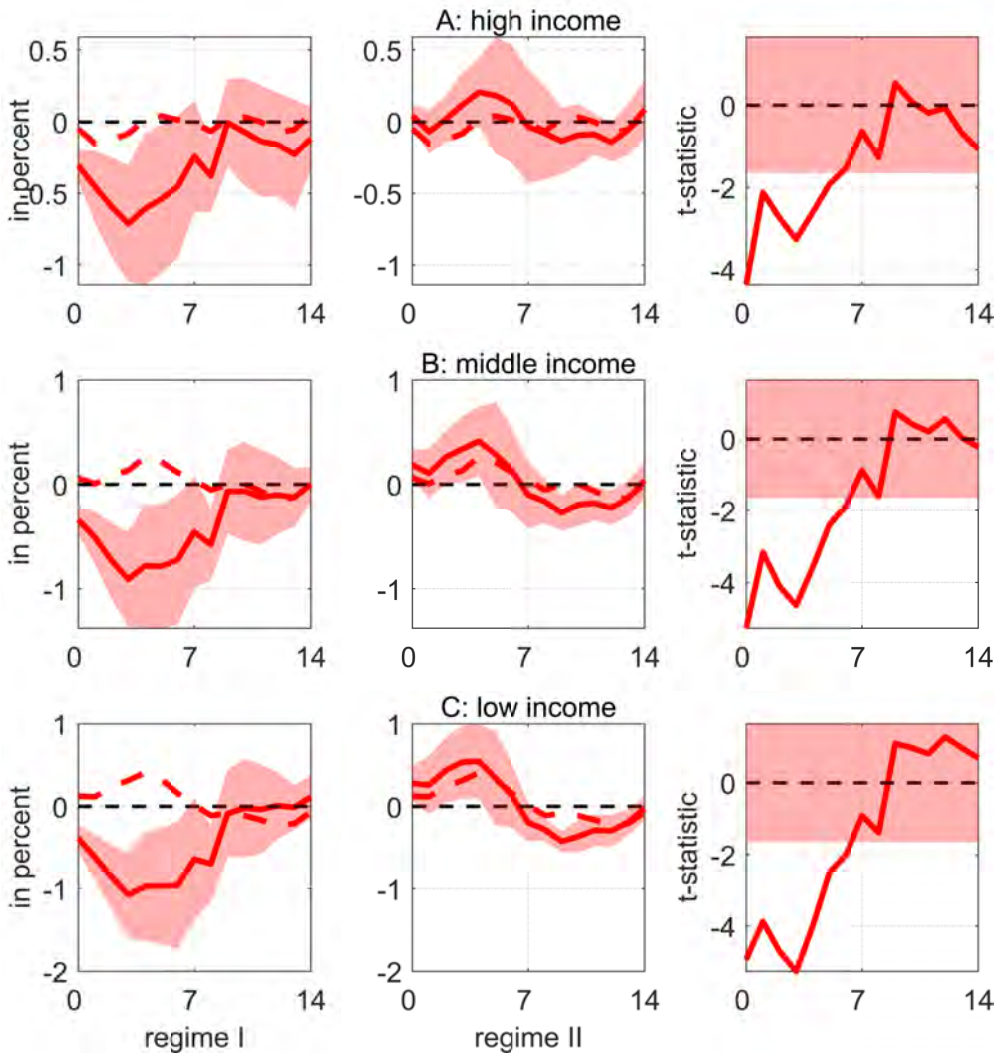

Notes: The first column shows the impulse response coefficients (red-solid) β_h^I for $h = 0, ..., H$ in regime I following a pandemic shock (one standard deviation); the second column shows the corresponding impulse response coefficients β_h^{II} in regime II. In both cases, the red-shaded area corresponds to the 90 percent confidence interval relying on Driscoll-Kraay standard errors. The red-dotted lines in the first two columns correspond to the impulse response coefficients from the linear model without allowing for state-dependent effects. The third column shows the $t-$statistics testing the null that $H_0 : \beta_h^I - \beta_h^{II} = 0$ for each horizon using the Driscoll-Kraay method. The red-shaded area covers the $t-$critical values for a 90% confidence interval, i.e. ±1.645.

Covid Economics 47, 4 September 2020: 35-69

Figure 13: Response of Total Spending: alternative II

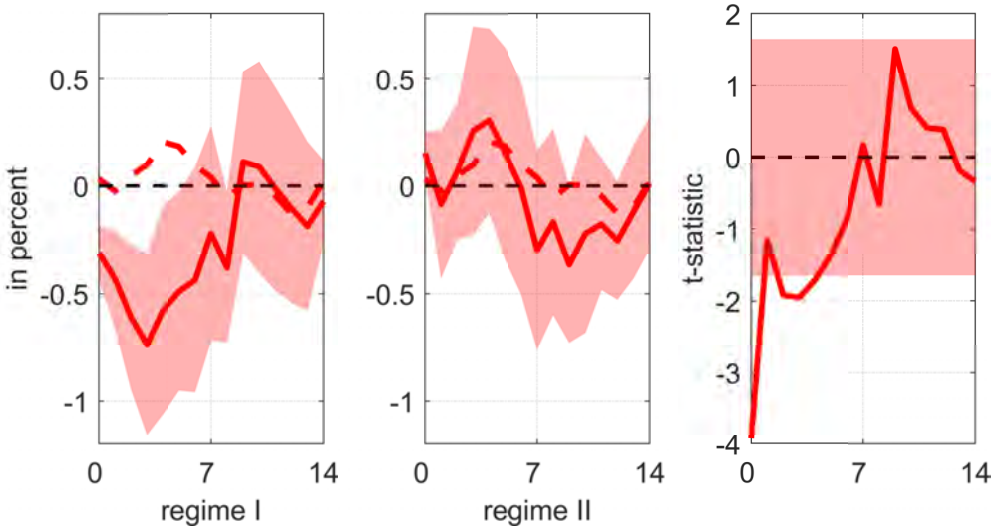

Notes: The first column shows the impulse response coefficients (red-solid) β_h^I for $h = 0, ..., H$ in regime I following a pandemic shock (one standard deviation); the second column shows the corresponding impulse response coefficients β_h^{II} in regime II. In both cases, the red-shaded area corresponds to the 90 percent confidence interval relying on Driscoll-Kraay standard errors. The red-dotted lines in the first two columns correspond to the impulse response coefficients from the linear model without allowing for state-dependent effects. The third column shows the $t-$statistics testing the null that $H_0 : \beta_h^I - \beta_h^{II} = 0$ for each horizon using the Driscoll-Kraay method. The red-shaded area covers the $t-$critical values for a 90% confidence interval, i.e. ±1.645.

Covid Economics 47, 4 September 2020: 35-69

Figure 14: Response of Spending Across Income Quartiles: alternative II

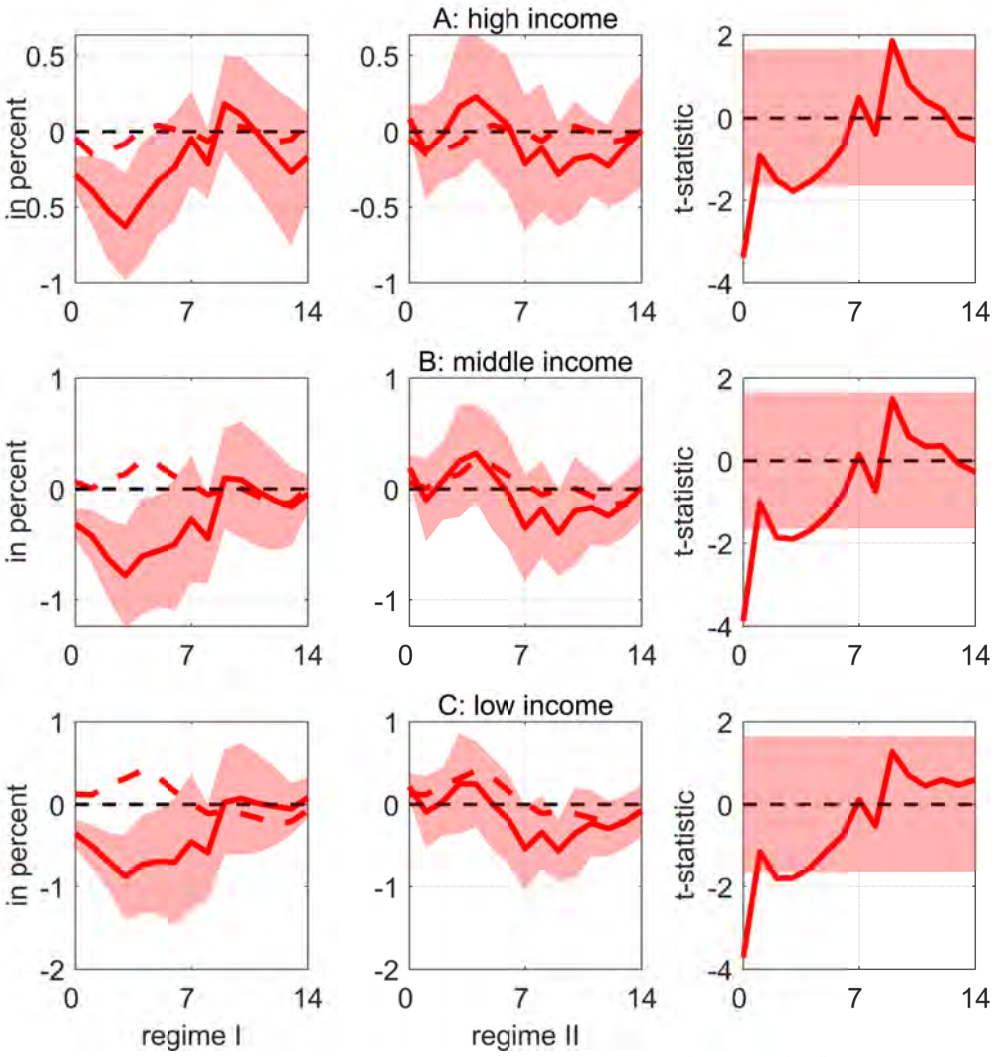

Notes: The first column shows the impulse response coefficients (red-solid) β_h^I for $h = 0, ..., H$ in regime I following a pandemic shock (one standard deviation); the second column shows the corresponding impulse response coefficients β_h^{II} in regime II. In both cases, the red-shaded area corresponds to the 90 percent confidence interval relying on Driscoll-Kraay standard errors. The red-dotted lines in the first two columns correspond to the impulse response coefficients from the linear model without allowing for state-dependent effects. The third column shows the $t-$statistics testing the null that $H_0 : \beta_h^I - \beta_h^{II} = 0$ for each horizon using the Driscoll-Kraay method. The red-shaded area covers the $t-$critical values for a 90% confidence interval, i.e. ±1.645.

Covid Economics **Issue 47, 4 September 2020**

The consequences of the Covid-19 job losses: Who will suffer most and by how much?[1]

Andreas Gulyas[2] and Krzysztof Pytka[3]

Date submitted: 18 August 2020; Date accepted: 1 September 2020

Using the universe of Austrian unemployment insurance records until May 2020, we document that the composition of UI claimants during the Covid-19 outbreak is substantially different compared to past times. Using a machine-learning algorithm from Gulyas and Pytka (2020), we identify individual earnings losses conditional on worker and job characteristics. Covid-19-related job terminations are associated with lower losses in earnings and wages compared to the Great Recession, but similar employment losses. We further derive an accurate but simple policy rule targeting individuals vulnerable to long-term wage losses.

Covid Economics 47, 4 September 2020: 70-107

1 Funding by the German Research Foundation (DFG) through CRC TR 224 (Project A3) is gratefully acknowledged. We thank Michèle Tertilt for useful comments. Further results can be explored interactively using the companion web applet available at: https://gulyas-pytka.app/earnloss.

2 University of Mannheim.
3 University of Mannheim.

Covid Economics 47, 4 September 2020: 70-107

I. Introduction

The Covid-19 epidemics have seen an unprecedented number of job losses around the world. A large economic literature documents that workers displaced during mass layoffs experience significant and long-lasting income losses, which are even larger during recessions.[1] The question naturally arises whether the millions of layoffs during the Covid-19 epidemics will have similar detrimental long-term consequences. Understanding this is not only important for predicting the shape of the recovery from the current downturn. Many policy interventions aimed at avoiding job losses such as firm bail-outs and short-time work subsidy schemes, or policies aimed at insuring workers through unemployment insurance extensions and top-ups should optimally depend on the severity of earnings losses. Therefore it is key to provide an accurate estimation of the long-term consequences of the job losses incurred during the Covid-19 outbreak.

In this paper, we comprehensively document which segments of the labor market were more affected by Covid-19 layoffs and we use a machine-learning approach to predict their long-term consequences. We draw upon the universe of all new UI claims up until May 31st 2020 and contrast the recent experience with the Great Recession of 2008/2009. The administrative nature of our data allows us to document the compositional pool without any measurement errors and small sample issues, and allows us to study worker and firm dimensions which cannot be measured in surveys, such as layoffs along the firm wage premium distribution. Similarly to other countries, Austria experienced an unprecedented scale of layoffs during the pandemic. New UI claims reached an all-time high in March 2020, more than three times the caseload during the peak of the financial crisis. The unemployment rate exceeded 12 percent in April 2020, the highest level recorded in the last 65 years.

We document that the current downturn in the labor market is not only unprecedented in its magnitude, but also unusual in terms of the segments of the labor market that are affected. Typically, during recessions the composition of UI claimants shifts towards worker and job characteristics that are associated with better labor market outcomes. During the Great Recession, UI claims increased more for well earning and male workers, and in larger, older and better-paying firms. The pattern of layoffs during Covid-19 is completely the opposite to the experience during the Great Recession. During the first three months of this downturn, UI claims increased more for workers earning below €25,000, for foreign citizens,

[1] Jacobson *et al.* (1993), Neal (1995), Couch and Placzek (2010), Davis and Von Wachter (2011), Farber (2011), Farber (2017), Davis and Von Wachter (2011), Schmieder *et al.* (2020), and Gulyas and Pytka (2020), among many others.

Covid Economics 47, 4 September 2020: 70-107

and for workers earning less than what would be expected according to their characteristics. In addition, UI claims are more concentrated among smaller, younger and lower-paying firms.

Given the worker and job characteristics of unemployment insurance (henceforth UI) claimants are so different during the Covid-19 epidemics, it is unclear whether the long-term consequences of an average job loser documented in the literature so far will be representative for the Pandemic Recession. To answer this question, we build on the machine-learning approach developed in Gulyas and Pytka (2020). This methodology allows us to estimate the long-term consequences of layoffs conditional on high dimensional worker and job characteristics. The machine-learning algorithm is trained on Austrian social security data from 1984 to 2019. This recession might be different in dimensions our machine learning algorithm does not capture. Nevertheless, we believe it is an important exercise since our approach enables us to explicitly take into account the different compositional pool of laid off workers during the Covid-19 epidemics.

Using the machine-learning algorithm we predict the long-term consequences of job losses for UI claimants from mass layoffs from March to May 2020 and compare these to the ones from the financial crises in 2009, as well as to the boom years just before these two recessions. While before the Pandemic Recession the average 11-year cumulative earnings losses of workers displaced in mass layoffs oscillated between 191-206% of their pre-displacement annual income, during the Covid-19 episode total losses are expected to be only 143%. This decrease is highly unusual because typically job terminations in downturns are associated with higher losses.[2] For our understanding of the labor-market recovery from the downturn, it is important to study whether those lower earnings losses stem from people finding jobs quicker or from lower long-term declines in wages. Although UI claimants exhibit very different characteristics, we predict employment losses to be as severe as during the financial crises. Over the next 11 years, we predict displaced workers to forgo 1.3 years of employment. Based on these findings, the danger of another jobless recovery looms.

The expected wage losses are of particular interest as they provide a forecast whether the wage growth will be as sluggish as after the financial crisis, which caused a lot of concerns among policy makers. In addition, wage losses provide the measure of human-capital destruction of job terminations. Here our findings provide a silver lining. The group of workers affected by the Covid-19 job losses is expected to have much lower wage losses upon re-employment compared to previous experiences. We show that this is due to the different composition of displaced workers during the Pandemic Recession. Almost all of the worker

[2]See e.g. Davis and Von Wachter (2011).

Covid Economics 47, 4 September 2020: 70-107

and job characteristics which are more heavily affected by job losses during the Covid-19 recessions are associated with lower wage declines. In particular, relying on our previous findings from (Gulyas and Pytka, 2020), the lower firm wage premia of displaced workers during the pandemic is able to explain the observed differences in estimated earnings losses. This observation is consistent with a simple job search model in the spirit of McCall (1970).[3]

Furthermore, we show that the low average wage losses of the Covid-19 job losses mask a lot of heterogeneity. While many individuals face significant long-lasting declines in income, 30% of individuals can expected wage gains after reemployment. Therefore, targeting policy interventions such as firm bail-outs, short-time work subsidy schemes, or UI extensions towards high-loss individuals would likely yield welfare gains. In order to guide policy makers, we use an algorithmic approach to derive a decision rule to identify individuals with positive wage losses. Despite its simplicity, the tree classifies 86.82% of individuals with positive wage losses correctly. Our policy recommendation suggests targeting (i) workers displaced from employers paying above the median and (ii) workers with a relatively long job tenure displaced from low paying firms in regions with fewer good jobs on the market.

Literature review. Our paper contributes to an emerging literature that documents that the Covid-19 downturn affected very different labor market segments compared to previous recessions (Dingel and Neiman, 2020; Mongey *et al.*, 2020; Alstadsæter *et al.*, 2020; Alon *et al.*, 2020; Adams-Prassl *et al.*, 2020; Cajner *et al.*, 2020; Kahn *et al.*, 2020; Coibion *et al.*, 2020). What distinguishes our study from the other papers is that we estimate the long-term consequences of the the Covid-19-related layoffs. To this end, we build on generalized random forests (Athey *et al.*, 2019) and undertake the systematic study of heterogeneity of earnings losses.

II. Layoffs during Covid-19

The Covid-19 crisis had similar devastating effects on the Austrian labor market as in other countries. The number of new monthly unemployment claims reached an unprecedented record high of 175,000 workers in April 2020, more than 3 times the peak during the Great Recession of 2009. The number of unemployed workers exceeded half a million for the first time since World War II, which implied an unprecedented unemployment rate of 12.7 percent in April 2020, nearly doubling compared to the previous year.[4] This increase in

[3] Workers employed at low paying firms expect higher wages in their new jobs whereas workers with in above average paying firms are much more likely to suffer more from a job displacement.

[4] Figure 5 in the Appendix plots the evolution of unemployment and UI claims over time.

Covid Economics 47, 4 September 2020: 70-107

unemployment occurred despite a generous short time work (STW) subsidy scheme, which covered at its peak almost a quarter of the Austrian workforce.

We start by documenting which segments of the labor market are comparably more affected during the COVID-19 epidemics and how the experience differs from the Great Recession. We use administrative employment and unemployment records from the social security administration in Austria until May 2020 for unemployment records and beginning of August 2020 for the employment records. This data comprises day-to-day information on all employment and unemployment spells covered by social security in Austria (Zweimüller *et al.*, 2009). It contains information on yearly earnings for each worker-establishment pair, in addition to basic socio-demographic information at the worker level such as age, gender, occupation, and citizenship.[5] Each establishment (we use firm and establishment exchangeably from here on) has a unique identifier, which allows us to study how unemployed workers differ in employer specific characteristics. At the establishment level we have data on the geographic location and a 4-digit industry classifier.

From the social security records we select all separations that are followed by a UI claim within 90 days. In order to focus on workers with some prior labor market attachment, we impose that workers need to have had positive earnings in the year prior to the UI claim and had at least 180 days of job tenure. We construct a number of variables in addition to the ones readily available in the social security dataset to provide a comprehensive picture of the worker and job characteristics of newly unemployed workers. These include job tenure, number of previous employers, firm size, regional and industry unemployment rates and the firm pay premium as job characteristics. The firm pay premium is computed using the seminal two-way fixed effect model of Abowd *et al.* (1999). We estimate:

$$\ln(w_{it}) = \psi_{J(i,t)} + \alpha_i + \theta_t + x_{it}\beta + \epsilon_{it}, \tag{1}$$

where $\ln(w_{it})$ is the log daily wage of the dominant employer in period t[6], α_i the worker fixed effect, θ_t the year fixed effect, x_{it} are time varying observables, comprising of a cubic polynomial of age, and $\psi_{J(i,t)}$ represents the establishment fixed effect of the employer of worker i at period t, which measure the pay premium relative to a baseline firm.[7] Using these firm wage premium estimates, we in addition compute the average firm wage premium in the region.[8]

[5] We deflate all earnings to 2017 level using the CPI index provided by the Austrian Statistical Agency.
[6] The dominant employer is selected based on the total earnings in calendar year t.
[7] We use data from 1984-2019 to estimate the firm pay premia.
[8] We compute the average firm wage premia of all jobs in a given region leaving out all jobs of

We are also interested how workers with different match qualities are affected during recessions. We estimate the match effect of worker i employed at firm $J(i,t)$ as the residual term ϵ_{it} from the following regression:

$$\ln(w_{it}) = \alpha_i + \hat{\psi}_{J(i,t)} + \theta_t + f(age_{it}) + f(tenure_{it}) + \epsilon_{it}, \tag{2}$$

where $f(age_{it})$ and $f(tenure_{it})$ are cubic polynomials and $\hat{\psi}_{J(i,t)}$ is the estimated firm fixed effect from regression (1).

With all the worker and job characteristics defined, we now turn to the analysis of which parts of the labor market were more affected by the Covid-19 recession, and how the recent experience differs from the Great Recession. Figure 1 displays the change in the number of UI take-ups during the last two recessions compared to pre-recession periods by different worker and job characteristics, broken down by the type of layoff. We distinguish between temporary layoffs (bottom panels), which we define as a UI claimant who is recalled within two months to her previous employer, and permanent layoffs (top panels). The left panels plot the change in UI claimants from March to May 2020 compared to the average during same time period of 2018 and 2019. The right panels plot the change from the Great Recession (2009) compared to 2007.[9]

First of all, the plot highlights the unprecedented magnitude of the Covid-19 shock on the labor market. As shown by the grey dotted lines, the overall number of UI claimants with a permanent layoff increased by 124 percent during the Covid-19 epidemics compared to pre-recession levels and temporary layoffs increased by a staggering 600 percent, albeit from a very low base.[10] During the Great Recession, UI claims from permanent and temporary layoffs increased by 28 and 35 percent in comparison. Especially the stark increase in furloughs is noteworthy, because Austria had a generous STW subsidy scheme in place, which covered at its peak almost a quarter of all employed workers. During the Corona Pandemic, firms were allowed to cut back hours and thus the wage bill by up to 90 percent, with the government replacing 80-90 percent of the workers' forgone income. The significant spike in temporary layoffs points towards many firms shunning STW, perhaps because

the worker's current employer. Formally for every worker i employed at firm $J(i,t)$ we compute $\sum_{k \notin J(i,t) \wedge k \in r(i)} \hat{\psi}_{J(k,t)} / \#(k \notin J(i,t) \wedge k \in r(i))$, where $r(i)$ is the region of the worker i.

[9] For the Great Recession, it is harder to pin down the exact starting and end point of the recession. In Austria, UI take-ups peaked in 2009, therefore we choose 2009 as the recession year. Throughout 2007, the number of unemployed was still falling and thus we choose it as the pre-recession comparison. See Figure 5 in the Appendix for the evolution of the number of unemployed and UI-take ups.

[10] In March-May 2018 and 2019, only 8 percent of UI claimants were temporarily laid off.

Covid Economics 47, 4 September 2020: 70-107

Covid Economics 47, 4 September 2020: 70-107

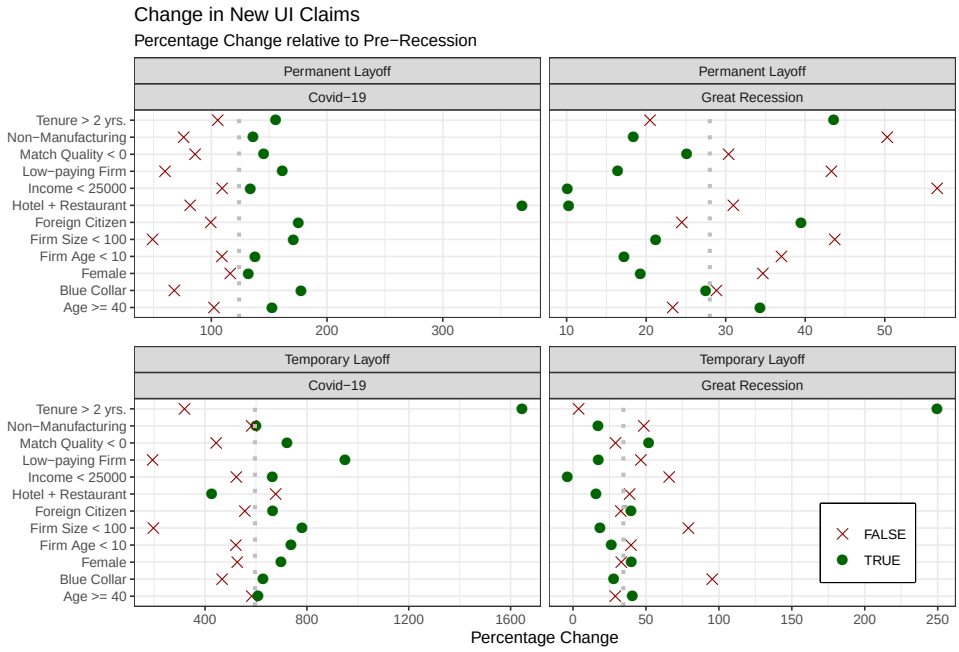

Figure 1: The figure shows the percentage change in the number of new UI claims March 2020 - May 2020 relative to the same period in 2019 and 2018 (Covid-19) and 2009 compared to 2007 (Great Recession), for temporary and permanent layoffs. Temporary layoff is defined as a recall within 2 months. The grey dotted line represents the overall change in UI take-ups. Sample consists of all UI claimants with positive earnings in the prior year and more than 180 days of job tenure. Source: Authors calculations using the AMDB data.

the restrictions on firing were perceived as too restrictive, or because of the administrative burden.[11]

The other striking feature of the Covid-19 recession is that very different parts of the labor market were affected compared to the previous recession. This is especially true for permanent layoffs, which constitute the overwhelming majority of UI claimants. Similarly to other countries, Austria enacted a strict lock-down in March 2020 with mandatory closures of all hotels, restaurants, and non-essential shops. Therefore, perhaps unsurprisingly, permanent layoffs in the hotel and restaurant industry increased much more than in other industries, whereas in the Great Recession, this industry was more resilient. The hotel and

[11]Firms are not allowed to downsize or lay off workers during the STW scheme, although exceptions are allowed with the permission of the work council.

Covid Economics 47, 4 September 2020: 70-107

restaurant industry seems also more pessimistic about a potential quick recovery. Not only did furloughs increase more than in other industries, but it is the only group in this figure where permanent layoffs increased more than temporary ones. In contrast, manufacturing was less affected by layoffs compared to the Great Recession.

Typically, during recessions the pool of unemployed shifts towards worker and job characteristics that are associated with better labor market outcomes. For example, in the Great Recession, permanent layoffs with prior yearly income *above* €25,000 increased six times more than for workers earning below this threshold.[12] In contrast, the Covid-19 recession affected workers earning *below* €25,000 relatively more than higher paid individuals. In addition, UI claims increased more for workers earning less than what would be expected based on their characteristics, again the opposite pattern to the Great Recession. UI claims from blue collar occupations, which are harder to perform via remote working, increased more than in white collar occupations, a pattern documented as well in (Mongey *et al.*, 2020). This is again in contrast to the Great Recession, where UI take-ups increased less for blue collar occupations. In the Covid-19 recession, job losses are more severe for females, which is very atypical for recessions (Alon *et al.*, 2020). This is likely due to an over-representation of females in the most affected sectors in addition to schools and daycare closures forcing more mothers to leave their jobs (Fuchs-Schündeln *et al.*, 2020).[13]

The administrative nature of our dataset also allows us to study a number of firm characteristics which are not readily available in other datasets. During the Great Recession, the composition of UI-claimants shifted towards larger, older and better paying firms. Here again the experience during the Covid-19 epidemics stands out. Layoffs were more concentrated in smaller, younger, and lower paying firms.

To summarize, contrary to the Great Recession, the composition of UI claimants shifted towards workers and job characteristics that are associated with worse labor market outcomes. As a result, as Table 2 in the Appendix shows, the composition of UI claimants is much more female, less Austrian, and consists of more workers from smaller, younger and lower paying firms and lower quality matches. A worker displaced from a bad quality match at a firm that pays well below market wage is likely facing different wage losses than a worker separating from a region's flagship company. These large compositional differences of the Covid-19 layoffs in comparison to the previous recession highlights the need for a method of estimating long-term consequences of job losses that takes the different worker and job char-

[12]For the United States, Mueller (2017) documents a similar pattern during previous recessions.

[13]55 percent of all workers in the hotel and restaurant industry are female, whereas only 25 percent of manufacturing workers are female.

acteristics of UI claimants into account. The methodological details of the machine-learning algorithm are presented in the next section.

III. Employed Methodology

The ultimate goal of our exercise is to predict the long-term cost of job termination occurred on the eve of the Pandemic Recession borne by displaced workers. In the earnings-loss literature the cost of job loss has been studied typically in a quasi-experimental setup using mass layoffs as a proxy for random treatments.[14] Consequently, by employing an event-study analysis the average long-term cost of job displacement can be estimated for workers separating during a mass-layoff event.[15] Nonetheless, given the fact that there is very strong heterogeneity in earnings losses across individuals as documented in Gulyas and Pytka (2020) and that the composition of workers displaced during the Covid-19 episode is substantially different from past events as we presented in the previous section, the identified average cost may not be a good representation for the current pandemic event. For this reason, we adapt the generalized random forest methodology (Athey *et al.*, 2019) to a difference-in-difference setting in a similar way to our companion paper (Gulyas and Pytka, 2020). The implemented algorithm is able to identify the conditional average cost of job loss at the worker level as a function of individual characteristics. Equipped with a random forest grown to detect heterogeneity in treatment effects, we are in a position to provide a prediction of earnings losses for each individual separately. Then, we can recover the average cost of job termination during the beginning of the Pandemic Recession simply by computing the average of individual predictions for the recently displaced employees.

For the definition of mass layoff displacement events, we follow the typically applied definitions and sample restrictions as much as possible. A worker is considered displaced if she separated from her employer that experienced a mass layoff in the given year. We define a mass-layoff event at the firm level in year t if it declined by more then 30 percent in size during year t.[16] To have a meaningful measure of firm growth, we only consider

[14] Just to cite but a few seminal examples: Jacobson *et al.* (1993), Neal (1995), Couch and Placzek (2010), Davis and Von Wachter (2011), Farber (2011), Farber (2017).

[15] In our study our treatment group is selected from mass-layoffs event that happened from 1989 through 2009. The control group is generated using propensity score matching.

[16] For the training of our machine learning procedure, we additionally apply the following sample restrictions. To avoid selecting volatile firms, we exclude firms that either grew rapidly the years before the mass layoff, or rebounded in size 3 years after the mass layoff event. That is, we exclude firms that grew by more than 30 percent in either $t-1$, or $t-2$, as well as firms that are larger 3 years after the event than before. In addition, to avoid mis-specifying mergers, outsourcing or firm restructures as mass layoffs, we compute a

Covid Economics 47, 4 September 2020: 70-107

establishment with at least 30 employees. We also exclude temporary layoffs by excluding anyone who is recalled to their previous employer.

Average cost of job displacement. In our study we are interested in the cumulative 11-year losses. Those losses can be identified by estimating a difference-in-difference setup:[17]

$$y_{it} = \tau \mathbb{1}(t \geq t^*) \times D_i + \theta D_i + \gamma_t + \epsilon_{it}, \tag{3}$$

where D_i is an indicator for displaced persons, t^* the displacement year and t the current year, period fixed effects γ_t control for the evolution of the control group's outcomes, and τ measures the average change of the variable of the interest in the horizon of 10 years after the displacement.[18] On the left-hand side as y_{it}, we use consider three specifications with different dependent variables: total annual labor earnings, employment days, and log average daily wages. An important concern is that the average cost from Equation (3) estimated with events from 1989 through 2009 may be not representative for the recent COVID-19–related job terminations. The reason for this is that heterogeneity in individual losses and different composition of displaced workers between the past and the presence might shape the average cost in a completely different way.

Conditional average cost of job displacement. One way to address the different composition of individuals displaced during the COVID-19 crisis is to identify the cost of job displacement, $\tau(\mathbf{z})$, as a function of some observables $\mathbf{z}$. In theory, this could be identified by running a modified version of (3) for all values of $\mathbf{z}$. Then the average cost $\mathbb{E}_{covid}\tau(\mathbf{z})$ related to the pandemic job layoffs could be computed simply by reweighing $\mathbf{z}$ according to the distribution $F^{covid}(\mathbf{z})$. That being said, estimation of $\tau(\mathbf{z})$ would require many observations for *each* combination of values in $\mathbf{z}$ and such a procedure would be extremely inefficient or, in practice, even infeasible. For this reason we employ a machine-learning technique, which is our adaptation of generalized random forests by Athey *et al.* (2019) in the difference-in-difference setup as in (Gulyas and Pytka, 2020), to detect individuals with similar values of

cross flow matrix for all firms in each year. We exclude all firms where more than 30 percent of its workforce ends up working for the same employer in $t + 1$. Thereby we exclude mass layoff firms with large worker flows to other firms.

[17] A more general specification with event-study coefficients is relegated to Appendix B.

[18] Table 4 in the Appendix shows the estimates from this regression for different specifications for the mass layoffs events that occurred events between 1989 and 2009. Column (1) reports the estimates for Equation (3) without any controls, column (2) and (3) a polynomial in age and worker fixed effects are added. In all specifications, the yearly earnings losses amount to close to €5,900 per year, or close to €65,000 over 11 years.

Covid Economics 47, 4 September 2020: 70-107

the treatment effect. The general idea relies on building trees which maximize heterogeneity in the estimated losses across different groups of workers. Growing a single tree consists in partitioning the dataset into smaller subsamples with different displacement costs, τ. The algorithm decides upon which variables and their cutoff values the dataset is split into two subsets. The splitting criteria maximizes the (adjusted) between-group heterogeneity in displacements costs. Having divided the dataset, the procedure is recursively repeated for two newly created subsets. The process continues until no new satisfactory splits can be obtained or the maximum depth of the tree is achieved. More formally, the procedure is presented in Algorithm 1.

Algorithm 1 Tree Algorithm of Recursive Partitioning

i. Start with the whole dataset and consider it as one large data partition, $\mathcal{P}$.

ii. For each explanatory variable z_k and its every occurring value $\overline{z}$, split partition $\mathcal{P}$ into two complementary sets of individuals i such that $\mathcal{P}_l = \{i \in \mathcal{P} : z_{ki} \leq \overline{z}\}$ and $\mathcal{P}_r = \mathcal{P} \setminus \mathcal{P}_l$ and estimate cumulative earnings losses τ_l and τ_r for both partitions by running two separate regressions of form (3) on $\mathcal{P}_l$ and $\mathcal{P}_r$.

iii. Choose the variable z_k and value $\overline{z}$ that maximizes:

$$(\tau_l - \tau_r)^2 \frac{n_l \cdot n_r}{N^2}, \tag{4}$$

where n_l and n_r are sizes of $\mathcal{P}_l$ and $\mathcal{P}_r$ and N is the sample size of $\mathcal{P}$.

iv. If (4) is smaller than a tolerance improvement threshold, then stop. Otherwise, go to step (ii) and repeat the splitting procedure for $\mathcal{P}_l$ and $\mathcal{P}_r$ separately, where $\mathcal{P}_l$ and $\mathcal{P}_r$ are new partitions subject to the splitting procedure, $\mathcal{P}$.

In the literature (e.g., Efron and Hastie, 2016; Hastie *et al.*, 2017) the shortcomings of a single tree such as high variance, overfitness and low stability are well known. To address those issues, a random forest, which is an ensemble of many trees trained on random subsamples with a random subset of explanatory variables, is recommended. In our application we built the random forest with 2,000 trees. Then, the displacement cost $\tau(\mathbf{z}_i)$ of individual i is identified by weighted-least squares estimation of Equation 3. The weight of each observation relevant in estimating $\tau(\mathbf{z}_i)$ is recovered from the random forest. Intuitively, those weights capture the frequency with which other observations fall into the same final node as the observation of our interest. We present the algorithm of building those weights more formally in Appendix C.

Covid Economics 47, 4 September 2020: 70-107

Covid Economics 47, 4 September 2020: 70-107

Explanatory variables. In our analysis we consider 16 different explanatory variables **z** for estimating the cost of job loss, which cover the most prominent theories from the earnings loss literature. We include worker characteristics such as age, gender, the number of previous employers, job tenure at the last job, and indicators for Blue-collar job and Austrian citizenship. In addition we include firm wage premia obtained from Equation (1), the match quality measured by the residual of Equation (2). Apart from the firm FE, other firm-related variables are: firm size, a manufacturing dummy, and the firm separation rate. The current state of the economy is reflected by five additional variables, *i.e.* regional and industry-specific unemployment rates and its year-to-year changes, Herfindahl-Hirschman index of labor market concentration, the regional average of the firm FE and a dummy accounting for recession years according to the OECD definition.

The Covid-19 outbreak was an unprecedented event in the modern history and thus the looming recession may be different in many dimensions. That being said, our machine-learning procedure takes into account some of the differences through our choice of explanatory variables. More specifically, we use multiple business cycle indicators at the national, regional, and industry level to account for any geographic- or industry-specific shocks of the Covid-19 recession. In addition, because of the rapid increase in unemployment during the Pandemic Recession, we not only use unemployment levels but also their year-to-year changes.

IV. Long-Term Consequences of Covid-19 Layoffs

Equipped with our random forest, we can predict the long-term cost for each displaced worker. In our main analysis, we focus on workers with at least two years of tenure separating from their employers in a mass-layoff. These are the same restriction that are typically applied in the literature and that were used to train the random forest. As mentioned before, we are aware that the Pandemic Recession might be different from previous recessions. Our machine-learning algorithm is trained on past mass-layoff events, which implies that in our prediction exercise it is implicitly assumed that the impact of all included channels has not changed. At the moment of writing this paper we do not know whether we will observe some structural changes. Nonetheless, as we show further, abstracting from plausible structural breaks and focusing only on changes in pools of displaced workers is sufficient to document that the Covid-19-related earnings losses are very different from the past ones. This difference might be amplified even more if some new and currently unknown properties

Covid Economics 47, 4 September 2020: 70-107

Table 1: Consequences of job loss - mass layoffs only

	Prior to Great Recession	Great Recession	Prior to Covid-19	Covid-19
All				
Pre-displ. Income	33,281.620	35,229.560	33,255.900	26,600.030
Earnings Losses (Euros)	63,600.580	72,700.760	60,947.730	38,062.180
Earnings Losses (% of Pre-displ. Income)	191%	206%	183%	143%
Emp. Losses (Days)	439.552	476.516	494.559	478.354
Log Wage Losses	0.061	0.076	0.055	0.019
Cor(Emp. Loss , Earn. Loss)	0.547	0.464	0.537	0.589
Female				
Pre-displ. Income	25,897.740	26,882.620	26,618.460	22,325.920
Earnings Losses (Euros)	52,380.900	58,560.430	53,396.870	30,714.660
Earnings Losses (% of Pre-displ. Income)	202%	218%	201%	138%
Emp. Losses (Days)	447.578	501.669	515.076	471.180
Log Wage Losses	0.057	0.071	0.054	0.017
Cor(Emp. Loss , Earn. Loss)	0.570	0.480	0.534	0.642
Male				
Pre-displ. Income	39,585.170	39,223.190	38,829.210	29,646.810
Earnings Losses (Euros)	73,178.720	79,466.260	67,288.020	43,299.820
Earnings Losses (% of Pre-displ. Income)	185%	203%	173%	146%
Emp. Losses (Days)	432.701	464.481	477.331	483.468
Log Wage Losses	0.064	0.079	0.056	0.020
Cor(Emp. Loss , Earn. Loss)	0.574	0.512	0.576	0.585

Earnings, employment and log-wage losses of all masslayoff UI claimants with 2+ years of job tenure, see text for definition of mass layoff. Covid-19 refers to March-May 2020, Pre Covid-19 to March-May 2018 and 2019, Great Recession to 2009 and Pre Great Recession to 2007. Earnings and employment losses are cumulative over 11 year, while log-wage losses are average declines. Results from a generalized random forest. Positive number imply losses, while negative numbers imply gains.

of the Pandemic Recession emerge in the near future.

A. Average cost of job displacement

Table 1 presents the average cost in terms of earnings, employment, and log-wage losses of job terminations during mass-layoff events. The reported statistics are broken down by gender for layoffs that occurred in four different periods: prior to the Great Recession, the Great Recession, prior to the COVID-19 crisis, and the COVID-19 crisis. First, in comparison to years prior to the COVID-19 outbreak, the predicted earnings losses in 2020 are substantially lower. While in the previous episodes the average long-term losses of job termination were estimated at the level of almost 200% of the pre-displacement annual income, recently displaced workers can expect much lower losses amounting to 143%. The dynamics of losses is quite interesting. Typically, job terminations in downturns are associated with higher losses.[19] In fact, this was observed during the Great Recession, when both employment and wage losses increased, which lead to an overall rise in earnings losses. In contrast, both wage and employment losses decreased for job terminations during the pandemic in comparison to the pre-COVID-19 levels. Recent job losers can expect yearly wages to decline by 2 percent on average for the next 11 years, compared to the control group who kept their jobs. This number is strikingly low in comparison to the previous years, where wage losses are three to four times as high.

The dynamics of losses by gender are the same as for the whole population. For all periods the predicted employment losses for women were higher than for men, likely a result of the lower labor market attachment of women. The log-wage losses are nearly the same for both gender for all periods. For all episodes except the Pandemic Recession, women's average costs exceeded 200% and was much higher than for males. Only during the current COVID-19 crisis the gender gap in the relative earnings losses reduced to a one-digit number equal to 8 percentage points.

Our findings can help to understand the shape of the recovery from the Pandemic Recession. Because we expect workers to incur employment losses of a similar magnitude as in the Great Recession, we predict a similar sluggish employment recovery as after the Great Recession. Another well documented fact of the Great Recession was the extremely slow wage growth during the recovery (Pinheiro and Yang, 2017). Here our findings provide a silver lining. The group of workers affected by the COVID-19 job losses is expected to have much lower wage losses upon re-employment compared to previous experiences. This sug-

[19] See e.g. Davis and Von Wachter (2011).

Covid Economics 47, 4 September 2020: 70-107

Covid Economics 47, 4 September 2020: 70-107

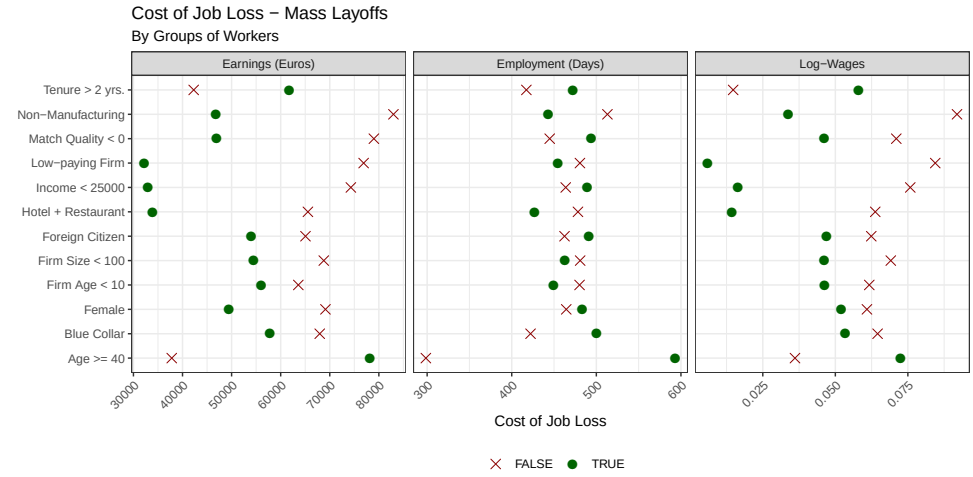

Figure 2: The figure shows the estimated cost of job losses for different groups of workers. Subgroups indicated by green dots experienced larger increases in UI claims, see Figure 1. Sample consists of UI claimants pooled over all samples conditional on mass-layoff, see text for definition. Estimated earnings losses from a generalized random forest.

gests that purely from the different composition of UI claimants we can expect less human capital being destroyed which points towards a quicker recovery in wages after the end of the Pandemic Recession.

B. Who losses more?

To understand why the predicted losses decreased for COVID-19 job losses and increased during the Great Recession we take a closer look on losses across displaced employees. Figure 2 shows average losses in earnings, employment, and wages for different groups of workers. This also allows us to judge the plausibility of our predictions. As mentioned before, usually during recessions the pool of unemployed shifts towards worker and job characteristics that are associated with better labor market outcomes. In Gulyas and Pytka (2020) we show that this compositional change almost entirely explains why workers displaced during recessions face higher earnings losses. During the COVID-19 episode we observed something completely different. Almost all groups whose UI take-ups increased proportionally more during the Pandemic Recession (green dots) are also associated with *lower* earnings and wage losses. The COVID-19 layoffs disproportionately affected the hotel and restau-

Covid Economics 47, 4 September 2020: 70-107

rant industry and other non-manufacturing sectors which employ many low income workers and in addition typically have the lowest firm wage premia.[20] UI claimants during the first three months of the Pandemic recession not only earned 25 percent less than the average UI claimant during the Great Recession, but also lost jobs with a whopping 24 percent lower employer-specific wage component (see table 3 in the appendix). Interpreted through a job-ladder model, it will be easier for workers to find a similarly paying job if they were not very high up on the firm quality ladder. This is consistent with the pattern seen in the right panel in Figure 2, where the workers with prior lower firm wage premia experience lower log-wage losses. This is also confirmed by Gulyas and Pytka (2020) and Schmieder *et al.* (2020), who show that firm wage premia is an important factor in explaining earnings losses. Given this information, it is not surprising that our machine-learning procedure predicts lower wage losses for the Covid-19 UI claimants.

Furthermore, recent layoffs were more common for smaller and younger firms, which are typically financially less stable companies.[21] As Figure 2 shows, job losses at these companies are associated with lower earnings losses. This potentially can be explained by the future earnings dynamics of workers from the control group. The employees who kept their jobs at such firms can be fired in future events or their future wage promotion can be slower than in other firms. Consequently, this can explain why the displacement cost from such employers is relatively lower.

Overall, almost all groups that are relatively more affected by layoffs during Covid-19 are also groups that experience lower earnings losses in general. The lower predicted wage losses are a reflection of the fact that the Pandemic recession hit groups of workers that were already disadvantaged in terms of income, firm wage premia, and match quality. This pattern is not observed for employment losses, which explains why we predict a similar employment losses compared to the Great Recession.

C. Heterogenous costs of job displacement

Documenting the differences in average cost of job loss is important to our understanding of the recovery from the current Pandemic Recession. But as Figure 3 shows, the averages mask a lot of individual heterogeneity in the long-term consequences of job losses. First, we can see that heterogeneity is substantial for all periods. For example, before the Covid-19 shock, almost a quarter of workers were experiencing wage gains after mass layoffs, whereas

[20] See e.g. Krueger and Summers (1988).
[21] A similar finding was made by Alstadsæter *et al.* (2020) for Norway.

Covid Economics 47, 4 September 2020: 70-107

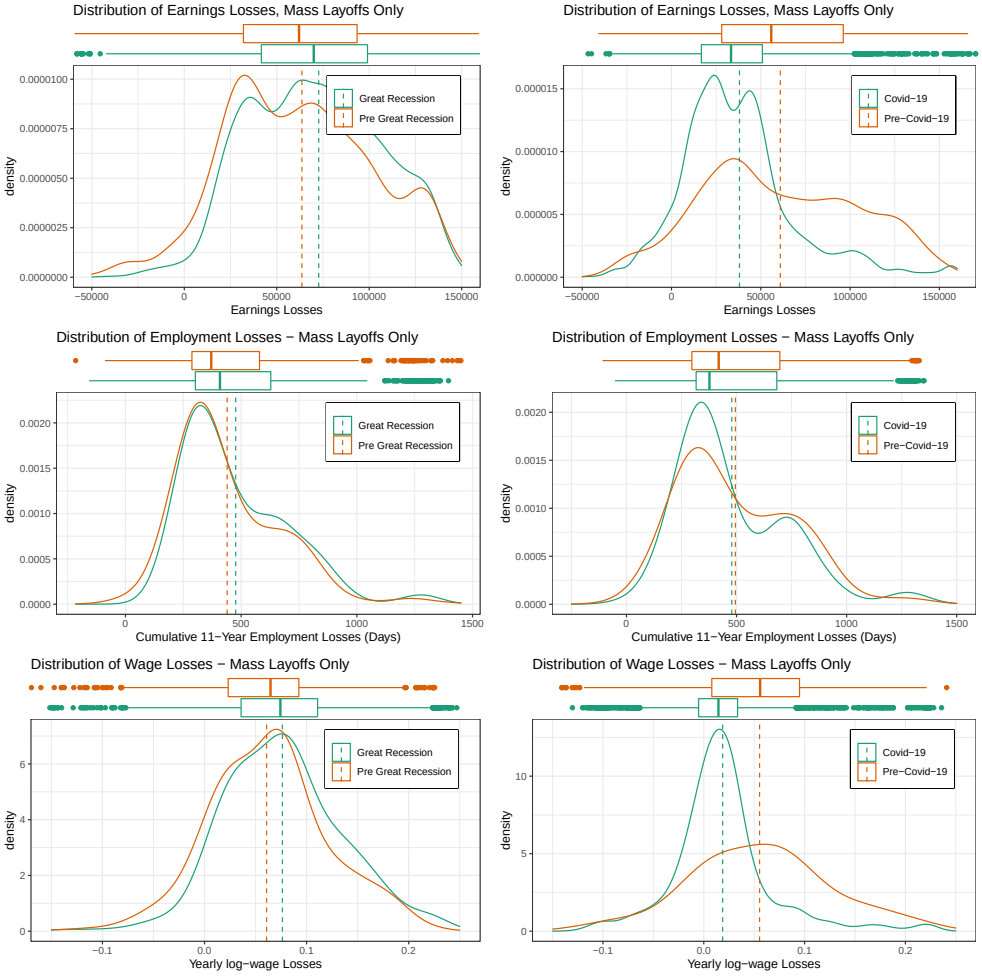

Figure 3: The figure shows the distribution of predicted earnings losses for every mass-layoff UI claimant with 180+ days of job tenure and positive earnings in the year prior to the separation. Covid-19 refers to March-May 2019, Pre Covid-19 to March-May 2018 and 2019, Great Recession to 2009 and Pre Great Recession to 2007. Predicted earnings losses from a generalized random forest. Earnings and employment losses are cumulative over 11 years, while log-wage losses are average declines. Positive numbers imply losses, while negative numbers imply gains. On the top of each panel there is a boxplot with quartiles and outliers. Dashed lines show means.

Covid Economics 47, 4 September 2020: 70-107

another quarter suffered permanent wage declines by more than 10 percent.

Second, while the distribution of employment losses during the Pandemic Recession is comparable to before, the distributions of log-wage and earnings losses stand out. Not only did the whole distributions of log-wage and earnings losses shift towards lower losses, but the distribution shows much lower dispersion. The interquartile range prior to the Pandemic Recession was equal to 8.4 log points and it decreased by over 50 percent to 4 log points. This is something new in comparison to previous experiences. During the previous crisis the wage losses were characterized with a higher average but similar dispersion. This is likely because the Covid-19 recession hit a much narrower segment of the labor market, compared to the Great Recession, which saw job losses across the board.

We also documented the distribution of earnings, employment and log-wages for the Covid-19 job losses separately by gender (Figure 10 in the Appendix). The distribution of employment and wage losses look surprisingly similar for men and women. The only noteworthy difference between men and women is perhaps that earnings losses for men are somewhat more dispersed, which is due to the higher dispersion in earnings for men.

Given the large amount of heterogeneity in earnings losses across workers, where a considerable fraction of workers even experience wage gains, any government intervention should likely be target. The next section presents how our algorithm can be used to identify high loss individuals.

V. Targeting Policies

Even though we expect lower earnings losses from the Pandemic Recession compared to the past, the average worker affected by a mass layoff still faces significant declines in income. Thus, policy interventions such as avoiding costly job losses through firm bail-outs and short-time work subsidy schemes, or policies aimed at insuring workers from the income losses through unemployment insurance extensions and top-ups are likely warranted. Moreover, we showed in the previous section that there is substantial heterogeneity in losses across different workers. For instance, 30% of workers can expect higher wages after re-employment. Thus, targeting policy interventions towards individuals that can expect wage losses would likely result in welfare gains. To detect workers with positive log wage losses we build a simple policy tree in the spirit of Athey and Wager (2017).[22] In general, depending on the welfare

[22]A certain caveat needs to be applied here. The reported losses are identified with our random forest, which was grown using pre-Covid-19 mass-layoff events. Our machine-learning technique allows us to predict individual earnings losses. As discussed before, the Covid-19 episode may be quantitatively different also

Covid Economics 47, 4 September 2020: 70-107

criteria of the policy maker and budgetary generosity of the intervention optimal trees might look different. That being said, we decided to focus on wage losses due to its persistency.[23]

In the considered time window of the Pandemic Recession, 3,227 workers were displaced in mass-layoff events and have not been recalled by their previous employer. Using our methodology we identified 2,104 individuals with losses in log wages and 1,123 people that are predicted to benefit from a job termination in terms of their reemployment wages. The tree forecasts whether estimated wage losses of each individual is positive ($y = 1$ if so, $y = 0$ otherwise). To provide an accurate but simple decision rule, we keep the max depth of the tree to 4.[24] Figure 4 illustrates the generated classification tree. Each node is characterized with three numbers. The dominant category in each node is reported on the top. The fraction of observations with positive wage losses in the node and the fraction of overall observations that fall in the node are shown in the middle and the bottom, respectively. Table 7 in the Appendix presents its confusion matrix computed on the set of people displaced in COVID-19 mass layoffs. Despite its simplicity, the prediction performance with an overall accuracy 86.02% is very good. 86.82% of individuals with positive wage losses are detected correctly.[25] Workers who are classified by our tree for targeting are expected to suffer a wage declines by 3.96 log points on average. Those workers who would not be selected in contrast are expected to see wage gains of more than two percent. This highlights the potential usefulness of the algorithmic decision tree for policy targeting.

Inspecting the policy tree further also reveals more about the underlying channels of wage losses. The first split chosen by the algorithm is associated with firm wage premia, which only reconfirms the importance of this variable for explaining the losses. It is quite striking that 97% of workers displaced from employers paying above the median face wage losses which amount to close to six percent on average.

On the other hand, for workers fired from low-paying firms it is much easier to find jobs with better pays. An interaction of a job-specific accumulated human capital, firm rents at other employers in a region, and a worker's age determines how likely it will be. Most of those employees who in addition have a relatively shorter job tenure will find better paying

in how observations with certain worker, job, and business-cycle characteristics are affected by a job loss. Our analysis does not include this effect.

[23] In Appendix F, we present an alternative tree grown to detect heterogeneity in the overall earnings losses.

[24] This also rules out potential problems of overfitting.

[25] In designing targeting policies the latter statistics can be even more important than the accuracy. Given budgetary constraints policy makers might want to sacrifice the accuracy and be less stringent in classifying somebody as needing help so as to reduce the false negative error rate, which in our case is equal to the fraction of people with actual wage losses predicted to have no losses.

CEPR PRESS

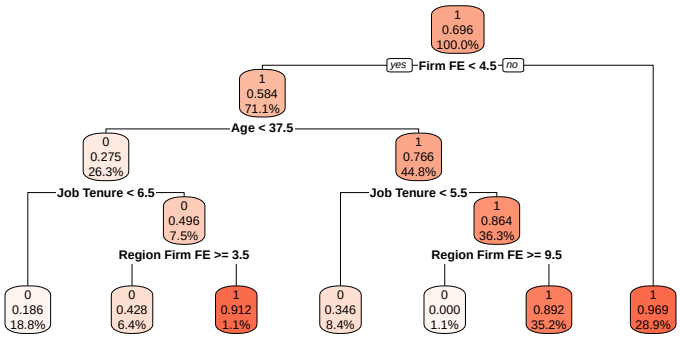

Figure 4: Classification tree classifying individuals with wage losses. On the top there is the most common value. The fraction of observations with wage losses in a node is reported in the middle. The fraction of observations in the global sample is shown in the bottom.

jobs. Depending on age it varies between $(100\% - 18.6\% =)81.4\%$ for younger workers and $(100\% - 34.6\% =)65.4\%$ for older workers. This difference might suggest that younger people are better skilled in looking for jobs (*e.g.*, due to better computer literacy) or that prospective employers discriminate older workers with similar characteristics. Next, lost job-specific human capital accumulated at a previous employer can be offset with availability of good jobs on the market. Again, it will be easier for younger workers. For them even slightly below-median regional firm premia are enough. Older workers are able to compensate wage losses implied by destructed job-specific human capital only if they will look for jobs in regions with the best paying firms.

We fully acknowledge that our decision tree does not provide a comprehensive welfare analysis of these policy recommendations. But we believe that by revealing which factors are more important drivers of earnings losses, our decision rule provides important insights for policy makers.

VI. Conclusions

Using the universe of Austrian unemployment insurance records, we document that the composition of UI claimants during the pandemic crisis was substantially different compared to previous experiences. In contrast to a typical recession, the pool of Covid-19 UI claimants shifted towards worker and job characteristics that are associated with worse labor market

Covid Economics 47, 4 September 2020: 70-107

outcomes. During the first three months of the Pandemic Recession, UI claims increased relatively more for females, low paid workers, as well as for younger, smaller and worse-paying firms. Using a machine-learning algorithm developed in Gulyas and Pytka (2020) we predict the individual cost of job loss for COVID-19 job losers conditional on their worker and job characteristics. As we show, those job terminations are associated with much lower losses in earnings and wages compared to the Great Recession, but similar employment losses.

The COVID-19 layoffs disproportionately affected the hotel and restaurant industry and other non-manufacturing sectors which employ many low income workers and typically have the lowest firm wage premia. In general, our study reconfirms our previous finding from Gulyas and Pytka (2020) stressing that firm wage premia is the most important factor in explaining earnings losses. Interpreted through a job-ladder model, it will be easier for workers to find a similarly paying job if they were not very high up on the ladder. Moreover, we document that recent layoffs were more common for smaller and younger firms, where job terminations are associated with lower earnings losses. Therefore, it is very important to take compositional changes of UI claimants into account for estimating earnings losses.

Given this significant heterogeneity in earnings losses across individuals, any policy intervention aimed at avoiding job losses such as firm bail-outs and short-time subsidy schemes should likely be targeted. We present a simple but accurate decision rule for policy makers to target individuals with high wage losses: (i) workers displaced from employers paying above the median and (ii) workers with a relatively long job tenure displaced from low paying firms in regions with fewer well-paying jobs on the market.

REFERENCES

ABOWD, J. M., KRAMARZ, F. and MARGOLIS, D. N. (1999). High wage workers and high wage firms. *Econometrica*, **67** (2), 251–333.

ADAMS-PRASSL, A., BONEVA, T., GOLIN, M. and RAUH, C. (2020). Inequality in the impact of the coronavirus shock: Evidence from real time surveys. *Journal of Public Economics*, p. 104245.

ALON, T., DOEPKE, M., OLMSTEAD-RUMSEY, J. and TERTILT, M. (2020). *This Time It's Different: The Role of Women's Employment in a Pandemic Recession*. Tech. rep., Working paper.

ALSTADSÆTER, A., BRATSBERG, B., EIELSEN, G., KOPCZUK, W., MARKUSSEN, S.,

Covid Economics 47, 4 September 2020: 70-107

Raaum, O. and Røed, K. (2020). The first weeks of the coronavirus crisis: Who got hit, when and why? evidence from norway. *Covid Economics*, **15** (May, 15).

Athey, S., Tibshirani, J. and Wager, S. (2019). Generalized random forests. *The Annals of Statistics*, **47** (2), 1148–1178.

— and Wager, S. (2017). Efficient policy learning. *arXiv preprint arXiv:1702.02896*.

Breiman, L. (2001). Random forests. *Machine Learning*, **45** (1), 5–32.

Cajner, T., Crane, L. D., Decker, R. A., Grigsby, J., Hamins-Puertolas, A., Hurst, E., Kurz, C. and Yildirmaz, A. (2020). *The U.S. Labor Market during the Beginning of the Pandemic Recession*. Working Paper 27159, National Bureau of Economic Research.

Coibion, O., Gorodnichenko, Y. and Weber, M. (2020). Labor markets during the covid-19 crisis: A preliminary view. *Covid Economics*, **21** (May, 22).

Couch, K. A. and Placzek, D. W. (2010). Earnings losses of displaced workers revisited. *The American Economic Review*, pp. 572–589.

Davis, S. J. and Von Wachter, T. (2011). Recessions and the costs of job loss. *Brookings Papers on Economic Activity*, **43** (2 (Fall)), 1–72.

Dingel, J. I. and Neiman, B. (2020). How many jobs can be done at home? *Journal of Public Economics*, **189**, 104235.

Efron, B. and Hastie, T. (2016). *Computer Age Statistical Inference: Algorithms, Evidence, and Data Science*. New York, NY, USA: Cambridge University Press, 1st edn.

Farber, H. S. (2011). *Job loss in the Great Recession: Historical perspective from the displaced workers survey, 1984-2010*. Tech. rep., National Bureau of Economic Research.

— (2017). Employment, hours, and earnings consequences of job loss: Us evidence from the displaced workers survey. *Journal of Labor Economics*, **35** (S1), S235–S272.

Fuchs-Schündeln, N., Kuhn, M. and Tertilt, M. (2020). *The Short-Run Macro Implications of School and Child-Care Closures*. Tech. rep., Institute of Labor Economics (IZA).

Covid Economics 47, 4 September 2020: 70-107

Gulyas, A. and Pytka, K. (2020). *Understanding the Sources of Earnings Losses After Job Displacement: A Machine-Learning Approach*. Tech. rep., Working paper.

Hastie, T., Tibshirani, R. and Friedman, J. H. (2017). *The elements of statistical learning: data mining, inference, and prediction, 2nd Edition*. Springer series in statistics, Springer.

Jacobson, L., LaLonde, R. and Sullivan, D. (1993). Earnings losses of displaced workers. *The American Economic Review*, pp. 685–709.

Kahn, L. B., Lange, F. and Wiczer, D. G. (2020). *Labor Demand in the Time of COVID-19: Evidence from Vacancy Postings and UI Claims*. Working Paper 27061, National Bureau of Economic Research.

Krueger, A. B. and Summers, L. H. (1988). Efficiency wages and the inter-industry wage structure. *Econometrica: Journal of the Econometric Society*, pp. 259–293.

McCall, J. (1970). Economics of information and job search. *The Quarterly Journal of Economics*, pp. 113–126.

Mongey, S., Pilossoph, L. and Weinberg, A. (2020). Which workers bear the burden of social distancing policies? *Covid Economics*, **12** (May, 1).

Mueller, A. I. (2017). Separations, sorting, and cyclical unemployment. *American Economic Review*, **107** (7), 2081–2107.

Neal, D. (1995). Industry-specific human capital: Evidence from displaced workers. *Journal of Labor Economics*, **13** (4), pp. 653–677.

Pinheiro, R. and Yang, M. (2017). Wage growth after the great recession. *Economic Commentary*, (2017-04).

Schmieder, J. F., von Wachter, T. and Heining, J. (2020). The Costs of Job Displacement over the Business Cycle and Its Sources: Evidence from Germany.

Zweimüller, J., Winter-Ebmer, R., Lalive, R., Kuhn, A., Wuellrich, J.-P., Ruf, O. and Büchi, S. (2009). Austrian social security database. *Available at SSRN 1399350*.

Covid Economics 47, 4 September 2020: 70-107

A. Appendix

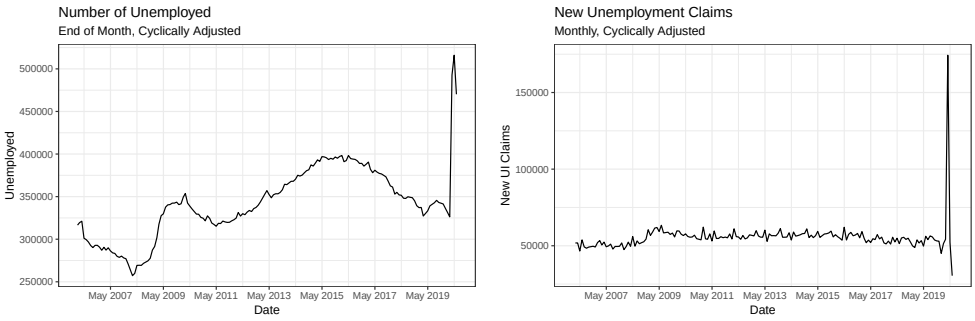

Figure 5: Evolution of number of unemployed and number of UI claiments in Austria. Authors calculation using AMDB data.

Covid Economics 47, 4 September 2020: 70-107

Table 2

	2007	2009	2018 & 2019	COVID-19
New UI Claims	215,894	278,482	94,462	124,178
Mass Layoffs (Share)	0.013	0.023	0.017	0.026
Temporary Layoff (Share)	0.151	0.157	0.082	0.218
Austrian (Share)	0.763	0.744	0.674	0.603
Blue-Collar (Share)	0.658	0.651	0.535	0.678
Female (Share)	0.400	0.375	0.482	0.497
Age (yrs)	37.351	37.795	38.308	39.798
Manufacturing (Share)	0.131	0.213	0.129	0.092
Hotel & Restaurants (Share)	0.113	0.098	0.147	0.269
Firm-Tenure (yrs)	2.355	2.881	2.748	3.167
Income t-1 (Euros)	23,177.290	25,938.530	23,963.470	23,475.610
Firm Size	300.111	328.436	469.929	239.738
Firm Wage Premium	-0.064	-0.037	-0.092	-0.203
Firm Age	16.976	17.797	19.754	17.728
Match Quality	0.026	0.031	-0.088	-0.152
Regional Firm Wage Premium	0.003	0.003	0.013	0.005

Notes: Sample statistics of all new UI claimants conditional on positive earnings in the last year and more than 180 days of job tenure. COVID-19 column refers to new UI claims from March 2020-May 2020, who have not returned to work as of beginning of August.

Covid Economics 47, 4 September 2020: 70-107

Covid Economics 47, 4 September 2020: 70-107

Table 3

	2007	2009	2018 & 2019	COVID-19
Mass Layoffs	2,762	6,313	1,595	3,227
Austrian (Share)	0.756	0.729	0.752	0.477
Blue-Collar (Share)	0.504	0.631	0.445	0.850
Female (Share)	0.461	0.324	0.456	0.416
Age (yrs)	40.919	41.940	42.488	41.866
Manufacturing (Share)	0.301	0.522	0.340	0.084
Hotel & Restaurants (Share)	0.040	0.031	0.031	0.440
Firm-Tenure (yrs)	6.929	7.016	7.153	5.424
Income t-1 (Euros)	33,281.620	35,229.560	33,255.900	26,600.030
Firm Size	393.981	188.450	391.951	218.830
Firm Wage Premium	0.066	0.098	0.003	-0.139
Firm Age	19.979	20.963	24.357	19.112
Match Quality	0.008	0.033	-0.076	-0.189
Regional Firm Wage Premium	0.018	0.002	0.012	0.021

Notes: Sample statistics of all UI claimants originating from mass layoffs, conditional on more than 2 years of job tenure. COVID-19 column refers to new UI claims from March 2020-May 2020, who have not returned to their previous employer as of August 10th.

B. Average cost of job displacement

The average causal cost of job termination of workers displaced in the past mass layoffs can be estimated from the following regression model:

$$y_{it} = \sum_{j=-4}^{10} \delta_j \mathbb{1}(t = t^* + j) \times D_i + \theta D_i + \gamma_t + \epsilon_{it}, \tag{5}$$

where D_i is an indicator for displaced persons, t^* the displacement year and t the current year. To control for the evolution of the control group's earning and initial differences in earnings year fixed effects γ_t and a displacement dummy D_i have been included. On the left-hand side as y_{it}, we use consider three specifications with different dependent variables: total annual labor earnings, employment days, and log average daily wages. Then $\{\delta_j\}_{j=-4}^{10}$

Covid Economics 47, 4 September 2020: 70-107

measure the change in the variable of the interest relative to the baseline year $t^* - 5$, after controlling for differences in initial earnings between the two groups.[26] One year after job displacement, earnings losses amount to approximately €8,000, which on average is the result of employment losses of approximately 70 days and wages decline by about 3 log points. In the following years earnings increase, but the recovery fades out after 5-6 year, after which the losses still amount to €5,000 yearly and log wage losses increase to 6-7.5 log points. The log-wages do not recover.

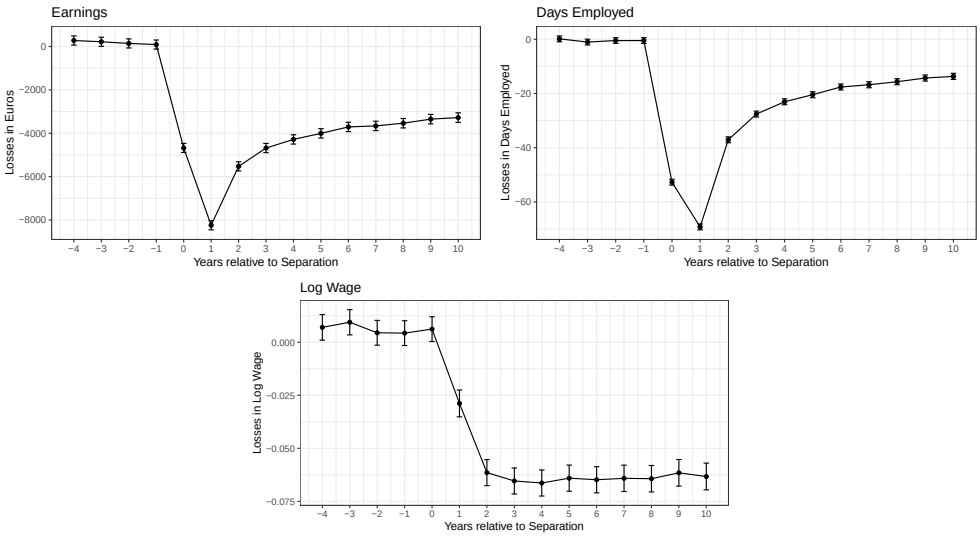

Figure 6: Earnings Losses of displaced workers - Eventstudy regression estimates of Equation (5). Period 0 corresponds to the separation year. Earnings and days employed are computed for the whole year, log wages are computed as the log average daily wage from the employer on 1st January. Control group is selected via propensity score matching.

[26] Figure 6 in the Appendix of this paper depicts event study coefficients δ_t for all periods (before and after displacement), for three variables of the interest. Because of the fact we analyzed mass-layoffs events from 1989 through 2009, the event-study coefficients are estimated using observations from 1984 through 2019.

	Dependent variable:		
	Yearly Income		
	(1)	(2)	(3)
$\hat{\tau}$	−5,850.6	−5,981.3	−5,952.0
	(55.2)	(33.0)	(32.1)
Worker FE		✓	✓
f(age)			✓
Observations	1,365,468	1,365,468	1,365,468
R^2	0.04	0.7	0.7
Adjusted R^2	0.04	0.7	0.7

Table 4: DiD Regression. Estimation results of Equation (3) for different sets of controls

C. Similarity Weights: Machine-Learning Algorithm

It is well known that a single tree tends to exhibit high prediction variance (e.g., Efron and Hastie, 2016; Hastie *et al.*, 2017). For this reason, just as in Athey *et al.* (2019), we have extended our procedure to a random forest in the spirit of Breiman (2001). The idea of this refinement is to grow many trees with bootstrapped datasets and sampling a subset of considered variables for each generated split. Thanks to this procedure, the prediction variance is very often reduced considerably and the impact of variables is smoother.

Equipped with the structure of the random forest, we are in a position to build weights used for estimating (3). Those weights capture the frequency with which other observations fall into the same leaf as the observation of our interest. Note that this means that for each individual the displacement cost is estimated separately using a different set of implied weights. Suppose that there is a forest with B trees indexed by b. Then weight $\alpha_{it}^b(\mathbf{z})$ measures the similarity of observation (i,t) with $\mathbf{z}$ and is defined as:

$$\alpha_{it}^b(\mathbf{z}) := \begin{cases} \frac{1}{|L_b(\mathbf{z})|}, & \mathbf{z}_{it} \in L_b(\mathbf{z}) \\ 0, & \text{otherwise,} \end{cases} \tag{6}$$

Covid Economics 47, 4 September 2020: 70-107

where $L_b(\mathbf{z})$ is the set of all observations, which share the same terminal node ("leaf") with an individual with characteristics $\mathbf{z}$ in tree b and $|L_b(\mathbf{z})|$ is the size of this set. The weight $\alpha_i(\mathbf{z})$ is the average across all trees: $\alpha_i(\mathbf{z}) := \frac{1}{B}\sum_{b=1}^{B}\alpha_{it}^{b}(\mathbf{z})$.

D. Who losses more?

Table 5 presents the average characteristics of displaced workers broken down by the size of the cumulative earnings losses. As can be seen, workers with predicted higher losses are displaced from firms with higher wage premia. While one can also observe some relationships of other variables such as age in quartiles of the predicted costs, we know that the earnings losses by far are the most sensitive to changes in the firm wage premia.[27] Workers who bear the smallest losses (column Tercile 1 in Table 5) are relatively younger and are fired from firms paying substantially (almost 20 log points) below the average market wage. This group of workers is better off in terms of wages and they only suffer a lower number of employment days than the control group. On average the group of the recently displaced workers can expect higher wages than before (wage losses are negative). However, employments losses offset small wage increase, which leads to overall earnings losses. On the other extreme, there are workers with the highest losses (column Tercile 3 in Table 5). They are fired from firms paying only 7.9 log points below the market wage. Those employees are predicted to look for new jobs much longer and to find lower wages in comparison to the previous employers. A quite analogous picture can be drawn if we juxtapose the previous layoffs with the most current ones. As can be seen in Table 3, in 2007 and 2009 terminated jobs came from firms paying above the average market wage (between 6.6 and 9.8 log points) and prior to the Covid-19 episode firing firms were paying at the market average (0.3 log point above to be precise). As a result, on average workers who were recently laid off are predicted to weather the losses relatively well as they are fired from worse firms with worse match quality.[28]

[27] Here we rely on a finding from our previous paper (Gulyas and Pytka, 2020, section VI) where we are able to identify the impact of each variable on the losses separately while keeping all other confounding factors fixed. This result is extremely robust and we arrived at that conclusion through several complementary analyses.

[28] This can be illustrated quite easily in the vanilla labor-search model by McCall (1970). Workers paid below the market wage expect higher wages in their new jobs while workers with above average income are much more likely to suffer more from a job displacement.

Covid Economics 47, 4 September 2020: 70-107

Table 5: Worker and Job Characteristics by Earnings Losses - Mass Layoffs Only

	Tercile 1	Tercile 2	Tercile 3
Earn. Losses	7,231.448	33,406.200	73,581.900
Empl. Losses	297.314	455.434	682.503
Wage Losses	−0.018	0.016	0.058
Blue Collar	0.825	0.878	0.847
Austrian	0.404	0.427	0.600
Manufacturing	0.017	0.046	0.211
Female	0.459	0.473	0.316
Age	32.288	42.231	51.086
Job Tenure	3.713	4.218	8.342
Number of Employers	4.230	6.189	7.720
Firm Size	150.664	294.629	211.188
Match Quality	-0.301	-0.261	-0.007
Firm Wage Premium	-0.203	-0.136	-0.079
Avg. F. Wage Premia	0.031	0.018	0.013
Herfindahl Index	0.015	0.021	0.027
Industry UE-Rate	0.373	0.326	0.281
Regional UE-Rate	0.137	0.139	0.139

Notes: Masslayoffs Only. Table shows mean baseline characteristics for each tercile of predicted treatment effects. Predictions from a causal forest

Covid Economics 47, 4 September 2020: 70-107

Covid Economics 47, 4 September 2020: 70-107

E. Long Term Consequences of Mass Layoffs by Gender

Figure 7

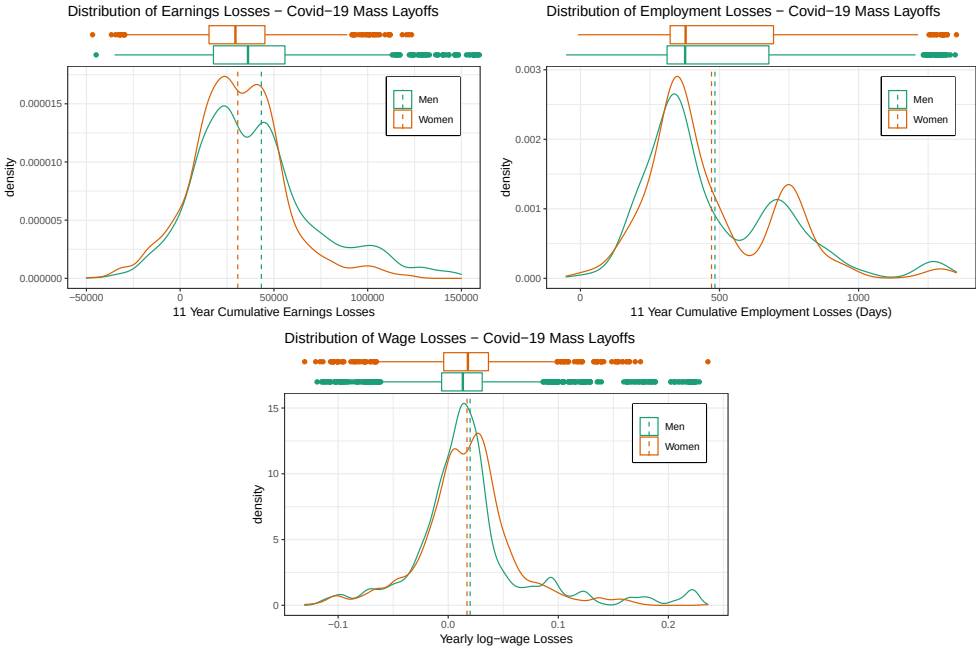

	Predicted wage losses		
Actual wage losses	Negative	Positive	Sum
Negative	25.63%	4.8%	30.43%
Positive	9.17%	60.4%	69.6%
Sum	34.8%	65.2%	100.00%

Table 7: Confusion matrix for the classification tree from Figure 4.

Table 6

	Male	Female
Mass Layoffs	1,884	1,343
Austrian (Share)	0.473	0.482
Blue-Collar (Share)	0.901	0.779
Age (yrs)	42.153	41.462
Manufacturing (Share)	0.107	0.052
Hotel & Restaurants (Share)	0.436	0.445
Firm-Tenure (yrs)	5.781	4.922
Income t-1 (Euros)	29,646.810	22,325.920
Firm Size	209.313	232.180
Firm Wage Premium	-0.124	-0.161
Firm Age	19.107	19.121
Match Quality	-0.106	-0.307
Regional Firm Wage Premium	0.022	0.019

Notes: Sample statistics of all UI claimants originating from mass layoffs, conditional more than 2 years of job tenure. COVID-19 column refers to new UI claims from March 2020-May 2020, who have not returned to work as of beginning of August.

F. Targeting Individuals with High Earnings Losses

Figure 8 depicts the generated tree. The tree forecasts whether estimated earnings losses of each individual is above the median level ($y = 1$ if so, $y = 0$ otherwise). For simplicity the max depth of the tree was set to 2. As can be seen, there are two groups with above-median earnings losses. The first group consists of workers older than 45 years located in all regions except those ones with the highest firm wage premia. In this group of people accounting

Covid Economics 47, 4 September 2020: 70-107

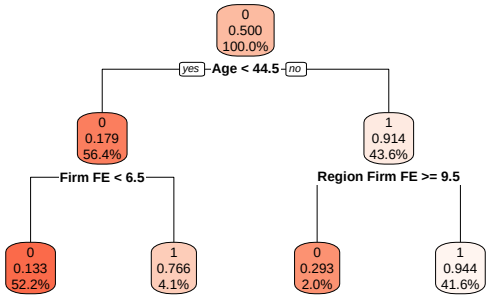

Figure 8: Classification tree predicting earnings losses above the median level. On the top there is the most common value. In the middle there is a fraction of observations with earnings losses above the median. In the bottom there is a fraction of observations in the global sample.

for 40.6% of displaced workers, the overwhelming majority of 94.2% exhibit losses above the median. The second group consists of workers not older than 45 who were displaced from well-paying firms. This group is much smaller though. This very simple criteria allows us to classify 89.96% of displaced individuals correctly and to identify 82.95% of workers with high earnings losses.

G. Analysis for all UI-claimants

This section presents the analysis without conditioning on mass layoffs. The only sample restrictions are that the UI claimant had positive earnings in the year prior to the UI claim, had more than 180 days of job tenure at their previous job, and was not recalled to their previous employer.

Covid Economics 47, 4 September 2020: 70-107

Table 8: Consequences of job loss

	Pre Great Recession	Great Recession	Pre COVID-19	COVID-19
All				
Pre-displ Inc.	23,261.010	25,569.370	24,140.740	23,456.840
Earnings Losses (Euros)	39,711.100	45,188.860	37,832.440	37,674.120
Employment Losses (Days)	369.153	387.481	413.143	447.939
Log Wage Losses	0.017	0.025	0.010	0.013
Cor(Emp. Loss , Earn. Loss)	0.488	0.488	0.487	0.489
Female				
Pre-displ Income	19,088.710	20,023.900	20,190.390	19,719.790
Earnings Losses (Euros)	31,346.670	34,833.750	31,961.990	32,865.590
Employment Losses (Days)	379.732	396.756	427.031	461.439
Log Wage Losses	0.007	0.013	0.003	0.012
Cor(Emp. Loss , Earn. Loss)	0.486	0.489	0.505	0.512
Male				
Pre-displ. Income	26,984.350	29,981.970	27,950.110	27,159.810
Earnings Losses (Euros)	47,175.500	53,428.540	43,493.390	42,438.790
Employment Losses (Days)	359.712	380.101	399.751	434.562
Log Wage Losses	0.025	0.035	0.017	0.014
Cor(Emp. Loss , Earn. Loss)	0.533	0.528	0.502	0.499

Earnings, employment and log-wage losses of all UI claimants with positive earnings in the last year and more than 180 days of job tenure. COVID-19 refers to March-May 2019, Pre COVID-19 to March-May 2018 and 2019, Great Recession to 2009 and Pre Great Recession to 2007. Predicted earnings losses from a generalized random forest. Earnings and employment losses are cumulative over 11 years, while log-wage losses are average declines. Positive numbers imply losses, while negative numbers imply gains.

Covid Economics 47, 4 September 2020: 70-107

Covid Economics 47, 4 September 2020: 70-107

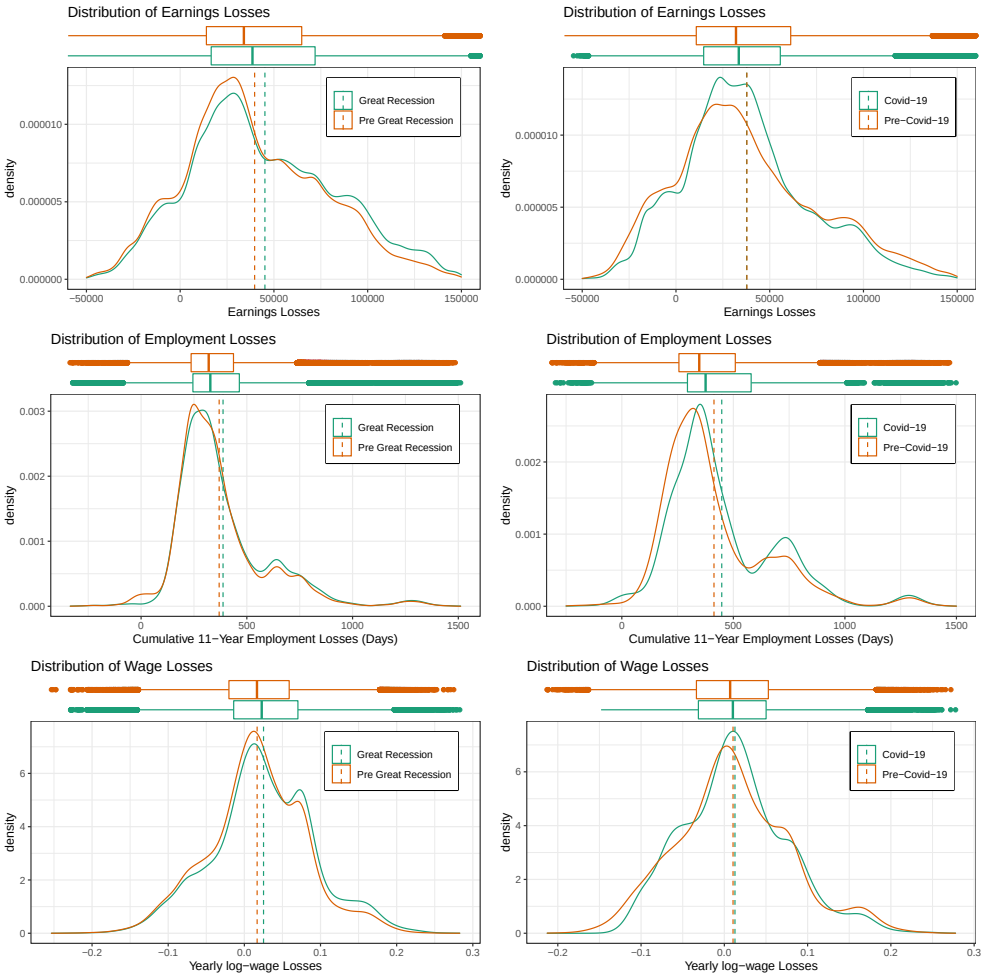

Figure 9: The figure shows the distribution of predicted earnings losses for every UI claimant with 180+ days of job tenure and positive earnings in the year prior to the separation. COVID-19 refers to March-May 2019, Pre COVID-19 to March-May 2018 and 2019, Great Recession to 2009 and Pre Great Recession to 2007. Predicted earnings losses from a generalized random forest. Earnings and employment losses are cumulative over 11 years, while log-wage losses are average declines. Positive numbers imply losses, while negative numbers imply gains.

Covid Economics 47, 4 September 2020: 70-107

Figure 10

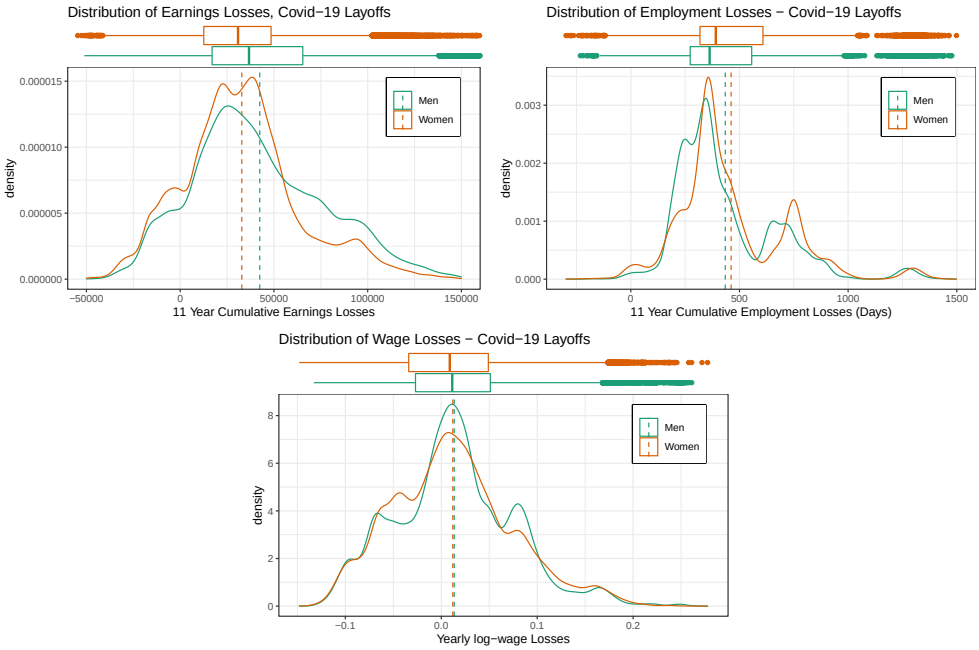

Table 9

	Male	Female
UI Claimants	41,445	41,067
Austrian (Share)	0.578	0.644
Blue-Collar (Share)	0.709	0.506
Age (yrs)	39.073	39.803
Manufacturing (Share)	0.137	0.077
Hotel & Restaurants (Share)	0.201	0.245
Firm-Tenure (yrs)	2.942	3.011
Income t-1 (Euros)	27,159.810	19,719.790
Firm Size	287.514	356.109
Firm Wage Premium	-0.146	-0.216
Firm Age	17.809	18.661
Match Quality	-0.035	-0.284
Regional Firm Wage Premium	0.013	0.009

Notes: Sample statistics of all UI claimants, conditional on 180+ days of job tenure and positive earnings in the year before UI claim. COVID-19 column refers to new UI claims from March 2020-May 2020, who have not returned to work August 1st.

Covid Economics 47, 4 September 2020: 70-107

CEPR PRESS

Table 10: Worker and Job Characteristics by Earnings Losses

	Tercile 1	Tercile 2	Tercile 3
Earn. Losses	2,765.381	33,639.600	76,617.370
Empl. Losses	287.359	477.507	578.951
Wage Losses	-0.036	0.009	0.065
Blue Collar	0.663	0.659	0.501
Austrian	0.545	0.585	0.704
Manufacturing	0.086	0.144	0.259
Female	0.544	0.543	0.407
Age	30.862	41.614	45.834
Job Tenure	1.971	2.621	4.337
Number of Employers	5.021	7.452	8.321
Firm Size	326.776	305.145	333.041
Match Quality	-0.261	-0.277	0.059
Firm Wage Premium	-0.285	-0.197	-0.061
Avg. F. Wage Premia	0.020	0.006	0.007
Herfindahl Index	0.023	0.027	0.030
Industry UE-Rate	0.260	0.231	0.169
Regional UE-Rate	0.133	0.135	0.134

Notes: Table shows mean baseline characteristics for each quartile of predicted treatment effects. Predictions from a causal forest

Covid Economics 47, 4 September 2020: 70-107

Demand for health insurance in the time of COVID-19: Evidence from the Special Enrollment Period in the Washington State ACA Marketplace

Gerardo Ruiz Sánchez[1]

Date submitted: 28 August 2020; Date accepted: 1 September 2020

I study the demand for health insurance during the COVID-19 pandemic using Special Enrollment Period (SEP) individual-level enrollment data from the Washington State Affordable Care Act Marketplace. I document that most individuals enrolling in plans during the pandemic are those who lost minimum essential coverage, followed by uninsured individuals making use of Washington's limited-time SEP for uninsured individuals. I estimate a demand model and find that low-income individuals and young individuals are more premium sensitive. I find that 20.4 percent of the individuals in my analysis sample did not pay their initial premium. Individuals losing minimum essential coverage are less likely to pay their initial premium than individuals using the SEP for other qualifying events. Lower income individuals are less likely to pay the initial premium than higher income individuals. My results suggest three reasons for considering more generous premium subsidies during the remainder of the pandemic: (1) individuals losing minimum essential coverage are already using the exchange to replace lost coverage, (2) consumers are premium sensitive, and (3) there are meaningful differences across demographic groups in the probability of paying the first premium, which is necessary for coverage to take effect.

1 Assistant Professor of Economics, Trinity College.

Covid Economics 47, 4 September 2020: 108-129

Covid Economics 47, 4 September 2020: 108-129

Demand for Health Insurance in the Time of COVID-19: Evidence from the Special Enrollment Period in the Washington State ACA Marketplace

1 Introduction

A growing body of research has found that the COVID-19 pandemic has led to significant job loss in the United States (U.S.) (Cajner et al., 2020; Coibion et al., 2020; Cowan, 2020; Forsythe et al., 2020). It is also well known that employer-sponsored health insurance covers over half of the non-elderly population in the U.S. (Kaiser Family Foundation, 2019). Because health insurance coverage is tied to employment for a significant share of the U.S. population, the COVID-19 pandemic will put many individuals at risk of losing coverage and will expose them to financial risks associated with health shocks. Moreover, recent surveys have found that small businesses that still offer health insurance benefits to their employees during the pandemic are not sure they will be able to keep up with premium payments beyond August 2020 (Dafny et al., 2020). It is therefore likely that millions of Americans will lose their employer-sponsored health insurance as the COVID-19 pandemic evolves. Individuals who face this situation will mainly rely on two public programs to replace their lost health insurance coverage: Medicaid and the Affordable Care Act ("ACA") Marketplaces.

The ACA Marketplaces may become increasingly important during the COVID-19 pandemic since low-income individuals receive subsidies to purchase health insurance plans through the Marketplaces. Typically, most individuals select a health plan during the Open Enrollment Period which happens before the plan year begins. After the Open Enrollment Period, individuals can enroll in a plan using the ACA Marketplaces Special Enrollment Period ("SEP") only if they can show they are undergoing a qualifying life event. These events include the loss of minimum essential coverage (e.g., loss of employer-sponsored insurance), a change in household size (e.g., getting married or having a baby), a change in primary place of living (e.g., moving to a new county or moving to the United States), among others.

In this paper, I study the demand for health insurance plans during the COVID-19 pandemic in the context of the Washington State ACA Marketplace SEP using data on individual-level enrollment and plan premiums. The Washington State ACA Marketplace provides an ideal opportunity to analyze the demand for health insurance during the COVID-19 pandemic for two reasons. First, in response to the pandemic, the Washington Health Benefit Exchange ("WAHBE") opened an Uninsured SEP for uninsured individuals from March 10, 2020 to May 8, 2020. This was a limited-time SEP for individuals who were not able to get insurance during the Open Enrollment Period but were not necessarily going through a typical qualifying life event. Second, the exchange also continued to help individuals that were undergoing a qualifying life event (e.g., loss of employer-sponsored health insurance coverage, change in household size, etc.) as part of their usual SEP operations. The overlap of these SEPs with the pandemic make this an ideal situation to study the demand for insurance during the COVID-19 pandemic.

I combine data from plan selections during the COVID-19 pandemic in the Washington State ACA Marketplace with a model of insurance demand to make three key findings in this paper.

First, summary statistics provide evidence that most individuals using the exchange during the COVID-19 pandemic decided to use the exchange because they indicated they had lost minimum essential coverage or because they were uninsured. Approximately 18,200 individuals in my analysis sample enrolled during the pandemic in 2020 due to lack of coverage or loss of minimum essential coverage. Although I do not have individual-level enrollment data from the 2019 SEP that would enable me to compare my data to the previous year, public reports from the WAHBE state that the increase in plan selections during March and April 2020 (relative to the same period in 2019) was driven by the almost 7,000 uninsured customers using the "Uninsured SEP" and an 80 percent increase in the customers using the existing SEP for loss of coverage

(Washington Health Benefit Exchange, 2020). These facts suggest that the ACA Marketplaces are playing a crucial role in helping individuals who lost or did not have coverage during the pandemic.

Second, my demand model estimates imply substantial heterogeneity in preferences across demographic groups using the exchange during the COVID-19 pandemic. I find that uninsured individuals using the SEP are more price sensitive than those who lost minimum essential coverage. I find that that low-income, subsidized individuals are more premium sensitive than high-income nonsubsidized individuals, and I estimate that younger individuals are more premium sensitive.

Third, I find that having lost minimum essential coverage is strongly associated with a lower probability of not effectuating enrollment relative to other demographic groups. If a person has not effectuated their enrollment, they select and enroll in a plan but never pay the first premium, which means the plan never takes effect. This finding means that even though the descriptive evidence indicates that most individuals selecting a plan in the Washington Marketplace during the COVID-19 pandemic are doing so because they lost minimum essential coverage, these individuals are also less likely to make the first premium payment and effectuate enrollment relative to other demographic groups. I also find that individuals belonging to a higher income category are more likely to effectuate enrollment relative to lower-income individuals.

In order to arrive to these findings, I provide summary statistics and estimate the demand for health insurance during the COVID-19 pandemic using two data sources: (1) administrative individual-level enrollment data from the WAHBE between March 10, 2020 and July 1, 2020; and (2) 2020 plan year insurer rate filings from the Office of the Insurance Commissioner of Washington State. The enrollment data contain individual-level demographic information that is useful to compute pre-subsidy and net-of-subsidy annual premiums (i.e., income as a percentage of the federal poverty line, age group, and county of residence). The enrollment data do not contain information on exactly which plan was selected by the individual. However, I am able observe the county, metal tier, and insurance company of the plan selected in the enrollment data. I can therefore combine the enrollment data with the insurers' rate filings data to construct the average net-of-subsidy premium that individuals faced for each metal-insurer combination in their choice set, where this choice set is determined by their county of residence.

I use this dataset to formulate and estimate an individual-level demand model in which individuals have heterogenous preferences for metal-insurer combinations in their choice set. Preferences for plans in my model depend on the average net-of-subsidy annual premium they pay, the plan's generosity measured by the actuarial value of the plan (accounting for cost sharing reductions when applicable), a metal-insurer fixed effect, and individual demographic characteristics. I allow for the premium and actuarial value coefficients in the demand model to vary across age groups, income categories, and qualifying event groups. I then use pricing rules from the exchange to estimate my model and address the potential endogeneity of premiums. Because 21-year-old base annual premiums are adjusted by age factors and income-based subsidies to determine the net annual premiums faced by consumers, I estimate demand for health plans using a conditional indirect utility specification with metal-insurer fixed effects so that I capture any unobservable factors that might affect pricing decisions of insurance companies (e.g. hospital networks). Conditional on the fixed effects, the exchange pricing and subsidy regulations generate individual-level exogenous variation in net-of-subsidy premiums across individuals with different ages and income. I also exploit the fact that choice sets vary across counties. My approach is similar to the literature estimating demand in the ACA Marketplaces and leveraging market regulations that induce exogenous variation in prices to estimate demand (e.g., Polyakova and Ryan, 2019; Saltzman, 2019; and Tebaldi, 2020).

Following the literature that studies consumers' premium sensitivity in the individual market (e.g., Chan and Gruber, 2010; Ericson and Starc, 2015; Hackmann and Kowalski, 2015; Shepard, 2016; Abraham et

Covid Economics 47, 4 September 2020: 108-129

al., 2017; Jaffe and Shepard, 2017; Finkelstein, Hendren, and Shepard, 2019; Drake, 2019; Saltzman, 2019; Tebaldi, 2020), I calculate the own-premium semi-elasticities implied by my estimation results across different demographic groups. My estimation results imply that individuals selecting plans through the exchange during the COVID-19 pandemic are extremely sensitive to premium changes. I estimate that younger individuals are significantly more price sensitive. I also find that low-income individuals (those who do not receive premium subsidies) are more premium sensitive.

Finally, I use the data to explore which individuals are more likely to make the first premium payment to the insurance company issuing the plan they selected. That is, who selects a plan and effectuates the enrollment. I use ordinary least squares and binomial logit models to estimate the probability that an individual effectuates enrollment as a function of individual demographic variables and characteristics of the selected plan.

2 Related literature and main contributions

This paper makes three main contributions. First, my paper contributes to the literature studying the Affordable Care Act Marketplaces (Frean et. al 2017; Sacks, 2017; Abraham et al., 2017; Drake, 2019; Saltzman, 2019; Tebaldi, 2020) by studying the demand for insurance in the context of the COVID-19 pandemic. To the best of my knowledge, this is the first paper to study the demand for insurance during the COVID-19 pandemic using individual-level data and insurers' rate filings price data from the ACA Marketplaces. In contrast with previous studies in the literature, I study demand for insurance during the Special Enrollment Period in the ACA Marketplaces because it is an ideal situation to analyze whether individuals losing minimum essential coverage (i.e., mostly losing employer-sponsored health coverage during the pandemic) are using the exchanges during the pandemic.

Second, previous studies of the ACA Marketplaces do not explore whether enrollment in the selected plan is effectuated or not among the individuals who selected a plan in the exchange. One of the reasons for not doing this is that under normal circumstances, Marketplace effectuation rates are relatively high. For example, according to a recent report (Centers for Medicare and Medicaid Services, 2020) based on data from Marketplaces of all states the effectuation rate for consumers who made plan selections during the 2020 Open Enrollment period was 94 percent. However, in the context of the COVID-19 pandemic, where individuals are losing their jobs and are more financially constrained than usual, the probability of making the first premium payment may go down during the SEP. Indeed, my data reveal that the effectuation rate within my analysis sample was only 79.6 percent during early months of the pandemic. I therefore use my data to estimate the probability that an individual makes the first premium payment for the selected plan as a function of individual demographic variables and the characteristics of the plan selected. My paper contributes to the ACA Marketplaces literature by exploring whether there are meaningful differences in effectuation rates across demographic groups during the COVID-19 pandemic.

Finally, my paper contributes to the literature examining consumer premium sensitivity in the health insurance exchanges (Chan and Gruber, 2010; Ericson and Starc, 2015; Shepard, 2017; Jaffe and Shepard, 2017; Finkelstein, Hendren, and Shepard, 2017; Abraham et al., 2017; Drake, 2019; Saltzman, 2019; Tebaldi, 2020). My paper complements this literature because I formulate and estimate an insurance demand model to provide own-premium semi-elasticity estimates across demographic groups during the COVID-19 pandemic.

Covid Economics 47, 4 September 2020: 108-129

Covid Economics 47, 4 September 2020: 108-129

3 The Washington Health Benefit Exchange (WAHBE): Institutional background and data

3.1 WAHBE institutional background

The WAHBE is Washington State's ACA Marketplace, where eligible individuals can compare, select, and pay monthly premiums for plans that have been certified to meet certain standards for essential health benefits. The marketplace web site displays information on premiums and plan generosity to consumers. Plans are classified using a metal label that represents the plan's actuarial value, or generosity. The actuarial value ("AV") of a health plan is equal to the percentage of average costs for covered benefits that will be paid by that health insurance plan. The higher the actuarial value, the more generous the plan coverage is. The metal labels are gold (80% AV), silver (70% AV) and bronze (60% AV). A type of high-deductible plan called a "catastrophic" plan is only available for people under the age of 30 or people with a hardship exemption (e.g., homelessness, domestic violence). Insurance companies can offer plans in all counties in the state or may choose to offer them only in a subset of counties.

Low-income households are eligible to receive two forms of financial assistance: advanced premium tax credits ("premium subsidies"), which reduce the monthly premium payments, and cost-sharing reduction subsidies ("cost-sharing subsidies"), which increase the actuarial value of silver plans bought by low-income households. To be eligible to receive premium subsidies, household income must be below 400 percent of the federal poverty line. To be eligible to receive cost-sharing subsidies, an individual must meet the following criteria: enroll in a silver plan and have an annual income below 250 percent of the federal poverty line.

Under the ACA, health insurance companies must charge the same annual premium regardless of pre-existing conditions or health status. However, pricing regulations allow insurers to vary premiums across ages in a predetermined way. Insurers must first submit 21-year-old base annual premiums for each plan. Given the submitted base prices, the pre-subsidy annual premium (also equal to the revenue for the insurer) for a given individual is computed using an age adjustment factor table. The age adjustment starts from 0.765 for the 0-14 age group, is equal to 1 for 21-year-old individuals, increases to 1.5 at age 46, and reaches 3 for individuals above 64 years old.

Net-of-subsidy annual premiums are computed by subtracting the premium subsidy that an individual qualifies for from the pre-subsidy annual premiums of the plans in their choice set (except catastrophic plans). The size of the premium subsidy depends on (1) the individual's income as a share of the federal poverty line and (2) the annual premium of the second cheapest silver plan in that individual's county of residence. The ACA subsidy regulation establishes a cap on the premium amount the individual should pay for the second cheapest silver plan. The cap does not vary by age and is only a function of the individual's income as a share of the federal poverty line. This cap increases with income so that higher income individuals receive lower premium subsidies.

Formally, the net-of-subsidy annual premium of plan k for individual i living in county c is given by the following formula:

$$max\left\{0, AgeFactor_i * BasePremium_k - max\{0, AgeFactor_i * Benchmark_c - IncomeCap_i^{FPL}\}\right\}$$

where $BasePremium_k$ is the 21-year-old base annual premium for plan k and $Benchmark_c$ is the 21-year-old base annual premium for the second cheapest silver plan in county c where both $BasePremium_k$ and $Benchmark_c$ are adjusted by the age factors described above. If the subsidy is high enough, there can be zero-premium health insurance plans available to low-income consumers (see, for example, Branham and DeLeire, 2019). I provide more detail on how I calculate these prices in **Appendix A**.

Covid Economics 47, 4 September 2020: 108-129

3.2 Data from the Washington Health Benefit Exchange

I obtained anonymized individual-level administrative data for all individuals who selected a health insurance plan through the WAHBE between March 10, 2020 and July 1, 2020. This includes the "Uninsured SEP" that was open for uninsured individuals from March 10 to May 8. These data are a rich source of individual-level characteristics for individuals who selected a plan during the first months of the COVID-19 pandemic. Each observation contains a unique individual-level identifier, gender, age group (e.g., 0-17, 18-25, 26-34, 35-44, etc.), county of residence, whether the individual received a subsidy or not, income as a percent of the federal poverty line (FPL), and the type of qualifying event that applied to the individual seeking coverage during the SEP. I also observe whether the enrollment in the plan selected was effectuated (i.e., whether the insurer received the first premium payment from the enrollee).

The data also contain information about the plans these individuals selected. I observe the selected plan's metal tier (Catastrophic, Bronze, Silver, or Gold) and the selected plan's health insurance issuer (e.g. BridgeSpan, Molina, etc.). One limitation of my data is that I do not observe exactly which health plan was selected. My demand model therefore models choices at the individual-county-insurer-metal level using an average net-of-subsidy annual premium at the county-insurer-metal level. **Appendix A** provides further details on why using these averages as prices is a reasonable way to deal with the limitations of my data. In particular, many insurers only offer one plan for a given metal tier, and there is limited variation in base annual premiums that belong to the same county-insurer-metal combination when there is more than one plan to construct the average premiums.

The raw dataset originally contains 30,882 plan selection records from March 10, 2020 to July 1, 2020. As explained further in **Appendix A**, I discard observations that have missing variables to arrive at an individual-level dataset of 27,871 plan selection records that I use in the main analysis of this paper.

3.3 Data from the Office of the Insurance Commissioner of Washington State

I collected plan-level information for all plans offered in the Washington Marketplace for the 2020 plan year using the rate filings that can be found in the Office of the Insurance Commissioner of Washington State webpage. The plan-level information found on the rate filing documents include the plan's name, the insurance company offering the plan, the metal tier of the plan, the set of counties where the plan is available and the annual premiums that will be charged for each type of individual based on their age and county of residence.

I first use these rate filings to construct the average annual premium for a 21-year old at the county-insurer-metal level. This enables me to compute average pre-subsidy annual premiums at the county-insurer-metal level for different age groups using the age rating factors used in the exchange. Since the individual enrollment data contains a county of residence variable, I can use the rate filings data to determine their insurer-metal choice set. I then merge the average pre-subsidy annual premiums onto the enrollment data such that each individual has the appropriate choice set for their county of residence. Finally, I use the demographic information in the enrollment data to compute average net-of-subsidy annual premiums at the county-insurer-metal level for individuals who are reported to have a subsidy in the enrollment data. **Appendix A** also provides more details on this process.

3.4 Summary statistics of the analysis sample

Table 1 displays summary statistics for the individuals in my analysis sample who selected a plan through the exchange between March 10, 2020 and July 1, 2020.

This table provides important descriptive evidence that the ACA exchanges are serving individuals who lost minimum essential coverage (e.g., loss of employer-sponsored coverage) and individuals who were uninsured that otherwise would not have been able to use the exchange were it not for the Uninsured SEP during the pandemic. For example, note that 41.2 percent of individuals in my analysis sample report selecting a plan because they lost minimum essential coverage. In addition, 24.2 percent of individuals in my analysis sample report selecting a plan because they were uninsured and took advantage of WAHBE's SEP for uninsured individuals. The other 34.6 percent includes individuals whose SEP qualifying event is a change in household size, an exceptional circumstance, a change in primary place of living, an enrollment plan error, an income change, a tax reconciliation, and so on.

Table 1

Summary statistics for the analysis sample: demographic and choice distribution

Qualifying Life Event		Insurance Company Selected	
Loss of Minimum Essential Coverage	41.2	BridgeSpan	1.8
Uninsured	24.2	Coordinated Care	18.7
Other	34.6	Kaiser Northwest	2.7
Age group		Kaiser WA	21.1
0-17	5.3	LifeWise	17.6
18-25	9.7	Molina	29.1
26-34	23.7	Pacific Source	2.0
35-44	19.6	Premera	6.5
45-54	18.1	Providence	0.4
55-64	22.3	Plan Type Selected	
65 +	1.3	EPO	29.0
Income group		HMO	69.4
0% to 138% FPL	8.32	PPO	1.6
138% to 250% FPL	40.83	Annual premium to be paid if enrollment is effectuated	
250% to 400% FPL	21.32	0% to 138% FPL	$256
No Premium Subsidy (over 400% FPL)	29.54	138% to 250% FPL	$1,337
Gender		250% to 400% FPL	$3,151
Male	44.8	No Premium Subsidy (over 400% FPL)	$5,034
Female	55.2	Was enrollment effectuated?	
Metal Tier Selected		Yes	79.6
Bronze	45.6	No	20.4
Silver	41.6		
Gold	10.2		
Catastrophic	2.6	Number of individuals in the analysis sample	27,871

Data source: Individuals who selected a plan during the Special Enrollment Period between March 10, 2020 and July 1,2020 in the Washington Health Benefit Exchange (WAHBE). Note: FPL = Federal Poverty Line.

The data also reveal that 23.6 percent of the individuals selecting a plan are 55 years old or older. Since older people are an important risk group during the COVID-19 pandemic, it is not surprising that they comprise a considerable share of individuals seeking coverage in the exchange. Individuals with incomes below 400 percent of the federal poverty line make up roughly 70 percent of the analysis sample and individuals with incomes below 250 percent of the federal poverty line make up roughly 49 percent of the analysis sample. In other words, a considerable share of people seeking coverage through the exchange during the pandemic are receiving premium subsidies and cost-sharing subsidies. The data also reveal that 55.2 percent of individuals seeking coverage during the pandemic are women.

In terms of preferences across metal tiers, bronze plans were the most selected option during the early months of the COVID-19 pandemic, followed very closely by silver plans. Gold plans are, on average, more expensive, which hints at why only 10 percent of the individuals in my analysis sample selected a gold plan even though they provide more generous coverage. Coordinated Care, Kaiser Washington (WA), LifeWise, and Molina were the most selected insurers.

Covid Economics 47, 4 September 2020: 108-129

The data also reveal that more than 20 percent of the individuals in my analysis sample had not effectuated enrollment of the plan they selected. At the end of this paper, I exploit this feature of the data to model the probability of enrollment effectuation as a function of individual demographics and plan characteristics of the selected plan.

Finally, using the rate filings data, the individual demographics in the enrollment data, and the selected insurer-metal tier combination, I compute the average annual net-of-subsidy premium to be paid if enrollment is effectuated after selecting the insurer-metal combination. As we can see in **Table 1**, net-of-subsidy annual premiums are considerably lower among low-income individuals due to the ACA premium subsidy rules. For example, the nonsubsidized individual must pay on average $5,034 per year so that enrollment in their selected plan is effectuated. In contrast, an individual whose income lies between 138 and 250 percent of the federal poverty line will have to pay on average $1,337 per year. In the next section I will leverage the variation in net-of-subsidy annual premiums induced by ACA pricing regulations to estimate demand.

4 Empirical strategy

In this section, I formulate an individual-level discrete choice demand model in which individuals have heterogenous preferences for insurer-metal tier combinations in their choice set. I also explain how I use exogenous variation in premiums induced by ACA regulations to identify the premium parameters in my model, following a similar approach to previous papers that estimate demand in the ACA Marketplaces.

4.1 Demand model

In this section, I formulate and estimate an individual-level discrete choice demand model in which individuals have heterogenous preferences for insurer-metal tier combinations in their choice set. It is important to note that this model incorporates the ACA regulations that affect the plan characteristics faced by consumers in the exchange. For example, the specification of the model accounts for the fact that the effective plan characteristics faced by an individual when purchasing a plan on the exchange depend on the individual's age group, their income as a percent of the federal poverty line, and the subsidy regulations for the exchange. I also take into consideration the fact that the set of insurer and metal tier combinations available to the individual depend on the individual's county of residence.

I do not observe specifically which plan was selected in the enrollment data, but I observe the selected plan's metal tier (Catastrophic, Bronze, Silver, Gold) and the selected plan's health insurance company. Therefore, as mentioned earlier when discussing the data, my demand model will be modeling individuals' choices at the individual-insurer-metal-county level. It is important to mention that my choice of modeling the utility function as a function of plan characteristics and allowing for the parameters to vary across demographic groups is mostly following the existing literature modeling demand for health insurance coverage in the ACA Marketplaces (e.g., Polyakova and Ryan, 2019; Saltzman, 2019; Tebaldi, 2020). My modelling approach is closer to Polyakova and Ryan (2019), as I use premiums and actuarial values to model demand.

Formally, I assume that the conditional indirect utility of individual i from selecting a metal-insurer combination $j = 1,2, \dots, J_c$ in county c is given by:

$$u_{ijc} = \alpha_i P_{ijc} + \beta_i AV_{ijc} + \delta_j + \epsilon_{ijc}$$

where P_{ijc} is the average net-of-subsidy annual premium for plans that belong to the same metal-insurer combination j (in thousands of dollars) for individual i in county c and AV_{ijc} denotes the applicable (net of

Covid Economics 47, 4 September 2020: 108-129

cost-sharing subsidies) actuarial value for plans in the metal-insurer combination j that individual i faces in county c. I include a metal-insurer fixed effect δ_j in my specification, and I assume that individuals select the insurer-metal combination j that yields the highest utility for them. It is important to mention that I am not allowing for an outside option $j = 0$ for two reasons. First, the size of the group choosing the outside option is hard to estimate because of rapidly evolving unemployment or loss of coverage. This means I cannot follow the previous literature that uses the American Community Survey to approximate its size. Second, even if I could approximate the size, I would need individual characteristics of the individuals in the group to construct the premiums they would face in the exchange.

Note that P_{ijc} is an individual-insurer-metal-specific average price since consumers face different average net-of-subsidy annual premiums for the same insurer-metal combination j in county c given that an individual's income and age group determine their premium subsidies. I also allow for AV_{ijc} to be individual-specific to accommodate the fact individuals with incomes below 250% FPL receive cost-sharing subsidies and face a higher actuarial value for silver plans.

The model allows for the premium coefficient α_i and the actuarial value coefficient β_i to vary across individuals. In particular, I will allow these marginal utility parameters to vary across 30 demographic groups, which are combinations of 5 age group categories (0-25, 26-34 ,35-44 ,45-54, 55+), 2 income categories (subsidized individuals with income below 400% FPL and nonsubsidized individuals with income above 400% FPL), and 3 qualifying event groups (loss of minimum essential coverage, uninsured, and other).

Finally, I assume that the individual shock ϵ_{ijt} is distributed i.i.d. with an Extreme Value Type I distribution so that I can predict the probability of an individual selecting a plan as a function of the average net annual premium, plan generosity measured in actuarial value, the metal-insurer fixed effect and the parameters of the model. I estimate the parameters of the model via maximum likelihood.

4.2 Endogeneity of Premiums and Variation in the Data to Estimate the Demand Parameters

My utility specification includes a metal-insurer combination fixed effect that controls for unobservable demand shocks at the insurer-metal level. This specification addresses the fact that P_{ijc} is endogenous and that unobserved characteristics that vary at the insurer-metal level (such as provider networks) could be correlated with P_{ijc}. I am also able to estimate the premium parameters α_i since the pricing and subsidy regulations generate variation in premiums faced by consumers that are independent of those demand shocks. That is, conditional on the fixed effect, individuals will face different prices depending on whether they are subsidized and depending on their age.

The intuition is that, under the ACA age pricing and subsidy regulations, two consumers of the same age that live in the same county will be facing different net-of-subsidy premiums for the same metal-insurer combination j if their income is different. Similarly, two consumers with the same income that live in the same county will be facing different net-of-subsidy premiums for the same metal-insurer combination j if their ages are different. Therefore, the parameters α_i are identified because I leverage this variation in net-of-subsidy premiums to estimate the effect of price on demand after controlling for unobservable insurer-metal level characteristics with the fixed effect in my specification.

The substantial variation in net-of-subsidy premiums faced by consumers across ages and income can be seen in **Table 2**. This table provides evidence of how those premiums vary by age groups, income, and metal tiers. The table is divided into four sections, where each section corresponds to a different income

Covid Economics 47, 4 September 2020: 108-129

group. Individuals cannot use premium subsidies to purchase Catastrophic plans, and these plans are only available for individuals under 30 and those with certain hardship exemptions.

The lower right section in the table corresponds to individuals who do not receive premium subsidies. These premiums are equal to the amount of money received by insurance companies as revenue. In addition, the ACA age pricing regulations that allow insurers to vary premiums across ages can be seen in this section of the table: premiums for non-subsidized individuals in the 55-64 age group are three times larger than those for the non-subsidized individuals in the 18-25 age group.

However, most individuals purchasing through the ACA exchanges are subsidized, and the subsidy formula significantly alters the prices they face. For example, bronze plan net-of-subsidy premiums decrease as age increases for low-income individuals. Silver plan net-of-subsidy premiums do not vary as much across ages, and gold plan net-of-subsidy premiums grow as age increases, but they do not exhibit the one to three ratio that unsubsidized gold plans have across ages. I use this variation in the prices faced by consumers of different ages and income to estimate my demand model.

Table 2

Average annual premiums faced by consumers across income, age and metal tiers.

150% Federal Poverty Line					200% Federal Poverty Line				
	Catastrophic	**Bronze**	**Silver**	**Gold**		**Catastrophic**	**Bronze**	**Silver**	**Gold**
0-17	2,208	295	1,056	1,437	**0-17**	2,208	1,094	1,911	2,293
18-25	2,576	260	1,104	1,547	**18-25**	2,576	1,007	1,957	2,403
26-34	2,970	231	1,155	1,665	**26-34**	2,970	914	2,007	2,521
35-44	-	209	1,210	1,792	**35-44**	-	819	2,059	2,647
45-54	-	171	1,374	2,164	**45-54**	-	621	2,218	3,016
55-64	-	136	1,693	2,869	**55-64**	-	446	2,521	3,717
65 +	-	132	1,818	3,146	**65 +**	-	413	2,642	3,994

250% Federal Poverty Line					No Premium Subsidy (over 400% FPL)				
	Catastrophic	**Bronze**	**Silver**	**Gold**		**Catastrophic**	**Bronze**	**Silver**	**Gold**
0-17	2,208	2,070	2,888	3,270	**0-17**	2,208	2,678	3,453	3,836
18-25	2,576	1,980	2,934	3,380	**18-25**	2,576	3,124	4,029	4,475
26-34	2,970	1,883	2,983	3,498	**26-34**	2,970	3,602	4,646	5,160
35-44	-	1,780	3,036	3,623	**35-44**	-	4,112	5,303	5,891
45-54	-	1,488	3,191	3,993	**45-54**	-	5,611	7,235	8,037
55-64	-	1,039	3,489	4,691	**55-64**	-	8,448	10,894	12,101
65 +	-	944	3,608	4,966	**65 +**	-	9,564	12,333	13,699

Notes: The first three panels show average net-of-subsidy annual premiums for low-income subsidized individuals.
Premium subsidies can't be used to buy a catastrophic plan and they are only available for people under thirty years old.
Individuals who qualify for premium subsidies can purchase a catastrophic plan but the premium subsidy will not apply.
I observe 3 individuals in my analysis sample who qualify for a premium subsidy but purchased a catastrophic plan.

It is also important to mention that variation in actuarial values of the silver plans faced by the lower-income individuals helps identify the β_i parameters. The intuition is that individuals of the same age living in the same county will face different actuarial values for the same insurer-silver plan combinations if their income is different. These discontinuous changes in the actuarial values of silver plans across individuals create exogenous variation that I leverage to estimate the β_i parameters. Finally, the fact that choice sets vary across counties also aids in the identification of both the premium and actuarial value parameters.

Covid Economics 47, 4 September 2020: 108-129

Covid Economics 47, 4 September 2020: 108-129

5 Estimation results: premium sensitivity

In this section, I report estimates of my demand model. I then use my demand estimates to provide own-price semi-elasticities.

Table 3 reports the estimated demand coefficients. The main takeaway from this table is that the marginal utility parameter α_i associated with the net-of-premium subsidy P_{ijc} varies in a meaningful way across demographic groups. This will have implications in the degree of premium sensitivity across these demographic groups. I also find that the marginal utility parameter β_i associated with the generosity of the plan AV_{ijt} as measured in actuarial value varies across demographic groups. For example, the marginal utility of the actuarial value of a plan is considerably higher for the low-income nonsubsidized groups.

Table 3
Demand Model Parameter Estimates across Demographic Groups.

Demographic group (income-age-qualifying life event bin)			Premium Coefficient Estimate	Robust Standard Error	Actuarial Value Coeffcient Estimate	Robust Standard Error
Subsidized Group (low-income)	0-25	Loss MEC	-1.84***	0.10	0.09***	0.01
		Uninsured	-2.96***	0.15	0.13***	0.01
		Other	-2.29***	0.10	0.12***	0.01
Subsidized Group (low-income)	26-34	Loss MEC	-1.87***	0.07	0.11***	0.00
		Uninsured	-2.27***	0.10	0.13***	0.01
		Other	-2.02***	0.07	0.11***	0.00
Subsidized Group (low-income)	35-44	Loss MEC	-1.65***	0.07	0.10***	0.00
		Uninsured	-2.21***	0.10	0.13***	0.01
		Other	-1.68***	0.07	0.11***	0.00
Subsidized Group (low-income)	45-54	Loss MEC	-1.25***	0.05	0.11***	0.00
		Uninsured	-1.53***	0.07	0.12***	0.01
		Other	-1.20***	0.05	0.10***	0.00
Subsidized Group (low-income)	55 or above	Loss MEC	-0.82***	0.03	0.10***	0.00
		Uninsured	-1.12***	0.05	0.13***	0.01
		Other	-0.79***	0.03	0.10***	0.00
No Subsidy Group (above 400% FPL)	0-25	Loss MEC	-1.21***	0.13	0.04***	0.01
		Uninsured	-1.64***	0.16	0.06***	0.01
		Other	-1.73***	0.16	0.10***	0.01
No Subsidy Group (above 400% FPL)	26-34	Loss MEC	-1.65***	0.10	0.08***	0.01
		Uninsured	-1.65***	0.12	0.10***	0.01
		Other	-1.36***	0.12	0.10***	0.01
No Subsidy Group (above 400% FPL)	35-44	Loss MEC	-1.11***	0.10	0.05***	0.01
		Uninsured	-1.32***	0.12	0.06***	0.01
		Other	-1.16***	0.12	0.12***	0.01
No Subsidy Group (above 400% FPL)	45-54	Loss MEC	-0.61***	0.07	0.02*	0.01
		Uninsured	-0.90***	0.09	0.04**	0.01
		Other	-0.66***	0.10	0.05***	0.02
No Subsidy Group (above 400% FPL)	55 or above	Loss MEC	-0.33***	0.05	0.00	0.01
		Uninsured	-0.46***	0.06	0.00	0.01
		Other	-0.42***	0.06	0.03*	0.02
Observations		427,684				
Pseudo R-squared		0.228				

Notes: Estimation includes metal-insurer fixed effects and the annual premium is measured in $1000s. MEC stands for Minimum Essential Coverage
*** p<0.01, ** p<0.05, * p<0.1

To provide some economic interpretation of these estimation results, I will now will follow the literature studying premium sensitivity in the marketplaces (e.g., Chan and Gruber, 2010; Ericson and Starc, 2015; Hackmann and Kowalski, 2015; Shepard, 2016; Jaffe and Shepard, 2017; Finkelstein, Hendren, and Shepard, 2017; Abraham et al., 2017; Drake, 2019; Saltzman, 2019; Tebaldi, 2020) and report mean own-premium semi-elasticities. For each individual i and insurer-metal combination j I calculate the percentage change in the probability of selecting j if the average premium increases by 100 dollars. I then use these individual "disaggregate" semi-elasticities to compute aggregate mean semi-elasticities across demographic groups. **Appendix B** contains more details on how I computed these results.

Table 4 shows how premium sensitivity varied across demographic groups during the COVID-19 pandemic in the WAHBE. I find that uninsured individuals are somewhat more price sensitive than individuals who lost minimum essential coverage. I also find that low-income subsidized individuals are more premium sensitive than non-subsidized individuals when selecting a plan during the pandemic. Additionally, younger individuals in the 0-25 age group are significantly more price sensitive than individuals in the 55 or older age group.

It is hard to make a sensible comparison of my semi-elasticity estimates with the previous literature because I am focusing on the special enrollment period of the Washington ACA Marketplace during the COVID-19 pandemic. However, Saltzman (2019) estimates demand and finds an overall own-premium semi-elasticity of -19.9 for the Washington ACA Marketplace using granular data from 2014 and 2015 plan years. I find this to be -11.6 for individual selecting plans during the COVID-19 pandemic, which suggests that premium sensitivity for insurance may potentially be lower during a pandemic. However, Saltzman (2019) and Tebaldi (2020) also find that younger individuals are more premium sensitive than older ones. This finding still holds when I estimate demand during the COVID-19 pandemic.

Table 4
Estimated mean own-premium semi-elasticities across demographic groups.

Mean own-premium semi-elasticity	-11.6
Qualifying Life Event	
Loss of Minimum Essential Coverage	-10.8
Uninsured	-12.8
Other	-11.6
Income group	
Low-income Subsidized	-12.2
No Premium Subsidy (over 400% FPL)	-9.9
Age	
0-25	-15.9
26-34	-15.3
35-44	-12.8
45-54	-9.1
55 or above	-5.9

6 Exploring which demographic groups are more likely to effectuate enrollment

In this section, I use a binomial logit model to estimate the probability that an individual effectuates enrollment as a function of individual demographic variables and characteristics of the selected plan. I also compute the average marginal effects implied by my estimation results to quantify the relationship between the covariates and the enrollment effectuation probability. The results are found in **Table 5**, where I also report the results of estimating the ordinary least squares version of the model (i.e., linear probability model).

Table 5 can be used to quantify the differences in probability of effectuation in a demographic group relative to the reference or omitted demographic group category keeping other covariates constant. For example, I find that individuals who lost minimum essential coverage and selected a plan in the exchange are less likely to effectuate enrollment than individuals who belong to the reference category. The reference

Covid Economics 47, 4 September 2020: 108-129

category "Other" groups individuals whose reported qualifying event for using the marketplace during the SEP includes a change in household size, a change in primary place of living, and so on. I also find that the uninsured individuals making use of the "Uninsured SEP" are more likely to effectuate enrollment. Hence, even though most individuals selecting a plan during the pandemic are doing so because they lost minimum essential coverage, my analysis shows that they are less likely to effectuate enrollment relative to other demographic groups. For example, the difference in probability between the uninsured group and the loss of minimum essential coverage group is approximately 0.27 using the logit estimates. The ordinary least squares estimation results imply similar differences.

Table 5

Ordinary Least Squares and Binary Logit Estimation Results.

Dependent variable: Was enrollment in the selected plan effectuated by the individual? Yes = 1 No = 0

	OLS		Binary Logit		
Explanatory Variable	Parameter Estimate	Standard Error	Parameter Estimate	Standard Error	Average Marginal Effect
Qualifying Life Event					
Loss of Minimum Essential Coverage	-0.187***	0.006	-1.155***	0.037	-0.169***
Uninsured	0.071***	0.005	0.823***	0.058	0.102***
Other	*omitted*	*omitted*	*omitted*	*omitted*	*omitted*
Age					
0-25	*omitted*	*omitted*	*omitted*	*omitted*	*omitted*
26-34	0.02*	0.008	0.149**	0.052	0.023**
35-44	0.047***	0.008	0.337***	0.055	0.05***
45-54	0.072***	0.008	0.524***	0.057	0.075***
55 or above	0.072***	0.008	0.515***	0.053	0.073***
Income group					
0% to 138% FPL	*omitted*	*omitted*	*omitted*	*omitted*	*omitted*
138% to 250% FPL	0.030***	0.009	0.23***	0.066	0.032***
250% to 400% FPL	0.037***	0.010	0.308***	0.073	0.041***
No Premium Subsidy (over 400% FPL)	0.115***	0.010	0.862***	0.075	0.11***
Gender					
Male	*omitted*	*omitted*	*omitted*	*omitted*	*omitted*
Female	0.007	0.005	0.051	0.032	0.007
Metal Tier Selected					
Bronze	0.131***	0.017	0.935***	0.102	0.125***
Silver	0.169***	0.018	1.188***	0.108	0.158***
Gold	0.133***	0.018	0.935***	0.110	0.108***
Catastrophic	*omitted*	*omitted*	*omitted*	*omitted*	*omitted*
Insurance Company Selected					
BridgeSpan	*omitted*	*omitted*	*omitted*	*omitted*	*omitted*
Coordinated Care	0.142***	0.020	1.106***	0.119	0.143***
Kaiser Northwest	0.163***	0.022	1.245***	0.162	0.155***
Kaiser WA	0.124***	0.019	0.905***	0.113	0.123***
LifeWise	-0.065**	0.020	-0.356**	0.110	-0.063***
Molina	0.012	0.020	0.043	0.109	0.007
Pacific Source	0.212***	0.023	1.676***	0.187	0.186***
Premera	-0.016	0.021	-0.109	0.119	-0.019
Providence	0.004	0.049	0.049	0.253	0.008
Constant	0.558***	0.028	-0.239	0.168	
R-squared/Pseudo R-squared	0.133		0.141		
Number of observations	27,871		27,871		

Note: Binary logit predicts 80.15 percent of the observations correctly.

* p<0.05, ** p<0.01, *** p<0.001

Covid Economics 47, 4 September 2020: 108-129

Covid Economics 47, 4 September 2020: 108-129

I also find that individuals not receiving subsidies are more likely to effectuate enrollment relative to individuals who receive subsidies. For example, the average marginal effect for the "No Premium Subsidy" category is approximately 0.11 under the logit estimates. This difference is important since the goal of the exchange is to help low-income individuals obtain coverage. So even though individuals with incomes below 400 percent of the federal poverty line make up 70 percent of the analysis sample, they are less likely to effectuate enrollment relative to their non-subsidized counterparts.

In terms of age groups, I find that older individuals are more likely to effectuate enrollment relative to young individuals during the COVID-19 pandemic. The difference between men and women is small and not significant.

Table 5 also reveals that individuals who select a silver plan are more likely to effectuate enrollment relative to individuals who select a different metal tier. So even though most of the individuals in my analysis sample select a bronze plan, it is those who select the silver plans that are more likely to effectuate enrollment when I control for other explanatory variables.

7 Conclusion

This paper studies demand for health insurance during the COVID-19 pandemic and provides important descriptive evidence that the Washington ACA Marketplace attracted a meaningful number of individuals who lost minimum essential coverage or who were uninsured. Dafny et al. (2020) found that small businesses are not sure they will be able to keep up with premium payments beyond August 2020. Therefore, it is not unreasonable to hypothesize that many Americans may lose coverage in the near future and that the ACA Marketplaces will play a crucial role in providing coverage before the 2021 Open Enrollment begins in November 2020, particularly among those who lose employer-sponsored coverage.

My results suggest that there are three reasons for considering more generous premium subsidies during the remainder of the pandemic. First, individuals losing minimum essential coverage are already using the exchange to replace lost coverage. Second, consumers are premium sensitive in a meaningful way. This finding coincides with previous work by Saltzman (2019) and Tebaldi (2020). Third, lower-income individuals and those who lost minimum essential coverage are less likely to effectuate enrollment relative to other demographic groups.

Covid Economics 47, 4 September 2020: 108-129

References

Abraham, J., Drake, C., Sacks, D., Simon, K., 2017. Demand for Health Insurance Marketplace Plans Was Highly Elastic in 2014-2015. Economic Letters. Vol 159, 69-73.

Branham, D.K., DeLeire, T., 2019. Zero-Premium Health Insurance Plans Become More Prevalent in Federal Marketplaces In 2018. Health Affairs. Vol 38, No. 5

Cajner, T., Crane, L., Decker, R., Grigsby, J., Hamins-Puertolas, A., Hurst, E., Kurz, C., Yildirmaz, A., 2020. The U.S. Labor Market during the Beginning of the Pandemic Recession. National Bureau of Economic Research. Working Paper No. 27159.

Center for Medicare and Medicaid Services, 2020. Early 2020 Effectuated Enrollment Snapshot. Released on July 23, 2020.

Chan, D., Gruber, J., 2010. How sensitive are low income families to health plan prices? American Economic Review. 100 (2), 292-296.

Coibion, O., Gorodnichenko, Y., Weber, M., 2020. Labor Markets During the COVID-19 Crisis: A Preliminary View. Covid Economics Vetted and Real-Time Papers. Issue 21, 40-58.

Cowan, B., 2020. Short-run Effects of COVID-19 on U.S. Worker Transitions. National Bureau of Economic Research. Working Paper No. 27315.

Drake, C., 2019. What are consumers willing to pay for a broad network health plan? Evidence from Covered California. Journal of Health Economics. 65, 63-77.

Dafny, L., Soon, Y.W., Cullen, Z., Stanton, C. 2020. How Has Covid-19 Affected Health Insurance Offered by Small Businesses in the U.S.? Early Evidence from a Survey. NEJM Catalyst.

Ericson, K., Starc, A., 2015. Pricing Regulation and Imperfect Competition on the Massachusetts Health Insurance Exchange. Review of Economics and Statistics. 97(3), 667-682.

Finkelstein, A., Hendren, N., Shepard, M., 2019. Subsidizing Health Insurance for Low-Income Adults: Evidence from Massachusetts. American Economic Review. 109(4), 1530-1567.

Forsythe, E., Kahn, L., Lange, F., Wiczer, D. 2020. Labor Demand in the Time of COVID-19: Evidence from Vacancy Postings and UI Claims. Journal of Public Economics 189, 104238.

Frean, M., Gruber, J., Sommers, B., 2017. Premium subsidies, the mandate, and Medicaid Expansion: Coverage Effects of the Affordable Care Act. Journal of Health Economics. 53, 72-86.

Hackmann, M., Kolstad, J., Kowalski, A., 2015. Adverse Selection and an Individual Mandate: When Theory Meets Practice. American Economic Review. 105(3), 1030-1066.

Jaffe, S., Shepard, M., 2017. Price-Linked Subsidies and Imperfect Competition in Health Insurance. National Bureau of Economic Research. Working Paper No. 23104.

Kaiser Foundation Family, 2019. Employer Health Benefits Survey, Washington D.C.

Polyakova, M., Ryan, S., 2019. Subsidy Targeting with Market Power. National Bureau of Economic Research. Working Paper No. 26367.

Saltzman, E., 2019. Demand for health insurance: Evidence from the California and Washington ACA exchanges. Journal of Health Economics. 63, 197-22.

Sacks, D., 2017. How Do the Mandate and Premium Tax Credit Affect the Individual Insurance Market? Working Paper.

Shepard, M., 2016. Hospital Network Competition and Adverse Selection: Evidence from the Massachusetts Health Insurance Exchange. National Bureau of Economic Research Working Paper No. 22600

Tebaldi, P., 2020. Estimating Equilibrium in Health Insurance Exchanges: Price Competition and Subsidy Design under the ACA. Working Paper.

Washington Health Benefit Exchange, 2020. Supplemental Report: Uninsured Special Enrollment Period. March 10-May 8, 2020.

Covid Economics 47, 4 September 2020: 108-129

Covid Economics 47, 4 September 2020: 108-129

Appendix A: Data

This appendix discusses (1) the construction of the analysis sample, (2) limitations of the data, (3) the construction of average premiums at the county-insurer-metal level, and (4) the definition of the actuarial value of silver plans for subsidized individuals.

1 Construction of analysis sample

The raw dataset originally contains 30,882 plan selection records from March 10, 2020 to July 1, 2020. I discard 2,596 observations that have missing values for the variables needed to compute average net-of-subsidy premiums used in the demand estimation. Because individuals must choose plans from insurance companies that entered their county of residence, I also drop 21 observations where the individual is choosing a plan from an insurance company that did not enter their county of residence. Because individuals should appear only once in the dataset to estimate demand, I also discard 394 duplicate observations: 390 of these observations are from individuals who appear twice in the data, and 4 of these observations are from 2 individuals who appear three times in the data. These exclusions produce a final individual-level dataset of 27,871 plan selection records that I use in the main analysis of this paper.

2 Limitations of the data

My dataset has four limitations: (1) I do not observe exact plan that was selected, only the insurer and metal level that was selected in a given county; (2) I do not have a household identifier that enables me to identify which individuals belong to the same household, (3) I do not observe the individual's exact age, only their age group; and (4) I do not see if an individual smokes.

The first limitation means that I am forced to model demand at the individual-metal-insurer-county level instead of modeling at the individual-plan-county level. The second limitation means that I am forced to model demand at the individual level instead of modeling demand at the household level like Saltzman (2019) and Tebaldi (2020). The third limitation means that I must use an average age factor rather than the exact age factor. And the fourth limitation implies that I cannot account for variation in premiums for smoking status.

To model demand at the individual-metal-insurer-county level I need to construct average prices. I describe the construction of these average prices in the next section.

3 Construction of average prices at the county-insurer-metal level

To construct average prices at the county-insurer-metal level—the P_{ijc} measure that I use in my demand model—I use the following four steps: (1) extract base monthly plan premiums from insurer rate filing PDFs, (2) calculate an average base monthly premium at the county-insurer-metal level, (3) multiply the base premium by an average age factor, and (4) apply the appropriate subsidy to the age-adjusted premium.

3.1 Extracting base premiums from insurer rate filings

First, I use insurer rate filing PDFs from the Office of the Insurance Commissioner of Washington State website to extract the plan-level base monthly premiums for all plans and counties

Source: https://www.insurance.wa.gov/individual-and-family-health-plans-premiums

Covid Economics 47, 4 September 2020: 108-129

3.2 Calculating an average base monthly premium

Next, because I do not observe the exact plan the individual chose, I construct the average annual premium for a 21-year-old non-smoker at the county-insurer-metal level. There are in total 360 county-insurer-metal combinations available on the exchange.

While this approach will introduce some measurement error, I believe that the limited variation in base premiums within county-insurer-metal combinations makes averaging a defensible method for dealing with the limitations of my data. For example, as shown in **Table A1**, many of the insurers only offer one plan for a given metal tier, which means that many county-insurer-metal combinations will only include one possible plan.

Table A1
Number of Counties Entered and Number of Plans Offered by Insurer

Insurer	Number of Counties Entered	Catastrophic	Bronze	Silver	Gold	Total
Bridgespan	4	-	12	4	4	**20**
Coordinated Care	20	-	1	7	2	**10**
Kaiser Northwest	2	1	3	2	2	**8**
Kaiser Washington	18	1	2	2	1	**6**
LifeWise	33	1	2	2	1	**6**
Molina	14	-	1	1	1	**3**
PacificSource	3	1	2	1	1	**5**
Premera	7	-	2	1	2	**5**
Providence	6	-	1	1	1	**3**
Total	-	**4**	**26**	**21**	**15**	**66**

Table A2 shows how many county-insurer-metal combinations include just one plan that is "averaged" or more than one plan whose premiums are averaged. More than half of the 360 county-insurer-metal combinations offer only one plan, which means I observe the real base premium that consumers faced for these combinations. Another 38 percent of the combinations are an average of just two plans. In addition to the 93 percent of county-insurer-metal combinations that include just one or two plans, Kaiser Northwest offers three different bronze plans in two counties, and Coordinated Care offers seven different silver plans in 20 counties.

Table A2
Number of Plans Averaged to Construct the Average
Base Monthly Premiums at the County-Insurer-Metal Level

Number of Plans Averaged	Number of County-Insurer-Metal Combinations	Percent of County-Insurer-Metal Combinations
1	197	54.7%
2	137	38.1%
3	6	1.7%
7	20	5.6%
Total	**360**	**100.0%**

Additionally, among the combinations that require the calculation of an average base monthly premium across two or more plans, there is little variation in price. **Table A3** provides summary statistics for the difference between the cheapest and most expensive plan within county-insurer-metal combinations. Among the combinations where an average base monthly premium is calculated, the mean absolute difference in price is $7.12 per month (or $85.44 per year), and the mean percent difference in price is 2.35 percent. The median absolute difference in price is only $3.57 per month (or $42.84 per year), and the median percent difference in price is only 1.25 percent. The largest absolute and percent differences in price are $27.70 per month (or $332.40 per year) and 9.17 percent, respectively. While this is not a negligible difference in price, only 5 of the 360 county-insurer-metal combinations have premium differences of more than $20 per month.

Table A3
Differences Between the Cheapest and Most Expensive Base Monthly
Premiums Used to Calculate County-Insurer-Metal Level
Average Base Monthly Premiums

Measure	Absolute Difference	Percent Difference
Mean Difference	$7.12	2.35%
Median Difference	$3.57	1.25%
Minimum Difference	$0.03	0.01%
Maximum Difference	$27.70	9.17%

Note: Includes the 163 county-insurer-metal combinations that have at least 2 plans. The 197 county-level-metal combinations with only 1 plan are excluded. Base monthly premiums are for a 21-year-old non-smoker.

After calculating these average base monthly premiums at the county-insurer-metal level, I multiply them by 12 to obtain the average annual premiums.

3.3 Applying the appropriate age factor using the age group found in the enrollment data

After calculating the average base annual premiums at the county-insurer-metal level for a 21-year-old non-smoker, I then scale these premiums by average age factors to compute average pre-subsidy annual premiums for different age groups. These age factors apply both subsidized and unsubsidized individuals. For unsubsidized individuals these are the prices they face.

Covid Economics 47, 4 September 2020: 108-129

Table A4
Age Factors by Age Group

Age Group	Age Factor
< 18	0.84
18 – 25	0.98
26 – 34	1.13
35 – 44	1.29
45 – 54	1.76
55 – 64	2.65
65+	3.00

Source: Centers for Medicare and Medicaid Services

Note that because I only observe an individual's age group in the enrollment data, not his or her exact age, I calculate the average age factor for the age bands observed in the enrollment data using the Centers for Medicare and Medicaid Services age curve variations, as shown in **Table A4**.

It is also important to point out that individuals who are over 65 and do not qualify for Medicare can buy a plan in the marketplace. These individuals may still be eligible for subsidies depending on their income.

This generally happens when seniors did not pay into Medicare for at least 10 years, which is sometimes the case for some Americans who may have come into the workforce late in their lives. It is also the case for some recent immigrants.

3.4 Applying the appropriate subsidy

The last step in calculating the measure of price P_{ijc} that consumers face when selecting an insurer-metal combination in their county is to construct the net-of-subsidy premium for subsidized individuals. To do this, I first compute the applicable subsidy for each individual and then subtract that subsidy from the average pre-subsidy annual premium computed above.

According to ACA regulations, an individual's subsidy is determined by (1) the premium for the second cheapest silver plan available in the individual's county of residence, and (2) the individual's income as a share of the federal poverty line (FPL).

First, the insurer rate filings allow me to identify the 21-year-old annual premium for the second cheapest silver plan in each individual's county of residence. I then adjust that 21-year-old premium by the age factor to compute the premium that individual would pay if he or she purchased that plan. This serves as the individual's age-adjusted benchmark plan, $AgeFactor_i * Benchmark_c$.

Second, I use the individual's income as share of the federal poverty line compute the share of income that the individual should pay towards the benchmark plan. The 2019 federal poverty line was set at $12,490 per year for an individual, and the IRS determines the share of an individual's income he or she should contribute based on the individual's income as a percentage of the federal poverty line (which I observe in the data). The individual's income times the share owed is denoted by $IncomeCap_i^{FPL}$.

Covid Economics 47, 4 September 2020: 108-129

Table A5
Share of Income Contributed by FPL

Income as a Percent of FPL	Share of Income Contributed
< 133	0.0208
133 – 150	0.0311 – 0.0415
151 – 200	0.0420 – 0.0654
201 – 250	0.0658 – 0.0836
251 – 299	0.0839 – 0.0983
300 – 400	0.0986

Source: IRS Form 8962 (2019), Table 2.

Using these inputs, the subsidy for each individual in the data is given by the following formula: $max\{0, AgeFactor_i * Benchmark_c - IncomeCap_i^{FPL}\}$.

To provide a stylized example with simple numbers, say there is an individual who earns $20,000, has a maximum contribution of 5 percent of their income, and lives in a county where the second cheapest silver plan for their age group is $4,800 per year. Their maximum contribution will be $1,000 (=20,000 × 0.05) per year, so the subsidy they will quality for is $3,800 (=4,800 – 1,000) per year. If the individual enrolls in the second cheapest silver plan, they will owe $1,000. If they enroll in a plan that costs $5,000 per year, they will owe $1,200 (=5,000 – 3,800). If they enroll in a plan that costs $4,000 per year, they will owe only $200 (=4,000 – 3,800). If they enroll in a plan that costs less than their $3,800 subsidy, they will pay $0, but they will be leaving money on the table. Additionally, if they enroll in a catastrophic plan, they will pay the full price of the plan because subsidies do not apply to catastrophic plans.

4 Silver plan actuarial values

Individuals whose income is less than 250 percent of the federal poverty line receive different actuarial values for silver plans than individuals making more than 250 percent of the federal poverty line. The following table provides details about these changes to silver plan actuarial values.

Table A6
Silver plan actuarial values faced by individuals on the exchange

Income as Percentage of FPL	Actuarial Value of Silver Plans
Below 150% FPL	94
150% to 200% FPL	87
200% to 250% FPL	73
Above 250% FPL	70

Note: Only individuals with incomes below 250% of the FPL receive cost-sharing subsidies that increase the actuarial value of the silver plans they face in the ACA Marketplaces.

Covid Economics 47, 4 September 2020: 108-129

Appendix B: Own-Premium Semi-Elasticities

This appendix defines the own-premium semi-elasticity formula of individual i for insurer-metal combination j in county c.

The probability that individual i selecting the insurer-metal combination j is given by:

$$s_{ijc} = \frac{\exp\left(\alpha_i P_{ijc} + \beta_i AV_{ijc} + \delta_j\right)}{\sum_{k=1}^{J_c} \exp\left(\alpha_i P_{ikc} + \beta_i AV_{ikc} + \delta_k\right)}$$

For each individual i and insurer-metal combination j I calculate the percentage change in the probability of selecting j if the average premium increases by 100 dollars using the following formula:

$$SemiElasticity_{ijc} = \alpha_i\left(1 - s_{ijc}\right) * 100$$

The premium parameter α_i can vary across the demographic groups defined in the main text.

I use these "disaggregate" semi-elasticities to compute the aggregate mean own-premium semi-elasticities across demographic groups reported in the paper. I also use the metal-insurer j market shares as weights to estimate the mean.

Covid Economics 47, 4 September 2020: 108-129

The distributional effects of COVID-19 and mitigation policies[1]

Sewon Hur[2]

Date submitted: 28 August 2020; Date accepted: 2 September 2020

This paper develops a quantitative life cycle model in which economic decisions impact the spread of the COVID-19 and, conversely, the virus affects economic decisions. The calibrated model is used to measure the welfare costs of the pandemic across the age, income, and wealth distribution and to study the effectiveness of various mitigation policies. In the absence of mitigation, young workers engage in too much economic activity relative to the social optimum, leading to higher rates of infection and death in the aggregate. The paper considers a subsidy-and-tax policy that imposes a tax on consumption and subsidizes reduced work compared to a lockdown policy that caps work hours. Both policies are welfare improving and lead to less infections and deaths. Notably, almost all agents favor the subsidy-and-tax policy, suggesting that there need not be a tradeoff between saving lives and economic welfare.

1 I thank Daniel Carroll, Andy Glover, Karel Mertens, and seminar participants at the Federal Reserve Bank of Dallas for helpful discussions. I also thank Anna Eckert and Andrew Johnson for outstanding research assistance. The views expressed herein are those of the author and not necessarily those of the Federal Reserve Bank of Dallas or the Federal Reserve System.

2 Federal Reserve Bank of Dallas.

Covid Economics 47, 4 September 2020: 130-161

Covid Economics 47, 4 September 2020: 130-161

1 Introduction

The COVID-19 pandemic represents dual public health and economic crises, and has spawned a quickly emerging literature on the economics of pandemics. Furthermore, the pandemic and mitigation efforts have had unequal impacts across the distribution: The virus has been particularly dangerous for older individuals, while mitigation policies, such as shutdowns, have affected working-age individuals. In particular, mitigation policies disproportionately harm low-wage workers who may be less likely to work from home and low-wealth workers who lack the resources to weather prolonged time away from work.

This paper develops a quantitative heterogeneous-agent life-cycle model in which economic decisions, such as how much to work and how much to consume, impact the spread of the virus and vice versa. The calibrated model is used to measure the welfare costs across the age, income, and wealth distribution and to study the effectiveness of various mitigation policies. In the absence of mitigation, young workers engage in too much economic activity relative to the social optimum, leading to higher rates of infection and death in the aggregate.

This paper considers two budget-neutral mitigation policies: a subsidy-and-tax policy that subsidizes reduced work—funded by a tax on consumption—and a lockdown policy that caps work hours. The subsidy-and-tax and lockdown policies lower the peak infection rate by 1.2 and 0.3 percentage points, respectively, and save approximately 470,000 and 46,000 lives, respectively. In terms of welfare, the lockdown policy benefits older individuals at the expense of younger, particularly low-wage workers. The approval among almost all agents for the subsidy-and-tax plan suggests that with well-designed policies, there need not be a tradeoff between saving lives and economic well being.

The model includes many, but not all, of the features relevant to studying the aggregate and distributional consequences of the pandemic and mitigation efforts. First and foremost, the model has heterogeneity by age, which is important because COVID-19 presents very different mortality risk by age, and various mitigation policies such as shutdowns mostly affect working-age individuals. Furthermore, lower income individuals appear less able to work from home (see, for example, Bick et al. 2020, Bartik et al. 2020, Dingel and Neiman 2020, Gascon and Ebsim 2020 and Mongey and Weinberg 2020), suggesting that heterogeneity across income is an important feature. The model builds on the epidemiological SIR

model of virus transmission that has become common in the literature.[2] Additionally, many studies have documented that the way viruses typically spread outside the home is through work or consumption-related activities, and like Eichenbaum et al. (2020), the model allows for these transmission mechanisms. Since many mitigation efforts are focused on reducing labor and consumption activities, I model endogenous labor supply, the ability to work from home, and optimization of consumption and saving. Finally, the model has other features that have become common in the literature such as hospital capacity constraints.

Related literature

The model combines the heterogeneous-agent overlapping-generations model (see, for example, Conesa et al. 2009, Favilukis et al. 2017, Heathcote et al. 2010, and Hur 2018) with an extension of the standard SIR epidemiological model similar to those used in Eichenbaum et al. (2020), Glover et al. (2020), and Jones et al. (2020). Workers face idiosyncratic productivity shocks and borrowing constraints within an incomplete market setting as in Aiyagari (1994), Bewley (1986), Huggett (1993), and Imrohoroğlu (1989).

The paper is most related to Bairoliya and Imrohoroglu (2020) and Glover et al. (2020). Bairoliya and Imrohoroglu (2020) study quarantine policies in a quantitative life-cycle model with heterogeneity across age, health, income, and wealth. They primarily focus on studying the effects of selective quarantines based on age and health. Relative to my paper, Bairoliya and Imrohoroglu (2020) study the disease progression at a lower frequency (yearly) and do not incorporate the economic-epidemiological feedback channel. Glover et al. (2020) study optimal mitigation policies in a model with three types of agents: retirees, young workers in the essential sector, and young workers in the non-essential sector. Relative to Glover et al. (2020), this paper features heterogeneity across not only age, but also income and wealth, and complements both papers by analyzing mitigation policies that specifically target the behavior of these different groups.

The epidemiological part of the model borrows from the economics literature that builds on the SIR model, originally developed by Kermack and McKendrick (1927). Atkeson (2020) was one of the first papers to use the SIR model in an economics context. Alvarez et al. (2020), Eichenbaum et al. (2020), Farboodi et al. (2020), and Jones et al. (2020) study opti-

[2] See Hur and Jenuwine (2020) for a review of this literature.

Covid Economics 47, 4 September 2020: 130-161

Covid Economics 47, 4 September 2020: 130-161

mal mitigation in SIR models extended with lockdowns, economic-epidemiological feedback, social distancing, and work from home with learning-by-doing, respectively. Bodenstein et al. (2020) and Krueger et al. (2020) study the SIR model with multiple sectors. Birinci et al. (2020), Garibaldi et al. (2020), and Kapicka and Rupert (2020) incorporate search and matching frictions into the SIR framework, while Berger et al. (2020), Chari et al. (2020), and Piguillem and Shi (2020) extend the SIR model to focus on testing and quarantine. Chudik et al. (2020) extend the SIR model to allow for compulsory and voluntary social distancing and estimate the model using data from Chinese provinces, while Argente et al. (2020) extend the SIR model with city structure, estimated with South Korean mobile phone data. Bognanni et al. (2020) develop a SIR model with multiple regions and estimate it on daily county-level US data. Aum et al. (2020) study the effects of lockdowns in a model with heterogeneous age, skill, and occupation choice, while Kaplan et al. (2020) study the distributional effects of the pandemic in a heterogeneous agent new Keynesian model.

By studying the heterogeneous welfare consequences of COVID-19 and mitigation efforts, this paper complements the empirical literature that has documented the early effects of the pandemic and various mitigation policies on different segments of the population, such as Chetty et al. (2020). Adams-Prassl et al. (2020) and Wozniak (2020) use survey data to document that COVID-19 has disproportionately impacted young and low-wage individuals in the US. Alstadsæter et al. (2020) use register data from Norway to document that pandemic-induced layoffs have disproportionately affected not only young and low-wage, but also low-wealth individuals. Additionally, Bertocchi and Dimico (2020) focus on differential effects of the COVID-19 crisis across race, Alon et al. (2020a,b) study the differences across gender, and Osotimehin and Popov (2020) study the heterogeneous impact by sector of employment.

2 Model

This section presents a model economy used to quantitatively analyze the welfare consequences of COVID-19 and to run policy counterfactuals. The setting combines the heterogeneous-agent overlapping-generations model with an extension of the standard SIR epidemiological model that is similar to those used in Eichenbaum et al. (2020). The economy is inhabited by overlapping generations of stochastically aging individuals. Time is discrete and indexed

by $t = 0, ..., \infty$. Workers face idiosyncratic productivity shocks and borrowing constraints within an incomplete market setting. I now describe the model in more detail.

2.1 Individuals

Individuals of age $j \in J \equiv \{1, 2, .., \overline{J}\}$ face conditional aging probabilities given by $\{\psi_j\}$.[3] Mandatory retirement occurs at age $j = J_R$. The period utility function is given by

$$u(c, \ell, h) = \frac{c^{1-\sigma}}{1-\sigma} - \varphi \frac{\ell^{1+\nu}}{1+\nu} + \bar{u} + \hat{u}_h \tag{1}$$

where c is consumption, ℓ is labor supply, and $\bar{u}$ and $\hat{u}_h$ govern the flow value of being alive and being in health state h, respectively.

An individual's health status is given by $h \in \{S, I, R, D\}$: *susceptible* agents are healthy but may contract the virus, *infected* agents have contracted the virus and may pass it onto others, and agents that exit the infection can either *recover* or *die*. Recovered agents are assumed to be immune from further infection.[4] The transition between health states builds on the widely used SIR model, originally developed by Kermack and McKendrick (1927). Susceptible individuals get infected with probability π_{It}, which depends on individual consumption and outside labor (c, ℓ^o) and the aggregate measure of infected individuals (μ_{It}) and their consumption and outside labor (C_{It}, L^o_{It}). Formally,

$$\pi_{It}(c, \ell^o; Z_t) = \beta_c c C_{It} + \beta_\ell \ell^o L^o_{It} + \beta_e \mu_{It}, \tag{2}$$

where $Z_t \equiv \{\mu_{It}, C_{It}, L^o_{It}\}$. This framework allows the virus to be contracted from consumption-related activities, labor-related activities, and from other settings. It also allows a feedback between disease progression and economic activities as in Eichenbaum et al. (2020), Glover et al. (2020), and Jones et al. (2020).

Infected individuals exit the infection with probability π_{Xt} and upon exit, they recover with probability $1 - \delta_{jt}(\mu_{It})$ and die with probability $\delta_{jt}(\mu_{It})$. The fatality rate depends on the individual's age and on the aggregate measure of infected individuals. If we assume that a vaccine and cure are developed and implemented in period $\hat{t}$, then the transition matrix

[3] Given that the model will be used to analyze disease progression at a high frequency, the assumption of stochastic aging greatly reduces the state space and computational burden.

[4] At this point, it is not clear whether individuals that have recovered from COVID-19 have lasting immunity. One could easily extend the model to have shorter durations of immunity.

Covid Economics 47, 4 September 2020: 130-161

between health states, for $t < \hat{t}$, is given by

$$\Pi_{jhh't}(c, \ell^o; Z_t) = \begin{array}{c|cccc} & S & I & R & D \\ \hline S & 1-\pi_{It}(c,\ell^o;Z_t) & \pi_{It}(c,\ell^o;Z_t) & 0 & 0 \\ I & 0 & 1-\pi_{Xt} & \pi_{Xt}(1-\delta_{jt}(Z_t)) & \pi_{Xt}\delta_{jt}(Z_t) \\ R & 0 & 0 & 1 & 0 \\ D & 0 & 0 & 0 & 1 \end{array} \tag{3}$$

and for $t \geq \hat{t}$,

$$\Pi_{jhh't}(c, \ell^o; Z_t) = \begin{array}{c|cccc} & S & I & R & D \\ \hline S & 0 & 0 & 1 & 0 \\ I & 0 & 0 & 1 & 0 \\ R & 0 & 0 & 1 & 0 \\ D & 0 & 0 & 0 & 1 \end{array} \tag{4}$$

Each period, workers receive idiosyncratic productivity shocks $\varepsilon \in E$, which follows a Markov process, with transition matrix Γ. Their labor income is given by $w_t \eta_{jh} \varepsilon \ell$, where w_t is the efficiency wage, η_{jh} is the health- and age-profile of efficiency units, and ℓ is total hours worked. Workers may choose to work up to a fraction $\bar{\theta}_j(\varepsilon)$ of their labor hours from home, where $\bar{\theta}_j(\varepsilon)$ is allowed to vary by age and productivity. Retirees are assumed to receive a fixed income of s each period.[5] Individuals can accumulate non-contingent assets k, which delivers a net return of r_t.

Given the sequence of prices $\{w_t, r_t\}$, consumption taxes $\{\tau_{ct}\}$, and aggregate states $\{Z_t\}$, a retiree with age $j \geq J_R$, wealth k, and health h in period t chooses consumption c and savings k' to solve:

$$\begin{aligned} V_{jt}(k,h) = \max_{c,k' \geq 0} \; & u(c,0,h) + \beta\psi_j \sum_{h' \in H} \Pi_{hh't}(c,0) V_{j+1,t+1}(k',h') \\ & + \beta(1-\psi_j) \sum_{h' \in H} \Pi_{hh't}(c,0) V_{j,t+1}(k',h') \\ \text{s.t. } & (1+\tau_{ct})c + k' \leq s + k(1+r_t) \end{aligned} \tag{5}$$

where β is the time discount factor. I assume that the value of death is zero and that $V_{\bar{J}+1,t} = 0$, which implies that agents in the last period of life ($j = \bar{J}$) may die due to stochastic aging and, if infected, due to the virus.

[5] This can readily be extended to depend on lifetime earnings as in Hur (2018).

Covid Economics 47, 4 September 2020: 130-161

Covid Economics 47, 4 September 2020: 130-161

Given the sequence of prices $\{w_t, r_t\}$, consumption and labor income taxes $\{\tau_{ct}, \tau_{\ell t}\}$, and aggregate states $\{Z_t\}$, a worker with age $j < J_R$, wealth k, productivity ε, and health h in period t chooses consumption c, total labor ℓ, outside labor ℓ^o and savings k' to solve:

$$\begin{aligned} v_{jt}(k,\varepsilon,h) = \max_{c,\ell,\ell^o,k'\geq 0} \; & u(c,\ell,h) + \beta\psi_j \sum_{\varepsilon'\in E}\sum_{h'\in H} \Gamma_{\varepsilon\varepsilon'}\Pi_{hh't}(c,\ell^o)v_{j+1,t+1}(k',\varepsilon',h') \\ & + \beta(1-\psi_j)\sum_{\varepsilon'\in E}\sum_{h'\in H} \Gamma_{\varepsilon\varepsilon'}\Pi_{hh't}(c,\ell^o)v_{j,t+1}(k',\varepsilon',h') \\ \text{s.t. } & (1+\tau_{ct})c + k' \leq w_t\eta_j^h(1-\tau_{\ell t})\varepsilon\ell + k(1+r_t) \\ & (1-\bar{\theta}_j(\varepsilon))\ell \leq \ell^o \leq \ell \end{aligned} \tag{6}$$

where $v_{jt}(k,\varepsilon,h) = V_{jt}(k,h)$ for $j \geq J_R$.

2.2 Production

A representative firm hires labor (L_{ft}) and capital (K_{ft}) to produce according to

$$Y_{ft} = K_{ft}^{\alpha} L_{ft}^{1-\alpha} \tag{7}$$

Taking prices as given, the firm solves

$$\max_{L_{ft},K_{ft}} Y_{ft} - w_t L_{ft} - (r_t + \delta)K_{ft}, \tag{8}$$

where δ is the deprecation rate of capital. Optimality conditions are given by

$$w_t = (1-\alpha)K_{ft}^{\alpha} L_{ft}^{-\alpha}, \tag{9}$$

$$r_t = \alpha K_{ft}^{\alpha-1} L_{ft}^{1-\alpha} - \delta. \tag{10}$$

2.3 Law of motion for aggregate states

Let C_{jht} and L^o_{jht} denote aggregate consumption and outside labor, respectively, of individuals with age j and health h in period t. Then, by the law of large numbers, equation (2) implies that new infections within an age-j cohort are given by

$$T_{jt} = \beta_c C_{jSt} C_{It} + \beta_\ell L^o_{jSt} L^o_{It} + \beta_e \mu_{jSt}\mu_{It} \tag{11}$$

where μ_{jSt} is the measure of susceptible age-j individuals in period t. The measure of infected agents is then given by $\mu_{I,t+1} = \sum_{j\in J} \mu_{jI,t+1}$ where, for $j > 1$,

$$\begin{aligned} \mu_{jI,t+1} = & \psi_j(\mu_{j-1,It}\,(1-\pi_{Xt}) + T_{j-1,t}) \\ & + (1-\psi_j)(\mu_{jIt}\,(1-\pi_{Xt}) + T_{jt}), \end{aligned} \tag{12}$$

and

$$\mu_{1I,t+1} = (1-\psi_1)(\mu_{1It}\,(1-\pi_{Xt}) + T_{1t}).$$

2.4 Equilibrium

We are ultimately interested in studying disease dynamics along a transition path. However, because most of the model parameters are calibrated to an initial pre-pandemic steady state, let's first define a stationary equilibrium in which $\mu_I = 0$. In this case, aggregate consumption and labor of infected individuals is trivially zero. Thus $Z = (0,0,0)$ and Π is the identity matrix. Define the state space over wealth, labor productivity, and health as $X = K \times E \times H$ and let a σ-algebra over X be defined by the Borel sets, $\mathcal{B}$, on X.

Definition. A *steady-state recursive equilibrium*, given fiscal policies $\{\tau_c, \tau_\ell, s\}$, is a set of value functions $\{v_j, V_j\}_{j\in J}$, policy functions $\{c_j, \ell_j, \ell_j^o, k_j'\}_{j\in J}$, prices $\{w, r\}$, producer plans $\{Y_f, L_f, K_f\}$, the distribution of newborns ω, and invariant measures $\{\mu_j\}_{j\in J}$ such that:

1. Given prices, workers and retirees solve (5) and (6).
2. Given prices, firms solve (8).
3. Markets clear:
   (a) $Y_f = \int_X \sum_{j\in J} (c_j(k,\varepsilon,h) + \delta k)\, d\mu_j(k,\varepsilon,h)$
   (b) $L_f = \int_X \sum_{j<J_R} l_j(k,\varepsilon,h) d\mu_j(k,\varepsilon,h)$
   (c) $K_f = \int_X \sum_{j\in J} k d\mu_j(k,\varepsilon,h)$
4. The government budget constraint holds:
$$\int_X \left[\tau_\ell w \sum_{j<J_R} \eta_{jh}\varepsilon \ell_j(k,\varepsilon,h) + \tau_c \sum_{j\in J} c_j(k,\varepsilon,h)\right] d\mu_j(k,\varepsilon,h) = s\int_X \sum_{j\geq J_R} d\mu_j(k,\varepsilon,h)$$
5. For any subset $(\mathcal{K},\mathcal{E},\mathcal{H}) \in \mathcal{B}$, the invariant measure μ_j satisfies, for $j > 1$,
$$\begin{aligned}\mu_j(\mathcal{K},\mathcal{E},\mathcal{H}) = &\int_X \psi_{j-1} \mathbb{1}_{\{k'_{j-1}(k,\varepsilon,h)\in\mathcal{K}\}} \sum_{\varepsilon'\in\mathcal{E}} \sum_{h'\in\mathcal{H}} \Gamma_{\varepsilon\varepsilon'}\Pi_{hh'} d\mu_{j-1}(k,\varepsilon,h) \\ &+ \int_X (1-\psi_j) \mathbb{1}_{\{k'_j(k,\varepsilon,h)\in\mathcal{K}\}} \sum_{\varepsilon'\in\mathcal{E}} \sum_{h'\in\mathcal{H}} \Gamma_{\varepsilon\varepsilon'}\Pi_{hh'} d\mu_j(k,\varepsilon,h)\end{aligned} \tag{13}$$

Covid Economics 47, 4 September 2020: 130-161

and

$$\mu_1(\mathcal{K},\mathcal{E},\mathcal{H}) = \int_X (1-\psi_1)\mathbb{1}_{\left\{k_1'(k,\varepsilon,h)\in\mathcal{K}\right\}} \sum_{\varepsilon'\in\mathcal{E}}\sum_{h'\in\mathcal{H}} \Gamma_{\varepsilon\varepsilon'}\Pi_{hh'} d\mu_1(k,\varepsilon,h) + \omega(\mathcal{K},\mathcal{E},\mathcal{H}) \quad (14)$$

6. The newborn distribution satisfies:

$$\int_X k d\omega(k,\varepsilon,h) = \int_X \psi_{\bar{J}} k'_{\bar{J}}(k,\varepsilon,h) d\mu_{\bar{J}}(k,\varepsilon,h) \quad (15)$$

3 Calibration

In this section, we begin by calibrating some of the model's parameters to the pre-pandemic steady state and discuss how other parameters are set. We will then use the calibrated model to analyze the distributional effects of the pandemic and mitigation policies. The parameters are summarized in Tables 1 and 2.

3.1 Economic parameters

A period in the model is two weeks. The aggregate measure of individuals in the steady state economy is normalized to one. The number of age cohorts, J, is set to 3, so that $j = 1$ corresponds to ages 25–44 (young), $j = 2$ corresponds to ages 45–64 (middle), and $j = J_R = \bar{J} = 3$ corresponds to ages 65–84 (old). The aging probability $\psi_j = \psi$ is set so that agents spend, on average, 20 years in each age cohort. The wealth of deceased individuals are rebated to a fraction of newborn individuals each period. Specifically, 85 percent of individuals are born with zero wealth, whereas 15 percent of individuals are endowed with 28 times annual per capita consumption.[6]

The age-profile of efficiency units, η_{jS}, is normalized to one for healthy young workers and healthy middle-age workers are assumed to be 35 percent more efficient, to match the wage ratio in the data (2014, *Panel Survey of Income Dynamics*). I assume that the efficiencies of recovered individuals are the same as that of susceptible individuals, $\eta_{jR} = \eta_{jS}$.[7] The

[6]This is based on the fact that 85 percent of households whose heads are between the ages of 21 and 25 had a cumulative net worth of zero in 2016 (*Survey of Consumer Finances*). The calibrated value of the endowment is rather large. Adding additional age groups would mitigate this issue, but would add to the computational burden.

[7]It is too early to conclude about the potentially long-lasting consequences of COVID-19. That said, if needed, the model can easily incorporate these changes in future work.

Covid Economics 47, 4 September 2020: 130-161

Covid Economics 47, 4 September 2020: 130-161

fraction of labor that can do done from home, $\bar{\theta}_j(\varepsilon)$ is set to match the average share of jobs that can be done from home by occupations grouped into five wage bins, computed based on Dingel and Neiman (2020). The average share of jobs that can be done from home ranges from 0.03 for the occupations in the bottom 20 percent of the wage distribution to 0.66 for those in the top 20 percent.

The time discount factor β is chosen so that the model replicates the US net-worth-to-GDP ratio (2014, *US Financial Accounts*). The parameter that governs the disutility from labor, φ, is set so that the model generates a share of disposable time spent working of 0.3, equivalent to 30 hours per week. I set risk aversion, σ, to be 2 and the Frisch elasticity, $1/\nu$, to be 0.5 (for example, see Chetty et al. (2011), which are both standard values in the literature.

To set the flow value of life, I follow Glover et al. (2020) who use a value of statistical life (VSL) of \$11.5 million, which corresponds to 7,475 times biweekly consumption per capita in the United States.[8] For simplicity, we can assume that the VSL is computed based on the consumption of a healthy infinitely-lived representative agent that discounts time at the rate of $\beta(1-\psi)$ in the pre-pandemic steady state, whose present discounted utility is given by

$$v = \frac{(\bar{c}+\Delta_c)^{1-\sigma}}{1-\sigma} + \bar{u} + \frac{\beta(1-\psi+\Delta_\psi)}{1-\beta(1-\psi)}\left(\frac{\bar{c}^{1-\sigma}}{1-\sigma}+\bar{u}\right) \tag{16}$$

where $\bar{c}$ denotes steady state consumption per capita and Δ_c and Δ_ψ denote small one-time deviations to consumption and survival probability. Then, the VSL—defined as the marginal rate of substitution between survival and consumption—can be expressed as

$$VSL = \left.\frac{\frac{\partial v}{\partial \Delta_\psi}}{\frac{\partial v}{\partial \Delta_c}}\right|_{\Delta_c=0} = \frac{\beta}{1-\beta(1-\psi)}\frac{\frac{\bar{c}^{1-\sigma}}{1-\sigma}+\bar{u}}{\bar{c}^{-\sigma}}. \tag{17}$$

Then, by substituting $VSL = 7475 \times \bar{c}$, we obtain

$$\bar{u} = 7475 \times \bar{c}^{1-\sigma}\frac{1-\beta(1-\psi)}{\beta} - \frac{\bar{c}^{1-\sigma}}{1-\sigma}. \tag{18}$$

The capital elasticity in the production function, α, is set to match the aggregate capital income share of 0.36. The consumption tax τ_c is set to zero, while the income tax τ_ℓ and

[8] As a robustness check, I use the VSL recommended by the Environmental Protection Agency, which is 7.4 million 2006 dollars, or 6,208 times biweekly consumption per capita in 2006. The main results of the paper are robust to this lower value.

Covid Economics 47, 4 September 2020: 130-161

Table 1: Calibration of economic parameters

Parameters	Values	Targets / Source
Discount factor, annualized, β	0.97	Wealth-to-GDP: 4.81 (2014)
Risk aversion, σ	2	Standard value
Disutility from labor, φ	114	Average hours: 30 hours per week
Frisch elasticity, $1/\nu$	0.50	Standard value
Flow value of life, $\bar{u}$	9.51	Value of statistical life: \$11.5 million
Aging probability, annualized, ψ	0.05	Expected duration: 20 years
Efficiency units, $\eta_{jS} = \eta_{jR}$	$\{1, 1.35\}_{j=1,2}$	Wage ratio of age 45-64 workers to age 25-44 workers (PSID)
Factor elasticity, α	0.36	Capital share
Capital depreciation, annualized, δ	0.05	Standard value
Retirement income, s	1.00	30% of average earnings per worker
Labor income tax, τ_ℓ	0.15	Government budget constraint
Consumption tax, τ_c	0.00	
Persistence, annual, ρ_ε	0.94	Author estimates (PSID)
Standard deviation, annual, σ_υ	0.19	Author estimates (PSID)

retirement income s are chosen so that retirement income is 30 percent of average labor earnings in the model and the government budget constraint is satisfied. The depreciation rate of capital, δ, is set at an annualized rate of 5 percent per year.

The labor productivity shocks ε are assumed to follow an order-one autoregressive process as follows:

$$\log \varepsilon_t = \rho_\varepsilon \log \varepsilon_{t-1} + \upsilon_t,\ \upsilon_t \sim N\left(0, \sigma_\upsilon^2\right). \tag{19}$$

This process is estimated using annual wages constructed from the PSID to find a persistence of $\rho_\varepsilon = 0.94$ and a standard deviation of $\sigma_\upsilon = 0.19$.[9] These parameters are then converted to a higher frequency, following Krueger et al. (2016). The process is approximated with a seven-state Markov process using the Rouwenhurst procedure described in Kopecky and Suen (2010).

[9]The wages are constructed similarly to Floden and Lindé (2001) and the sample selection and estimation procedures closely follow Krueger et al. (2016) and Carroll and Hur (2020). See Appendix A for details.

Covid Economics 47, 4 September 2020: 130-161

3.2 Parameters related to COVID-19

The exit rate, π_X is set to 14/18 so that the expected duration of the infection is 18 days, as in Atkeson (2020) and Eichenbaum et al. (2020). For the unconstrained case fatality rates, I use data from South Korea's Ministry of Health and Welfare to compute a fatality rate of 8.47 percent for ages 65–84, 0.94 percent for ages 45–64, and 0.09 percent for ages 25–44. I use South Korean data because testing has been abundant since the outbreak began[10], the peak in infections was early enough that case fatality rates are not biased due to lags in deaths, and hospitals were not overwhelmed, as the number of active cases never exceeded 0.015 percent of the population.[11]

Next, we discuss the hospital capacity constraints and how they affect death rates. Following Piguillem and Shi (2020), I use the functional form

$$\delta_j(\mu_I) = \delta_j^u \min\left\{1, \frac{\kappa}{\mu_I}\right\} + \delta_j^c \max\left\{0, 1 - \frac{\kappa}{\mu_I}\right\} \tag{20}$$

where δ_j^u and δ_j^c denote the unconstrained and constrained death rates and κ denotes the number of infected individuals that can be treated without the constraint binding. According to the American Hospital Association, there are roughly 924,000 hospital beds in the US, corresponding to 0.28 percent of the population.[12] Since not all infected cases require hospitalization, I use a generous capacity constraint, H, of 1 percent. The unconstrained death rates, δ_j^u, are set to match those documented for South Korea, and the constrained death rates are set as $\delta_j^c = 2\delta_j^u$, following Piguillem and Shi (2020).

There is quite a bit of uncertainty regarding the basic reproduction number (R_0), which corresponds to the number of people to whom the average infected person passes the disease absent mitigation efforts, though most estimates range between 2.2 and 3.1 (see for example, Wang et al. 2020 and Fauci et al. 2020). Using equation (11), total new infections in a given period is given by

$$T = \beta_c C_S C_I + \beta_\ell L_S^o L_I^o + \beta_e \mu_S \mu_I, \tag{21}$$

[10]For example, see https://www.bloomberg.com/news/articles/2020-04-18/seoul-s-full-cafes-apple-store-lines-show-mass-testing-success. Aum et al. (2020) also discuss the success of early testing and tracing efforts in South Korea.

[11]Active infection cases in South Korea peaked at 7,362 on March 11, 2020, according to Worldometer. See https://www.worldometers.info/coronavirus/country/south-korea/

[12]See https://www.aha.org/statistics/fast-facts-us-hospitals.

Covid Economics 47, 4 September 2020: 130-161

where C_h and L_h^o are the aggregate steady state consumption and labor supply of individuals with health status $h \in H$. In the pre-pandemic steady state, workers are indifferent between working outside or working from home. Thus, I assume that all steady state work is done outside, which can be obtained by introducing an arbitrarily small difference in either productivity or preference in favor of working outside. If we assume that when the virus is first introduced into the model, we have that $L_S/\mu_S = L_I/\mu_I$ and $C_S/\mu_S = C_I/\mu_I$, then by taking $\mu_S \to 1$, the basic reproduction number is given by[13]

$$R_0 = \frac{\beta_c C_S^2 + \beta_\ell L_S^2 + \beta_e}{\pi_X}. \tag{22}$$

Thus given values for the basic reproduction number, R_0, the exit rate, π_X, the steady state values for aggregate consumption and labor, C_S and L_S, we need to assign values to the fractions of new infections occurring through consumption activities, work activities, and other channels in order to pin down the values for β_c, β_ℓ, and β_e. Evidence on how COVID-19 is transmitted is limited, but in the case of other infectious diseases, Ferguson et al. (2006) report that 70 percent of transmissions occur outside of the household. In another study that investigates the transmission channels of infectious diseases, Mossong et al. (2008) find that 35 percent of high-intensity contacts occur in workplaces and schools. Based on these studies, I assume that one-third of initial transmission occurs through consumption activities, one-third through labor activities, and one-third through other channels.

For the value of being infected, Glover et al. (2020) assume a 30 percent reduction in the flow value of life for an average infected agent with mild symptoms and a 100 percent reduction in the flow value of life for an average infected agent with severe symptoms. I take an intermediate value of 50 percent by setting $\hat{u}_I = -0.5(\bar{c}^{1-\sigma}/(1-\sigma) + \bar{u})$ and set $\hat{u}_S = \hat{u}_R = 0$.[14]

Next, I discuss how the efficiency units change when an individual gets infected. It is reasonable to expect that those with no symptoms would suffer little, if any, efficiency loss, whereas those that experience very severe symptoms would suffer something close to a 100 percent efficiency loss. Without sufficient evidence regarding how COVID-19 affects labor productivity and the fraction of infected individuals suffering severe symptoms, I assume

[13] These assumptions allow the calibration of these epidemiological parameters using steady state values. These may also be reasonable assumptions, given that the very first infected individuals may not change their behavior given the lack of testing and information regarding the pandemic in the early stages.

[14] The results are robust to a 30 percent reduction in the flow value of life, as shown in Appendix B

Covid Economics 47, 4 September 2020: 130-161

Table 2: Calibration of Epidemiological parameters

Parameters	Values	Targets / Source
Infection exit rate, π_X	0.78	Expected infection duration: 18 days
Unconstrained death rate,		Fatality rates in South Korea
$\delta_1^u \times 100$	0.09	
$\delta_2^u \times 100$	0.94	
$\delta_3^u \times 100$	8.47	
Constrained death rate, δ_j^c	$2\delta_j^u$	Piguillem and Shi (2020)
Hospital capacity, κ	0.01	See discussion above
Transmission parameters,		Basic reproduction number, $R_0 = 2.2$,
consumption-related, β_c	0.08	and initial transmission equally
labor-related, β_ℓ	14.20	likely through three channels
other, β_e	0.57	
Flow value of infection $\hat{u}_I$	–4.57	50 percent reduction in flow utility value of average agent
Efficiency units η_{jI}	$0.5\eta_{jS}$	See discussion above

that infected individuals suffer a 50 percent loss in efficiency.[15]

4 Pandemic

This section uses the model to investigate the distributional consequences of the pandemic and various mitigation measures. First, I will explore how the endogenous transmission model—one in which economic interactions change the spread of the virus—differs from an exogenous transmission model—one in which the spread of the virus only depends on the number of susceptible and infected agents. This can also be thought of as the role of private mitigation. Second, I will explore the effect of various mitigation policies. In particular, I contrast a *lockdown*, implemented in the model by imposing a maximum labor supply of 20 hours per week for all agents, with a *subsidy-and-tax* policy that subsidizes working less than 20 hours per week, funded by a tax on consumption. While both policies reduce infections and deaths and raise welfare, the subsidy-and-tax policy delivers a higher welfare gain and is

[15] Appendix B shows that the main results are robust to assuming a 30 percent loss in efficiency.

Covid Economics 47, 4 September 2020: 130-161

favored by almost all agents in the economy, whereas the lockdown benefits older individuals at the expense of younger, low-wage workers.

The economy starts in the pre-pandemic steady state in period $t = 0$. Then, in period $t = 1$ (April 1, 2020), the virus is introduced into the model so that 0.1 percent of the population is infected. I assume that a vaccine and cure is developed and fully implemented by April 1, 2022, after which the model transits back toward its steady state.[16] An important caveat is that, while the steady state analysis was done in general equilibrium, the transition path analysis is done in partial equilibrium, meaning that wages and capital rental rates are fixed at their steady-state levels. I also do not require the government budgets to be balanced nor do I change the measure of newborns and their wealth distribution throughout the transition. This implies that, as a result of the pandemic, the measure of agents in the economy may be less than 1 during the transition.

To solve the transition, the economy begins in the steady-state distribution, μ_j, at $t = 0$. Then, the virus is introduced in $t = 1$, and I solve for a sequence of value functions, $\{V_{jt}, v_{jt}\}_{t=1}^{\infty}$, policy functions, $\{c_{jt}, \ell_{jt}, \ell^o_{jt}, k'_{jt}\}_{t=1}^{\infty}$, distributions μ_{jt}, fiscal policies, $\{\tau_{ct}, \tau_{\ell t}\}_{t=1}^{\infty}$, for $j \in J$, such that given prices, households make optimal decisions and distributions are consistent with shocks, the invariant distribution of newborns, and household decisions.

4.1 Endogenous virus transmission

To better understand how the baseline model—the "SIR Macro" model with endogenous transmission—works, we can contrast it with the alternative "SIR" model with exogenous transmission, where $\beta_c = \beta_\ell = 0$. In the SIR model, we set $\beta_e = 1.71$ so that the model has the same basic reproduction number, $R_0 = 2.2$, as in the baseline SIR Macro model.

Figure 1 shows that even though the SIR Macro and SIR models begin with the same reproduction number (panel a), the SIR Macro model exhibits a quicker decline in the reproduction number and consequently a lower number of infections (panel b) and deaths (panel c). This is because, in response to the pandemic, agents in the SIR Macro model reduce their consumption and hours dramatically, as can be seen in Figure 1, panels (d) and

[16] While there is a lot of uncertainty regarding when a vaccine might be approved and distributed, this approach allows the computational burden to be reduced dramatically. An alternative approach would be to model the arrival of a vaccine and cure probabilistically.

Covid Economics 47, 4 September 2020: 130-161

Figure 1: Engodenous vs. exogenous transmission (no mitigation)

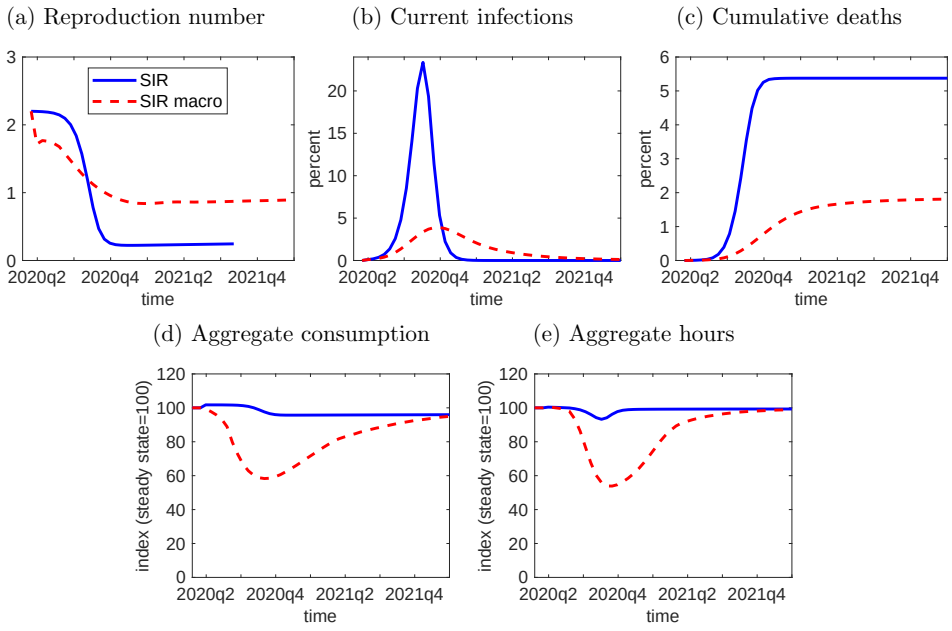

(e).

Taking a closer look at the baseline model, consider the policy functions for consumption and outside labor of susceptible agents across the age, income, and wealth distribution (Figure 2). The decline in hours and consumption is broad based. However, the decline in consumption is much greater for middle-aged and old agents than for young agents (panels a–c), and the decline in hours is much larger and more sustained for middle-aged workers than for young workers (panels d–e). This reflects the lower fatality risk for young agents. Moreover, among young workers, the declines in consumption and outside hours are the smallest for low-wage and low-wealth workers. Low-wage, high-wealth workers sit out the labor market altogether during the infection peak, suggesting that the lack of precautionary savings to draw from prevents low-wealth individuals from reducing their labor supply by more. Overall, young workers experience a much larger increase in infections, as shown in panel (f).

Covid Economics 47, 4 September 2020: 130-161

Figure 2: Response to pandemic (no mitigation)

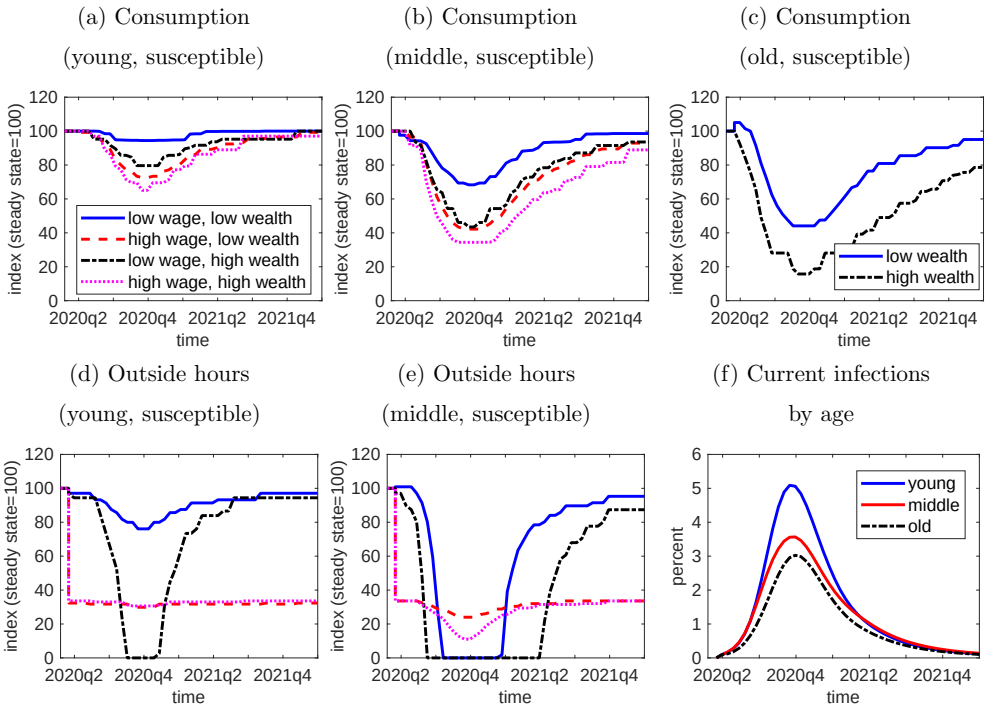

Notes: Low income and high income correspond to 10th and 90th percentiles of the steady state wage distribution. Low wealth and high wealth correspond to the 25th and 75th percentiles of the steady state wealth distribution.

Covid Economics 47, 4 September 2020: 130-161

4.2 Mitigation policies

The previous subsection highlighted the externalities at work: Young workers do not reduce their consumption and labor as much as their older counterparts and incur higher infections. These responses are individually rational in the sense that young workers do not face high fatality risk. However, higher rates of infection among young agents also lead to higher infections among older individuals, who face higher fatality rates.

In this subsection, we explore several mitigation policies that reduce infection and death rates. In particular, we compare and contrast two different mitigation policies. The first is a blanket *lockdown*, implemented in the model by restricting outside labor supply to less than 20 hours per week for all agents, beginning April 1, 2020, with a gradual relaxation after August 1, 2020. The outside hours cap increases linearly, reaching 40 hours by March 1, 2021, and is no longer binding for any individual after May 1, 2021. The second is a *subsidy-and-tax* policy, which incentivizes reduced work by providing a subsidy amount of 25 percent of consumption per capita, equivalent to roughly $200 per week, for any working-age individual working less than 20 hours per week.[17] The subsidy begins April 1, 2020, with a gradual reduction after August 1, 2020. The subsidy declines to $100 by February 1, 2021, and to zero by April 1, 2022. The subsidy is funded by a 17 percent consumption tax, beginning April 1, 2020, with a gradual phase-out after August 1, 2020, reaching zero by April 1, 2022. The tax and subsidy do not clear period-by-period, but rather they clear in net present value. Thus, both policies are budget neutral from the government's perspective.

Figure 3 panels (a)–(c) plot the evolution of the disease under the laissez-faire scenario as well as the two mitigation scenarios. Relative to the case with no mitigation, both mitigation policies reduce the reproduction number faster, leading to a lower peak in infection rates and less deaths. However, the subsidy-and-tax policy is much more effective in reducing the number of deaths than the blanket lockdown policy. Panels (d) and (e) show that this is obtained by lower hours throughout the transition and generally lower consumption as well.

Figure 4 panels (a)–(c) and (d)–(e) show the policy functions for consumption and outside

[17] Here, I assume that, for administrative purposes, the criteria to qualify for the subsidy is for total hours worked as it may be difficult for the administrator to ascertain what fraction of hours were outside versus at home. This is in contrast to the lockdown policy, where I assume that the hours cap is for outside labor. The idea is that the lockdown is administered at the firm-level whereas the subsidy is administered at the individual level.

Covid Economics 47, 4 September 2020: 130-161

Figure 3: Disease transmission (with and without mitigation)

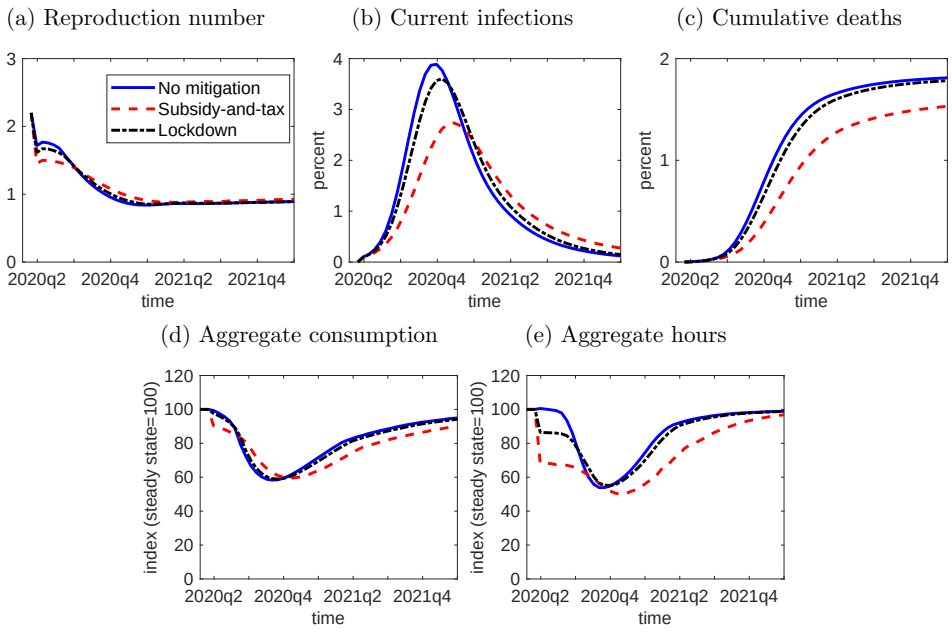

Covid Economics 47, 4 September 2020: 130-161

Figure 4: Response to pandemic (subsidy-and-tax)

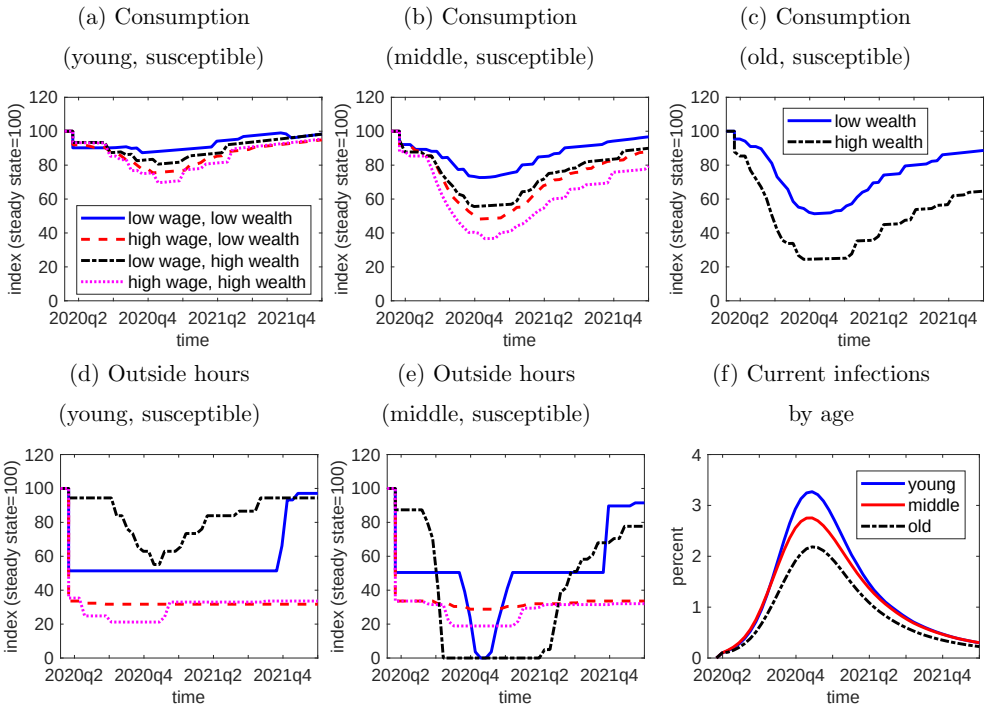

Notes: Low income and high income correspond to 10th and 90th percentiles of the steady state wage distribution. Low wealth and high wealth correspond to the 25th and 75th percentiles of the steady state wealth distribution.

hours, respectively, for susceptible individuals under the subsidy-and-tax policy. Relative to the case with no mitigation, the reduction in consumption and outside hours is more broad-based, including declines in consumption and hours for young low-wage, low-wealth workers. As a result, the peak infection rate for young agents declines from 5.1 percent to 3.3 percent (panel f).

Qualitatively, the blanket lockdown policy has similar properties as the subsidy-and-tax policy in the sense that they both reduce consumption and labor, infection, and death rates. However, in terms of welfare, measured in consumption equivalents, the blanket lockdown policy is vastly inferior.[18] The subsidy-and-tax policy reduces the average welfare loss from

[18]Specifically, the consumption equivalent is defined as what percentage change of remaining lifetime

Covid Economics 47, 4 September 2020: 130-161

Table 3: Welfare consequences of pandemic and mitigation policies

	consumption equivalents (percent)				
	low wealth		high wealth		average
	low wage	high wage	low wage	high wage	
No mitigation					–19.3
young	–2.7	–3.6	–3.8	–4.7	
middle	–11.4	–14.7	–15.2	–20.4	
old	–29.6		–45.3		
Subsidy-and-tax					–17.5
young	–2.3	$-3.7^{\dagger}$	–3.3	–4.5	
middle	–9.7	–13.2	–13.5	–18.5	
old	–26.7		-41.6^{*}		
Lockdown					–19.2
young	$-3.1^{\dagger}$	–3.6	–3.8	–4.7	
middle	–11.5	–14.6	–15.1	–20.3	
old	–29.2		-44.9^{*}		

Notes: Low (high) wage corresponds to below (above) the median wage. Low (high) wealth corresponds to below (above) the median wealth. * and † denote the largest and smallest welfare gains from the mitigation policies, respectively.

the pandemic by 1.8 percentage points, whereas the lockdown policy reduces the average welfare loss by only 0.1 percentage points, as can be seen in Table 3. This is because the lockdown policy is mainly favored by older agents who most value the lower risk of death induced by the policy and is opposed by young low-wage, low-wealth workers for whom the lockdown policy is most binding. For middle-aged workers, the benefit of the lower death risk is mostly offset by the cost of the hours cap. Overall, the lockdown policy is favored by 84.4 percent of the initial population. In contrast, the subsidy-and-tax policy is is favored by almost all agents in the economy.

There has been plenty of debate about the tradeoff between output and health. It is also the case that the mitigation policies studied in this paper induce larger output losses than

consumption in the steady state would make the individual indifferent to the pandemic and, if applicable, mitigation policies.

Covid Economics 47, 4 September 2020: 130-161

Figure 5: Welfare and lives

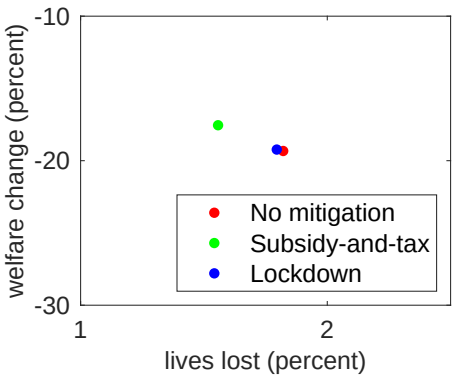

the no mitigation case. However, in terms of welfare, for the appropriately designed policy, there seems to be no tradeoff, as can be seen in Figure 5.

5 Conclusion

In this paper, I developed a quantitative life-cycle economic-epidemiology model that was used to measure the heterogeneous welfare consequences of COVID-19, with and without mitigation efforts. The paper also shows that, with well-designed policies, there is no trade-off between economic well-being and saving lives. In particular, a policy that subsidizes individuals to work less hours, funded by a tax on consumption, saves nearly a half-million lives and is favored by almost all individuals, regardless of age, income, or wealth.

Covid Economics 47, 4 September 2020: 130-161

References

Adams-Prassl, A., T. Boneva, M. Golin, and C. Rauh (2020): "Inequality in the impact of the coronavirus shock: Evidence from real time surveys," *Journal of Public Economics*, 189, https://doi.org/10.1016/j.jpubeco.2020.104245.

Aiyagari, S. R. (1994): "Uninsured Idiosyncratic Risk and Aggregate Saving," *The Quarterly Journal of Economics*, 109, 659–684, https://doi.org/10.2307/2118417.

Alon, T., M. Doepke, J. Olmstead-Rumsey, and M. Tertilt (2020a): "This Time It's Different: The Role of Women's Employment in a Pandemic Recession," Tech. rep., National Bureau of Economic Research, https://doi.org/10.3386/w27660.

Alon, T. M., M. Doepke, J. Olmstead-Rumsey, and M. Tertilt (2020b): "The Impact of COVID-19 on Gender Inequality," *Covid Economics*, 4, 65–85, https://doi.org/10.3386/w26947.

Alstadsæter, A., B. Bratsberg, G. Eielsen, W. Kopczuk, S. Markussen, O. Raaum, and K. Røed (2020): "The first weeks of the coronavirus crisis: Who got hit, when and why? Evidence from Norway," Tech. rep., National Bureau of Economic Research, https://doi.org/10.3386/w27131.

Alvarez, F., D. Argente, and F. Lippi (2020): "A Simple Planning Problem for COVID-19 Lockdown," *Covid Economics*, 14, 1–32, https://doi.org/10.3386/w26981.

Argente, D. O., C.-T. Hsieh, and M. Lee (2020): "The Cost of Privacy: Welfare Effect of the Disclosure of COVID-19 Cases," Tech. rep., National Bureau of Economic Research, https://doi.org/10.3386/w27220.

Atkeson, A. (2020): "What will be the economic impact of COVID-19 in the US? Rough estimates of disease scenarios," Tech. rep., National Bureau of Economic Research, https://doi.org/10.3386/w26867.

Aum, S., S. Y. T. Lee, and Y. Shin (2020): "Inequality of fear and self-quarantine: Is there a trade-off between GDP and public health?" *Covid Economics*, 14, 143–174, https://doi.org/10.3386/w27100.

Bairoliya, N. and A. Imrohoroglu (2020): "Macroeconomic Consequences of Stay-At-Home Policies During the COVID-19 Pandemic," *Covid Economics*, 13, 71–90, https://www.marshall.usc.edu/sites/default/files/bairoliy/intellcont/macroeffects_of_corona-1.pdf.

Bartik, A. W., Z. B. Cullen, E. L. Glaeser, M. Luca, and C. T. Stanton (2020): "What jobs are being done at home during the COVID-19 crisis? Evidence from firm-level surveys," Tech. rep., National Bureau of Economic Research, https://doi.org/10.3386/w27422.

Berger, D. W., K. F. Herkenhoff, and S. Mongey (2020): "An seir infectious disease model with testing and conditional quarantine," *Covid Economics*, 13, 1–30, https://doi.org/10.3386/w26901.

Bertocchi, G. and A. Dimico (2020): "COVID-19, Race, and Redlining," *Covid Economics*, 38, 129–195, https://doi.org/10.1101/2020.07.11.20148486.

Bewley, T. (1986): "Stationary monetary equilibrium with a continuum of independently fluctuating consumers," in *Contributions to mathematical economics in honor of Gérard Debreu*, ed. by W. Hildenbrand and A. Mas-Colell, North-Holland Amsterdam, vol. 79.

Bick, A., A. Blandin, and K. Mertens (2020): "Work from home after the COVID-19 Outbreak," Tech. rep., https://doi.org/10.24149/wp2017r1.

Birinci, S., F. Karahan, Y. Mercan, and K. See (2020): "Labor Market Policies during an Epidemic," Tech. rep., https://doi.org/10.20955/wp.2020.024.

Bodenstein, M., G. Corsetti, and L. Guerrieri (2020): "Social distancing and supply disruptions in a pandemic," *Covid Economics*, 19, 1–52, https://ssrn.com/abstract=3594260.

Bognanni, M., D. Hanley, D. Kolliner, and K. Mitman (2020): "Economic Activity and COVID-19 Transmission: Evidence from an Estimated Economic-Epidemiological Model," Tech. rep., University of Pittsburgh, https://doughanley.com/files/papers/COVID.pdf.

Covid Economics 47, 4 September 2020: 130-161

Carroll, D. and S. Hur (2020): "On the distributional effects of international tariffs," Tech. rep., Federal Reserve Bank of Cleveland, https://doi.org/10.26509/frbc-wp-202018.

Chari, V. V., R. Kirpalani, and C. Phelan (2020): "The hammer and the scalpel: On the economics of indiscriminate versus targeted isolation policies during pandemics," Tech. rep., National Bureau of Economic Research, https://doi.org/10.3386/w27232.

Chetty, R., J. N. Friedman, N. Hendren, M. Stepner, et al. (2020): "How did covid-19 and stabilization policies affect spending and employment? a new real-time economic tracker based on private sector data," Tech. rep., National Bureau of Economic Research, https://doi.org/10.3386/w27232.

Chetty, R., A. Guren, D. Manoli, and A. Weber (2011): "Are micro and macro labor supply elasticities consistent? A review of evidence on the intensive and extensive margins," *American Economic Review*, 101, 471–75, https://doi.org/10.1257/aer.101.3.471.

Chudik, A., M. H. Pesaran, and A. Rebucci (2020): "Voluntary and mandatory social distancing: Evidence on covid-19 exposure rates from chinese provinces and selected countries," *Covid Economics*, 15, 26–62, https://doi.org/10.3386/w27039.

Conesa, J. C., S. Kitao, and D. Krueger (2009): "Taxing capital? Not a bad idea after all!" *American Economic Review*, 99, 25–48, https://doi.org/10.1257/aer.99.1.25.

Dingel, J. I. and B. Neiman (2020): "How many jobs can be done at home?" *Covid Economics*, 1, 16–24, https://doi.org/10.3386/w26948.

Eichenbaum, M. S., S. Rebelo, and M. Trabandt (2020): "The macroeconomics of epidemics," Tech. rep., National Bureau of Economic Research, https://doi.org/10.3386/w26882.

Farboodi, M., G. Jarosch, and R. Shimer (2020): "Internal and external effects of social distancing in a pandemic," *Covid Economics*, 9, 22–58, https://doi.org/10.3386/w27059.

Fauci, A. S., H. C. Lane, and R. R. Redfield (2020): "Covid-19-navigating the uncharted," *New England Journal of Medicine*, 382, 1268–1269, https://doi.org/10.1056/NEJMe2002387.

Covid Economics 47, 4 September 2020: 130-161

Favilukis, J., S. C. Ludvigson, and S. Van Nieuwerburgh (2017): "The macroeconomic effects of housing wealth, housing finance, and limited risk sharing in general equilibrium," *Journal of Political Economy*, 125, 140–223, https://doi.org/10.1086/689606.

Ferguson, N. M., D. A. Cummings, C. Fraser, J. C. Cajka, P. C. Cooley, and D. S. Burke (2006): "Strategies for mitigating an influenza pandemic," *Nature*, 442, 448–452, https://doi.org/10.1038/nature04795.

Floden, M. and J. Lindé (2001): "Idiosyncratic risk in the United States and Sweden: Is there a role for government insurance?" *Review of Economic dynamics*, 4, 406–437, https://doi.org/10.1006/redy.2000.0121.

Garibaldi, P., E. R. Moen, and C. A. Pissarides (2020): "Modelling contacts and transitions in the SIR epidemics model," *Covid Economics*, 5, 1–20, https://www.carloalberto.org/wp-content/uploads/2020/04/garibaldi.pdf.

Gascon, C. and M. Ebsim (2020): "How Many Employees Are Prepared to Work from Home?" Tech. rep., https://www.stlouisfed.org/on-the-economy/2020/march/employees-work-home.

Glover, A., J. Heathcote, D. Krueger, and J.-V. Rios-Rull (2020): "Health versus Wealth: On the Distributional Effects of Controlling a Pandemic," *Covid Economics*, 6, 22–64, https://doi.org/10.1006/redy.2000.0121.

Heathcote, J., K. Storesletten, and G. L. Violante (2010): "The macroeconomic implications of rising wage inequality in the United States," *Journal of Political Economy*, 118, 681–722, https://doi.org/10.1086/656632.

Huggett, M. (1993): "The risk-free rate in heterogeneous-agent incomplete-insurance economies," *Journal of Economic Dynamics and Control*, 17, 953–969, https://doi.org/10.1016/0165-1889(93)90024-m.

Hur, S. (2018): "The lost generation of the Great Recession," *Review of Economic Dynamics*, 30, 179–202, https://doi.org/10.1016/j.red.2018.05.004.

Hur, S. and M. Jenuwine (2020): "Lessons on the Economics of Pandemics from Recent Research," *Economic Commentary*, https://doi.org/10.26509/frbc-ec-202011.

Covid Economics 47, 4 September 2020: 130-161

Imrohoroğlu, A. (1989): "Cost of Business Cycles with Indivisibilities and Liquidity Constraints," *Journal of Political Economy*, 97, 1364–1383, https://doi.org/10.1086/261658.

Jones, C., T. Philippon, and V. Venkateswaran (2020): "Optimal Mitigation Policies in a Pandemic: Social Distancing and Working from Home," Tech. rep., https://doi.org/10.3386/w26984.

Kapicka, M. and P. Rupert (2020): "Labor markets during pandemics," *Manuscript, UC Santa Barbara*.

Kaplan, G., B. Moll, and G. Violante (2020): "Pandemics According to HANK," Tech. rep., Virtual Presentation on March 31, 2020.

Kermack, W. O. and A. G. McKendrick (1927): "A contribution to the mathematical theory of epidemics," *Proceedings of the royal society of london. Series A, Containing papers of a mathematical and physical character*, 115, 700–721, https://doi.org/10.1098/rspa.1927.0118.

Kopecky, K. A. and R. M. Suen (2010): "Finite state Markov-chain approximations to highly persistent processes," *Review of Economic Dynamics*, 13, 701–714, https://doi.org/10.1016/j.red.2010.02.002.

Krueger, D., K. Mitman, and F. Perri (2016): "Macroeconomics and household heterogeneity," in *Handbook of Macroeconomics*, Elsevier, vol. 2, 843–921, https://doi.org/10.1016/bs.hesmac.2016.04.003.

Krueger, D., H. Uhlig, and T. Xie (2020): "Macroeconomic dynamics and reallocation in an epidemic," *Covid Economics*, 5, 21–55, https://doi.org/10.3386/w27047.

Mongey, S. and A. Weinberg (2020): "Characteristics of workers in low work-from-home and high personal-proximity occupations," *Becker Friedman Institute for Economic White Paper*, https://bfi.uchicago.edu/wp-content/uploads/BFI_White-Paper_Mongey_3.2020.pdf.

Mossong, J., N. Hens, M. Jit, P. Beutels, K. Auranen, R. Mikolajczyk, M. Massari, S. Salmaso, G. S. Tomba, J. Wallinga, et al. (2008): "Social con-

Covid Economics 47, 4 September 2020: 130-161

tacts and mixing patterns relevant to the spread of infectious diseases," *PLoS medicine*, 5, https://doi.org/10.1371/journal.pmed.0050074.

Osotimehin, S. and L. Popov (2020): "Sectoral Impact of COVID-19: Cascading Risks," Tech. rep., Federal Reserve Bank of Minneapolis, https://doi.org/10.21034/iwp.31.

Piguillem, F. and L. Shi (2020): "The Optimal COVID-19 Quarantine and Testing Policies," Tech. rep., Einaudi Institute for Economics and Finance (EIEF), http://www.eief.it/eief/images/WP_20.04.pdf.

Wang, H., Z. Wang, Y. Dong, R. Chang, C. Xu, X. Yu, S. Zhang, L. Tsamlag, M. Shang, J. Huang, et al. (2020): "Phase-adjusted estimation of the number of coronavirus disease 2019 cases in Wuhan, China," *Cell Discovery*, 6, 1–8, https://doi.org/10.1038/s41421-020-0148-0.

Wozniak, A. (2020): "Disparities and Mitigation Behavior during COVID-19," Tech. rep., Federal Reserve Bank of Minneapolis, https://doi.org/10.21034/iwp.32.

Covid Economics 47, 4 September 2020: 130-161

Covid Economics 47, 4 September 2020: 130-161

A Estimation of Wage Processes

The sample selection and estimation procedure closely follows the procedure described in Krueger et al. (2016) and Hur (2018). I use annual income data from the PSID core sample (1970–1997), selecting all household heads, ages 23 to 64. For waves before 1993, I use the variable Total Labor Income of Head, which is the sum of wages, tips, labor part of farm and business income, and other items. For waves after 1993, I compute total head labor income as the sum of the head's labor income (excluding farm and business income), head's labor part of business income, and 50 percent of household farm income, divided by two if married. Next, I construct wages by dividing head's total labor income by hours, where hours is the sum of hours worked, hours unemployed, and sick hours. I drop observations with missing education, with wages that are less than half of the minimum wage, with top-coded income, and with fewer than 1,000 hours per year. On this sample, I regress the log wage on age and education dummies, their interaction, and year dummies. I then exclude all individual wage sequences shorter than 5 years, leaving final samples of 4,524 individuals, with an average length of 9 years. On these samples, I compute the autocovariance matrix of the residuals. The stochastic process in equation (19) is estimated using GMM, targeting the covariance matrix, where the weighting matrix is the identity matrix. I thank Chris Tonetti for providing the Matlab routines that perform the estimation.

B Sensitivity analysis

B.1 Value of Statistical Life

In the baseline calibration, I used a VSL of $11.5 million, or 7,475 times biweekly consumption per capita in the US. As a robustness check, I use the VSL that is recommended by the EPA, which is 7.4 million 2006 dollars, or 6,208 times biweekly consumption per capita in 2006. I find that the main results are robust to this alternative value. Table 4 shows that a smaller value of statistical life decreases the welfare loss from the pandemic overall, but does not affect much distribution of welfare losses or the net effect of the mitigation policies.

Covid Economics 47, 4 September 2020: 130-161

Table 4: Welfare consequences (with $vsl = 6208\bar{c}$)

	consumption equivalents (percent)				
	low wealth		high wealth		average
	low wage	high wage	low wage	high wage	
No mitigation					–19.2
young	–2.3	–3.1	–3.3	–4.1	
middle	–11.2	–14.5	–15.0	–20.1	
old	–29.8		–45.5		
Subsidy-and-tax					–17.4
young	–2.0	$-3.3^{\dagger}$	–2.8	–3.9	
middle	–9.5	–12.9	–13.2	–18.2	
old	–26.8		-41.8^{*}		
Lockdown					–19.0
young	$-2.7^{\dagger}$	–3.1	–3.3	–4.0	
middle	–11.4	–14.3	–14.9	–20.0	
old	-29.4		-45.0^{*}		

Notes: Low (high) wage corresponds to below (above) the median wage. Low (high) wealth corresponds to below (above) the median wealth. * and † denote the largest and smallest welfare gains from the mitigation policies, respectively.

Covid Economics 47, 4 September 2020: 130-161

Table 5: Welfare consequences (with $\hat{u}_I = -2.74$)

	consumption equivalents (percent)				
	low wealth		high wealth		average
	low wage	high wage	low wage	high wage	
No mitigation					–17.3
young	–2.0	–2.7	–2.9	–3.5	
middle	–9.9	–12.8	–13.3	–18.0	
old	–26.7		–42.1		
Subsidy-and-tax					–15.7
young	–1.7	$-2.9^{\dagger}$	–2.4	–3.5	
middle	–8.4	–11.5	–11.7	–16.3	
old	–24.1		-38.6^{*}		
Lockdown					–17.2
young	$-2.4^{\dagger}$	–2.7	–2.8	–3.5	
middle	–10.0	–12.7	–13.2	–17.9	
old	–26.3		-41.6^{*}		

Notes: Low (high) wage corresponds to below (above) the median wage. Low (high) wealth corresponds to below (above) the median wealth. * and † denote the largest and smallest welfare gains from the mitigation policies, respectively.

B.2 Utility loss during infection

In the baseline calibration, I assumed that infection was associated with a 50 percent reduction in the flow value of the average healthy individual. Here, I investigate how the results change if an infection causes a 30 percent reduction. Table 5 shows that the distributional effects of pandemic and mitigation policies are largely unchanged from the baseline. Assuming a smaller utility loss during infection *decreases* the welfare loss of the pandemic for young individuals, but *increases* the welfare loss for old individuals. This is because the smaller utility loss induces more economic activity among susceptible individuals, relative to the baseline calibration, leading to higher infections. Without mitigation, the peak infection rate is 4.0 percent, compared with 3.9 percent in the baseline. This leads to a larger welfare loss for old individuals, who face a greater fatality risk.

CEPR PRESS

Table 6: Welfare consequences (with $\eta_{jI} = 0.7\eta_{jS}$)

	consumption equivalents (percent)				
	low wealth		high wealth		average
	low wage	high wage	low wage	high wage	
No mitigation					–19.7
young	–2.8	–3.7	–3.9	–4.8	
middle	–11.7	–15.0	–15.5	–20.7	
old	–30.2		–45.9		
Subsidy-and-tax					–17.7
young	–2.4	$-3.8^{\dagger}$	–3.4	–4.6	
middle	–9.9	–13.4	–13.7	–18.8	
old	–26.9		-42.0^{*}		
Lockdown					–19.5
young	$-3.2^{\dagger}$	–3.7	–3.9	–4.8	
middle	–11.8	–14.9	–15.4	–20.6	
old	-29.7		-45.4^{*}		

Notes: Low (high) wage corresponds to below (above) the median wage. Low (high) wealth corresponds to below (above) the median wealth. * and † denote the largest and smallest welfare gains from the mitigation policies, respectively.

B.3 Efficiency during infection

In the baseline calibration, I assumed that the efficiency of infected individuals was 50 percent that of susceptible and recovered individuals. Table 6 shows the results when the efficiency of infected individuals is assumed to be 70 percent that of susceptible and recovered individuals. The distributional effects of pandemic and mitigation policies are very similar to the baseline. Notably, assuming a smaller efficiency loss during infection *increases* the welfare loss of the pandemic and *increases* the welfare gain from mitigation policies. This is because infected individuals engage in more economic activity, relative to the baseline calibration, leading to higher infections and deaths in the aggregate. Without mitigation, the peak infection rate is 4.1 percent, compared to 3.9 percent in the baseline.

Covid Economics 47, 4 September 2020: 130-161

Mass outdoor events and the spread of an airborne virus: English football and Covid-19[1]

Matthew Olczak,[2] J. James Reade[3] and Matthew Yeo[4]

Date submitted: 27 August 2020; Date accepted: 29 August 2020

Mass attendance events are a mainstay of economic and social activity. Such events have public health consequences, facilitating the spreading of disease, with attendant economic consequences. There is uncertainty over the impact such events can have on the spread of disease. We investigate the impact of regular mass outdoor meetings on the spread of a virus by considering football matches in England in February and March 2020 and the spread of Covid-19 into April 2020. There were 340 league and cup football matches with a combined attendance of 1.625m people in March, taking place over 188 of 313 local areas. We look at the occurrence and attendance at matches, and how full the stadia were, and how these variables are related to the spread of Covid-19 in April. We evaluate Covid-19 cases, deaths and excess deaths, all as rates of 100,000 people in an area. We find evidence that mass outdoor events were consistent with more cases and deaths, even after controlling for measurable characteristics of local areas. We find that a football match is consistent with around six additional Covid-19 cases per 100,000 people, two additional Covid-19 deaths per 100,000 people, and three additional excess deaths per 100,000 people. This effect is slightly stronger for the areas of away teams in March, and slightly weaker for matches in February. These results suggest caution in returning to unrestricted spectator attendance at matches. We caveat our analysis though by noting that stadium access and egress routes can be adapted such that some of the opportunities for the spread of an airborne virus could be

1 We would like to thank Gary Ekins from footballwebpages.co.uk and Peter Ormosi for their help in constructing the datasets used in this paper, and Steven Bosworth, Stephen Kastoryano and Carl Singleton, along with seminar participants at the University of Reading for their comments on an earlier version of this paper. All errors remain our own.

2 Senior Lecturer, Aston Business School, Aston University.
3 Professor, Department of Economics, University of Reading.
4 Doctoral Student, Department of Economics, University of Reading.

Covid Economics 47, 4 September 2020: 162-183

mitigated. We recommend that the relevant authorities conduct pilot events before determining to what extent fans can return to mass outdoor events.

Covid Economics 47, 4 September 2020: 162-183

Covid Economics 47, 4 September 2020: 162-183

1 Introduction

Mass events are a mainstay of economic activity, be they work-related networking events, or ostensibly leisure events like music concerts or sporting events. Yet the concentration of people in relatively small areas has public health consequences; diseases can spread, with subsequent consequences for economic activity. The balance of these benefits and risks are usually tipped in favour of allowing mass events to take place. In the Covid-19 pandemic of 2020, the balance swung against holding such events, as the risks to public health infrastructure were judged to be so severe.[1]

An important aspect of making the decision regarding not only the value but also the health risk of mass events is to build up an evidence base. There have been some attempts to do that already; it appears that mass events do act as *superspreaders* of airborne viruses, as this is the clear conclusion of research by Stoecker et al. (2016), Ahammer et al. (2020) and Cardazzi et al. (2020). Ahammer et al. (2020) look at mass indoor events in the context of Covid-19, Cardazzi et al. (2020) consider indoor and outdoor events and their effect on influenza, and Stoecker et al. (2016) assess the impact of a local American Football team's participation in the Superbowl on influenza deaths. But what about mass outdoor events and their impact on the spread of Covid-19?

In this paper, we investigate the impact that outdoor events may have on the spread of Covid-19. We look at football matches, which are mass outdoor events that take place on a frequent basis across large parts of the world, but in particular in England.[2] In the 2018–2019 season, the last one completed in England before the Covid-19 pandemic, 11,279 matches took place in England in domestic league and cup competitions, nationwide and regional, with a total attendance of almost 45m people. Furthermore, these events are spread all around the country; of the 313 geographic areas of England and Wales that we consider in this study, 247 have football being played in them on a regular basis. Ninety three of these have more than one football club across the top eight levels of English football.

Fans congregate in pubs and bars before and after matches, and travel together in groups to matches, often on public transport, but also privately. Fans in stadiums often pack tightly together to create 'atmosphere', and sing and shout. Taken together, there is great potential for these events to be 'super spreaders', where an airborne virus like Covid-19 can spread from person to person. Equally, however, there is a balance of risks; as countries cope with the pandemic, important questions need to be answered about the extent to which normal activities should be resumed.

The abundance of data associated with football matches in England, and their prevalence across the country, along with data on Covid-19 cases, deaths and excess deaths, make football an ideal subject to evaluate the impact of mass outdoor events on the spread of an airborne virus.

We consider specifically football matches in England in March 2020, shortly before football was suspended, and we evaluate their impact on Covid-19 cases, deaths and excess deaths in April 2020. We find that a football match is consistent with around six additional Covid-19 cases per 100,000 people in the area it took place, two additional Covid-19 deaths per 100,000 people in the area it took place, and three additional excess deaths per 100,000 people in the area it took place. These effects are slightly stronger for the areas of away teams following each match in March, and slightly weaker for matches in February. Therefore, our results suggest caution in returning to unrestricted spectator attendance at matches.

In Section 2 we outline the relevant literature, in Section 3 we introduce our data sources and

[1] For example, by April the only professional football league in the world still playing was in Belarus.

[2] For the avoidance of doubt, when we refer to football in the remainder of this paper we refer to association football, soccer, or European football, as opposed to American football.

present summary statistics. In Section 4 we present out methodolgy, and in Section 5 we present results. Section 6 concludes.

2 Literature

The demand for attendance at football matches is a richly studied phenomena; counts of spectators at events are public information, and are recorded for many sporting events (see, for example, Soebbing (2008) for Major League Baseball in the US, Coates and Humphreys (2010) for American football, Coates and Humphreys (2012) for ice hockey in North America, Forrest and Simmons (2006, 2002) for English football, Garcia and Rodríguez (2002) for Spanish football, Owen and Weatherston (2004) for rugby union in Australia, and Paton and Cooke (2005); Sacheti et al. (2014) cricket in England). A common determinant of attendance is believed to be the level of uncertainty surrounding the outcome. Equally, though, intriguing arrangements have attracted the attention of studies. Peel and Thomas (1996) look at repeat fixtures, while Szymanski (2001) compare matches between the same pairs of teams in different competitions in English football. Wallrafen et al. (2019) consider lower division football, and Chabros et al. (2019) look at non-league football in England, paying particular attention to the rules prohibiting the live broadcasting of matches on a Saturday afternoon.

The determinants of attendance though in these studies have not included the presence of a global pandemic, at least, pre-Covid-19. Gitter (2017) is the notable exception, looking at Mexian baseball attendance during the H1N1 pandemic in 2009. Reade and Singleton (2020) look at the impact of the Covid-19 pandemic as it spread throughout Western Europe on the top football leagues in the region, finding mixed effects, while Reade et al. (2020) consider the one professional football league in Europe that did not suspend during the Covid-19 pandemic, that of Belarus. They find that fans did self-distance spontenously, even as their government took a relaxed approach to the virus.

The extent to which agents do socially distance spontenously matters for public policy in the midst of a public health crisis like Covid-19, since it must dictate the policy response. Mass outdoor events, as described in the introduction, have the potential to act as *super spreaders* of an airborne virus like Covid-19. Equally, most economic activity has this potential, and yet a balance of risk must be struck. Part of that balance involves knowing what the risks are. Ahammer et al. (2020), Stoecker et al. (2016) and Cardazzi et al. (2020) consider the impact of sporting events as *super spreaders*. Ahammer et al. (2020) look at mass indoor events in the Covid-19 pandemic, and find that these events led to around 380 more Covid-19 cases, and 16 more deaths per one million people in the counties events took place in. Stoecker et al. (2016) find that a US city having a team in the Superbowl saw an 18% increase in influenza deaths amongst the over-65 population. Cardazzi et al. (2020) take a longer term look at the presence of sport team franchises in US cities over many decades, and find that their presence led to between 4% and 24% more influenza deaths in the years since.

We are unaware of any existing study that considers the impact of mass outdoor events like football matches on the spread of an airborne virus. As Sassano et al. (2020) note, this is a 'surprising gap' in our knowledge. This is particularly important from a public policy perspective, as football represents such a significant mass outdoor pastime across much of Europe and indeed the world, and patterns associated with attendance at football matches (e.g. transit to/from matches and travelling to away matches) differ significantly from patterns for attendance at North American sports.

The impact of events, be they indoor or outdoor, on the spread of an airborne virus, will depend on a huge range of confounding factors that are beyond the scope of any study. For example, the design

Covid Economics 47, 4 September 2020: 162-183

of indoor and outdoor arenas allowing for, or discouraging, access and egress of people, will matter, since they will affect the likelihood of groups of people gathering closely together. Larsson et al. (2020) consider the adequacy of stadium designs for egress from a fire safety perspective, and the principles considered here in terms of the flow of participants at an event could matter for the transmission of an airborne virus.

As such, any conclusions drawn from our study of football matches in March need not be immediately applicable to any potential return of spectators to sporting events, since stadia can be altered to mitigate the spread of an airborne virus.

3 Data

We collect data from a range of sources. We collect data on Covid-19 cases, Covid-19 recorded deaths and excess deaths from the Office for National Statistics. Figures 1–3 plot these series, and document the extent to which Covid-19 spread around England in March and April.

In Figure 1, the cumulative numbers of cases in each area of England are plotted for March and April. There is considerable variation across areas, with many well below 100 cases per 100,000 people at the end of April, a mass of areas up to about 400 cases per 100,000, and one area, Barrow-in-Furness, recording around 800 cases per 100,000.

Covid Economics 47, 4 September 2020: 162-183

Covid Economics 47, 4 September 2020: 162-183

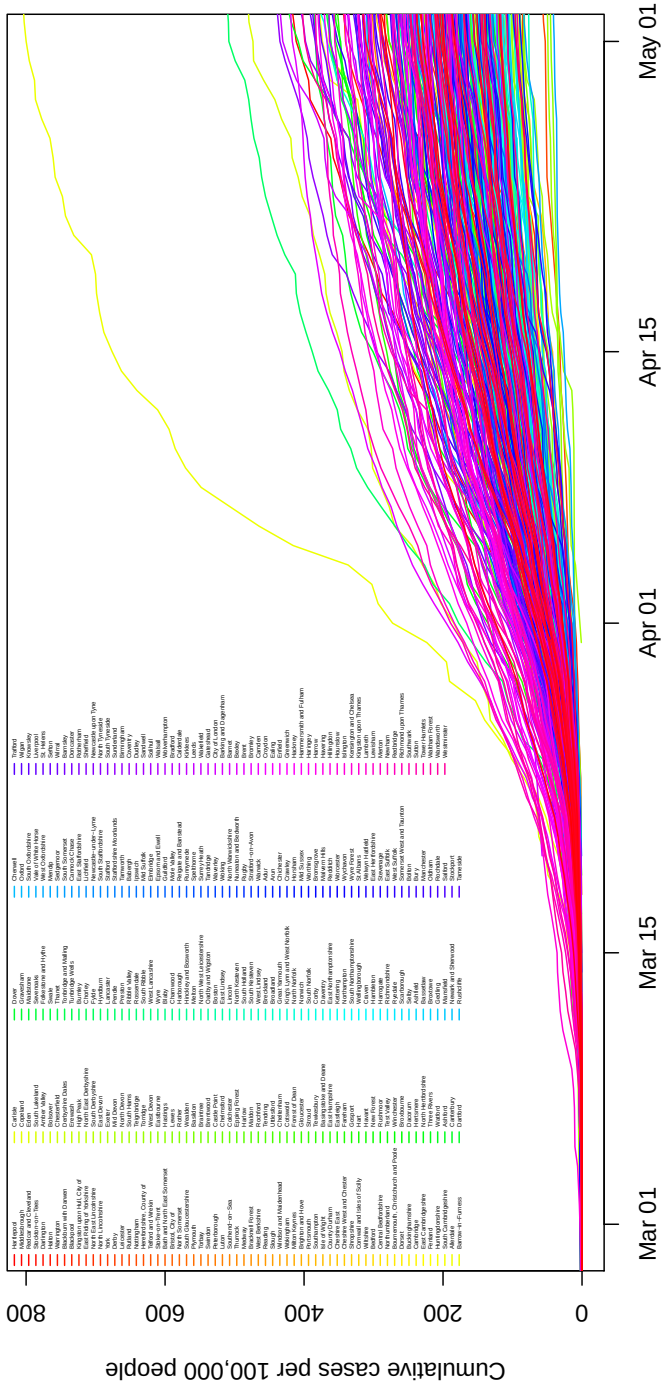

Figure 1: Time profile of Covid-19 cases per 100,000 people in all areas across England.

Covid Economics 47, 4 September 2020: 162-183

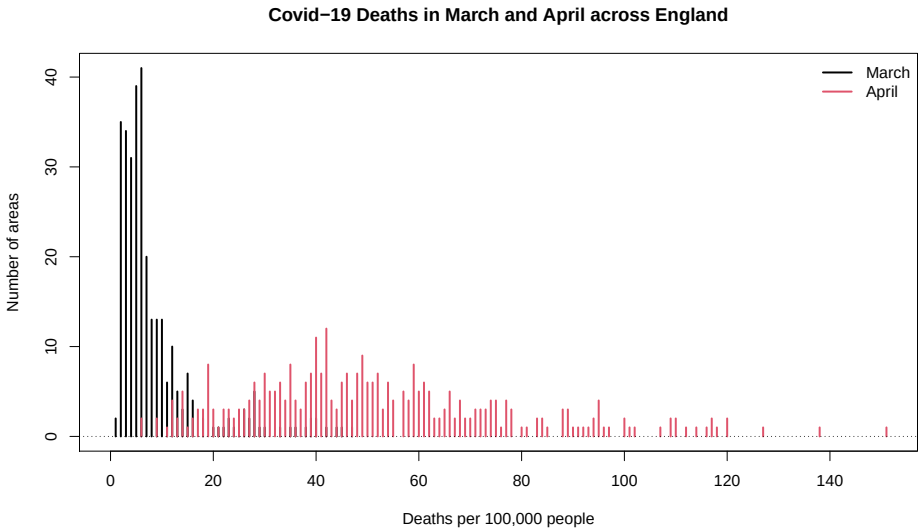

Figure 2: Distribution of Covid-19 deaths per 100,000 people in all areas across England.

In Figures 2 and 3, the distribution of deaths (Covid-19 and excess) per 100,000 people is plotted for March in black and April in red. For Covid-19 (Figure 2), the distribution is tightly centred between 5 and 10 deaths per 100,000 people in March, and much more spread in April around 40 deaths per 100,000 people. For excess deaths, the difference in distributions isn't quite so stark, but moves significantly to the right into April, centred around 130 deaths per 100,000 people.

Our football data are matches in the 2019–2020 season of English football, collected from football-webpages.co.uk, worldfootball.net, and footballgroundmap.com. Our data cover the top eight levels of the English football league system, the two major English cup competitions (the FA Cup and the League Cup), collected from footballwebpages.co.uk, and the two European competitions that English teams competed in (the Champions League and the Europa League), collected from worldfootball.net. We collected information on the capacities of stadia from footballgroundmap.com.

The data cover the English Premier League (288 matches), the top division in England, down to seven sub-regional leagues that constitute the eighth tier, via the English Football League (tiers 2 to 4, 1284 matches), the National League (tier 5, 452 matches), National League North and South (tier 6, 733 matches), four regional leagues covering the North, Midlands, South and East of England (tier 7, 1392 matches), and the seven sub-regional leagues below them (tier 8, 1956 matches).

The cup data consists of:

- 888 FA Cup matches that took place before the Covid-19 suspension, with 56 taking place in January, six in February and eight in March 2020.
- 121 League Cup matches, of which four took place in January (two-legged semi-finals), and one in March, the final at Wembley Stadium in London.

Covid Economics 47, 4 September 2020: 162-183

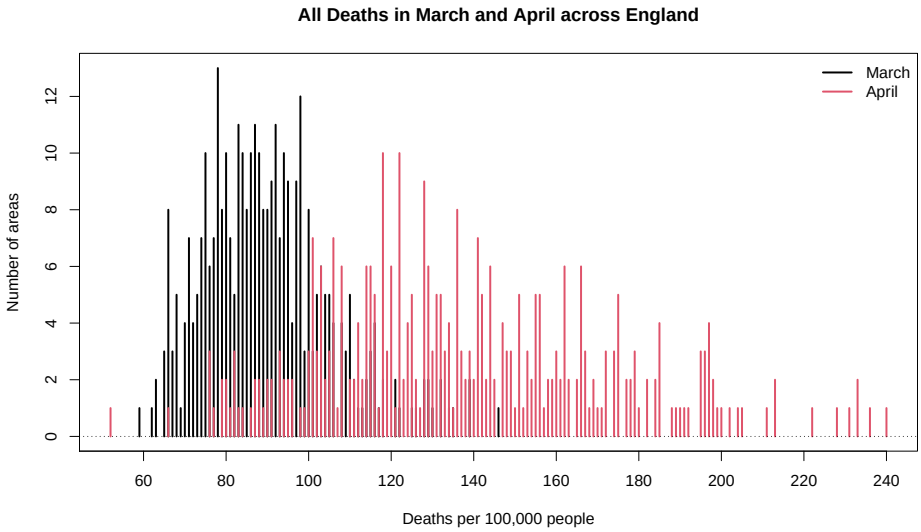

Figure 3: Distribution of excess deaths per 100,000 people in all areas across England.

- 15 Champions League, and 14 Europa League matches involving a visiting team from elsewhere in Europe, of which four were in late February and one was in March.

Table 1 provides further information on the spread of these matches over the months of the season up to the suspension in mid-March 2020. 340 matches took place in March, and 909 in February.

In the 2019–2020 season up until the suspension due to Covid-19, the average attendance in England's top tier was 39,410, from Table 2, and in the second tier it was almost 20,000. As low down as the sixth tier, average attendances were around 1,000 people. In Figure 4 the distribution of the percentage of stadia filled at matches during the 2019–2020 season is plotted. The bulk of matches are played in stadia less than 20% full, but there is also a concentration of matches with capacity above 90%, coinciding with generally Premier League matches. Of the 419 matches with capacity at or above 90%, 264 are in the Premier League, 82 are in the Championship, and 57 are in Cup competitions.

Fans attend matches, and often they are packed tightly together. In the top tier, on average 96.7% of a stadium's capacity was filled (Table 2). Even though in the fourth tier this falls to 45.1%, fans usually congregate in groups, often for the purpose of singing and shouting in support of their team, and congregate on concourses behind stands to purchase and consume refreshments and visit bathrooms. As such, even sparsely attended stadia may provide contexts in which an airborne virus can spread. Finally, crowds at football matches are noisy, shouting at the participants in the game. These are activities known to assist in the spreading of an airborne virus.

Another characteristic of football matches is the sizeable presence of visiting spectators. This naturally varies based on the distance between clubs, and the size of the following of different clubs, but away followings can amount to well in excess of a thousand spectators, down to a hundred or fewer.

Covid Economics 47, 4 September 2020: 162-183

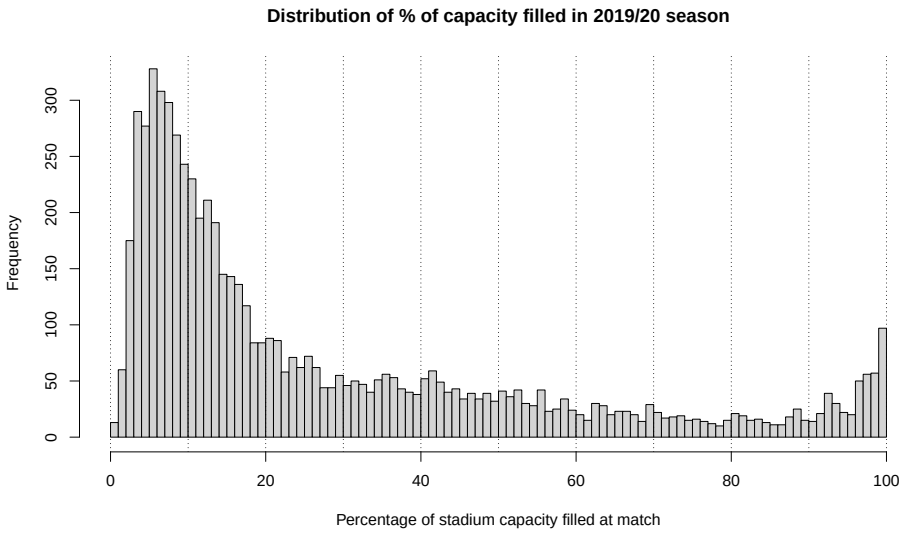

Figure 4: The distribution of the percentage of a stadium full in matches during the 2019–2020 season in all competitions covered in our dataset (6,612 matches).

Covid Economics 47, 4 September 2020: 162-183

Table 1: Breakdown of matches by competition/tier, and month.

	Aug 2019	Sep 2019	Oct 2019	Nov 2019	Dec 2019	Jan 2020	Feb 2020	Mar 2020
Champions League	0	1	5	5	1	0	2	1
Europa League	2	2	2	3	2	0	3	0
FA Cup	389	263	87	62	17	56	6	8
League Cup	84	17	8	0	4	4	0	4
Premier League	38	32	30	36	63	41	36	12
Championship	72	36	59	59	73	51	81	13
League One	64	51	50	34	56	56	72	17
League Two	72	60	56	35	58	72	71	16
National League	96	70	57	57	47	51	47	27
NL North and South	174	87	51	79	91	110	96	45
Tier 7	239	137	181	169	151	239	201	75
Tier 8	279	223	170	284	237	347	294	122
Total	1509	979	756	823	800	1027	909	340

Table 2: Stadium attendance statistics for English football in the 2019–2020 season.

Statistic	N	Mean	St. Dev.	Min	Pctl(25)	Pctl(75)	Max
Premier League							
Attendance	280	39,410	16,187	10,020	27,110	53,480	73,737
Proportion of capacity filled	280	0.967	0.038	0.808	0.956	0.993	1.024
Championship							
Attendance	435	18,592	6,368	8,965	13,011	22,611	36,514
Proportion of capacity filled	435	0.716	0.169	0.357	0.589	0.853	1.002
League One							
Attendance	388	8,790	6,403	1,816	4,882	9,436	33,821
Proportion of capacity filled	388	0.542	0.179	0.156	0.436	0.649	1.014
League Two							
Attendance	434	4,680	2,774	1,389	3,028	5,129	17,668
Proportion of capacity filled	434	0.451	0.144	0.155	0.347	0.547	0.928
National League							
Attendance	446	2,187	1,278	407	1,250	2,911	9,090
Proportion of capacity filled	446	0.316	0.138	0.090	0.218	0.384	1.053
National League North							
Attendance	360	1,076	680	160	574	1,356	4,019
Proportion of capacity filled	360	0.227	0.130	0.040	0.135	0.313	0.753
National League South							
Attendance	349	867	531	185	481	1,042	3,132
Proportion of capacity filled	349	0.247	0.165	0.074	0.131	0.304	1.044

Nonetheless, fans travel significant distances to football matches, via public and private transport, and usually in groups.

Football matches are a regular feature across most parts of the UK. Of the 313 geographic areas of England and Wales that we consider in this study, 247 have football being played in them on a regular basis. Ninety three of these have more than one football club across the top eight levels of English football. Thirty nine of these areas have regular matches with stadia more than 80% full. Such football matches take place, conventionally, on a fortnightly basis.

Across these 247 areas, 909 matches took place in our dataset during February 2020, and 340 in March 2020. Football in the top four tiers was suspended on March 13, with the remainder of the lower leagues the following week. As such, the final matches in our sample take place on March 14 2020.

4 Methodology

Our hypothesis is thus that football matches act to spread an airborne virus like Covid-19, and so we propose specifically that the incidence of football matches in particular areas may aid the spread of the virus in those areas. We investigate a number of models of the form:

$$y_i = \alpha_i + \beta football_i + \gamma X_i + \varepsilon_i. \tag{1}$$

That is, some measure of the spread of the virus in local area i, y_i, is a function of the existence of $football$ in area i, as well as a set of other variables X_{it}, which would include measures of the age profile of an area, its ethnic breakdown, and also lagged measures of the spread of the virus. The test of the hypothesis that football matches acted to spread the virus is whether $\beta > 0$.

For our measure of the spread of the virus, y_i, we consider three measures of mortality:

1. The cumulative rate of Covid-19 cases on April 30 2020, as per every 100,000 people in an area.
2. The rate of Covid-19 deaths in April 2020, as per every 100,000 people in an area.
3. The rate of excess deaths in April 2020, as per every 100,000 people in an area.

Our first measure of football in an area is the total number of matches over a time period, N_i, hence:

$$football_i = N_i. \tag{2}$$

Second, we sum up the attendance, A_n, across all matches in an area in a time period, so:

$$football_i = \sum_{n=1}^{N_i} A_n. \tag{3}$$

We then consider the following measures of capacity utilisation, where C_n is stadium capacity for match

Covid Economics 47, 4 September 2020: 162-183

n:

$$football_i = C_{k,i} = \sum_{n=1}^{N_i} 1_{\{A_n/C_n \geq k\}}, \tag{4}$$

$$football_i = C_{k,i} = \sum_{n=1}^{N_i} 1_{\{A_n/C_n < k\}}, \tag{5}$$

$$football_i = D_i = \frac{1}{N_i} \sum_{n=1}^{N_i} \left(\frac{A_n}{C_n}\right)^2. \tag{6}$$

We simply count the number of matches that were over (4) or under (5) a particular threshold of capacity k. Because the measures in (4) and (5) give a discrete representation of capacity utilisation across football matches in an area, in (6) we employ a continuous measure of capacity that weighs more heavily the matches that were close to capacity. We sum the squares of the attendance to capacity ratios and divide by the number of matches.

Our controls consist of the population density, the median age, the proportions of the local population between 16 and 64, the proportion of an area that is categorised as being of an ethnic minority, the average income level of an area, and the number of Football League clubs in an area.

Although there is a time element to (1), this is a cross section regression. We consider cumulative cases by a particular point, t, or deaths over a particular month, April, and consider the extent to which they are explained by standard controls, or by the presence of football matches in a preceding time period.

It is understood that the length of time from transmission of Covid-19 to it presenting itself is around two weeks (Lauer et al., 2020). It is further understood that Covid-19 can remain symptomless in many people (Bai et al., 2020), and as such, if somebody caught Covid-19 at a football match in early March, it is possible they may have passed the virus to others in mid-March whilst unaware, and the spread could be significantly larger as a result of the football match. Subsequent to that, cases may become more severe and result in a death.

As such, we consider the impact of matches taking place in February and March on Covid-19 case rates in March and April 2020. We similarly attempt to understand total reported Covid-19 death rates in April by looking at matches in February and March. Finally, as the Covid-19 testing procedure must be imperfect, and indeed many were not necessarily tested, we run regressions using total reported excess death rates April on football matches in February and March.

Our case and death rate data are presented graphically in Figures 1–3, and in Table 3 we present summary statistics relating to our data. The top panel describes the mortality measures, the middle panel the control variables, and the bottom panel a range of the football measures.

We consider the impact of matches taking place *in* an area on Covid-19 cases and deaths in that area, and we also consider the impact of matches *involving* teams from a area playing away from home. That is, if Bournemouth visit Liverpool for a match, as occurred on March 7, we consider the impact of this match on Covid-19 cases in Bournemouth, as well as on Covid-19 cases in Liverpool. Hence in Table 3 we report the number of matches involving areas, as well as matches in areas.

Covid Economics 47, 4 September 2020: 162-183

Covid Economics 47, 4 September 2020: 162-183

Table 3: Summary Statistics

Statistic	N	Mean	St. Dev.	Min	Pctl(25)	Pctl(75)	Max
Cumulative lab confirmed cases rate March 14 (per 100,000 people)	313	2.292	4.257	0	0	3	35
Cumulative lab confirmed cases rate April 30 (per 100,000 people)	313	188.388	108.122	0.000	126.300	247.900	795.400
March Covid-19 death rate (per 100,000 people)	313	8.018	8.937	0.000	2.800	9.500	47.100
April Covid-19 death rate (per 100,000 people)	313	51.840	26.600	0.000	32.900	66.600	150.700
March excess death rate (per 100,000 people)	313	90.486	16.199	59.200	78.500	99.700	146.300
April excess death rate (per 100,000 people)	313	138.280	35.299	51.900	113.600	161.700	239.900
Population (000s)	312	166.947	112.893	7.375	97.234	205.323	1,073.045
Population Density (people per square km)	313	1,816.553	2,664.425	25	229	2,423	16,427
Median Age	313	42.230	5.099	29	38	46	54
Working age 16–64	313	61.524	3.730	53	59	63	75
Proportion White English/Welsh/Scottish/Northern Irish	313	83.962	16.604	17	81	95	98
Income (GBP)	313	20,285.120	5,802.567	12,232	17,225	21,927	62,600
Number of Football Clubs	313	1.220	1.003	0	1	2	7
Number of League Football Clubs	313	0.284	0.524	0	0	1	3
Number of matches in area in March	313	1.058	1.213	0	0	2	8
Number of matches involving area in March	313	1.070	1.188	0	0	2	9
Number of matches in area in Feb	313	2.834	2.467	0	1	4	16
Number of matches involving area in Feb	313	2.818	2.607	0	1	4	22
Total attendance at matches in area in March	313	4.144	13.271	0.000	0.000	1.430	116.071
Total attendance at matches involving area in March	313	5.217	25.923	0.000	0.000	1.310	407.166
Number of matches in area in March with 90% full stadium	313	0.061	0.276	0	0	0	2
Number of matches involving area in March with 90% full stadium	313	0.073	0.398	0	0	0	5
Number of matches in area in March with 80% full stadium	313	0.077	0.311	0	0	0	2
Number of matches in area involving March with 80% full stadium	313	0.089	0.458	0	0	0	6
Number of matches in area in March with 70% full stadium	313	0.102	0.370	0	0	0	2
Number of matches in area involving March with 70% full stadium	313	0.118	0.489	0	0	0	6
Number of matches in area in March with 50% full stadium	313	0.169	0.474	0	0	0	3
Number of matches involving area in March with 50% full stadium	313	0.182	0.611	0	0	0	7

5 Results

Figure 5 gives a graphical summary of our results from running a range of variants of (1), varying the football measure, and the mortality measure. A subset of this information is provided in Tables 4–9 in numerical form. Each plot is for a different mortality measure, while the points represent coefficient estimates for different football measures (equations (2)–(6)). Each dot on each plot comes from a different regression equation, and each dot is an estimate of the β coefficient from (1)

In each plot, a solid dot represents the β coefficient estimate, and the lines represent the associated 90% confident interval. The first three coefficients from the left are the coefficients on the capacity measure (6), the number of matches (2) and the total attendance (3), and the subsequent coefficients to the right of the dashed line are measures (4) and (5) for 10% to 90% capacity, in 10 percentage point increments. A black dot or line represents matches *above* that threshold, a red dot or line represents matches *below* that threashold.

The capacity measure, being bounded on the unit interval, has the largest coefficient and suggests that the more full are matches in an area, the greater are case and death rates. The total attendance coefficient is very small, because attendances are in the thousands. The number of matches along the top panel, without any controls, is usually significant. This suggests that every football match in an area increases the number of cases and deaths, per 100,000 people.

To the right of the dashed line we look at the different thresholds of capacity, from 10% up to 90%, and here the red dots and lines represent a regression coefficient for *lower* than that threshold (5), and a black one for *above* it (4).

On the top row of Figure 5, without controls, matches closer to capacity are consistent with more cases and deaths in an area. That is, each match with attendance greater than or equal to 90% of capacity is consistent with more cases and deaths than each match with attendance greater than or

Covid Economics 47, 4 September 2020: 162-183

equal to 10% of capacity. The effect is around 50 additional cases per 100,000 people, and between 20 and 30 additional deaths per 100,000 people, for each extra match with attendance above 60% of capacity.

The red dots indicate that the effect of matches below each threshold is smaller, yet close to being significant, and as such, non-trivial.

Moving to the bottom row of plots, these are when control variables have been added (see middle section of Table 3). These control variables are for population density, and the age and ethnic profiles, the mean income level, and the number of football clubs for each area. The notable change here is that the below thresholds (5) are consistently larger, relative to without controls, while the above thresholds (4) tend to be more varied and less distinguishable from the below ones.

Because the mean capacity filled in a match in our sample is around 15% (Table 3), the below thresholds have smaller confidence bands and hence, to some extent, renders these more reliable indicators. For death rates (Covid-19 and excess), these are significant from around 20–30% upwards and are consistent with between 2 and 3 additional deaths per match. For deaths, the above thresholds peak in terms of significant at 30%, before dropping to insignificance, and registering essentially a zero coefficient for around 70% before jumping in magnitude for 90% matches.

The 30% peak, which is significant, suggests that matches above 30% are consistent with between 4 and 5 additional deaths per 100,000 people, whereas matches below 30% capacity are consistent with between 2 or 3 additional deaths per 100,000 people. These are both significant effects. At this level, the effect of matches on Covid-19 cases is significant, too, for matches above 30% capacity, and consistent with around 25 Covid-19 cases per 100,000 people.

Across the capacity thresholds, and based on the simple number of matches taking place, our results are consistent with around six additional Covid-19 cases per 100,000 people in the area the match took place, two additional Covid-19 deaths per 100,000 people in the area the match took place, and three additional excess deaths per 100,000 people in the area the match took place.

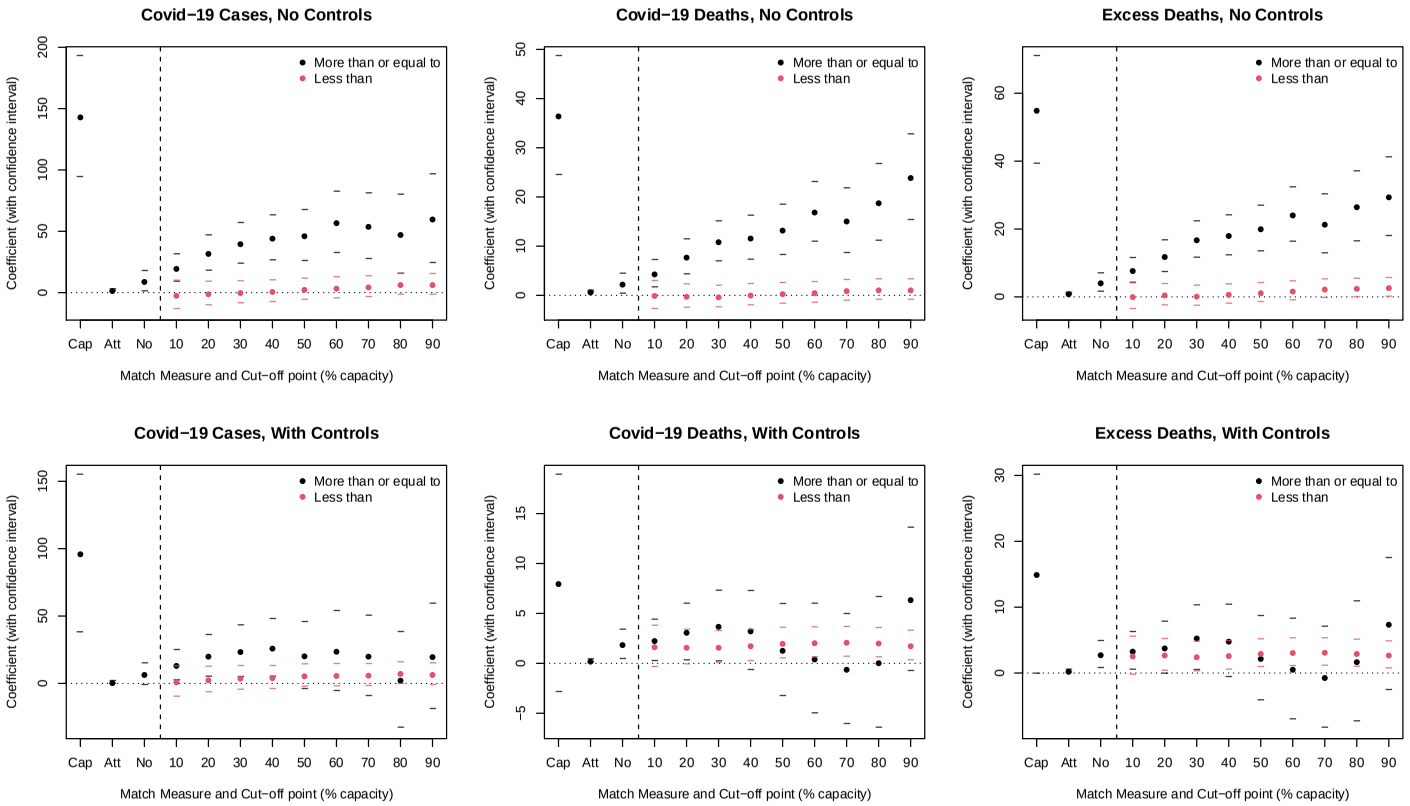

Figure 5: Summary of regression results of football match activity on mortality in the first half of 2020 in England. Each column of plots relates to a measure of mortality (Covid-19 cases, Covid-19 deaths, and excess deaths), the top row is without any control variables, and the bottom row adds control variables. Solid dots are regression coefficients on the footballing measure, and circles are the upper and lower confidence intervals (90% significance level).

Covid Economics 47, 4 September 2020: 162-183

Tables 4–6 we run (1) provide numerical information to supplement that in Figure 5, and in addition, include the impact of matches *involving* an area, as well as matches in February.

In Table 4, the impact of matches on Covid-19 cases per 100,000 people is summarised, again via the β estimated coefficient from (1), plus p-value. Down the columns, the effect of particular timing groupings of matches, hence $t-j$, is presented: matches *in* an area in March, matches *involving* an area in March, and then the same for February. Along the rows, particular measures of matches in those time frames, hence one of (2)–(6), are presented.

With the exception of the final row, matches that have attendance less than half the capacity of a stadium, by and large the effects are significant, and sizeable. The effects are also generally smaller for February relative to March, and for matches involving an area rather than matches in an area.

Tables 5 and 6 present the same effects of matches without controls, which tend to be significant.

	March (home)	March (away)	Feb (home)	Feb (away)
No..matches	8.73	10.33	6.54	5.82
X	0.08	0.04	0.01	0.01
Attendance	1.31	0.34	0.78	0.64
X.1	0.00	0.15	0.00	0.00
Cap..measure	142.84	86.59	95.38	104.77
X.2	0.00	0.00	0.00	0.00
X..of.matches...90..capacity	59.60	25.97	16.55	30.44
X.3	0.01	0.09	0.10	0.01
X..of.matches..90..capacity	6.12	7.37	5.99	4.50
X.4	0.23	0.19	0.02	0.06
X..of.matches...50..capacity	45.95	16.56	17.55	14.27
X.5	0.00	0.10	0.00	0.01
X..of.matches..50..capacity	2.23	6.13	2.68	3.05
X.6	0.67	0.29	0.33	0.23

Table 4: Effect of football matches on Covid-19 case rates, without adding controls

	March (home)	March (away)	Feb (home)	Feb (away)
No. matches (coef)	2.17	3.78	1.91	1.52
No. matches (p-value)	0.08	0.00	0.00	0.01
Attendance (coef)	0.58	0.17	0.30	0.29
Attendance (p-value)	0.00	0.00	0.00	0.00
Cap. measure (coef)	36.38	29.38	36.04	36.94
Cap. measure (p-value)	0.00	0.00	0.00	0.00
% of matches >=90% capacity (coef)	23.84	11.47	11.07	13.62
% of matches >=90% capacity (p-value)	0.00	0.00	0.00	0.00
% of matches <90% capacity (coef)	1.00	2.49	1.29	0.89
% of matches <90% capacity (p-value)	0.43	0.07	0.04	0.13
% of matches >=50% capacity (coef)	13.15	7.68	6.00	5.77
% of matches >=50% capacity (p-value)	0.00	0.00	0.00	0.00
% of matches <50% capacity (coef)	0.23	1.76	0.47	0.29
% of matches <50% capacity (p-value)	0.86	0.22	0.49	0.64

Table 5: Effect of football matches on Covid-19 death rates, without adding controls

In Tables 7–9 we report the same effects of measured football match activity in areas once the controls

	March (home)	March (away)	Feb (home)	Feb (away)
No. matches (coef)	4.00	4.96	3.00	2.67
No. matches (p-value)	0.01	0.00	0.00	0.00
Attendance (coef)	0.77	0.25	0.43	0.45
Attendance (p-value)	0.00	0.00	0.00	0.00
Cap. measure (coef)	54.84	49.77	57.79	63.96
Cap. measure (p-value)	0.00	0.00	0.00	0.00
% of matches >=90% capacity (coef)	29.34	17.62	16.11	20.66
% of matches >=90% capacity (p-value)	0.00	0.00	0.00	0.00
% of matches <90% capacity (coef)	2.59	3.11	2.13	1.72
% of matches <90% capacity (p-value)	0.12	0.09	0.01	0.03
% of matches >=50% capacity (coef)	19.92	12.10	8.80	9.56
% of matches >=50% capacity (p-value)	0.00	0.00	0.00	0.00
% of matches <50% capacity (coef)	1.09	1.81	0.95	0.65
% of matches <50% capacity (p-value)	0.52	0.34	0.29	0.43

Table 6: Effect of football matches on excess death rates, without adding controls

outlined in Section 4 are added. These coefficients correspond to the lower row of plots in Figure 5. These is very little significance in terms of cases, but for Covid-19 and excess deaths, the number of matches is significant at a 10% level of significance for matches in and involving an area in March, and also in February. Matches in March add 2–3 deaths per 100,000 people, both in and involving an area, and matches in February around one death per 100,000 people. The effect is similarly significant for matches with less than 90%, and less than 50% of capacity, and again for all timings and locations of matches — in and involving areas in March and February. In particular, for matches involving an area in March, the effect of a match appears to be larger than for matches in an area.

	March (home)	March (away)	Feb (home)	Feb (away)
No. matches (coef)	6.27	6.88	3.23	3.43
No. matches (p-value)	0.20	0.17	0.22	0.16
Attendance (coef)	0.18	-0.14	0.21	-0.39
Attendance (p-value)	0.74	0.59	0.49	0.28
Cap. measure (coef)	95.83	7.80	3.19	4.74
Cap. measure (p-value)	0.01	0.83	0.93	0.91
% of matches >=90% capacity (coef)	19.50	-5.53	-13.06	-4.05
% of matches >=90% capacity (p-value)	0.41	0.74	0.24	0.77
% of matches <90% capacity (coef)	6.27	7.48	4.04	3.40
% of matches <90% capacity (p-value)	0.20	0.16	0.12	0.16
% of matches >=50% capacity (coef)	20.08	-10.19	3.12	-12.28
% of matches >=50% capacity (p-value)	0.19	0.38	0.69	0.21
% of matches <50% capacity (coef)	5.28	10.01	3.10	4.03
% of matches <50% capacity (p-value)	0.30	0.07	0.25	0.10

Table 7: Effect of football matches on Covid-19 case rates, adding controls

The control variables, x_{it}, are an important part of ensuring that the effect that is detected by the football match variables reflects the incidence of these matches, rather than the characteristics of areas that have football clubs. With the number of different football match measures, timings of matches, and mortality measures, there are 264 different tables representing the impact of adding control variables. In

Covid Economics 47, 4 September 2020: 162-183

Covid Economics 47, 4 September 2020: 162-183

	March (home)	March (away)	Feb (home)	Feb (away)
No. matches (coef)	1.83	2.61	0.93	0.90
No. matches (p-value)	0.04	0.00	0.06	0.05
Attendance (coef)	0.17	-0.01	0.09	-0.00
Attendance (p-value)	0.09	0.75	0.09	0.97
Cap. measure (coef)	7.94	-1.61	-4.01	-2.33
Cap. measure (p-value)	0.23	0.81	0.55	0.76
% of matches >=90% capacity (coef)	6.33	-0.73	-0.65	1.50
% of matches >=90% capacity (p-value)	0.15	0.81	0.75	0.55
% of matches <90% capacity (coef)	1.71	2.79	0.93	0.82
% of matches <90% capacity (p-value)	0.06	0.00	0.05	0.07
% of matches >=50% capacity (coef)	1.25	-1.09	-0.20	-1.20
% of matches >=50% capacity (p-value)	0.65	0.61	0.89	0.51
% of matches <50% capacity (coef)	1.95	3.26	0.95	0.94
% of matches <50% capacity (p-value)	0.04	0.00	0.05	0.04

Table 8: Effect of football matches on Covid-19 death rates, adding controls

	March (home)	March (away)	Feb (home)	Feb (away)
No. matches (coef)	2.70	2.50	1.15	1.39
No. matches (p-value)	0.03	0.05	0.09	0.03
Attendance (coef)	0.19	-0.03	0.12	0.05
Attendance (p-value)	0.17	0.61	0.14	0.62
Cap. measure (coef)	14.89	1.94	2.83	9.52
Cap. measure (p-value)	0.11	0.83	0.76	0.38
% of matches >=90% capacity (coef)	7.33	-1.46	0.65	3.48
% of matches >=90% capacity (p-value)	0.23	0.73	0.82	0.32
% of matches <90% capacity (coef)	2.65	2.75	1.11	1.21
% of matches <90% capacity (p-value)	0.03	0.04	0.10	0.05
% of matches >=50% capacity (coef)	2.14	-2.47	0.04	-0.09
% of matches >=50% capacity (p-value)	0.58	0.41	0.99	0.97
% of matches <50% capacity (coef)	2.90	3.45	1.19	1.33
% of matches <50% capacity (p-value)	0.02	0.02	0.08	0.03

Table 9: Effect of football matches on excess death rates, adding controls

Table 10 we present one such Table, for matches in March with attendance less than 30% of capacity.[3] Controls are added one by one across the Table, from left to right. The coefficient on matches jumps from essentially zero to 2.5 deaths per 100,000 people in an area for each match in March wtih attendance less than 30% of stadium capacity with the addition of population density. As such, once we control for the number of excess deaths that would be expected for a given population density (hence controlling for the level of urban development in an area), the impact of football matches becomes more apparent. In Tables 7–9 we present column (6) rather than column (7), where the latter includes as a control variable a lagged count of the mortality measure in question.

Figure 6 also provides a graphical representation, plotting the average trajectory of Covid-19 cases through March and April for areas that had zero, one, two or more matches with at least 30% capacity filled in their stadia. The lines for one (47 areas have one match) and two (15 areas) matches are above

[3]The remainder are available in an online appendix, which can be found here: https://www.dropbox.com/s/8vqno3eudyqj86n/covid-online-app.pdf?dl=0.

Covid Economics 47, 4 September 2020: 162-183

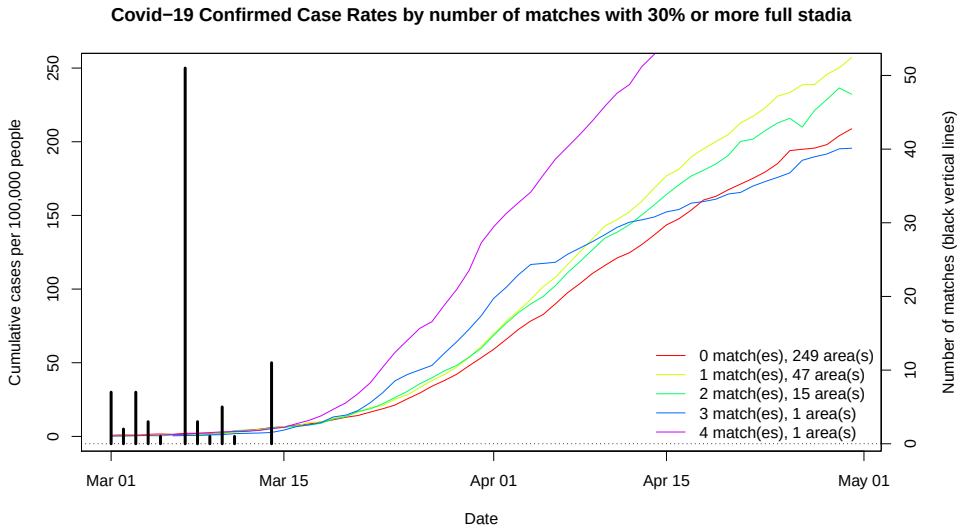

Figure 6: Cumulative cases per 100,000 people by the number of matches in March with stadia at least 30% full.

the line for no matches, while there is only one area with three matches, and one with four (Sheffield), and as such these two lines are somewhat unrepresentative of general patterns. Excluding Sheffield from the analysis does not affect the results.

Table 10: Excess death rate on number of football matches with stadium less than 30 percent full in area in March, adding controls

	Dependent variable:						
	Covid-19 cumulative case rate April 30						
	(1)	(2)	(3)	(4)	(5)	(6)	(7)
Constant	138.206***	124.610***	217.094***	273.006***	327.284***	314.592***	169.876***
	(2.436)	(2.560)	(16.311)	(16.705)	(19.239)	(21.022)	(24.893)
Number of Football Matches with Stadium less than 30 Percent Full	0.095	2.500	2.128	2.704*	2.092	2.394*	0.945
	(1.786)	(1.588)	(1.514)	(1.394)	(1.345)	(1.358)	(1.224)
Population Density (ppl/km2)		0.006***	0.001	0.003***	0.002	0.002	−0.001
		(0.001)	(0.001)	(0.001)	(0.001)	(0.001)	(0.001)
Prop. White British/Northern Irish			−0.989***	−1.147***	−0.750***	−0.759***	−0.532***
			(0.173)	(0.160)	(0.172)	(0.172)	(0.156)
Income				−0.002***	−0.002***	−0.002***	−0.001**
				(0.0003)	(0.0003)	(0.0003)	(0.0003)
Median Age					−2.211***	−1.965***	−1.447***
					(0.432)	(0.462)	(0.417)
Number of league clubs						4.917	4.687
						(3.315)	(2.962)
March rate							0.968***
							(0.109)
Observations	313	313	313	313	313	313	313
R^2	0.00001	0.231	0.305	0.415	0.461	0.465	0.574
Adjusted R^2	−0.003	0.226	0.299	0.407	0.452	0.454	0.564
Residual Std. Error	35.356 (df = 311)	31.047 (df = 310)	29.564 (df = 309)	27.178 (df = 308)	26.128 (df = 307)	26.077 (df = 306)	23.295 (df = 305)
F Statistic	0.003 (df = 1; 311)	46.660*** (df = 2; 310)	45.268*** (df = 3; 309)	54.583*** (df = 4; 308)	52.497*** (df = 5; 307)	44.285*** (df = 6; 306)	58.770*** (df = 7; 305)
Note:							*p<0.1; **p<0.05; ***p<0.01

Across the capacity thresholds, and based on the simple number of matches taking place, our results

are consistent with around six additional Covid-19 cases per 100,000 people in the area the match took place, two additional Covid-19 deaths per 100,000 people in the area the match took place, and three additional excess deaths per 100,000 people in the area the match took place. This effect is slightly stronger for the areas of away teams in March, and slightly weaker for matches in February.

6 Conclusions

In this paper, we study the potential impact of mass outdoor events on the spread of an airborne virus. We utilise local area level data on Covid-19 cases, deaths and excess deaths, alongside demographic and other regionally disaggregated variables to explain the prevalence of the virus in such local areas. We then consider the extent to which football matches, of which there are usually around 200 per week across England and Wales, did spread the virus as it emerged in the UK in the first half of 2020.

We find prima facie evidence that football matches were consistent with increased cases, and deaths, during April 2020. Once we control for a range of factors believed to help explain the spread of the virus other than mass outdoor events, we find that small but significant effects remain of football match activity in an area on measures of mortality in April. We find that the effect isn't constrained to matches in March, or even matches only in an area. The effect of fans travelling to away matches is apparent, as all mortality measures remain sizeable, and are generally significant, for matches involving teams in other parts of the country in both March and February 2020.

Concretely, across the capacity thresholds, and based on the simple number of matches taking place, our results are consistent with around six additional Covid-19 cases per 100,000 people in the area the match took place, two additional Covid-19 deaths per 100,000 people in the area the match took place, and three additional excess deaths per 100,000 people in the area the match took place. This effect is slightly stronger for the areas of away teams in March, and slightly weaker for matches in February.

This evidence suggests that the return of fans to stadia, even for outdoor events, and even for sparsely attended matches, may have significant effects on mortality measures, and the spread of Covid-19, and hence ought to be considered with caution. This evidence appears statistically significant, and it undoubtedly has economic significance for sports leagues and sports clubs, many of whom could not survive financially without the attendance of fans at matches.

The football matches that form the basis for this evidence took place in February and March, a time when in England social distancing was not at all widespread. Indeed Reade and Singleton (2020) find a very limited impact of publicly available information on Covid-19 on fan attendance at such mass events. It is possible that subsequent exposure to the virus in the time since March may have affected public attitudes towards social distancing. Reade et al. (2020) suggests that fans in Belarus spontaneously self-distanced, and as such changes in fan behaviour may be such that the impact noted from matches in March, which may have been from fans mingling in common areas in stadia (e.g. concourses to get refreshments, and pubs and bars before and after matches), rather than the match itself, particularly when sparsely attended. As such, we would suggest that in order to form policy regarding the return of fans to outdoor sporting events in the coming months, governments and sporting authorities ought to make use of pilot studies as well as the evidence contained within this study.

Covid Economics 47, 4 September 2020: 162-183

References

A. Ahammer, M. Halla, and M. Lackner. Mass Gatherings Contributed to Early COVID-19 Spread: Evidence from US Sports. *Covid Economics*, 30, 2020.

Y. Bai, L. Yao, T. Wei, F. Tian, D.-Y. Jin, L. Chen, and M. Wang. Presumed asymptomatic carrier transmission of COVID-19. *Jama*, 323(14):1406–1407, 2020.

A. Cardazzi, B.R. Humphreys, J.E. Ruseski, B. Soebbing, and N.S Watanabe. Professional Sporting Events Increase Seasonal Influenza Mortality in US Cities. Technical Report 3628649, SSRN, 2020.

M. Chabros, D. Agelos, C. Jones, and M. Olczak. The Determinants of Grassroots English Football Attendance. Working paper, Aston University, 2019.

D. Coates and B.R. Humphreys. Week-to-week attendance and competitive balance in the National Football League. *International Journal of Sport Finance*, 5(4):239, 2010.

D. Coates and B.R. Humphreys. Game attendance and outcome uncertainty in the National Hockey League. *Journal of Sports Economics*, 13(4):364–377, 2012.

D. Forrest and R. Simmons. New Issues in Attendance Demand: The case of the English Football League. *Journal of Sports Economics*, 7(3):247–263, 2006.

David Forrest and Robert Simmons. Outcome uncertainty and attendance demand in sport: the case of English soccer. *Journal of the Royal Statistical Society: Series D (The Statistician)*, 51(2):229–241, 2002.

J. Garcia and P. Rodríguez. The determinants of football match attendance revisited empirical evidence from the spanish football league. *Journal of Sports Economics*, 3(1):18–38, 2002.

S. Gitter. The H1N1 Virus and Mexican Baseball Attendance. *Athens Journal of Sports*, 4(4), 2017. doi: 10.30958/ajspo.4.4.2.

A. Larsson, E. Ranudd, E. Ronchi, A. Hunt, and S. Gwynne. The impact of crowd composition on egress performance. *Fire Safety Journal*, page 103040, 2020.

S.A. Lauer, K.H. Grantz, Q. Bi, F.K. Jones, Q. Zheng, H.R. Meredith, A.S. Azman, N.G. Reich, and J. Lessler. The incubation period of coronavirus disease 2019 (COVID-19) from publicly reported confirmed cases: estimation and application. *Annals of internal medicine*, 172(9):577–582, 2020.

D. Owen and C.R. Weatherston. Uncertainty of Outcome and Super 12 Attendance: Application of a General-To-Specific Modeling Strategy. *Journal of Sports Economics*, 5(4):347–370, 2004.

D. Paton and A. Cooke. Attendance at County Cricket: An Economic Analysis. *Journal of Sports Economics*, 6(1):24–45, 2005.

D. Peel and D. Thomas. Attendance demand: an investigation of repeat fixtures. *Applied Economics Letters*, 3(6):391–394, 1996.

J.J. Reade and C. Singleton. Demand for Public Events in the COVID-19 Pandemic: A Case Study of European Football. Discussion Paper em-dp2020-09, Department of Economics, University of Reading, 2020.

Covid Economics 47, 4 September 2020: 162-183

J.J. Reade, D. Schreyer, and C. Singleton. Stadium attendance demand during the COVID-19 crisis: First empirical evidence from Belarus. Discussion Paper em-dp2020-20, Department of Economics, University of Reading, 2020.

A. Sacheti, I. Gregory-Smith, and D. Paton. Uncertainty of Outcome or Strengths of Teams: An Economic Analysis of Attendance Demand for International Cricket. *Applied Economics*, 46(17): 2034–2046, 2014.

M. Sassano, M. McKee, W. Ricciardi, and S. Boccia. Transmission of SARS-CoV-2 and Other Infections at Large Sports Gatherings: A Surprising Gap in Our Knowledge. *Frontiers in Medicine*, 7, 2020.

B.P. Soebbing. Competitive Balance and Attendance in Major League Baseball: An Empirical Test of the Uncertainty of Outcome Hypothesis. *International Journal of Sports Finance*, 3:119–126, 2008.

C. Stoecker, N.J. Sanders, and A. Barreca. Success Is something to sneeze at: Influenza mortality in cities that participate in the Super Bowl. *American Journal of Health Economics*, 2(1):125–143, 2016.

S. Szymanski. Income inequality, competitive balance and the attractiveness of team sports: Some evidence and a natural experiment from English soccer. *Economic Journal*, 111(469):69–84, 2001.

T. Wallrafen, T. Pawlowski, and C. Deutscher. Substitution in sports: The case of lower division football attendance. *Journal of Sports Economics*, 20(3):319–343, 2019.

Covid Economics 47, 4 September 2020: 162-183